STUDIES ON CHEMICAL CONSTITUENTS AND BIOLOGICAL ACTIVITIES OF *NAUCLEA OFFICINALIS* AND *NAUCLEA SUBDITA*

LIEW SOOK YEE

THESIS SUBMITTED IN FULFILMENT OF THE REQUIREMENTS FOR THE DEGREE OF DOCTOR OF PHILOSOPHY

DEPARTMENT OF CHEMISTRY
FACULTY OF SCIENCE
UNIVERSITY OF MALAYA
KUALA LUMPUR

2014

UNIVERSITI MALAYA

ORIGINAL LITERARY WORK DECLARATION

Name of Candidate: **LIEW SOOK YEE** (I.C/Passport No: **870430-08-5382**)

Registration/Matric No: **SHC 100046**

Name of Degree: **DOCTOR OF PHILOSOPHY**

Title of Project Paper/Research Report/Dissertation/Thesis ("this Work"):
STUDIES ON CHEMICAL CONSTITUENTS AND BIOLOGICAL ACTIVITES OF *NAUCLEA OFFICINALIS* AND *NAUCLEA SUBDITA*

Field of Study:

I do solemnly and sincerely declare that:

(1) I am the sole author/writer of this Work;
(2) This Work is original;
(3) Any use of any work in which copyright exists was done by way of fair dealing and for permitted purposes and any excerpt or extract from, or reference to or reproduction of any copyright work has been disclosed expressly and sufficiently and the title of the Work and its authorship have been acknowledged in this Work;
(4) I do not have any actual knowledge nor do I ought reasonably to know that the making of this work constitutes an infringement of any copyright work;
(5) I hereby assign all and every rights in the copyright to this Work to the University of Malaya ("UM"), who henceforth shall be owner of the copyright in this Work and that any reproduction or use in any form or by any means whatsoever is prohibited without the written consent of UM having been first had and obtained;
(6) I am fully aware that if in the course of making this Work I have infringed any copyright whether intentionally or otherwise, I may be subject to legal action or any other action as may be determined by UM.

Candidate's Signature Date 10/9/2014

Subscribed and solemnly declared before,

Witness's Signature Date 10/9/2014

Name: Professor Dr. Khalijah Awang
Designation: Department of Chemistry,
Faculty Science, University Malaya,
50603 Kuala Lumpur.

ABSTRACT

The phytochemical studies on two species of Rubiaceae; *Nauclea officinalis* and *Nauclea subdita* have been carried out. Twenty one compounds were successfully isolated and purified using several chromatography techniques such as column chromatography (CC), thin layer chromatography (TLC), preparative thin layer chromatography (PTLC), and high performance liquid chromatography (HPLC). The compounds are naucline, nauclefine, naucletine, angustine, angustoline, 3,14-dihydroangustoline, angustidine, subditine, strictosamide, pumiloside, naucleficine, naucleactonin C, harmane, 1,2,3,4-tetrahydro-1-oxo-β-carboline, benzamide, cinnamide, blumenol B, blumenol A, β-sitosterol, stigmast-4-en-3-one and vanillin. Naucline and subditine are new indole alkaloids which were isolated from the bark of *Nauclea officinalis* and *Nauclea subdita* respectively. The structure of the isolated compounds were elucidated using various spectroscopic methods; 1D-NMR (^{1}H, ^{13}C, DEPT), 2D-NMR (COSY, HSQC, HMBC, NOESY), UV, mass spectrometry and comparison with literature reviews. Among five compounds, subditine exhibited good cytotoxic activity against human prostate cancer cells which are LNCaP and PC-3 with IC_{50} of 12.24 ± 0.19 µM and IC_{50} of 13.97 ± 0.32 µM respectively. IC_{50} values of angustoline, angustidine, angustine and nauclefine were in the range of 58.09-149.16 µM. Subditine showed higher selectivity against LNCaP and PC-3 prostate cancer cells than the normal prostate cells; RWPE-1 (selectivity index: [LNCaP/PC-3] = 2.49/2/18). In addition, ten alkaloids was tested for anticholinesterase activity. Only angustidine showed potent inhibition with IC_{50} of 6.54 ± 0.37 µM on acetylcholinesterase enzyme (AChE). On the other hand, for butyrylcholinesterae enzyme (BChE), three alkaloids exhibited potent inhibition; angustidine, angustine and nauclefine with IC_{50} of 0.31 ± 0.07 µM, 1.56 ± 0.05 µM and 2.21 ± 0.03 µM, respectively. Angustidine was the most potent inhibitor of BChE than the standard galanthamine. Enzyme kinetic studies and

molecular docking suggested that the most potent compound, angustidine possess mixed inhibition mode with inhibition constant, *Ki* value of 6.12 µM and its binding site was strongest at the bottom gorge of *h*BChE and formed hydrogen bonding with Ser 198 and His 438.

ABSTRAK

Kajian fitokimia terhadap dua spesis Rubiaceae; *Nauclea officinalis* dan *Nauclea subdita* telah dijalankan. Dua puluh satu sebatian telah berjaya diasingkan dan ditulenkan dengan menggunakan pelbagai kaedah kromatografi seperti kromatografi turus, kromatografi lapisan nipis, kromatografi lapisan nipis persediaan dan kromatografi cecair prestasi tinggi. Sebatian-sebatian tersebuat ialah are naucline, subditine, angustine, angustidine, angustoline, 3,14-dihydroangustoline, naucletine, nauclefine, naucleficine, naucleactonin C, 1,2,3,4-tetrahydro-1-oxo-β-carboline, harmane, cinnamide, benzamide, pumiloside, strictosamide, stigmast-4-en-3-one, β-sitosterol, blumenol A, blumenol B dan vanillin. Naucline dan subditine merupakan sebatian alkaloid baru yang masing-masing diasingkan daripada bahagian batang spesis *Nauclea officinalis* dan *Nauclea subdita*. Struktur bagi sebatian yang diasingkan telah dikenalpastikan dengan menggunakan pelbagai teknik spectroskopi; 1D-NMR (^{1}H, ^{13}C, DEPT), 2D-NMR (COSY, HSQC, HMBC, NOESY), UV, mass spectrometry dan perbandingan dengan kajian-kajian lepas. Subditine menunjukkan aktiviti sitotoksik yang bagus terhadap kanser sel prostat manusia iaitu LNCaP dan PC3 yang masing-masing dengan nilai IC_{50} 12.24 ± 0.19 µM dan 13.97 ± 0.32 µM di antara lima sebatian. Nilai IC_{50} bagi angustoline, angustidine, angustine dan nauclefine adalah dalam lingkungan 58.09-149.16 µM. Subditine menunjukkan kepilihan yang lebih tinggi terhadap kanser sel prostat manusia; LNCaP dan PC3 berbanding dengan normal sel prostat manusia; RWPE-1 (Indeks kepilihan: [LNCaP/PC-3] = 2.49/2/18). Selain itu, sepuluh sebatian alkaloid telah diujikan bagi aktiviti antikolinesterase. Hanya angustidine menunjukkan potensi yang bagus bagi perencatan dengan nilai IC_{50} 6.54 ± 0.37 µM bagi enzim asetilkolinesterase. Manakala, bagi enzim butirilkolinesterase, tiga sebatian alkaloid menunjukkan potensi yang bagus bagi perencatan; angustidine, angustine dan nauclefine yang masing-masing dengan IC_{50} 0.31 ± 0.07 µM, 1.56 ± 0.05

µM dan 2.21 ± 0.03 µM. Kajian kinetik enzim dan docking molekul mencadangkan compound yang paling bagus potensinya, angustidine mempunyai mod jenis perencatan campuran dengan nilai pemalar prencatan 6.12 µM dan mengikat pada bahagian bawah “gorge” dan membentuk ikatan hidrogen Ser 198 dan His 438.

ACKNOWLEDGEMENT

First and foremost, I want to thank to God for providing me infinite blessing . I would like to express my greatest gratitude and appreciation to my supervisors, Prof. Dr. Khalijah Awang and Prof. Dr. Mohd Rais bin Mustafa for their good supervision, concern, encouragement and constant guidance throughout my research study. I also wish to forward my greatest appreciation to my ex-supervisor, the late Assoc. Prof. Dr. Mat Ropi bin Mukhtar for his kind guidance, advices and patience.

My deepest appreciation is also dedicate to my friends in phytochemistry laboratory; Mrs. Syazreen Nadia, Mrs. Azeana, Mrs. Faizah, Mrs. Ayu Afiqah, Mrs. Wan Nurul Nazneem, Ms. Yasodha, Mrs. Shelly, Mr. Fadzli, Mr. Ang, Mrs. Kee, Mr. Azmi, Mrs. Munirah, Mr. Abbas, Ms. Masoumeh, Mrs. Chan, Ms. Rosalind, Mr. Jamil, Ms. Hazrina, Ms. Lailey, Ms. Haslinda, Ms. Nor Aimi, Ms. Dewi, Mrs. Julia, Mrs. Norsita, Mr. Chong, Mr. Tiong, Ms. Xe Min, Ms. Tien, Mr. Omer and Mr. Ahamd Kaleem for their great support, help and friendship.

I also would like to thank herbarium staffs; Mr. Din, Mr. Rafly, Mr. Teo for plant collection and hardware repair work in lab, as well as NMR and LCMS staffs; Ms. Norzalida, Mr. Fateh, Mrs. Dara Fiona, Mr. Zakaria and Mr. Siew for recording NMR and LCMS data.

Last but not least, I owed too much to my beloved parents; Mr. Liew Loi and Mrs. Chan Yit Yeen, my brother and sister in law; Mr Liew Yoong Sin, Mrs. Cheng Wei Ling , my sister, Liew Sook Huey and my friend, Lam Meng Chun for their infinite moral support, understanding and endurance that are greatly treasured throughout the study, Without their encouragement especially my father for always providing me shoulder to rest and ear to listen in tough time, I will never reach this far. Thank you for making my life so meaningful.

CONTENTS

CHAPTER 3: RESULTS AND DISCUSSION

LIST OF SCHEMES

LIST OF FIGURES

LIST OF TABLES

ABBREVIATIONS

α	Alpha
β	Beta
δ	Chemical shift
λ	Maximum wavelength
nm	Nanometer
µM	Micromolar
M	Molar
µL	Microlitre
mL	Mililitre
mM	Milimolar
mg/mL	Miligram per mililitre
µg/mL	Microgram per mililitre
m	Meter
g	Gram
kg	Kilogram
U/mL	Unit per mililitre
MHz	Mega Hertz
Hz	Hertz
UV	Ultraviolet
IR	Infrared
ppm	Part per million
cm^{-1}	Per centimeter
^{0}C	Degree celsius
Å	Angstrom
J	Coupling constant

s	Singlet
d	Doublet
dd	Doublet of doublets
dt	Doublet of triplets
t	Triplet
m	Multiplet
q	Quartet
$CHCl_3$	Chloroform
$CDCl_3$	Deuterated chloroform
CH_2Cl_2	Dichloromethane
MeOH	Methanol
MeOD	Deuterated methanol
DMSO-d_6	Dimethylsulphoxide-d_6
DMF-d_7	*N*,*N*-Dimethyl formamide-d_7
C_5D_5N	Pyridine-d_5
FA	Formic acid
NH_3	Ammonia
HCl	Hydrogen chloride
TLC	Thin layer chromatography
PTLC	Preparative thin layer chromatography
CC	Column chromatography
HPLC	High Performance Liquid Chromatography
CH_3	Methyl group
OH	Hydroxy group
NMR	Nuclear magnetic resonance
1D-NMR	One dimensional nuclear magnetic resonance

2D-NMR	Two dimensional nuclear magnetic resonance
^{1}H	Proton NMR
^{13}C	13-carbon NMR
COSY	^{1}H-^{1}H Correlation Spectroscopy
DEPT	Distortionless Enhancement by Polarization Transfer
HMBC	Heteronuclear Multiple Bond Coherence
HSQC	Heteronuclear Single Quantum Coherence
HMQC	Heteronuclear Multiple Quantum Coherence
NOESY	Nuclear Overhauser Effect Spectroscopy
LCMS-IT-TOF	Liquid Chromatography Mass Spectrometry-Ion Trap-Time of Flight
ESIMS	Electrospray Ionization Mass Spectrometry
m/z	Mass per charge
IC_{50}	Concentration required to inhibit 50% of activity
CO_2	Carbon dioxide
MTT	3-(4,5-dimethylthiazol-2-yl)-2,5-diphenyltetrazolium bromide
SI	Selectivity index
PDB	Protein data bank
Ki	Inhibition constant
LB plot	Lineweaver-Burk plot
OD	Optical density
*Tc*AChE	Torpedo californica acetylcholinesterase
*h*BChE	Human butyrylcholinesterase
TFA	Trifluroacetic acid
N.	Nauclea

SD	Standard Deviation
AD	Alzheimer disease

1.1 General

Pharmaceutical importance of plants has led to the discovery and adoption of plant extracts which are commonly used in traditional medicine.[1] Therefore, there are many medicinal plants which are being utilized as raw material sources in pharmaceutical manufacturing. For example, two terpenoid indole alkaloids, vinblastine **1** and vincristine **2** from *Catharanthus roseus*, are the natural anticancer agents to be clinically used.[2,3] Regardless of developing countries or developed ones, the demand for medicinal plants are high.

Medicinal plants have been shown to have genuine utility and a report by Okoro, Osagie and Asibor (2010) indicated that about 80% of the rural population depend on them as primary health care.[4] In fact, Newman and Cragg (2012) estimated that approximately 71% of the drugs that are available were either directly or indirectly derived from plants.[5]

Medicinal plants exhibit various effects on living system which include immuno-modulatory function, antiplasmodics, antioxidants, anti-inflammatory, cardio-protective, antipyretics, analgesic and sedatives.[6,7] The medicinal value of these plants originated from the chemical substances that produce a specific physiocological action on the human body.[8] There are wide variety of plant species that have potentials to become the source of drugs or lead compound that may be manipulated to develop potential therapeutics for the treatment of various diseases effectively. Examples of potent natural drugs and leads from plants are artemisinin **3** (antimalaria drug) from *Arternisia annua*, demecolcine **4** (antitumor drugs) from *Colchicum autumnale* and rescinnamine **5** (antihypertensive drug) from *Rauvolfia serpentine*. Hence, there is a need to continue and further investigate medicinal plant's potentials.

Malaysia has about 15,000 species of flowering plants of which around 10% of them have medicinal properties.[9,10,11] A large number of Malaysian plants possess a

multitude of pharmacological properties. For example, *Orthosiphonstamineus* Benth (Cat's whiskers), a medicinal plants in Malaysia, possess antiapoptotic and antioxidant activities.[12]

Rubiaceae is one of the plant families that is widely distributed in the Malaysian flora with 80 genera and 555 species among which is the genus *Nauclea*.[13] The *Nauclea* genus is known to be rich in indole alkaloids. Isolation of alkaloidal constituents from *N. parva, N. latifolia, N. pobeguinii, N. diderrichii* and *N. orientalis* have resulted in more than 50 alkaloids which include indolopyridine alkaloids, strictosidine-related monoterpenoid indole alkaloids and others.[14] Some of these alkaloids were reported to exert interesting biological activities such as antiproliferative (10-hydroxyangustine **6**)[15] and antirenin (latifoliamides C **7**)[16]. However, very few phytochemical and biological activity studies have been carried out on the *Nauclea* genus in Malaysia. In continuation of our scientific research on plants from the Rubiaceae family, a study of the chemical constituents of *N. officinalis* and *N. subdita* as well as evaluation on the cytotoxic and anti-cholinesterase activities have been carried out. These activities were chosen because alkaloids are well known to have potent cytotoxic (vinblastine and vincristine) and anti-cholinesterase activities (galanthamine and physostigmine).

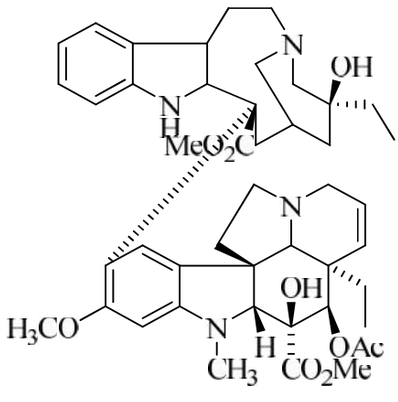

1

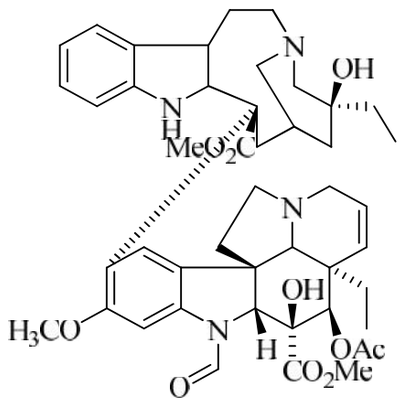

2

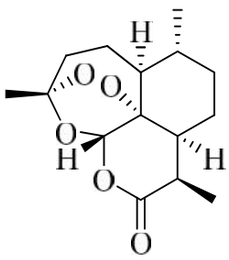

3

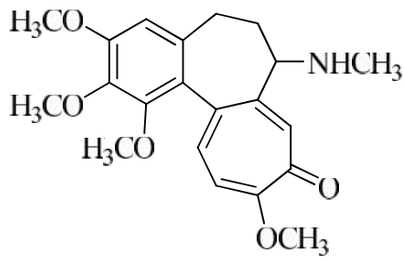

4

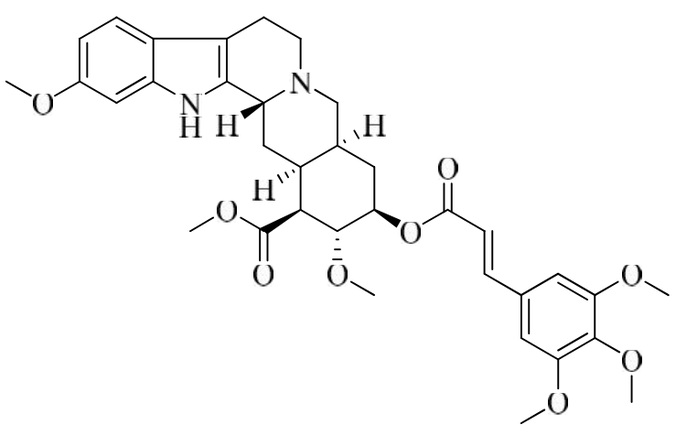

5

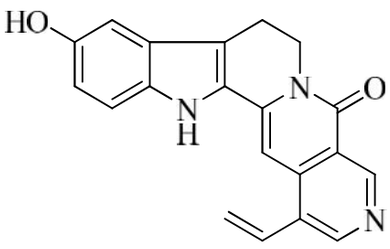

6

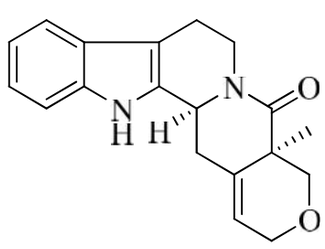

7

1.2 Rubiaceae: General appearance and morphology

Rubiaceae is also known as Madder or Bedstraw and comprises 637 genera and 10,700 species worldwide.[17] It is one of the fifth largest family of flowering plants (after Orchidaceae, Compositae, Leguminosae, Gramineae). In Malaysia, it is the largest family of trees, represented by 80 genera and 555 species of which some 244 species in 49 genres are trees.[13] The most recent and complete classification based on molecular, morphological and chemical evidence has subdivided this family into four subfamilies which are Cinchonoideae, Ixoroideae, Antirheoideae and Rubiodeae.[17,18]

The Rubiaceae is an important component of the lower strata of the rain forest. Only about a dozen species grow up to 30 m in height or taller and reaching 2 m in girth, the commonest being *Jackiopsis ornata*, *Metadina trichotoma*, *Mussaendopsis beccariana*, *Nauclea officinalis*, *Neolamarckia cadamba* and *Rothmannia schoemannii*. In all, only 50 species grow taller than 10 m.

Leaves are simple, occurring opposite in two rows or decussate or in whorls. In some taxa with one leaf reduced at successive nodes or alternate nodes or just below the inflorescence, or both leaves reduced at alternate nodes. Secondary veins on the lower leaf surface in some species characteristically with acarodomatia in their axils. Leaf tissue is exceptionally with dark bacterial wart-like nodules.

Flowers are bisexual or unisexual, mostly 4 to 5 merous. Calyces free or initially apically fused or later free or persistently fused. Sometimes with one lobe enlarged and conspicuously coloured. Corolla variously shaped with base united in a tube and lobes valvate or contorted in the bud .

It is free of fruits or connate into a compound fruit. It has many seeds per fruits. The seeds are in various shape and sometimes are winged, albuminous or exalbuminous.[13]

1.3 Classification of Rubiaceae

The classification of Rubiaceae is illustrated in Scheme 1.1. It is classified into four subfamilies which are Cinchonoideae, Ixoroideae, Antirheoideae and Rubiodeae.[17,18] The genus *Nauclea* is classified under the tribe of Naucleeae and subfamily of Cinchonoideae.[19]

Kingdom: Plantae

Division: Magnoliophyta

Class: Magnoliopsida

Order: Rubiales

Family: Rubiaceae

Subfamily: Cinchonoideae

Ixoroideae

Antirheoideae

Rubioideae

Tribe: Naucleeae

Scheme 1.1: Classification of tribe of Rubiaceae

1.4 Medicinal uses of Rubiaceae Plants

Plants of the Rubiaceae are known to have many natural substances which have been employed for various commercial and medicinal purposes. These plants are not only ornamental but they are also used in African folk medicine to treat several diseases. Based on the studies of Karou, Tchacondo, Ilboudo and Simpore (2011), more than 60 species are used for more than 70 medicinal treatments that include malaria, hepatitis, eczema, oedema, cough, hypertension, diabetes and sexual weakness. Besides, many of

these plants exhibited antimalarial, antimicrobial, antihypertension, antidiabetic, antioxidant and anti-inflammatory activities through biological screening following leads supplied by traditional healers.[20]

Morever, Pedersen, Gurib-Fakim, Subratty and Adsersen (1999) have carried out *in vitro* antibacterial, antifungal, pharmacological tests as well as chemical screenings on 27 plant extracts from 7 plants [*Antirhea borbonica* Gmel., *Chassalia coriaceae* Verdc., *Danais fragrans* (Lam.) Pers., *Gaertnera psychotrioides* Baker, *Mussaenda arcuata* Poiret in Lam., *Mussaenda landia* Poiret in Lam., *Paederia foetida* L.] of the Rubiaceae. 7 out of the 27 extracts showed antibacterial properties, five showed antifungal properties while two showed potent smooth muscle relaxation and contractile properties.[21]

Morinda ellipfica, locally known as "mengkudu kecil" is a medicinal plant which is normally used by the Malays in Peninsular Malaysia. Parts of the plant are used to treat various health problems and ailments. Ismail (1999) had carried out phytochemical studies on the roots of this plant that resulted in the isolation of some anthraquinones. The anthraquinones were subjected to a battery of bioactivity testings, which included antimicrobial, antiviral, cytotoxicity and antioxidant assays.[17] The results indicated that some of the compounds possessed interesting biological activities especially in the cytotoxicity and antioxidant assays. Damnacanthal and nordamnacanthal were found to be active against many cell lines tested that may have the potential to be developed as anticancer agents.[22]

Another species of Rubiaceae which also has medicinal uses is *Uncaria tomentosa* or commonly known as Cat's Claw. Traditionally, the bark of this plant is used for inflammatory arthritis and intestinal complaints such as stomach ulcers. The alkaloids present in the bark and roots of *Uncaria tomentosa* have been documented to stimulate the immune system. Studies indicate at least six of these oxindole alkaloids

have the ability to increase immune function by up to 50% in relatively small amounts. This finding has led to its uses around the world as an adjunctive treatment for cancer and AIDS as well as other diseases which has negatively impact the immune system.[23,24]

According to the studies by Singh and Ali (2012), 26 plant species which belong to Rubiaceae family have been explored for their medicinal properties. The medicinal properties of some of the plant species are listed in Table 1.1[25]:

Table 1.1: Medicinal properties of some of the *Rubiaceae* species

Species	Medicinal properties
Borreria articularis Linn. f.	The root of this plant is used to cure stomach pain and regulates excessive discharges during menses, seeds have wormicide property and is used to treat toothache.
Catunaregam nilotica Stapf.	Fruits are used as safest emetic in alternative system of medicine as well as it is used as a remedy for diarrhea and dysentery. The roots are frequently prescribed as paste in headache cases.
Dentella repens Linn.	The leaves are used to treat blood ailments and to purify blood. It is also used to improve the eyesight and is prescribed as a laxative for constipation.
Gardenia gummifera Linn.	The plant as a whole is made into a paste and applied on bone fracture and dislocation as fomentation to reduce pain as well as to enhance the callus formation. In veterinary, the paste of this plant is applied onto the sores of cattle to repel insects. Gum released from stem and bark is frequently used to treat toothache, dyspepsia and to disinfect the septic wounds. The gum is used to protect food grains from insect and mites.
Haldina cordifolia Roxb.	The bark of this plant is used as febrifuge, antiseptic and aphrodisiac. It cures inflammation, skin and blood diseases. The juice of this plant is applied onto sores to kill worms. The basal part of the stem is used as hepato-protective treatment in jaundice and other types of hepatitis. The root is given after menstruation to secure the birth of a male child.
Ixora arborea Roxb.	The roots and fruits are used by the tribals to

	cure micturation and urinary problems of females. The root bark is effective in treating skin diseases and chest pains. The juice of the roots and fruits is acclaimed as a cure for nerve problems. The flowers are pounded in fresh milk and is given to the patients to treat whooping cough. Its areal parts are effective in diabetes management.
Meyna spinosa Roxb.	The decoction of the whole plant is used by tribals to treat vertigo. For tetanus infection, a decoction of the root bark is very effective. The root is made into a paste and applied for painful urination. The powder of the leaf is an effective prescription to kill intestinal worms. It is also prescribed with black pepper to cure diphtheria. The powder of seeds has narcotic effect.
Oldenlandia corymbosa Linn.	Decoction of the plant is given in the treatment of intermittent fever with gastric irritation and nervous depression. The plant is also used for treating jaundice, hepatic diseases and as an anthelmintic. The leaves are made into a paste and applied to cure burning sensation of the soles and palms.
Paederia scandens Lour.	The whole plant is used, mainly the leaves and the tender twigs are used as anti arthritis, anti-spasmodic, astringent, carminative, anti emetic, emollient, expectorant. It is also indicated in asthma, diarrhea, diabetes, gout and seminal weakness. The root ash is used to treat various skin diseases. The leaf is made into a paste and its composition is taken to treat leucorrhoea.
Rubia cordifolia Linn.	The plant has properties like antidysentric, anthelmintic, astringent, carminative, expectorant and is used in cough, hepatic obstructions, indigestion, jaundice, ulcers, fracture, mental agony, obstructions in urinary passage and paralytic affections. The whole plant is used in diabetic treatment. Decoction of the roots is given to relieve cough, cold and respiratory problems especially in infants. The oil extract of the whole plant is used to cure eczema.

1.5 The genus *Nauclea*

The genus *Nauclea* consists of 35 species worldwide[26], of which ten are distributed throughout tropical Africa, Asia, and Australia along with one species in China.[27] The species of *Nauclea* include *N. orientalis*, *N. officinalis*, *N. cadamba*, *N. diderrichii*, *N. robinsonii*, *N. subdita*, *N. pobeguinii*, *N. gilletii*, *N. tenuiflora* and so on.[28]

These plants are usually medium to large sized trees. Its terminal vegetative bud is strongly flattened. Stipules are ovate, or obovate, flattened to strongly keeled, adpressed, deciduous or semi-persistent. Many flowered flowering heads in a groups of 2 to 5. Leaves are opposite, petiolate or blades chartaceous to coriaceous.[29]

1.6 Medicinal uses of *Nauclea* species

The genus *Nauclea* have been reported to be used for various medicinal purposes. For example, in West and South Africa, infusions and decoctions of the stem bark and leaves of *N. latifolia* are traditionally used for the treatment of malaria, stomach aches, fever, diarrhea and nematode infections in human and animals.[30] While in Kano, Nigeria, it is used as a chewing stick and as a remedy against stomach ache and tuberculosis.[31] The Fulani in Mubi use the leaves to de-worm their cattle. On the other hand, infusions and decoctions are used to cure malaria in Ivory Coast.[32]

N. orientalis is also known to have many medicinal uses. Its leaves and bark are used medicinally against abdominal pains, animal bites and wounds.[33] This plants can also act as an anti-pyretic, vulnerary and an anti-diarrhoeic as well as in the treatment of boils, tumors and toothaches.[34]

N. officinalis, a traditional Chinese medicine, has anti-inflammatory effect and widely used for treatment of pink eye, fever, acute jaundice and stomachache in China. Its root, stem and branch are cut into pieces, dried and used for medical purpose.[35,36,37]

N. subdita, is used for the treatment of stomach ache, diabetes, skin problems and blood pressure. Its young leaves are edible and is a source of traditional medicine to treat stomachache.[38]

1.7 *Nauclea officinalis*

N. officinalis (Pierre ex Pitard) Merr. & Chun is a medium to big sized tree up to 30 m and 70 cm girth. The bark is smooth to cracking and shallowly fissured, greyish to reddish brown. Its inner bark is yellow turning brown to orange on exposure. Sapwood is in pale yellow colour while twigs is in drying dark brown colour. Leaves are elliptic to obovate. Flowering heads are in group of 2 to 5, rarely single and each measuring 13 to 15 mm. This species is distributed throughout Malaysia, in lowlands to hill forests and also in swampy places. They also can be found in South China, Indo-China, Sumatra and Borneo.[13]

Figure 1.1: Bark of *N. officinalis*

Figure 1.2: Leaves of *N. officinalis*

1.8 *Nauclea subdita*

N. subdita (Korth.) Steud is a small or medium sized tree up to 25 m in height and 60 cm girth. The bark is smooth to fissured and cracking, sometimes scaly or greyish brown. Its inner bark is yellow to pale brown or pink or reddish and laminated with reddish purple layers. Sapwood is in yellow colour while twigs is in drying white to pale brown colour. Leaves are ovate, elliptic to obovate. This species is distributed throughout Malaysia, in lowlands to hill forests and also in swampy places and frequently along streams and rivers. They can also be found in Northeast India and Malesia.[13]

Figure 1.3: Bark and leaves of *N. subdita*

Figure 1.4: Leaves of *N. subdita*

1.9 Objectives of the study

The objectives of this study are:

1. To isolate chemical constituents from two Malaysian *Nauclea* species; *N. officinalis* and *N. subdita* by using chromatographic methods such as column chromatography (CC), preparative thin layer chromatography (PTLC) as well as high performance liquid chromatography (HPLC).
2. To elucidate the structure of the isolated compounds using spectroscopic methods such as 1D-NMR (^{1}H, ^{13}C and DEPT-135), 2D-NMR (COSY, HMBC, HSQC, NOESY), Ultraviolet (UV), Infrared (IR) and LCMS-IT-TOF analysis.
3. To study the biological activities of the compounds isolated from *N. officinalis* and *N. subdita* including anti-cancer and anti-cholinesterase activities as well molecular docking and enzyme kinetic studies on the potent compounds.

2.1 General

Phytochemical studies on Rubiaceae plants have produced alkaloids and non-alkaloid constituents (e.g. triterpenes, polyphenols, fatty acids). A number of chemical constituents have been isolated from this family especially alkaloids where their biological activities have been investigated and reported by researchers. Indole alkaloids in particular have diverse chemical structures and interesting biological activities. They have been subjected to chemical and biosynthetic studies. In this chapter, the general aspects of the indole alkaloids in terms of their classification and biogenesis will be briefly discussed.

2.2 Alkaloids

The term alkaloid was coined in 1818 by W. Meissner and meant simply as *alkali-like.* The first definition of alkaloids was given by Winterstein and Trier who described them in a broad sense as basic, nitrogen containing compounds of either plant or animal origin.[39]

A definition was given in Meyer's *Konversations-Lexikon* of 1896: "Alkaloids (plant bases) occur characteristically in plants, and are frequently distinguished by their remarkable physiological activities. They contain carbon, hydrogen and nitrogen, and in most cases oxygen as well; in many respects they resemble the alkalis (hence the name)".[40]

According to the IUPAC Gold Book, alkaloids are defined as basic nitrogen containing compounds (mostly heterocyclic) occurring mostly in the plant kingdom (but not excluding those of animal origin). Amino acids, peptides, proteins, nucleotides, nucleic acids, amino sugars and antibiotics are not normally regarded as alkaloids. By extension, certain neutral compounds biogenetically related to basic alkaloids are included[41].

The alkaloids are majorly distributed among flowering plants which are the angiosperms. There have been an increase in the discovery of their occurrence in animals, marine organisms, insects, fungi, algae and simple vascular plants over the recent years.[42,43] For example, Cai et al. (2010) had isolated two new indole alkaloids named as arsindoline A **8** and arsindoline B **9** from the marine-derived bacterium *Aeromonas* sp. CB101. In addition, Martínez-Luis, Gómez, Spadafora, Guzmán and Gutiérrez (2012) were able to isolate anti-trypanosomal alkaloids which were 3-hydroxyacetylindole **10**, *N*-acetyl-β-oxotryptamine **11** and 3-formylindole **12** from the marine bacterium, *Bacillus pumilus*.

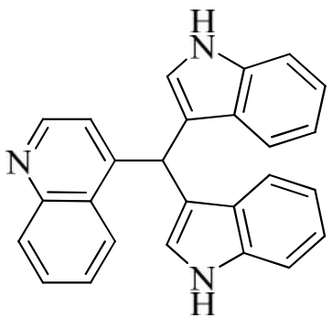

8

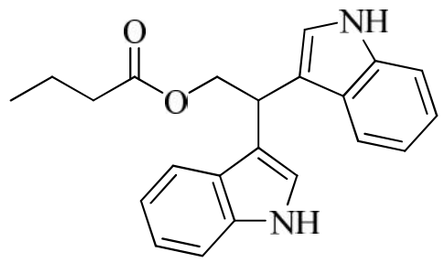

9

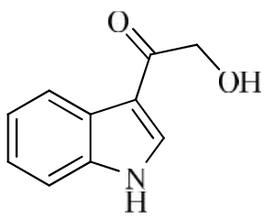

10

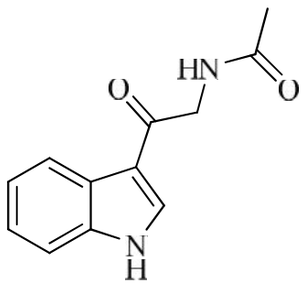

11

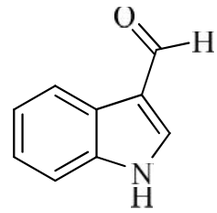

12

Known Alkaloids from marine-derived bacterium

2.3 Classification of alkaloids

Alkaloids can be classified according to biosynthetic, chemical, pharmacological and taxonomic classification.[46] Hegnauer (1963) distinguished 'true alkaloids' from other nitrogen-containing metabolites on the basis of their origin from amino acids.[47] He grouped the alkaloids into three types; true alkaloids, proto alkaloids and pseudo alkaloids. The explanation for these three types of alkaloids are given below.[43]

I. True alkaloids

The true alkaloids are compounds containing nitrogen in a heterocyclic ring and originate from amino acids. They are almost invariably basic. They are usually found as a salt of an organic acid in a plant. Examples are nicotine **13** and atropine **14**. There are however some exceptions to the types of alkaloids. For example, eventhough aristolochic acid **15** has no heterocyclic ring in its structure while coniine[48] **16** is not derived from an amino acid, yet they still belong to this group of alkaloids.

II. Proto alkaloids

The proto alkaloids are compounds which are derived from amino acids but the amino acid nitrogen is not in a heterocyclic ring. They are basic. Their characteristic examples are mescaline **17** and *N*-*N*-dimethyltryptamine **18**.

III. Pseudo alkaloids

The pseudo alkaloids are compounds containing nitrogen in a heterocyclic ring but they are not derived from amino acids. Their characteristic examples are conessine **19** (steroidal alkaloids) and theobromine **20** (purines).[49]

2.4 Pharmacological activities of alkaloids

Alkaloids are one of the important naturally occurring phytoconstituents. Nowadays, many alkaloids from natural sources are commonly used as drug and a number of alkaloidal drugs are still under clinical trial stages.

There are many well known alkaloids with pharmacological activities. For example, physostigmine **21** from *Physostigma venenosum* is used as synthetic parasympatholytic agents, cocaine **22** from *Erythroxylon coca* as local anesthetics and morphine **23** from *P. somniferum* as analgesics.[50]

Another example is berberine **24** from the roots and stem-bark of *Berberis* species; *B.aristata*, *B. petiolaris*, *B.vulgaris*, *B. aquifolium*, *B. thunbergii* and *B. asiatica*. [51,52,53] Berberine **24** has anti-proliferative, anti-migratory and anti-mircobial activities.[54] Other examples of alkaloids with their pharmacological activities are listed in Table 2.1.

Table 2.1: Pharmacological activities of some alkaloids[43]

Alkaloids	Source	Pharmacological acitivities
Ajmalicine 25	*Catharanthus roseus*	Hypotensive
Camptothecine 26	*Camptotheca acuminata*	Anti-cancer
Ephedrine 27	*Ephedra fragilis*	Spasmolytic
Quinidine 28	*Remijia sp.*	Cardiac depressant
Quinine 29	*Cinchona sp.*	Anti-malaria
Strychnine 30	*Strychnos nux vomica*	CNS depressant
Codeine 31	*Papaver somniferum*	Pain killer

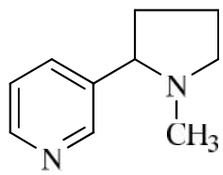

13

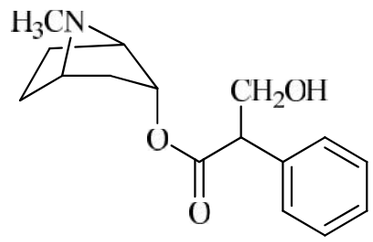

14

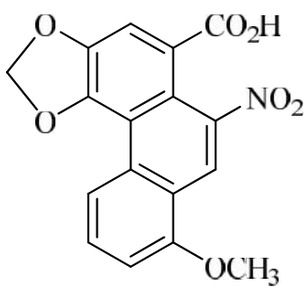

15

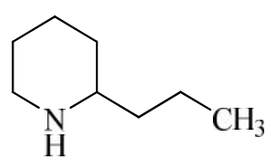

16

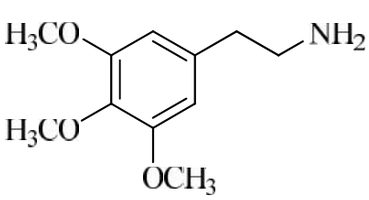

17

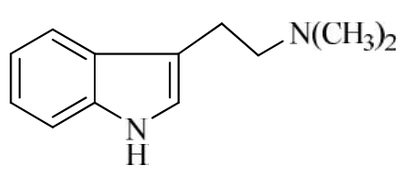

18

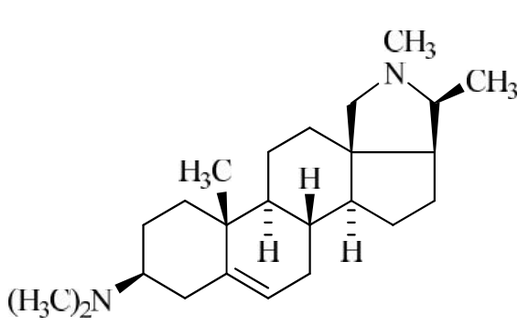

19

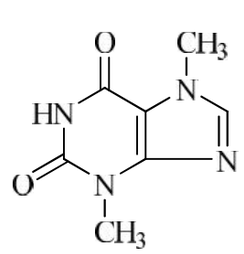

20

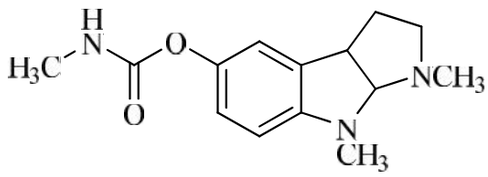

21

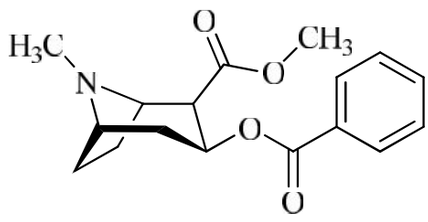

21

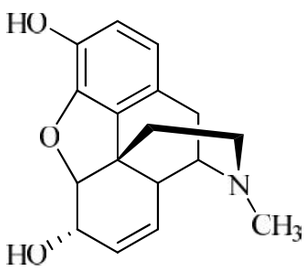

23

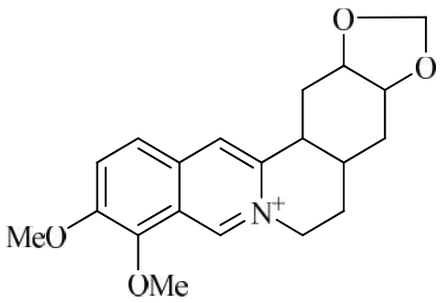

24

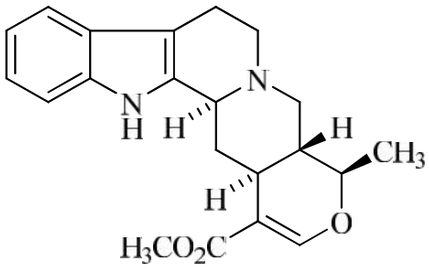

25

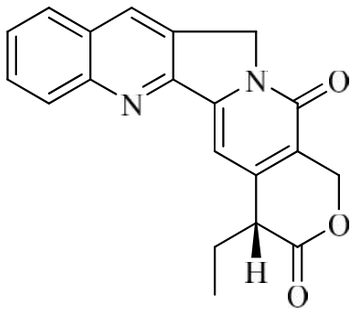

26

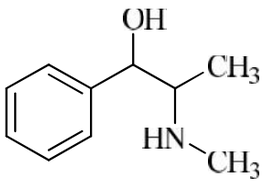

27

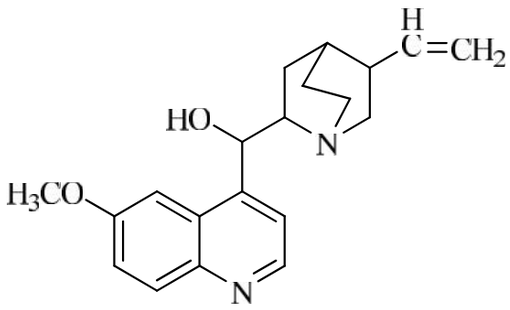

28

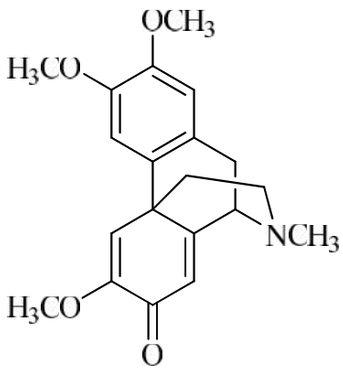

29

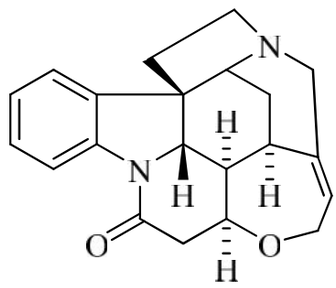

30

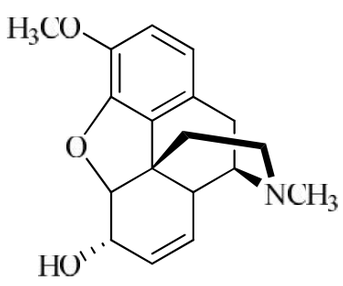

31

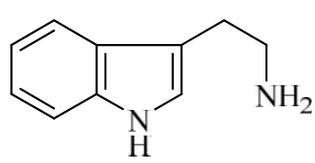

32

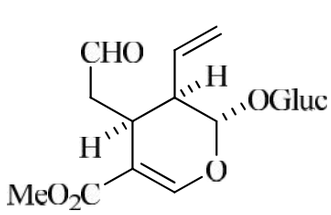

33

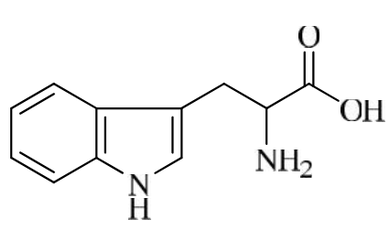

34

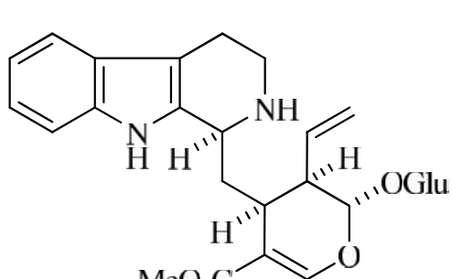

35

2.5 Indole Alkaloids

Accroding to Atta-Ur-Rahman and Basha (1982), all indole alkaloids can be classified into five classes; class I, class II, class III, class IV and class V, based on the skeleton of the non-tryptophan unit. Indole alkaloids, C_6C_2N are derived from tryptamine **32** (tryptophan **34**) and the iridoid, secologanin **33**[43] to give the intermediate of corynanthe indole, strictosidine **35**. Class I indole alkaloids are derived from secologanin **33**. Skeletal rearrangement will occur after the condensation of secologanin **33** with tryptophan **34**. Bond cleavage (oxidative cleavage) and the joining of a new bond of the class I skeleton will result in the formation of the class II (Aspidosperma) and class III (Iboga) indoles (Scheme 2.1).[55,56] Class I indoles consist of corynanthe, yohimbe and strychnos types where the yohimbe and strychnos types can be formed through cleavage at a certain bond and the formation of a new bond, respectively (Scheme 2.2).[57]

The secologanin skeleton system is no longer in its original form for class II indole alkaloids. Bond cleavage between C-3 and C-4 has occurred and a new bond between C-2,6 and C-4 has formed (Scheme 2.1). The third class of indole alkaloid, class III, is formed through the same C-C bond cleavage as class II but the formation of a new bond is between C-2,6 and C-5 instead (Scheme 2.1). The class IV indole alkaloids consist of non-trytophan indole alkaloids, non-isoprenoid tryptophan alkaloids and fungal (ergot) indole alkaloids while the class V indole alkaloids consist of binary indole alkaloids. Example of indole alkaloids of the five different classes of skeletons are shown in Table 2.2.[55]

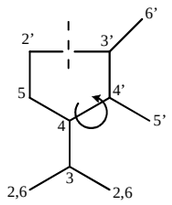

loganin

Skeletal rearragement
after condensation with
tryptophan

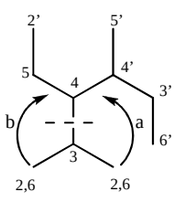

Class I skeleton (*Corynanthe, Yohimbe, Strychnos*)

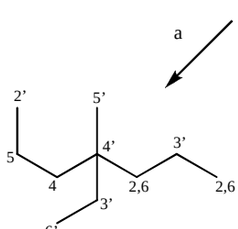

Class II skeleton
(*Aspidosperma*)

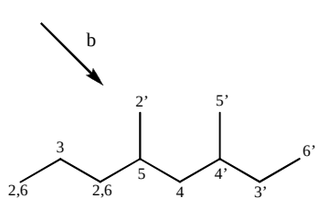

Class III skeleton
(*Iboga*)

Scheme 2.1: Three major skeletal of indole alkaloids from loganin[55,58]

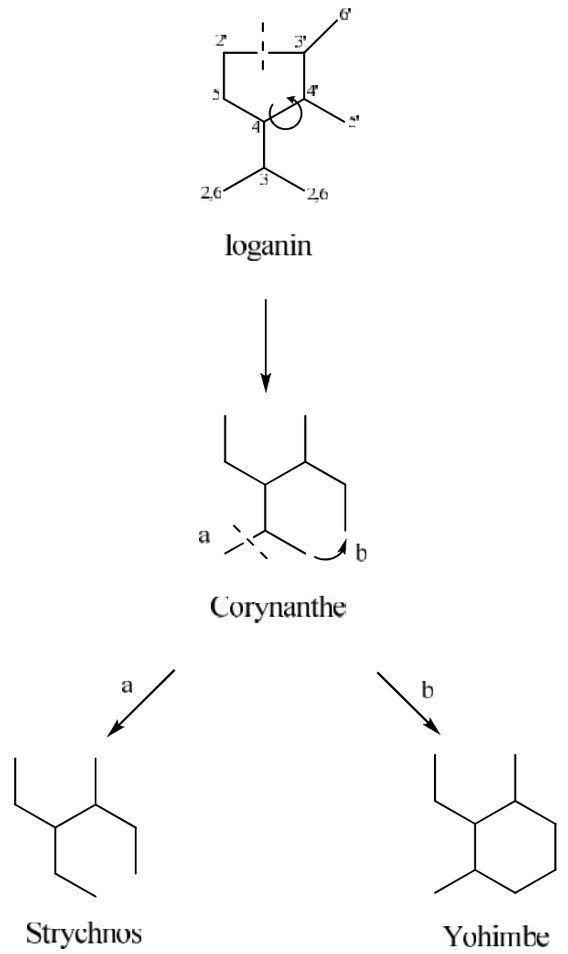

Scheme 2.2: Various skeletal types of indole alkaloids from rearrangement of corynanthe type (Class I)[55]

Table 2.2: Biogenetic Classification of Indole Alkaloids[55]

<table>
<tr><td colspan="2">Class I Alkaloids
 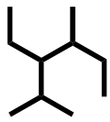 </td></tr>
<tr><td>Vincoside group
 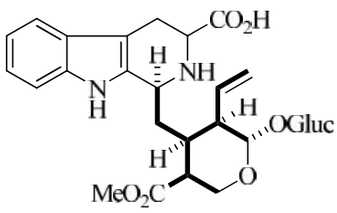
5α-carboxystrictosidine</td><td>Cadambine group
 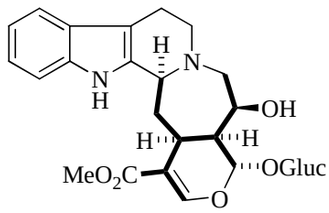
3α-dihydrocadambine</td></tr>
<tr><td>Strictosamide group
 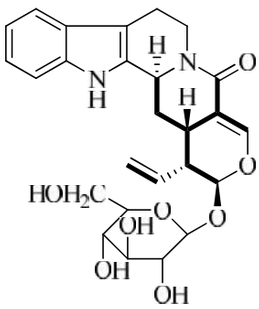
Strictosamide</td><td>Cadamine group
 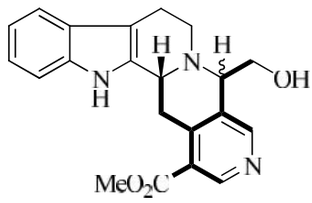
Cadamine</td></tr>
<tr><td>Corynantheine group
 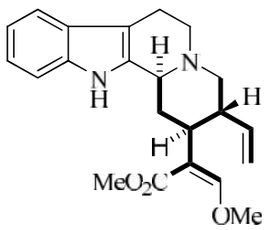
Corynantheine</td><td>Yohimbine group
 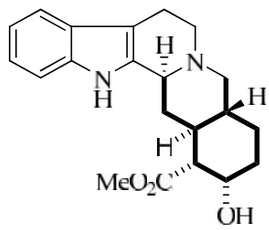
Yohimbine</td></tr>
</table>

Class II Alkaloids

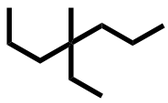

Aspidospermine group	Apodine group
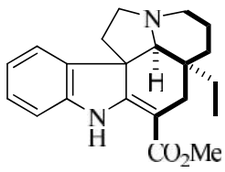	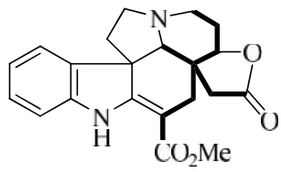
Vincadifformine	Apodine
Vincatine group	**Kopsone group**
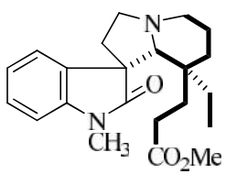	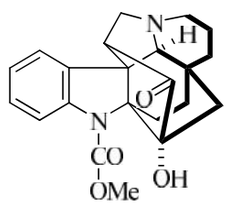
Vincatine	Kopsine
Schizozygine group	**Cuanzine group**
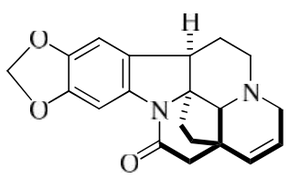	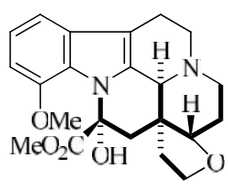
Schizozygine	Cuanzine

Class III Alkaloids

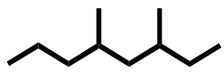

Catharanthine group	Pandoline group
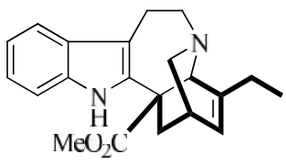	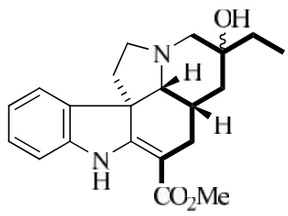
Catharanthine	Pandoline

Class IV Alkaloids (not derived from secologanin)

-Non-trytophan indole alkaloids

Murrayanine group	Girinimbine group
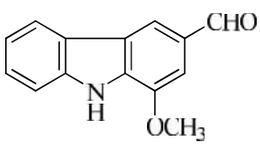	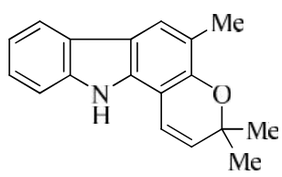
Murrayanine	Girinimbine
Murrayazolidine group	**Mahanimbidine**
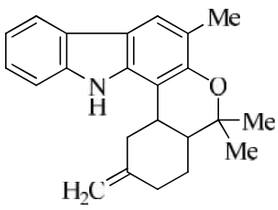	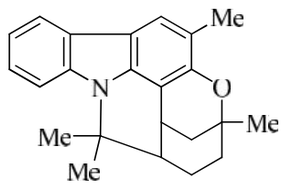
Murrayazolidine	Mahanimbidine

Subincanine group 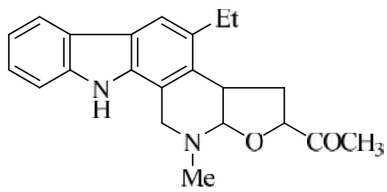 Subincanine	Couroupitine A group 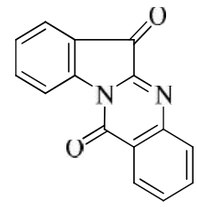 Couroupitine A
-Non-isoprenoid tryptophan alkaloids	
Tryptophan group 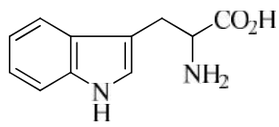 Tryptophan	Harmaline group 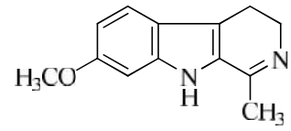 Harmaline
Indolopyridine 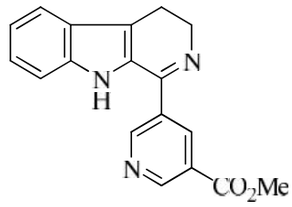 Indolopyridine ‘A’	Naufoline group 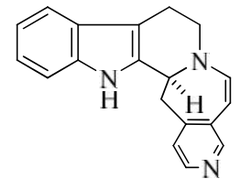 Naufoline
Nauclefine group 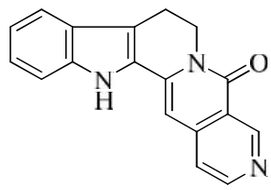 Nauclefine	Naulafine group 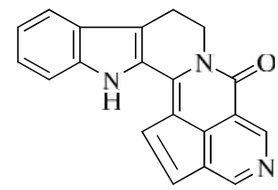 Nauclafine

-Isoprenoid tryptophan alkaloids (fungal indole alkaloids)

Agroclavine group

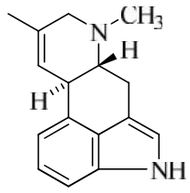

Agroclavine

Neoechinuline group

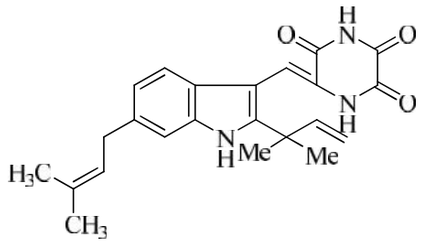

Neoechinuline

Alysinopsin group

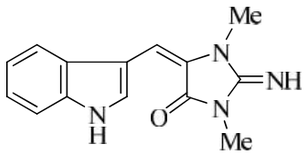

Alysinopsin

Olivacine group

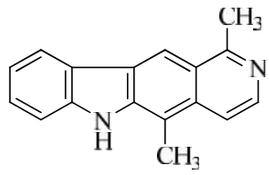

Olivacine

Akaferine group

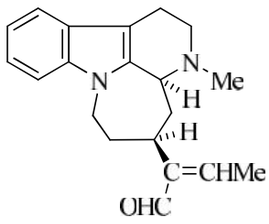

Akaferine

Aristoteline group

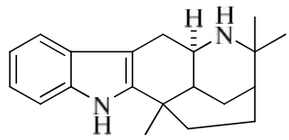

Aristoteline

Class V Alkaloids (binary indole alkaloids)

I-I group

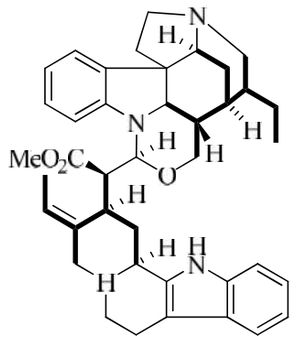

Geissospermine

I-III group

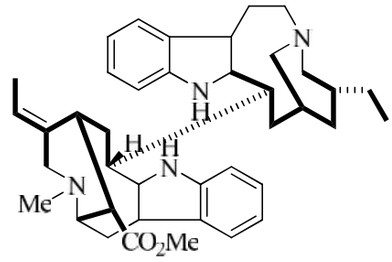

Dehydroxycopuvosine

I-III group

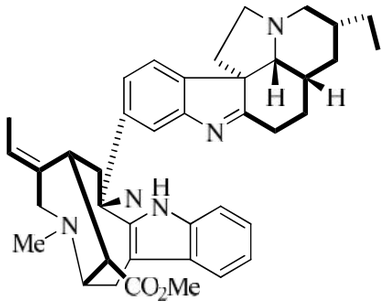

Capuvosidine

II-II group

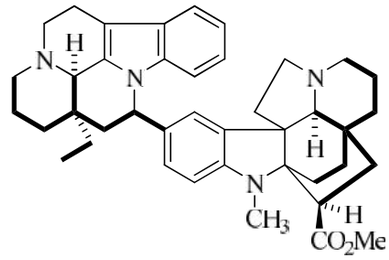

Pleiomutine

II-III group

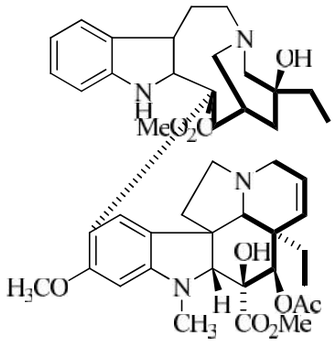

Vinblastine

III-III group

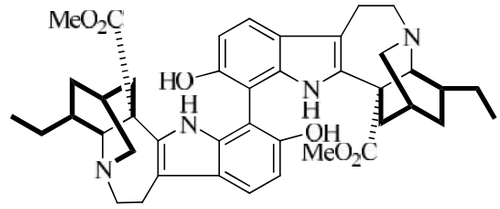

Bis-12-[11-hydroxycoronaridyl]

2.5.1 Biosynthesis of indole alkaloid

The aromatic part of the indole alkaloids is derived from the decarboxylation of tryptophan **34** to form tryptamine **32**. This idea was suggested by Perkin and Robinson (1919) and proved by Battersby, Burnett and Parsons (1969). The basic unit of indole alkaloids is derived from the Mannich condensation of tryptamine **32** with an aliphatic aldehyde (bearing nine or ten carbons) at the α or β-position of the indole nucleus to form a Schiff base **36**.[61] Intramolecular attack to the imine carbon (*) through the β carbon resulted in the formation of the indolenines **37** which then followed by a rearrangement to form a six membered ring intermediate **38.** Consecutive loss of H^+ will give the corresponding β carboline skeleton (Scheme 2.3).[55]

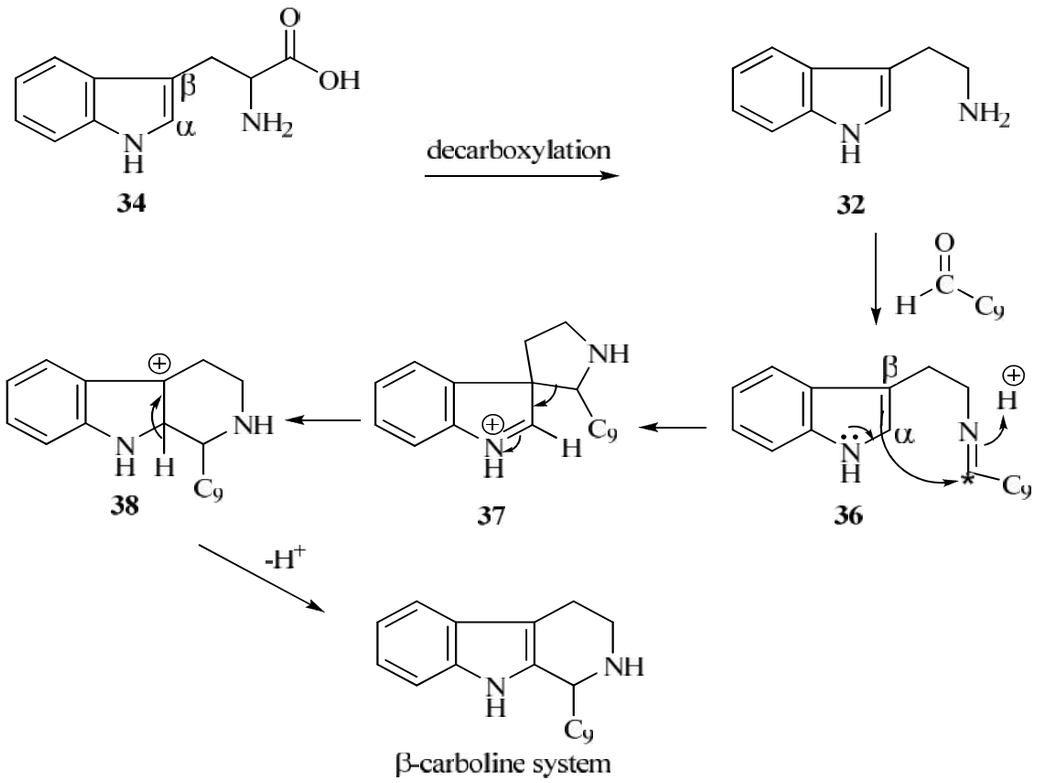

Scheme 2.3: Biosysnthetic pathway of basic structure of indole alkaloids

Aldehyde cannot undergo a condensation reaction directly with the α-position of the indole nucleus to form the β-carboline systems. This is shown through an examination of reaction mechanisms where such a direct attack would generate an intermediate **40** with a disturbed π electron cloud on the benzene ring and this kind of intermediate would be energically unfavorable. To avoid the formation of this intermediate, indolenine could have been formed by a β condensation to give a more stable intermediate **39** first followed by the migration of R_2 to the α-position (Scheme 2.4).[55] Such pathway has been proved by Jackson and Smith (1967) with experiments.

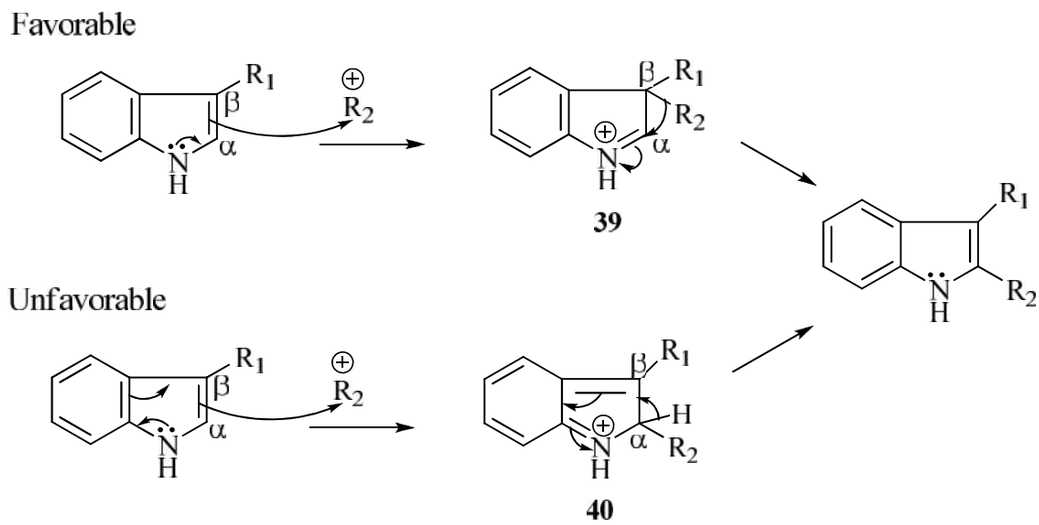

Scheme 2.4: Formation of indolenine with favourable and unfavourable pathways

2.5.2 Biogenesis of corynanthe and yohimbe indoles

Tryptamine **32** and secologanin **33** are the precursors for the biosynthesis of monoterpenoid indole alkaloids of classes I, II, III and V[63,64,65,66]. Strictosidine **35** could be formed from the condensation of both the precursors **32** and **33** in the presence of strictosidine synthase followed by the Pictet-Spengler reaction.[67] Hence, strictosidine **36** is the important key intermediate for the biosynthesis of pyridino-indolo-

quinolizidinone alkaloids (corynanthe type of indoles)[68,69] such as angustine **42** and yohimbe type of indoles such as yohimbine **52**. For corynanthe type of indoles, strictosidine **35** is transformed into strictosidine lactam **41** then followed by the formation of angustine **42**, angsutoline **43** and angustidine **44**. Most probably the nitrogen in the ring E (third nitrogen) could be come from the action of ammonia or amino acid on a glucosidic precursor[49] (Scheme 2.5). On the other hand, strictosidine **35** is hydrolyzed by β-glucosidase to form a reactive hemiacetal intermediate of **45** and followed by the opening of the lactol ring to form a dialdehyde intermediate of **46**. The aldehyde group formed in **46** reacts with a secondary amine of a strictosidine framework to produce 4,21-dehydrocorynantheine aldehyde **47**. The enol **48** or keto **49** form of dehydrogeissoschizine can be produced through allylic isomerization and enolization of **47**. Delocalization of electrons of the keto form of dehydrogeissoschizine **49** forms **50** where the aldehyde in turn attacks dienamine at the γ-position to yield α-yohimbine **51**. Hydrogenation of α-yohimbine **51** lead to formation of yohimbine **52** (Scheme 2.5).

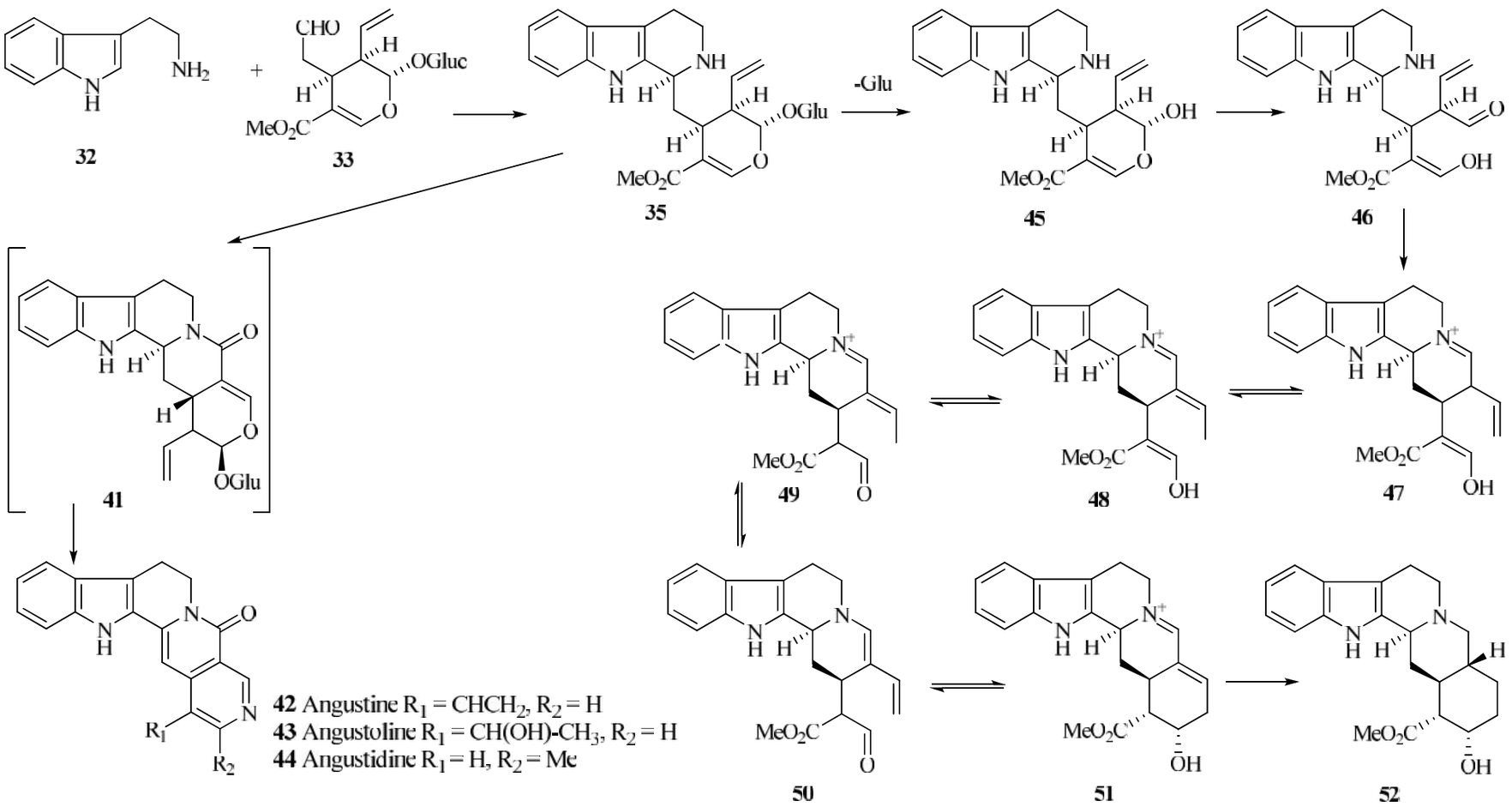

Scheme 2.5: Proposed biosynthetic pathway of angustine **42**, angustoline **43**, angustidine **44**[67,70] and yohimbine **52**[43,71]

In addition, Brown and co-workers has shown the biosynthesis of 18-19-dihydroangustine **55** (Scheme 2.6). This indole alkaloid can be formed through initial hydrolysis of 18,19-dihydrovincosamide **53** with a β-glucosidase enzyme followed by the condensation with ammonia which resulted in the formation of carbinolamine **54**. It will then be transformed to 18-19-dihydroangustine **55** through oxidation using TFA as the oxidising agent.

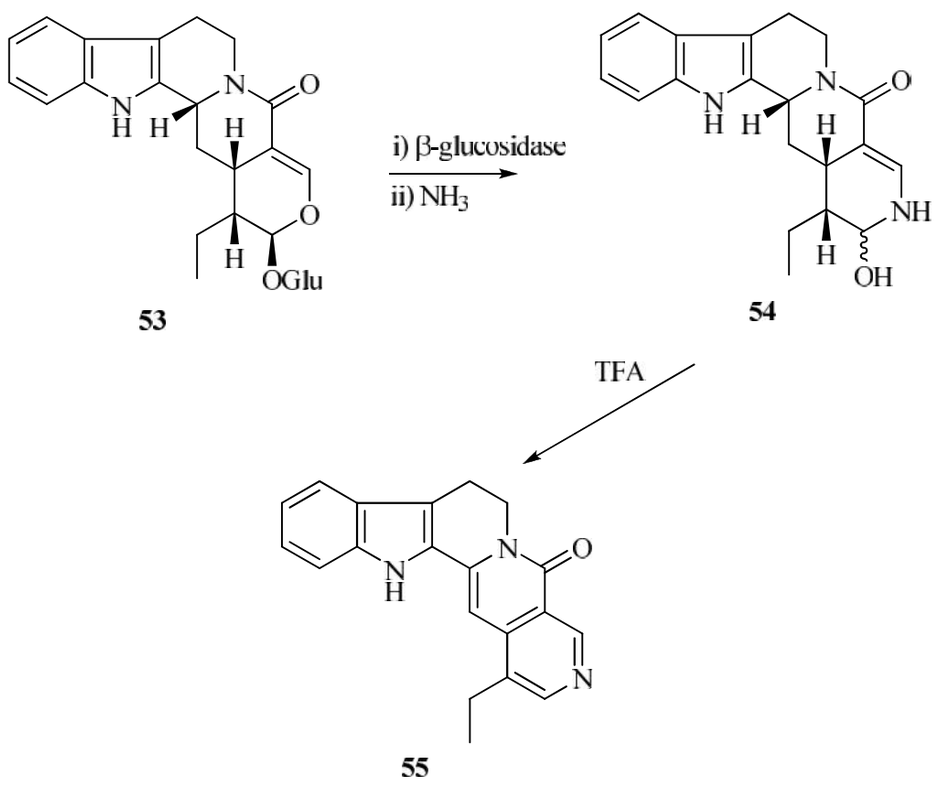

53 **54** **55**

Scheme 2.6: Biosynthetic pathway of 18-19-dihydroangustine **55**[43]

3.1 General

Bark and leaves of *N. officinalis* and *N. subdita* which belong to Rubiaceae family were studied in detail for their alkaloidal contents and other chemical constituents. The extraction and isolation procedures of the chemical constituents from these two species are described in chapter 6. The structures of all isolated compounds were elucidated with various spectroscopic methods such as 1D-NMR (^{1}H, ^{13}C, DEPT), 2D-NMR (COSY, HSQC, HMBC, NOESY), IR, UV, LCMS-IT-TOF and also by comparison with literature data.

3.2 Isolation and structural elucidation of chemical constituents from bark and leaves of *N. officinalis* (Madek), *N. officinalis* (Mersing) and *N. subdita*

Two sets of samples of *N. officinalis* were studied. They were collected from two different locations; Hutan Simpan Madek, Keluang, Johor and Hutan Simpan Mersing, Johor. Isolation and structural elucidation of chemical constituents from the bark of *N. officinalis* from both sites yieled one new compound and twelve known compounds. The new compound isolated was identified as naucline **56** while the known compounds were stigmast-4-en-3-one **57**, vanillin **58**, cinnamide **59**, 1,2,3,4-tetrahydro-1-oxo-β-carboline **60**, naucletine **61**, angustidine **44**, benzamide **62**, angustine **42**, nauclefine **63**, angustoline **43**, naucleficine **64** and naucleactonin C **65**. Besides, the leaves of *N. offcinalis* yieled seven known compounds; angustine **42**, blumenol A **66**, harmane **67**, 3,14-dihydroangustoline **68**, pumiloside **69** and strictosamide **70** and blumenol B **71.**

Furthermore, isolation and structural elucidation of chemical constituents from the bark of *N. subdita* yielded one new compound; subditine **72** and eleven known compounds; stigmast-4-en-3-one **57**, β-sitosterol **73**, naucleactonin C **65**, benzamide **62**, cinnamide **59**, 1,2,3,4-tetrahydro-1-oxo-β-carboline **60**, angustine **42**, angustidine **44**,

nauclefine **63**, harmane **67** and angustoline **43**. In addition, two compounds; angustine **42** and harmane **67** were isolated from the leaves of *N. subdita*. The compounds isolated from these three samples are summarized in Table 3.1

Table 3.1: Summarization of compounds isolated from the three samples

No.	Compounds
1	Naucline **56**
2	Nauclefine **63**
3	Naucletine **61**
4	Angustine **42**
5	Angustoline **43**
6	3,14-dihydroangustoline **68**
7	Angustidine **44**
8	Subditine **72**
9	Strictosamide **70**
10	Pumiloside **69**
11	Naucleficine **64**
12	Naucleactonin C **65**
13	Harmane **67**
14	1,2,3,4-tetrahydro-1-oxo-β-carboline **60**
15	Benzamide **62**
16	Cinnamide **59**
17	Blumenol B **71**
18	Blumenol A **66**
19	β-sitosterol **73**
20	Stigmast-4-en-3-one **57**
21	Vanillin **58**

3.2.1 Naucline 56

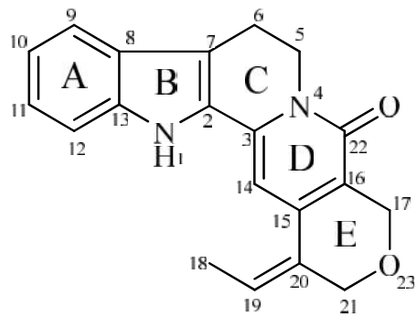

56

Naucline **56** was isolated as a brownish amorphous solid. The LCMS-IT-TOF spectrum (Figure 3.2) revealed a pseudomolecular ion peak $[M+H]^+$ at *m/z* 319.1450, corresponding to the molecular formula of $C_{20}H_{18}N_2O_2$. UV spectrum of naucline **56** showed strong absorptions at 391, 374 and 214 nm. In the IR spectrum, an absorption band due to a conjugated lactam carbonyl stretching vibration was observed at 1638 cm^{-1}.[72,73,74]

In the ^{1}H-NMR spectrum (Figure 3.3), the presence of four aromatic protons, a broad peak of N-H and one -CH_2-CH_2-N- group were observed, suggesting a tetrahydro-*β*-carboline skeleton.[75] Two of the four aromatic protons in ring A appeared as doublets at δ_H 7.48 and 7.33 attributable to H-9 (1H, *d*, J = 7.8 Hz) and H-12 (1H, *d*, J = 8.2 Hz) respectively. The other as two protons, H-10 (1H, *dd*, *J* = 7.8, 7.3 Hz) and H-11 (1H, *dd*, *J* = 7.3, 8.2 Hz), resonated at δ_H 7.10 and 7.21 as doublet of doublets (*dd*). H-14 of ring D appeared as a singlet at δ_H 6.32 indicating that a double bond could be formed between C-15 and C-16. In addition, the presence of downfield quartet at δ_H 5.76 (1H, *q*, *J* = 6.6 Hz, H-19) coupled with an upfield doublet at δ_H 1.46 (3H, *d*, *J* = 6.6 Hz, H_3-18) indicated the existence of a trisubstituted olefin group.

The ^{13}C-NMR and DEPT spectra (Figure 3.4 and Figure 3.5) of naucline **56** indicated a total of twenty carbon signals; one methyl, one carbonyl, four methylenes,

six methines and eight quaternary carbons. The presence of a carbonyl carbon was observed at δ_C 163.1 (C-22). The signals at δ_C 58.9 and 66.6 could be assigned to the resonances of two oxymethylenes, C-17 and C-21 respectively. HMBC correlations were observed between H_3-18 and C-19 (δ_C 125.9), H_3-18 and C-20 (δ_C 148.0), H-19 (δ_H 5.76) and C-20, H-19 and C-21, established the connectivity of trisubstituted olefin group to the pyran ring (ring E) through C-20. (Figure 3.1). The COSY spectrum (Figure 3.6) showed correlation peaks between H_2-5/H_2-6 and H_3-18/H-19 respectively.

Complete ^{1}H- and ^{13}C-NMR assignments (Table 3.2) of naucline **56** was accomplished through analysis of COSY, HMQC, HMBC and NOESY data. Thorough analysis of all spectral data led to the conclusion that naucline **56** is a new corynanthe indole alkaloid. Biogenesis pathway for naucline **56** was shown in Scheme 3.1.

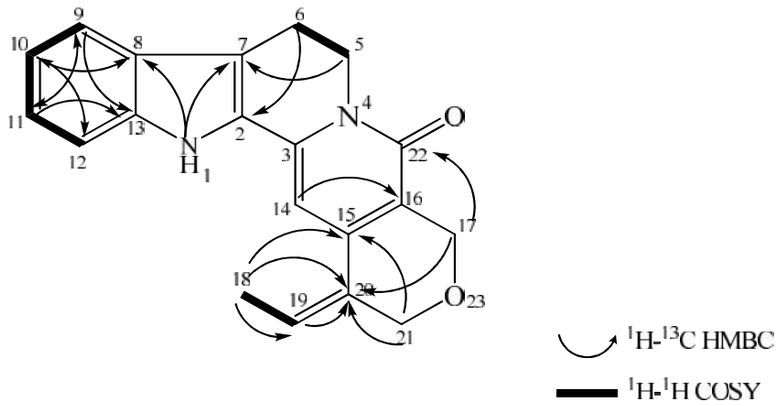

Figure 3.1: Selected COSY and HMBC Correlations for Naucline **56**.

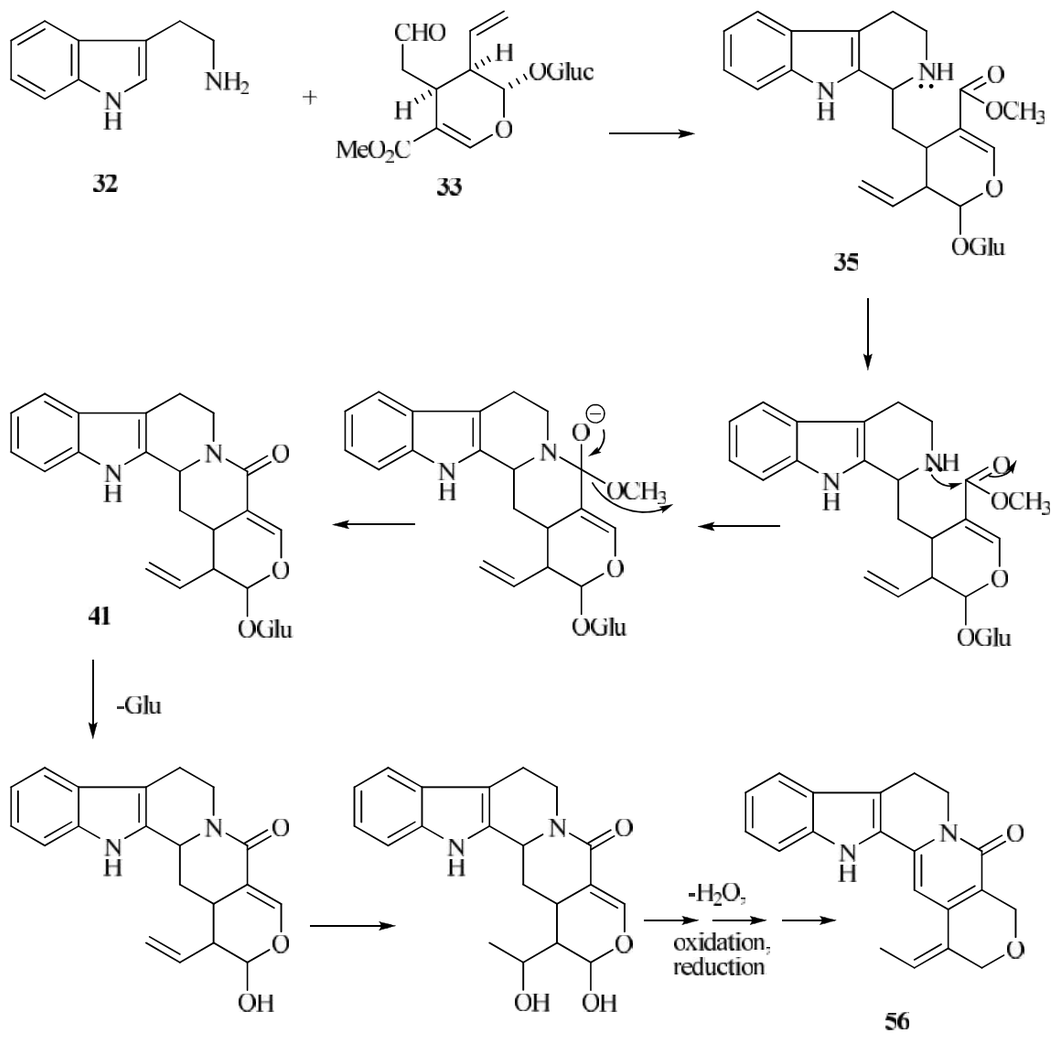

Scheme 3.1: Proposed biogenesis pathway for naucline **56**.

Table 3.2: ^{1}H-NMR (400 MHz) and ^{13}C-NMR (100 MHz) Spectral Data of Naucline **56** in $CDCl_3$.

Position	**^{1}H, δ_H (multiplicity, *J* in Hz)**	**^{13}C (δ_C)**
NH-1	9.72 (s)	-
2	-	127.4
3	-	137.9
5a	3.99-4.04 (*m*)	40.7
5b	4.58-4.61 (*m*)	
6	2.92-2.98 (*m*)	19.5
7	-	114.4
8	-	125.6
9	7.48 (*d*, 7.8)	119.5
10	7.10 (*dd*, 7.8, 7.3)	120.5
11	7.21 (*dd*, 7.3, 8.2)	124.7
12	7.33 (*d*, 8.2)	111.9
13	-	138.5
14	6.32 (*s*)	102.0
15	-	136.6
16	-	125.7
17a	4.36 (*br d*, 12.1)	58.9
17b	4.65 (*br d*, 12.1)	
18	1.46 (*d*, 6.6)	14.6
19	5.76 (*q*, 6.6)	125.9
20	-	148.0
21a	4.18 (*br d*, 11.9)	66.6
21b	4.20 (*br d*, 11.9)	
22	-	163.1

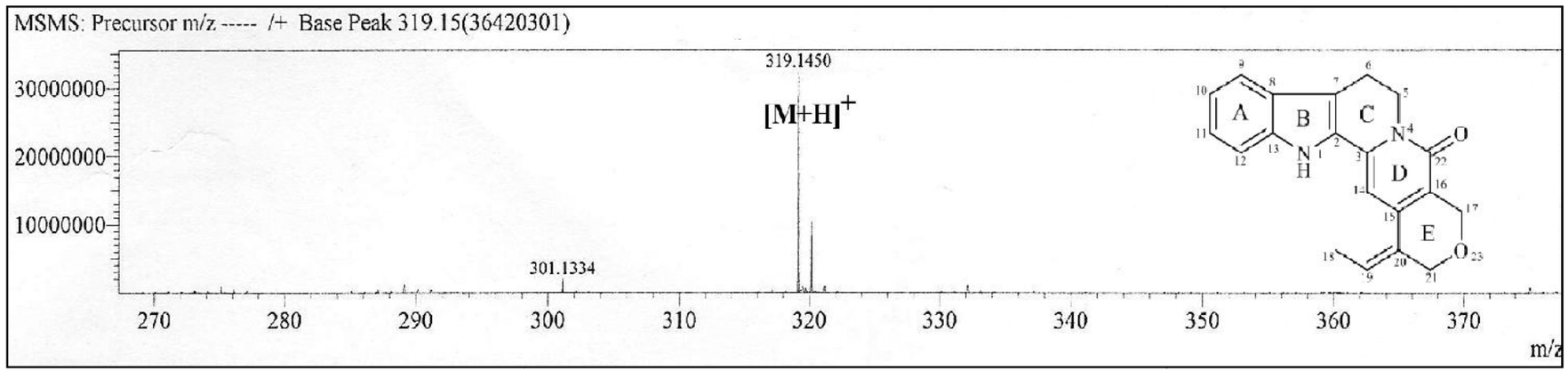

Figure 3.2: LCMS Spectrum of Naucline **56**

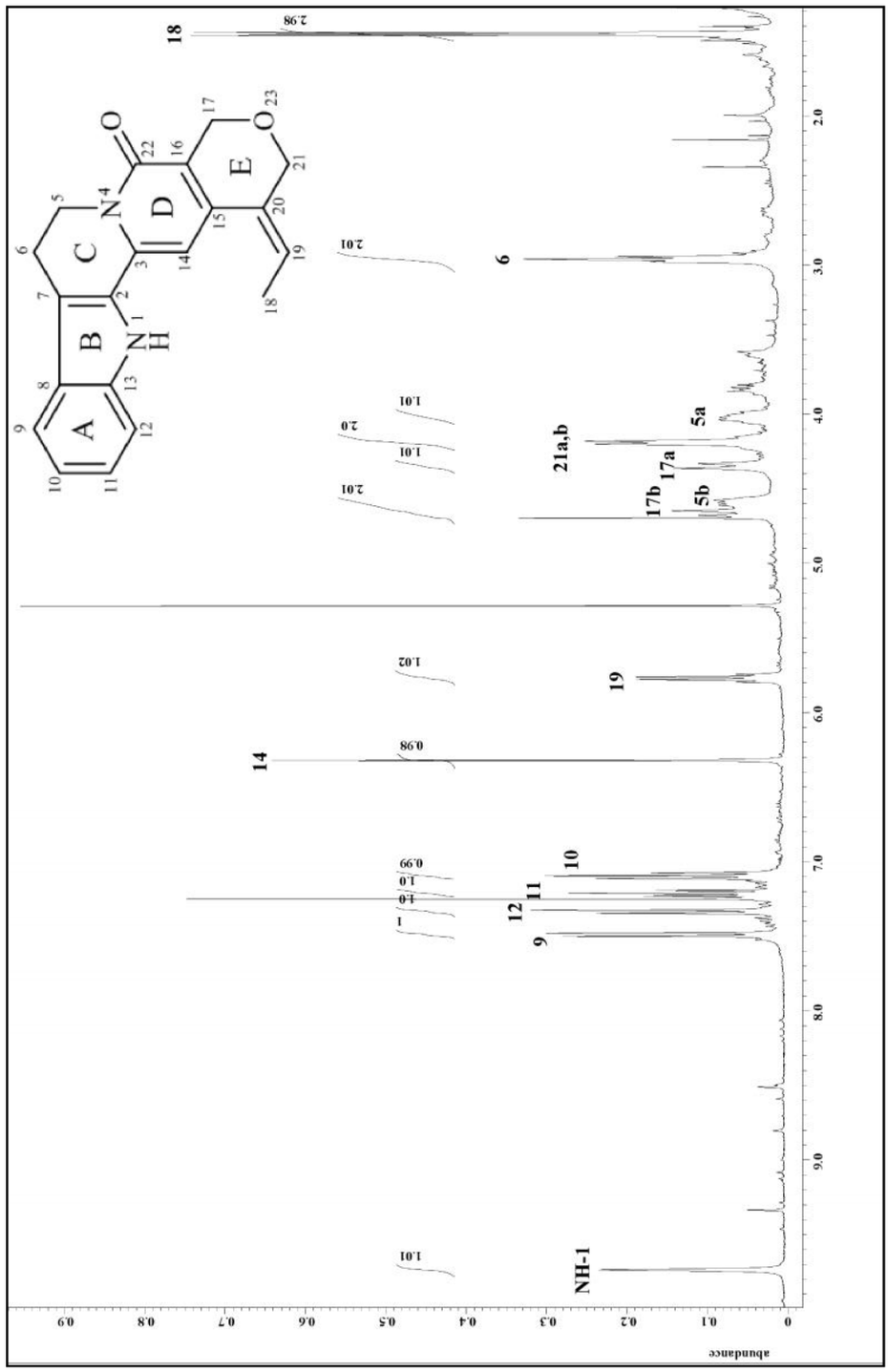

Figure 3.3: ^{1}H NMR Spectrum of Naucline **56**

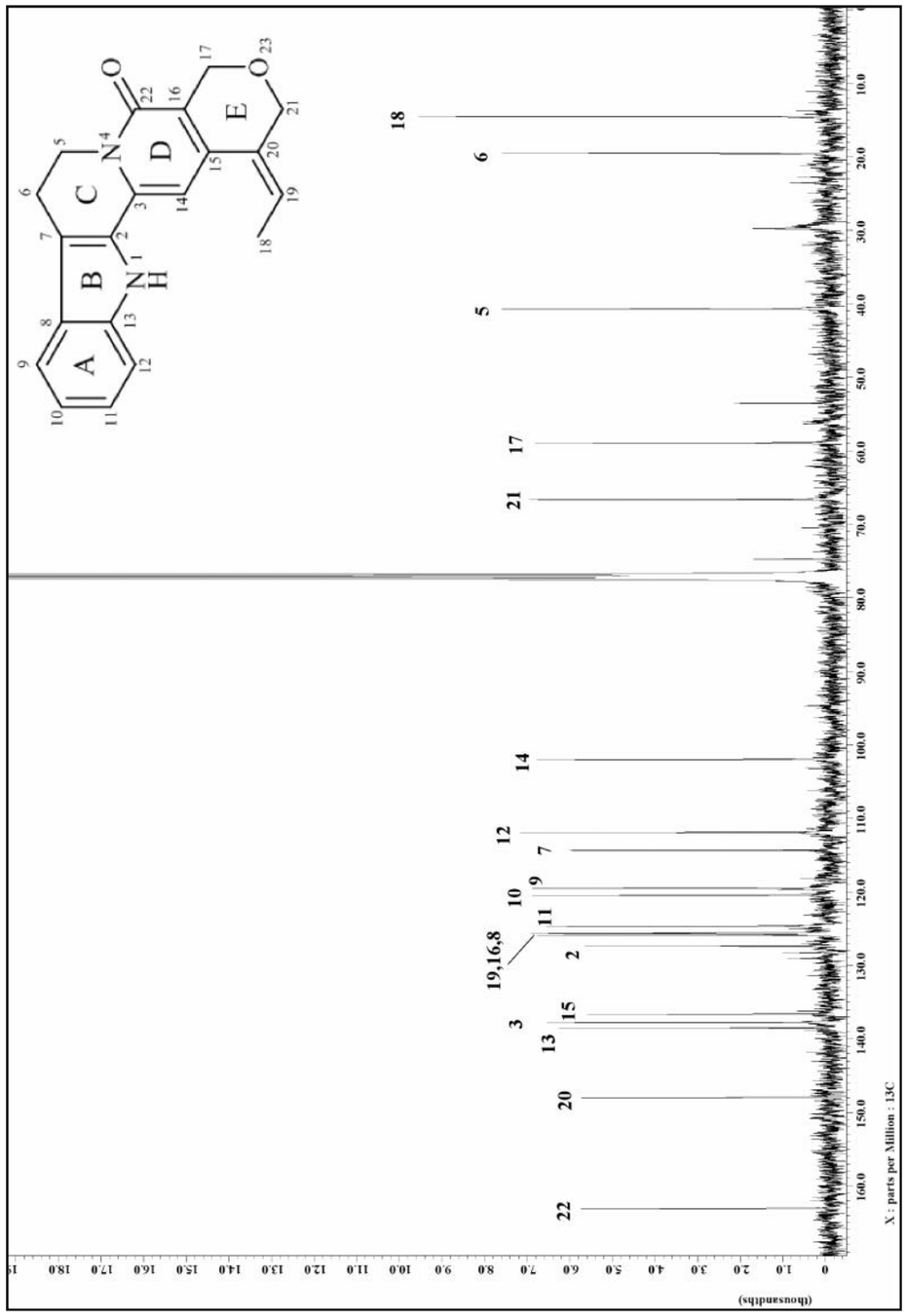

Figure 3.4: ^{13}C NMR Spectrum of Naucline **56**

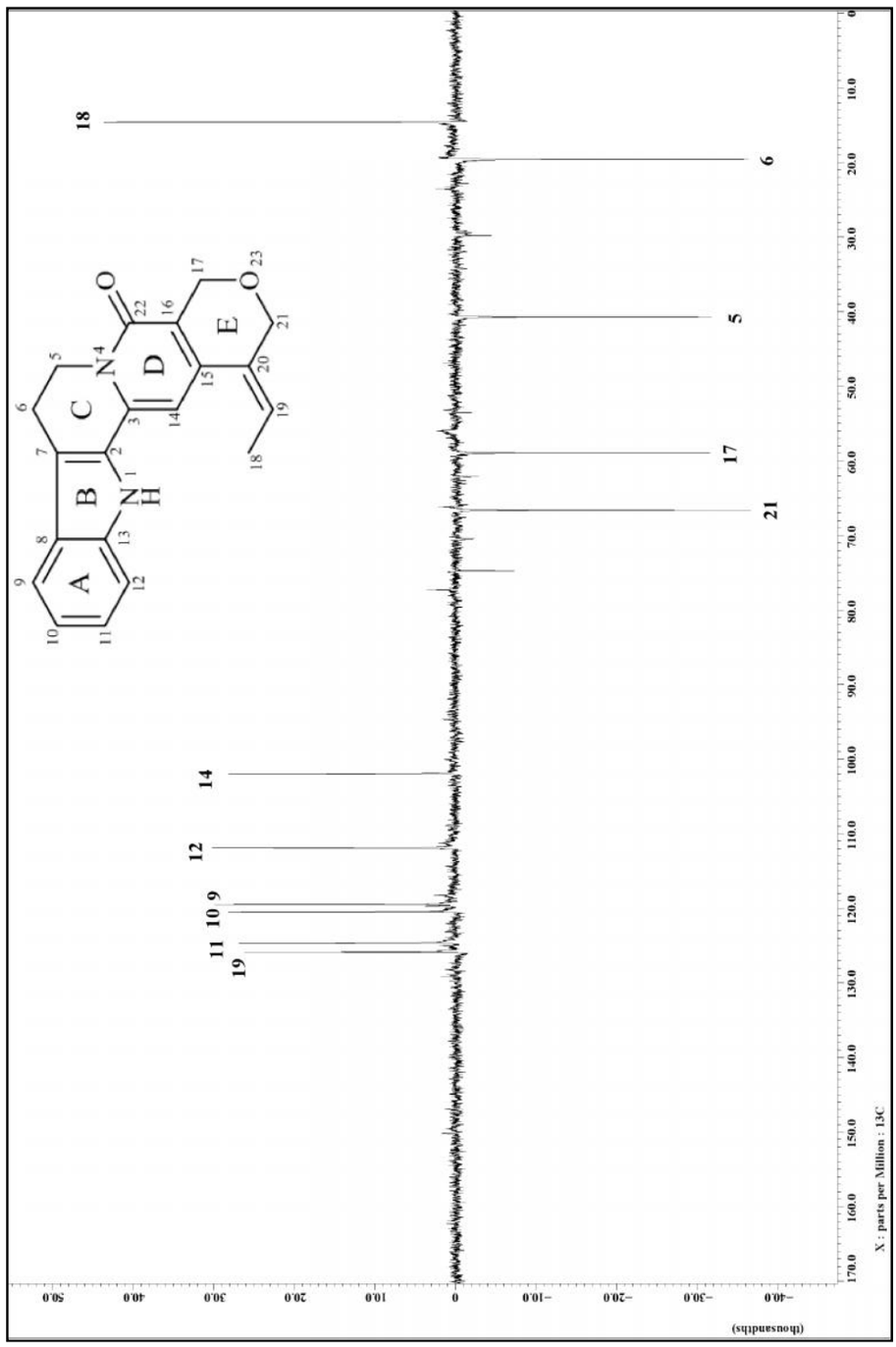

Figure 3.5: DEPT 135 Spectrum of Naucline **56**

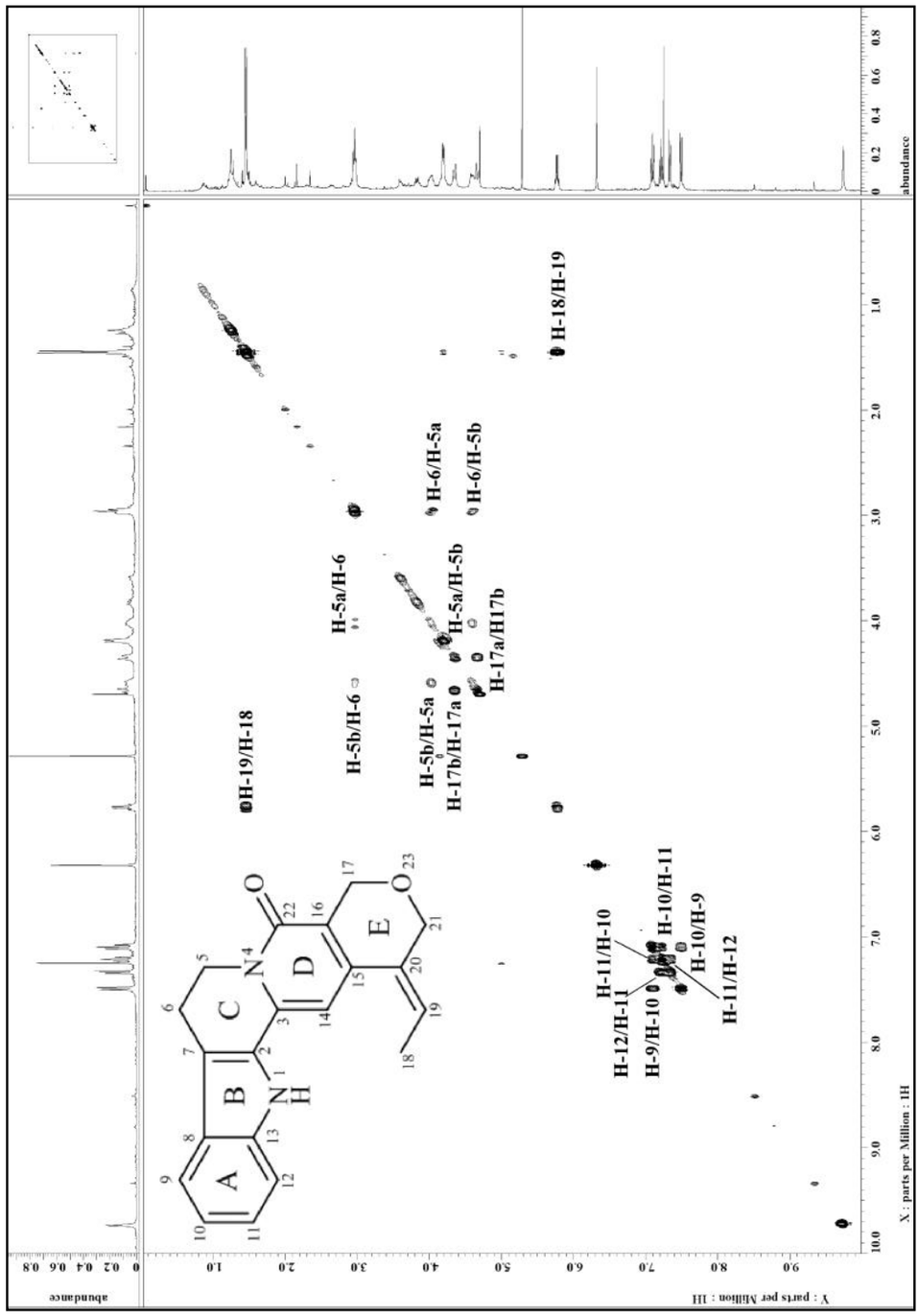

Figure 3.6: COSY Spectrum of Naucline **56**

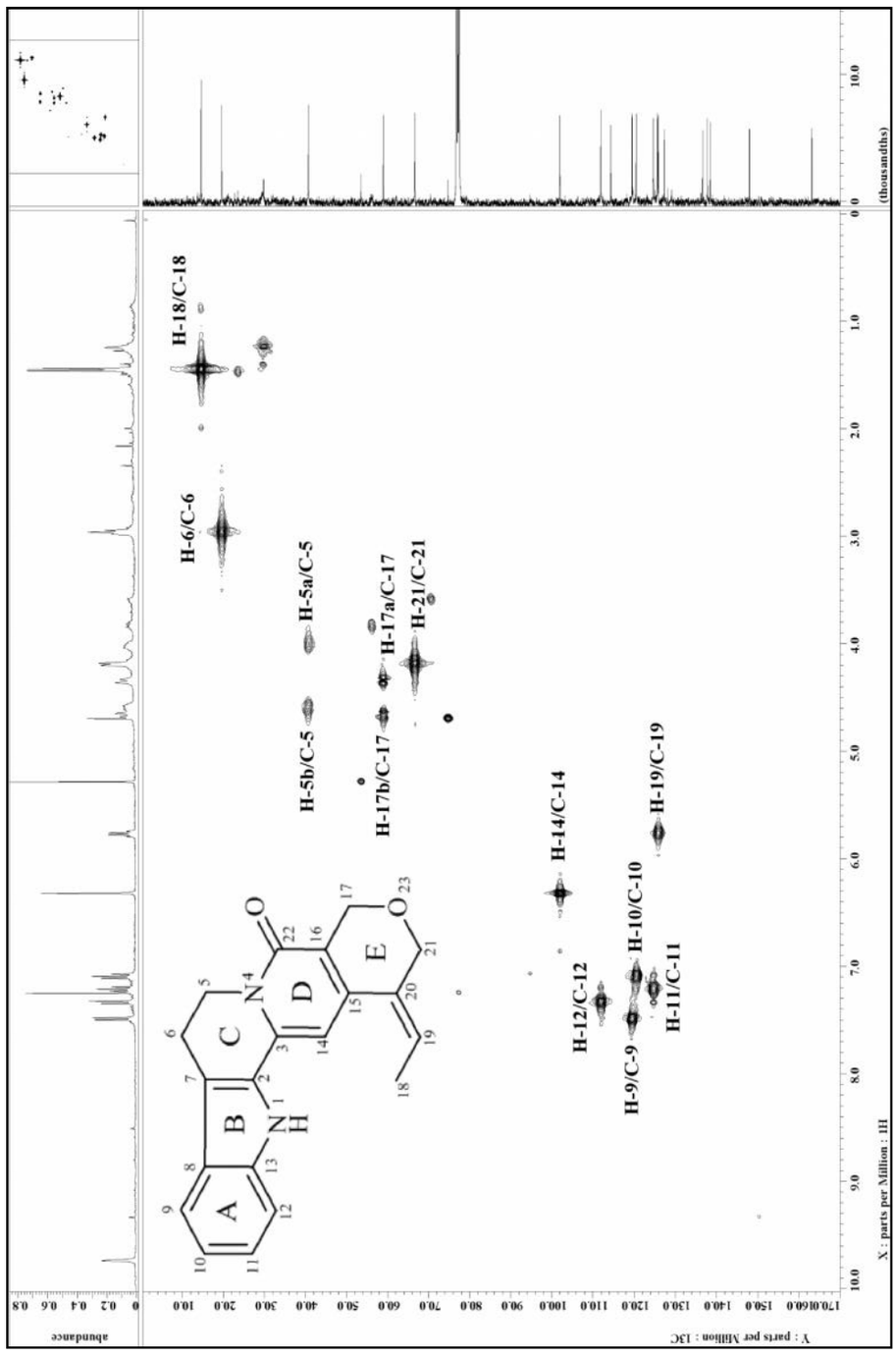

Figure 3.7: HMQC Spectrum of Naucline **56**

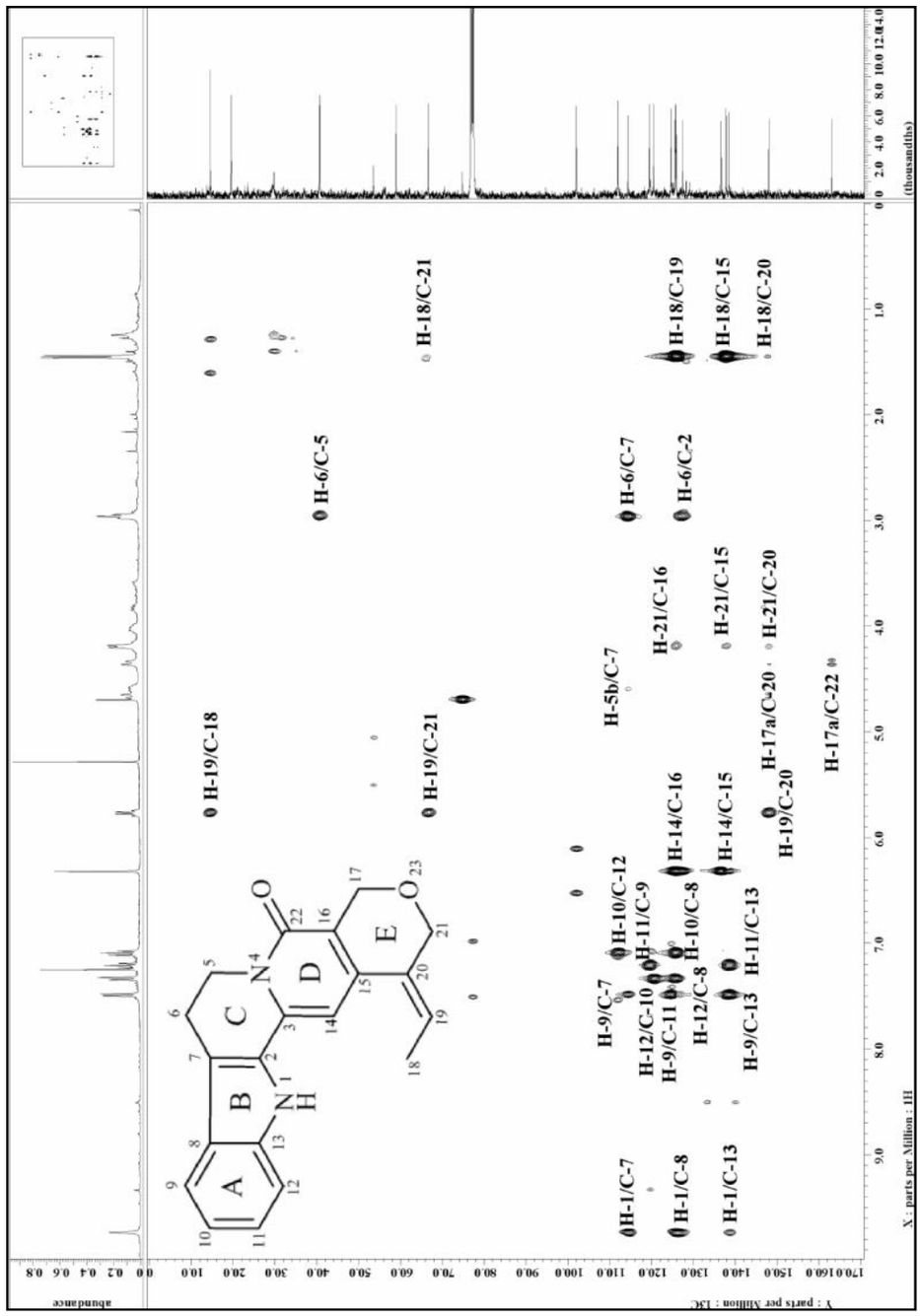

Figure 3.8: HMBC Spectrum of Naucline **56**

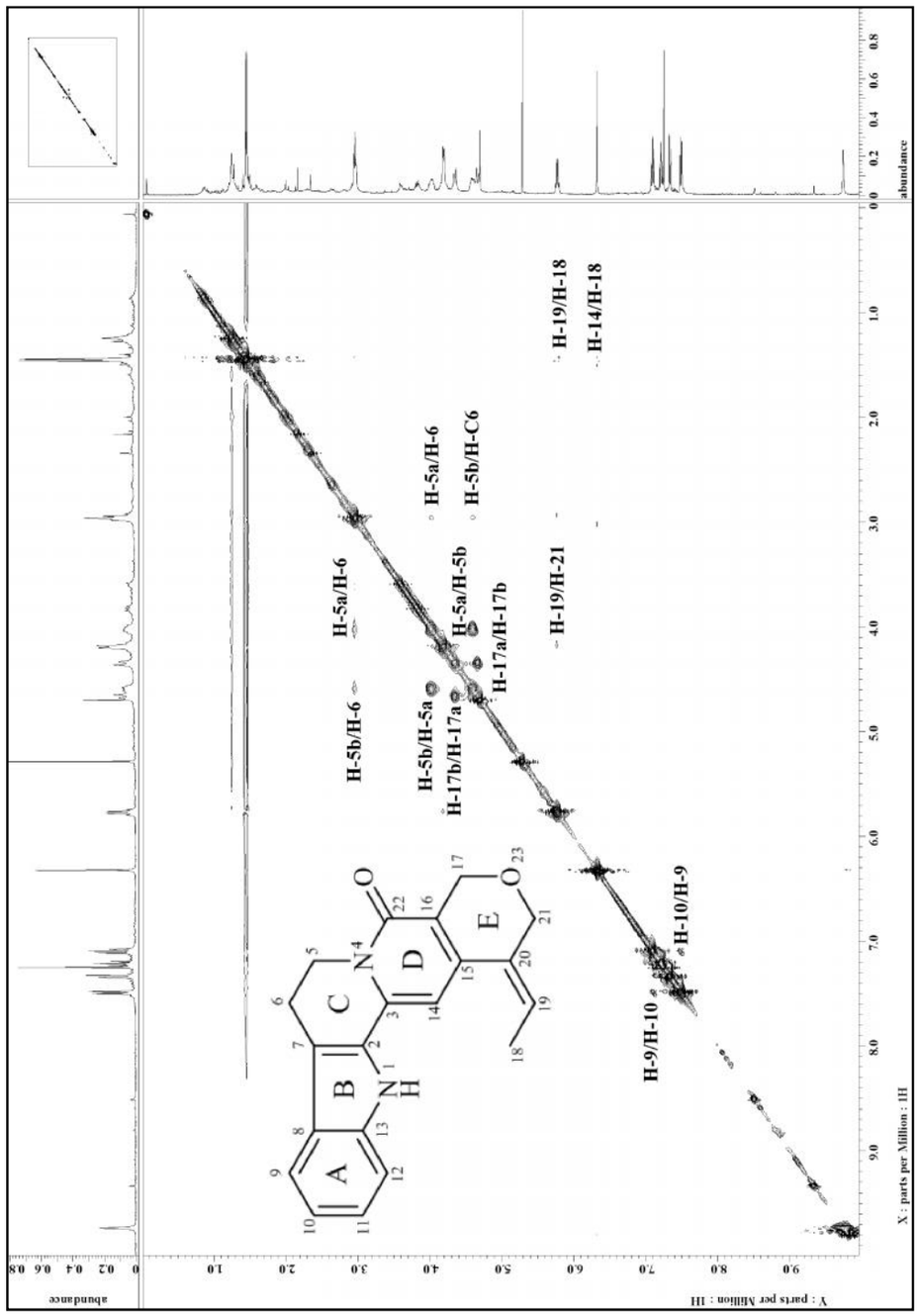

Figure 3.9: NOESY Spectrum of Naucline **56**

3.2.2 Nauclefine 63

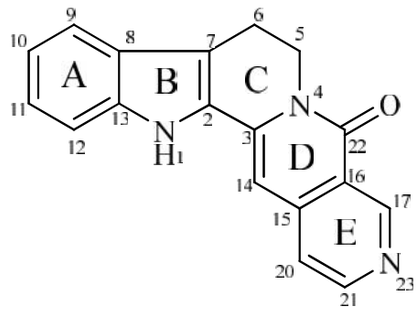

63

Nauclefine **63** was afforded as a yellowish amorphous solid. The ESIMS (Figure 3.11) showed a pseudomolecular ion peak $[M+H]^+$ at *m/z* 288.1155 which was in agreeable to the molecular formula of $C_{18}H_{13}N_3O$ (calc. 288.1131) with fourteen degrees of unsaturation which consisted nine double bonds and five rings. The UV spectrum exhibited maxima at 391, 372, 220 and 204 nm.[15,76,77] The IR spectrum of nauclefine **63** showed absorption bands at 3415 and 1650 cm^{-1}, indicative of N-H and conjugated lactam carbonyl functionalities respectively.[15,76]

In the ^{1}H-NMR spectrum (Figure 3.12), the presence of two doublets at δ_H 7.61 (1H, *d*, *J* = 7.9 Hz, H-9) and δ_H 7.42 (1H, *d*, *J* = 7.9 Hz, H-12), two triplets at δ_H 7.32 (1H, *t*, *J* = 7.9 Hz, H-11) and δ_H 7.19 (1H, *t*, *J* = 7.9 Hz, H-10), two methylenes at δ_H 4.53 (2H, *t*, *J* = 6.8, H_2-5) and δ_H 3.16 (2H, *t*, *J* = 6.8, H_2-6), suggesting a naucleamide derivative with substitution pattern in ring A and C.[35] Furthermore, this tetrahydro-*β*-carboline skeleton (ring A, B and C)[75] presence was confirmed with HMBC correlations of H_2-5 to C-3 (δ_C 136.7) and C-7 (δ_C 116.4), H_2-6 to C-2 (δ_C 127.5) and C-7, H-9 to C-7 and C-13 (δ_C 138.5) (Figure 3.10).

The ^{13}C-NMR and DEPT spectra (Figure 3.13 and Figure 3.14) of nauclefine **63** indicated a total of eighteen carbon signals; two methylenes, eight methines, seven quaternary carbons and one carbonyl carbon. The carbonyl of the δ lactam ring (ring D)

resonated at δ_C 162.0 (C-22). In addition, the HMBC spectrum showed correlation between H-14 (δ_H 6.57) and C-2, H-14 and C-3, H-5 and C-3, thus supporting the connectivity of ring C with ring D. Furthermore, HMBC correlations of H-14 to C-20 (δ_C 118.6), H-17 (δ_H 9.57) to C-15 (δ_C 141.8), H-21 (δ_H 8.64) to C-15 and H-17 to C-21 (δ_C 150.9), indicated that ring D is connected to a pyridine (ring E).

It is worth to note that nauclefine **63** is rather similar in structure with naucline **56**. They differ in ring E. The ring E component in the former is actually a pyridine ring while the latter, the ring E component is a pyran. The interesting characteristic features of nauclefine **63** is the coupling constant value of H-20 and H-21 which is ~5Hz due to the adjacent nitrogen atom. In addition, both H-17 and H-21 resonated very downfield at δ_H 9.57 and δ_H 8.64, respectively.

Thorough analysis of all the spectroscopic data (Table 3.3) obtained coupled with the literature values[15,78] confirmed, without doubt, the identity of nauclefine **63**.

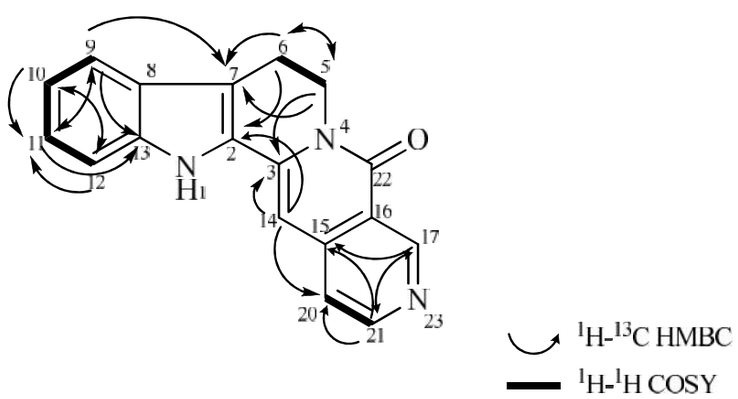

Figure 3.10: COSY and HMBC correlations of nauclefine **63**

Table 3.3: ^{1}H-NMR (400 MHz) and ^{13}C-NMR (100 MHz) Spectral Data of Nauclefine **63** in $CDCl_3$.

Position	**^{1}H**		**^{13}C**	
	δ_H (multiplicity, *J* in Hz)		**δ_C**	
	Experimental ($CDCl_3$)	**Reference* ($CDCl_3$:CD_3OD-4:1)**	**Experimental ($CDCl_3$)**	**Reference* (DMSO-d_6)**
NH-1	-	-	-	-
2	-	-	127.5	127.6
3	-	-	136.7	137.2
5	4.53 (*t*, 6.8)	4.52 (*t*, 6.6)	40.7	40.3
6	3.16 (*t*, 6.8)	3.18 (*t*, 6.6)	19.9	19.3
7	-	-	116.4	114.8
8	-	-	126.1	125.4
9	7.61 (*d*, 7.9)	7.62 (*d*, 7.9)	119.9	119.7
10	7.19 (*t*, 7.9)	7.17 (*t*, 7.5)	121.0	119.9
11	7.32 (*t*, 7.9)	7.31 (*t*, 7.5)	125.3	124.5
12	7.42 (*d*, 7.9)	7.44 (*d*, 7.9)	111.7	112.0
13	-	-	138.5	138.6
14	6.57 (*s*)	6.76 (*s*)	96.9	97.0
15	-	-	141.8	141.6
16	-	-	120.0	119.0
17	9.57 (*s*)	9.49 (*s*)	151.6	150.5
20	7.29 (*d*, 5.5)	7.36 (*d*, 5.5)	118.6	119.0
21	8.64 (*d*, 5.5)	8.57 (*d*, 5.5)	150.9	151.0
22	-	-	162.0	161.1

*Literature values from Erdelmeier et al. (1992) and Abreu and Pereira (1998).

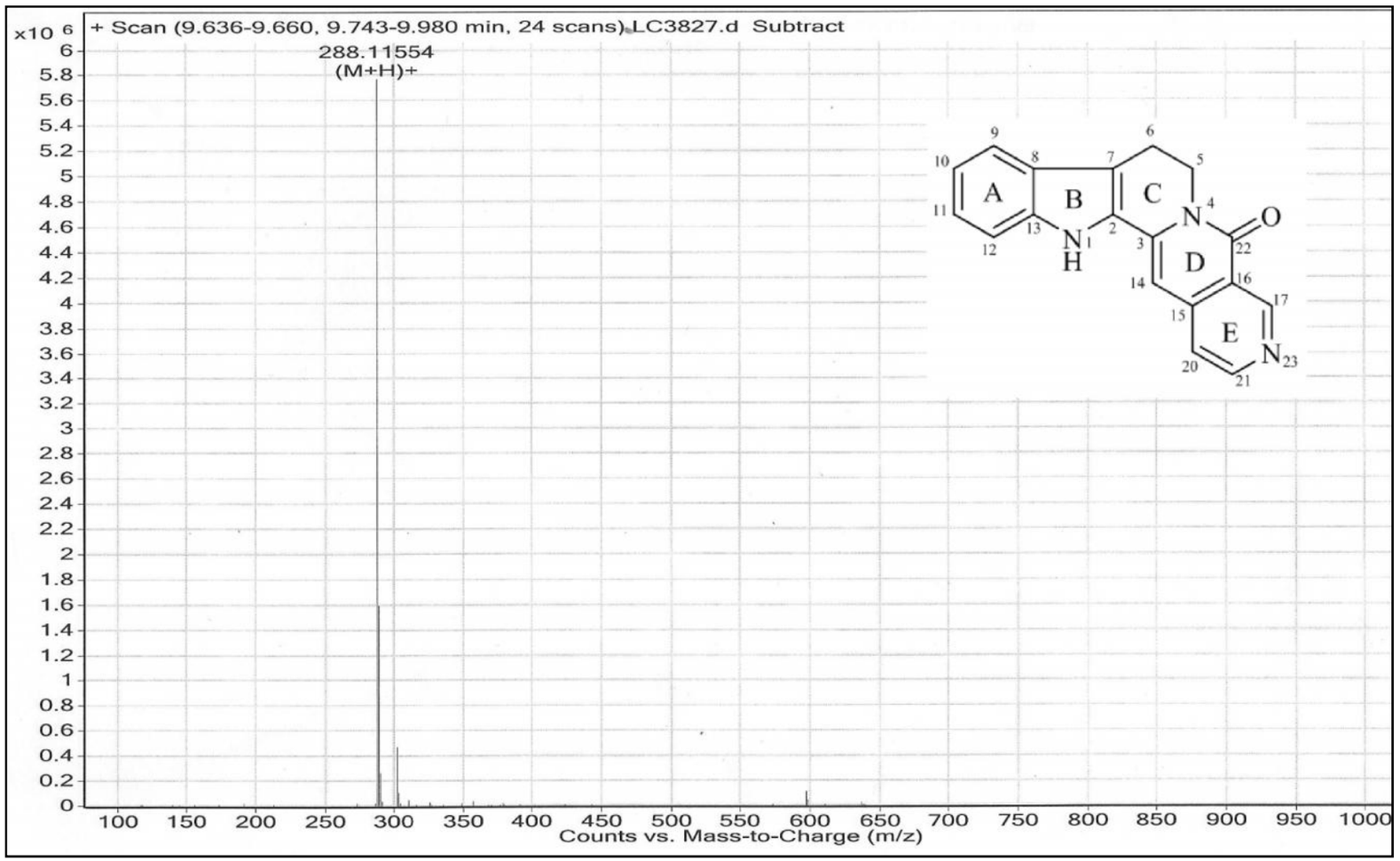

Figure 3.11: LCMS Spectrum of Nauclefine **63**

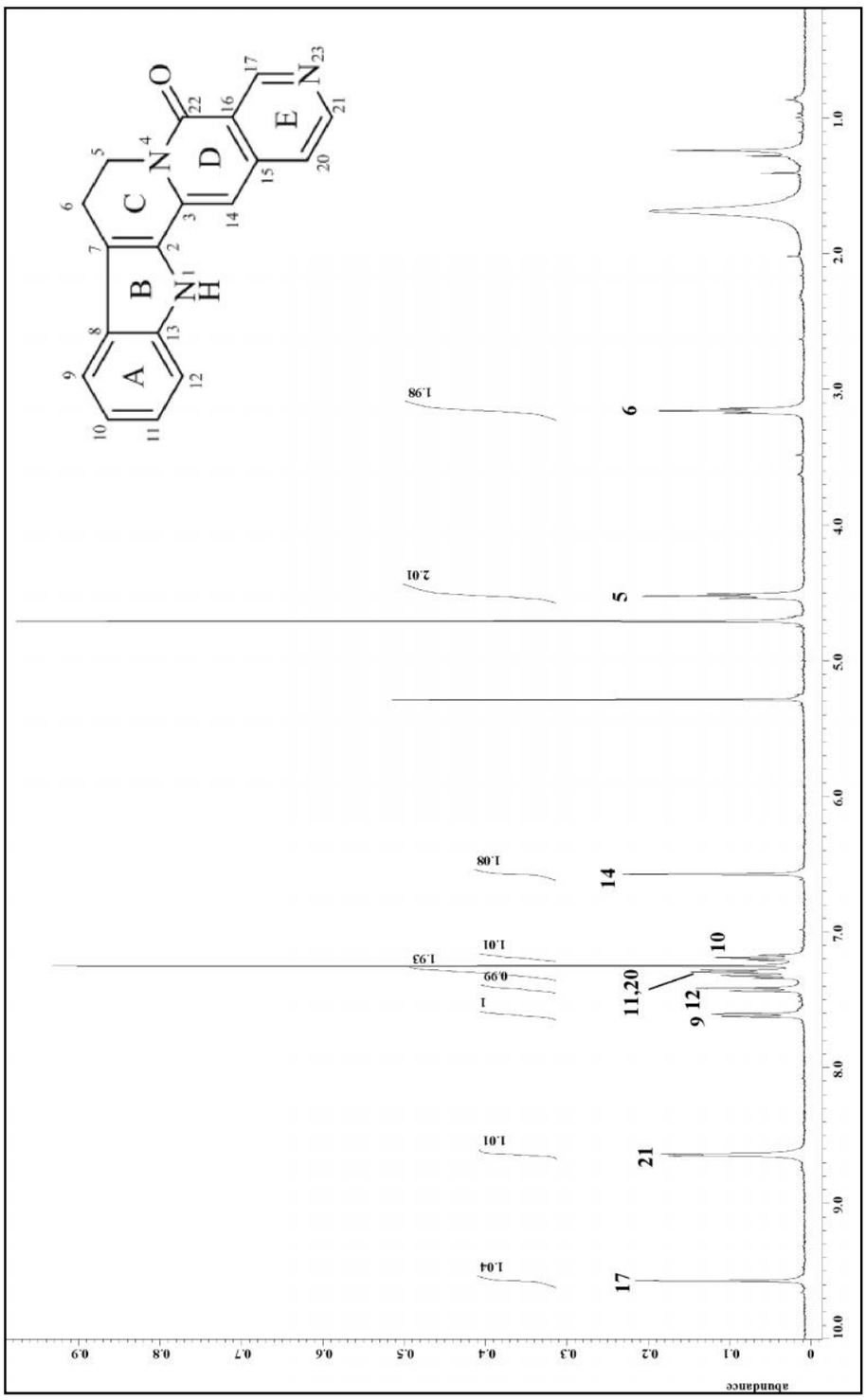

Figure 3.12: ^{1}H NMR Spectrum of Nauclefine **63**

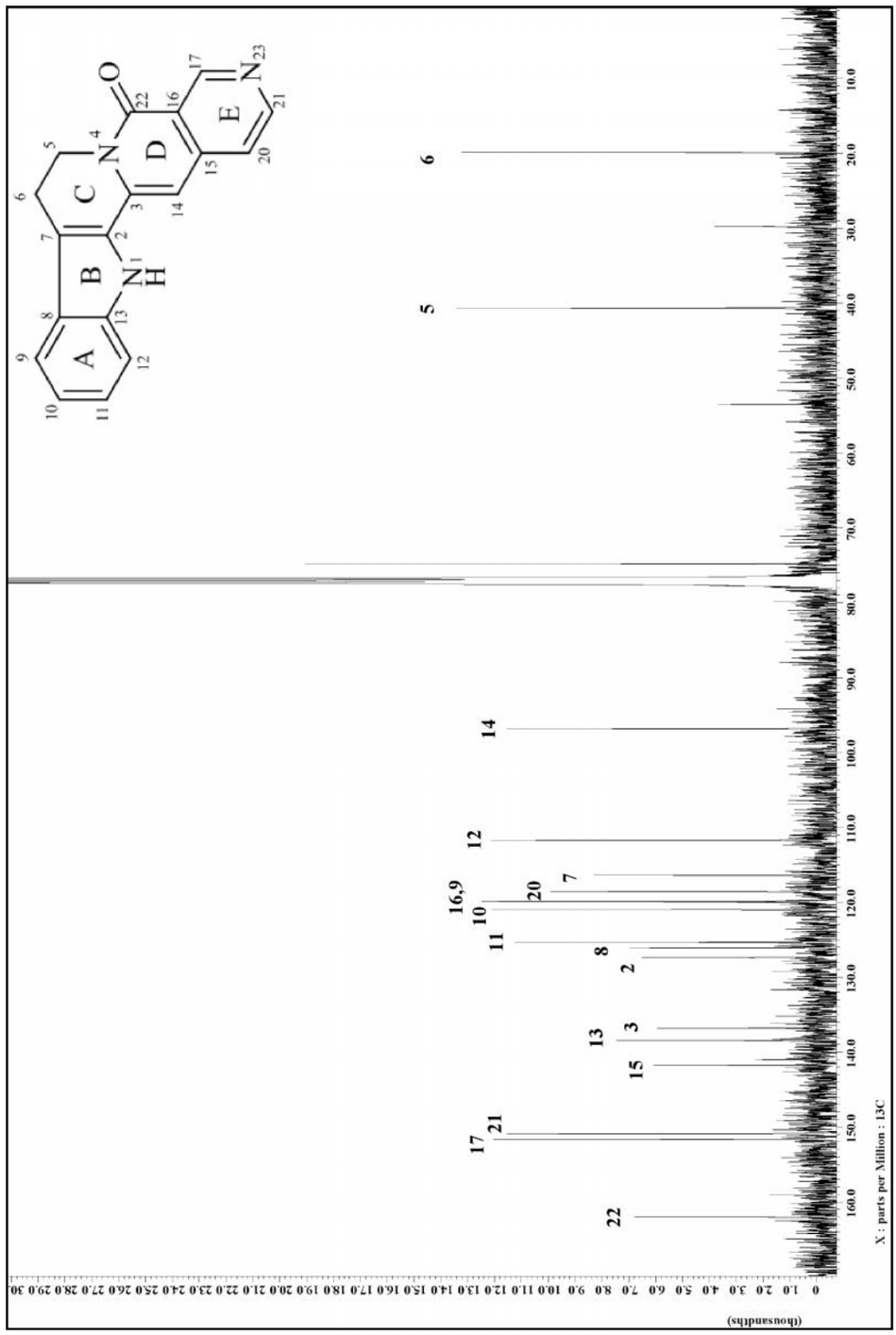

Figure 3.13: ^{13}C NMR Spectrum of Nauclefine **63**

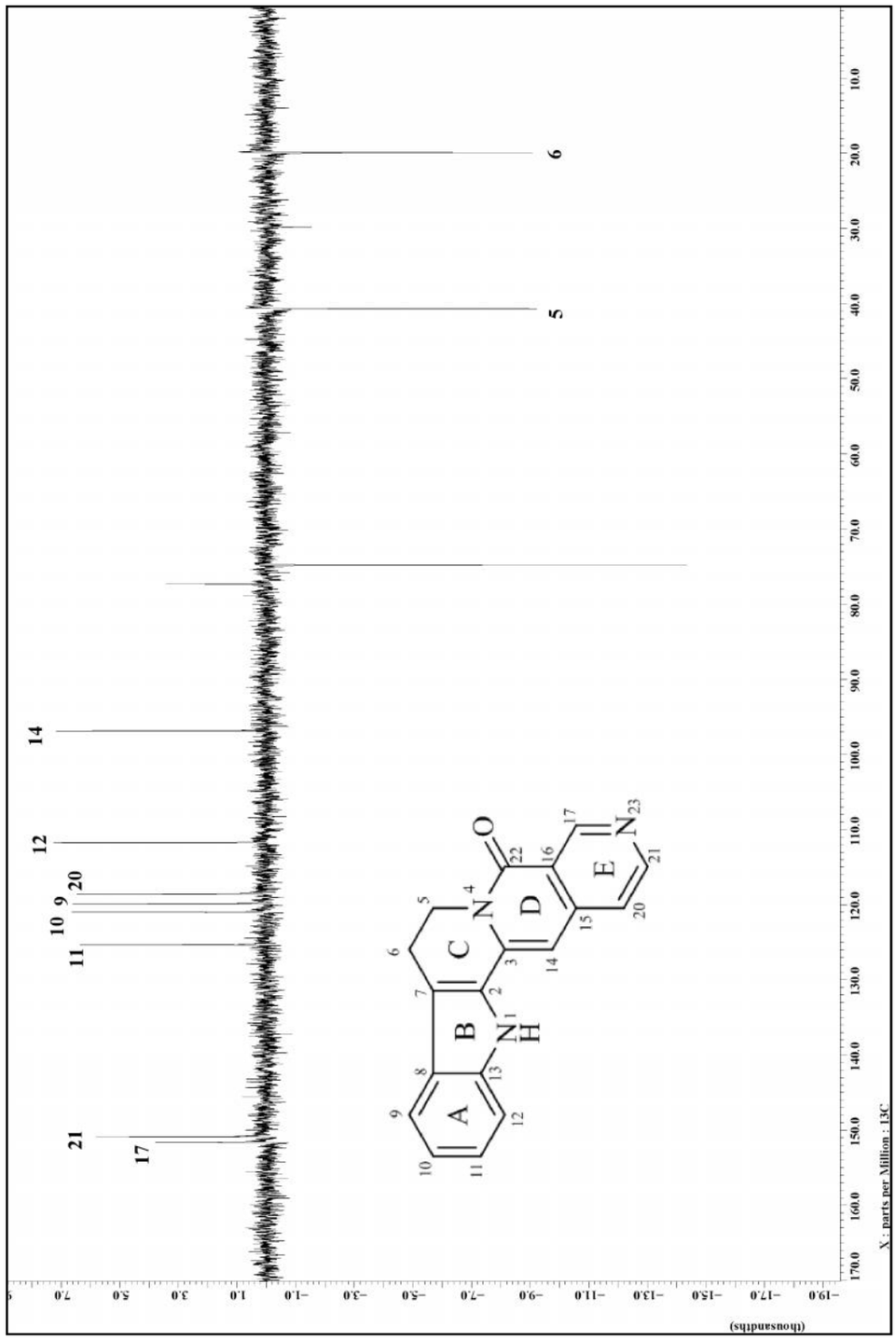

Figure 3.14: DEPT 135 Spectrum of Nauclefine **63**

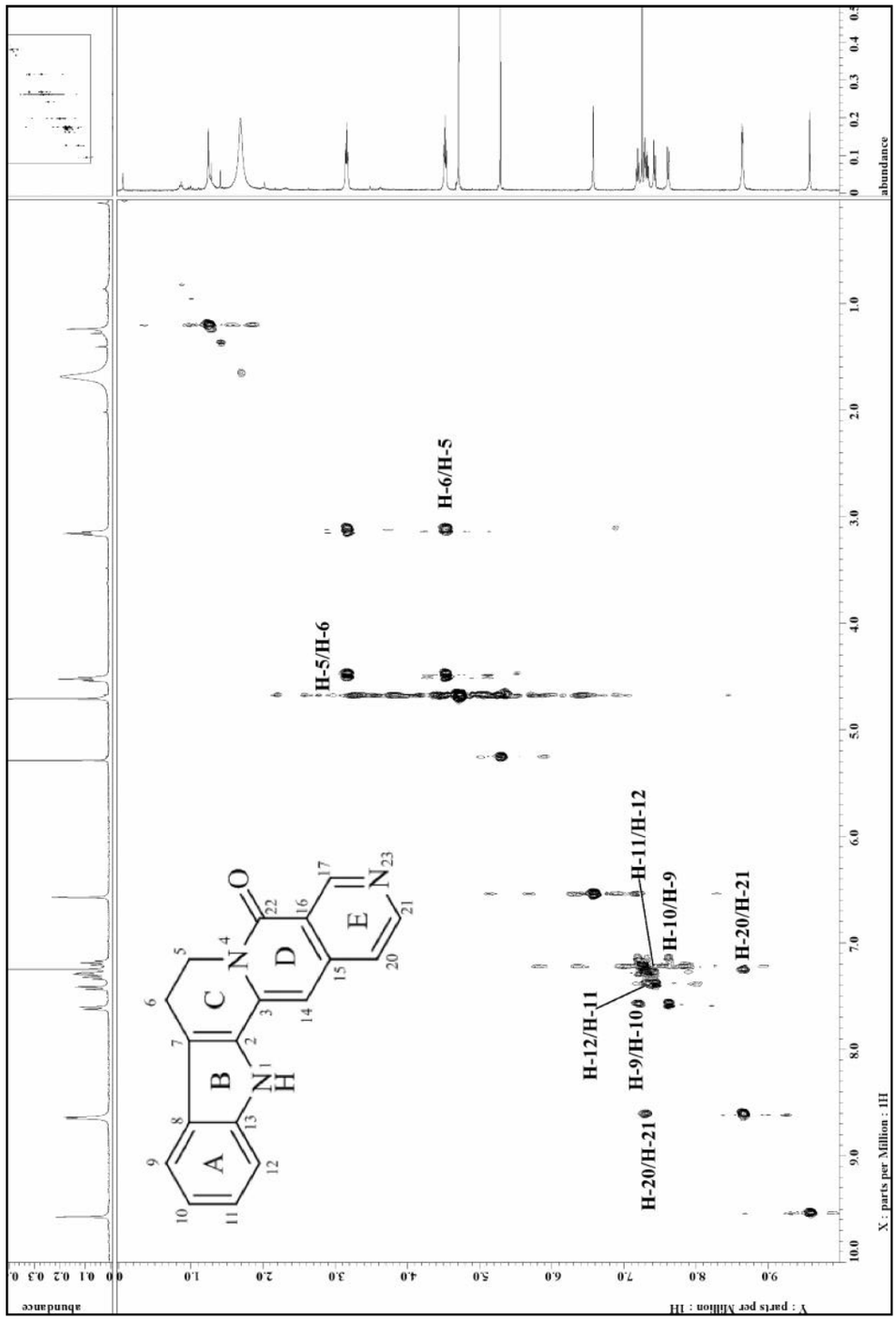

Figure 3.15: COSY Spectrum of Nauclefine **63**

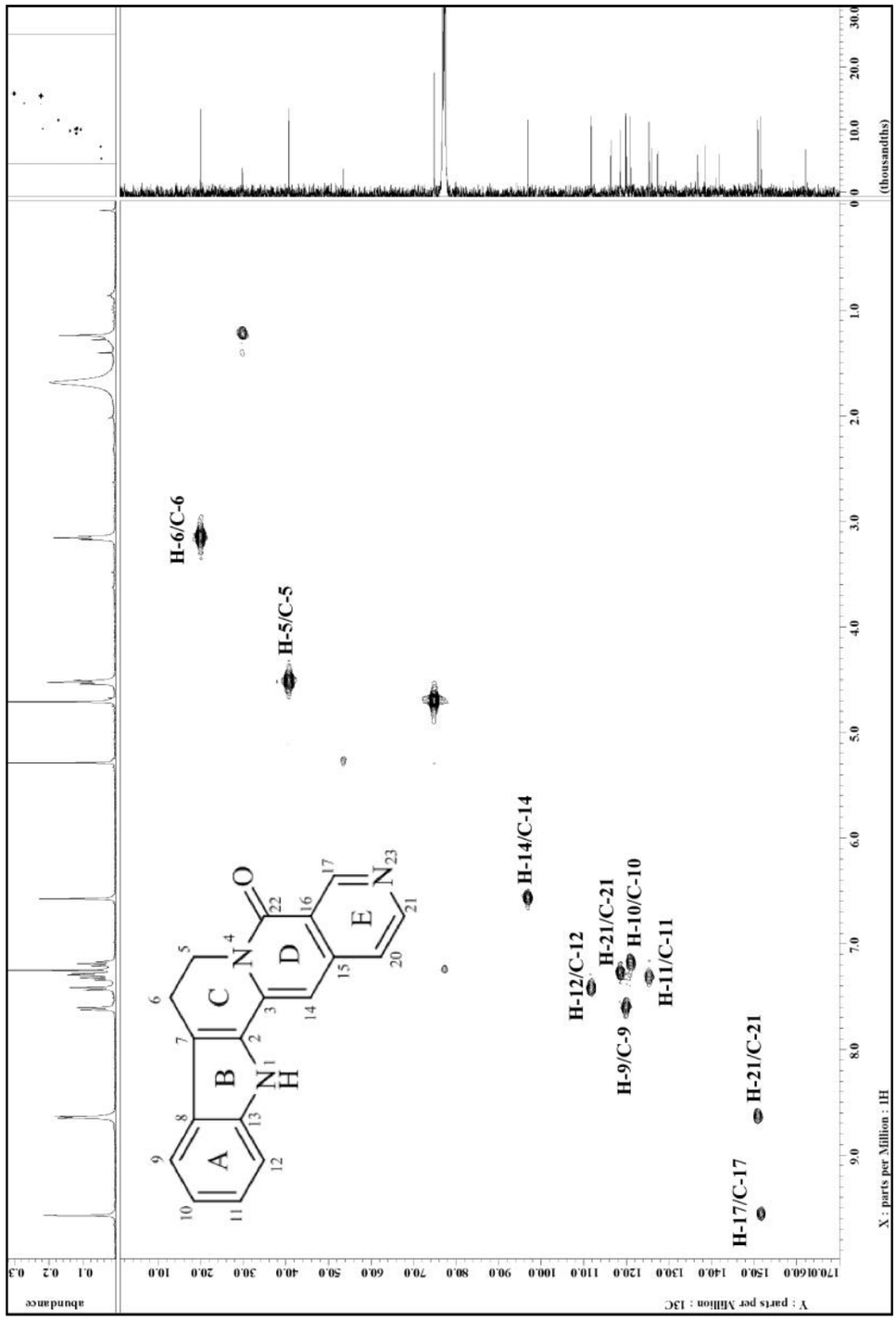

Figure 3.16: HMQC Spectrum of Nauclefine **63**

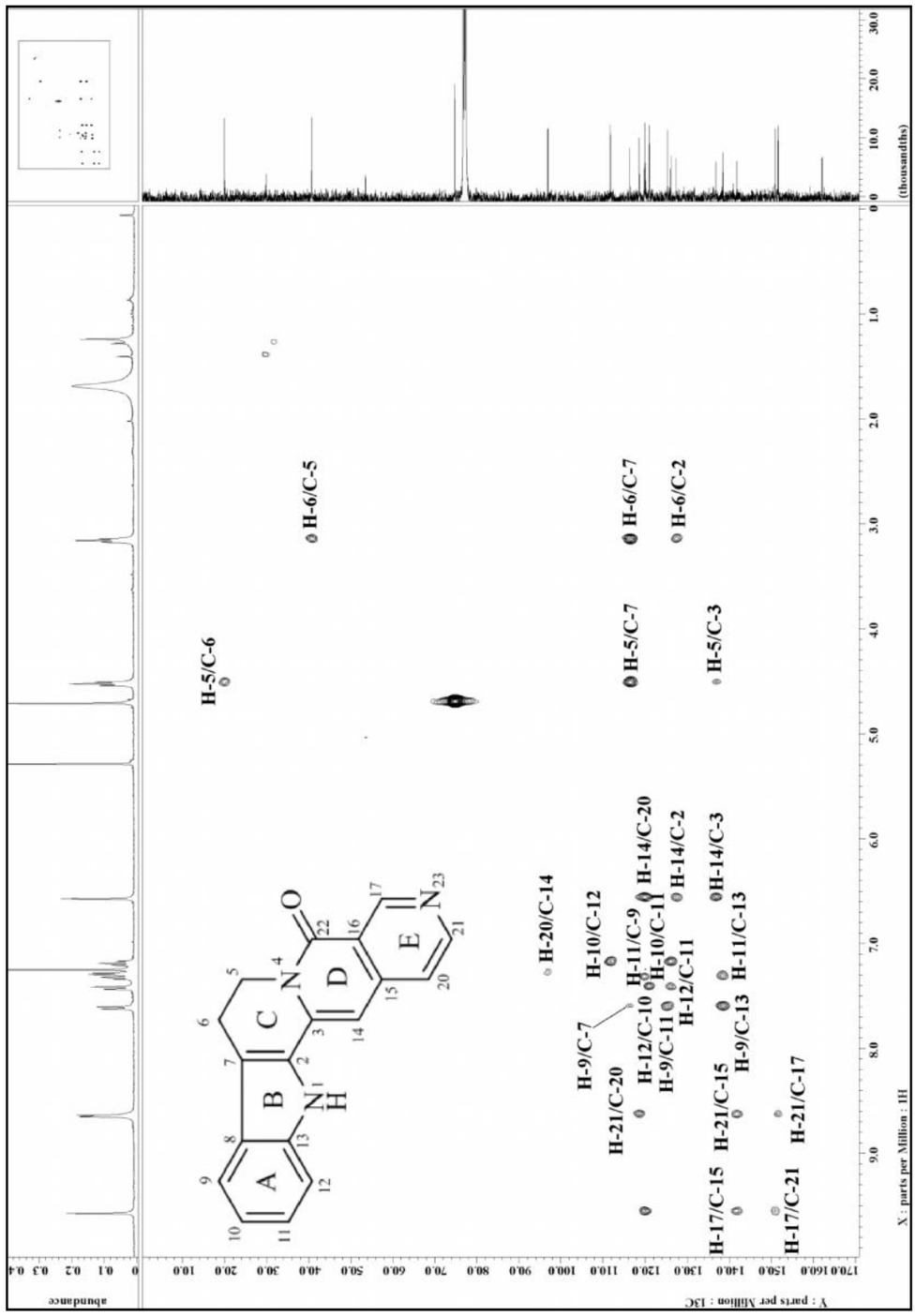

Figure 3.17: HMBC Spectrum of Nauclefine **63**

3.2.3 Naucletine 61

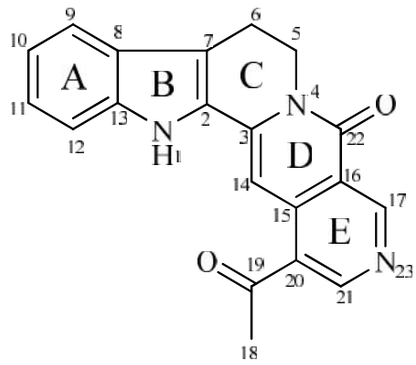

61

Naucletine **61** was obtained as a yellowish amorphous solid. The ESIMS (Figure 3.19) showed a pseudomolecular ion peak $[M+H]^+$ at *m/z* 330.1266, corresponding to the molecular formula of $C_{20}H_{15}N_3O_2$ (calc. 330.1237). The UV spectrum showed strong absorptions at 402, 312, 260 and 210 nm.[79] Naucletine **61** revealed absorption bands at 1675 and 1653 cm^{-1} in IR spectrum thus indicating the presence of conjugated carbonyl and lactam carbonyl (-NC=O) groups respectively.[80]

The ^{1}H-NMR (Figure 3.20) and ^{13}C-NMR (Figure 3.21) spectra of this alkaloid showed a similar pattern with that of nauclefine **63** by exhibiting two doublets at δ_H 7.64 (1H, *d, J* = 8.0 Hz, H-9) and δ_H 7.47 (1H, *d, J* = 8.0 Hz, H-12) together with two doublet of triplets (*dt*) at δ_H 7.20 (1H, *dt, J* = 8.0, 1.1 Hz, H-10) and δ_H 7.36 (1H, *dt, J* = 8.0, 1.1 Hz, H-11) in aromatic region. Two sets of triplets signals were also observed at δ_H 4.54 (2H, *t, J* = 6.9 Hz) and δ_H 3.20 (2H, t, *J* = 6.9 Hz), corresponding to methylene protons, H_2-5 and H_2-6 respectively. However, a marked difference between naucletine **61** and nauclefine **63** was observed in the coupling pattern of H-21. Naucletine **61** showed a singlet while nauclefine **63** revealed a doublet, therefore suggesting that C-20 is substituted. Interestingly, the former, naucletine **61**, showed a methyl singlet (H_3-18) of an acetyl group at δ_H 2.78. A broad singlet at δ_H 8.89 implied the presence of an NH unit.

The ^{13}C-NMR and DEPT (Figure 3.22) spectra of naucletine **61** indicated a total of twenty carbon signals; one methyl, two methylenes, seven methines, eight quaternary carbons and two carbonyl carbons. The carbonyl of an acetyl group resonated at δ_C 199.7 (C-19). In addition, the HMBC spectrum showed correlations between H-14 (δ_H 7.93) and C-3 (δ_C 138.8), H-14 and C-16 (δ_C 120.7), H_2-5 and C-22 (δ_C 161.6), thus supporting the presence of a δ lactam ring (ring D). HMBC correlations of H-14 to C-16, H-17 (δ_H 9.69) to C-15 (δ_C 140.7) and C-16, H-21 (δ_H 9.23) to C-15 indicated that ring D is attached to the pyridine (ring E). Connectivity of the acetyl group with the pyridine forming a 3-acetylpyridine unit was revealed by the HMBC correlations of H_3-18 to C-19 and C-21 (δ_C 155.3) (Figure 3.18).

From the analysis of the spectroscopic data obtained (Table 3.4) and comparison with the literature values[79,81,82], thus the structure of naucletine **61** was confirmed. This indole alkaloid has been isolated from other Rubiaceae plant such as *Sarcocephalus latifolia*[78] and synthesized by Ninomiya et al. (1976)

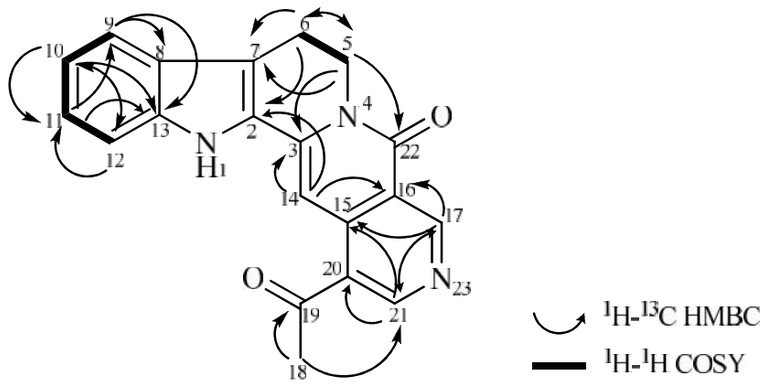

Figure 3.18: COSY and HMBC Correlations of Naucletine **61**

Table 3.4: ^{1}H-NMR (400 MHz) and ^{13}C-NMR (100 MHz) Spectral Data of Naucletine **61** in $CDCl_3$.

Position	**^{1}H**		**^{13}C**
	δ_H (multiplicity, *J* in Hz)		**δ_C**
	Experimental ($CDCl_3$)	**Reference* (DMSO-d_6)**	**Experimental ($CDCl_3$)**
NH-1	8.95 (*s*)	11.9 (*s*)	-
2	-	-	127.3
3	-	-	138.8
5	4.54 (*t*, 6.9)	4.39 (*t*, 6.9)	40.6
6	3.20 (*t*, 6.9)	3.12 (*t*, 6.9)	19.7
7	-	-	116.9
8	-	-	125.8
9	7.64 (*d*, 8.0)	7.65 (*d*, 8.0)	119.9
10	7.20 (*dt*, 8.0, 1.1)	7.07 (*m*)	120.9
11	7.36 (*dt*, 8.0, 1.1)	7.23 (*m*)	125.6
12	7.47 (*d*, 8.0)	7.45 (*d*, 8.1)	111.9
13	-	-	138.7
14	7.93 (*s*)	7.73 (*s*)	95.4
15	-	-	140.7
16	-	-	120.7
17	9.69 (*s*)	9.41 (*s*)	153.9
18	2.78 (*s*)	2.71 (*s*)	29.2
19	-	-	199.7
20	-	-	124.7
21	9.23 (*s*)	9.21 (*s*)	155.3
22	-	-	161.6

*Literature values from Lavilla et al. (1995).

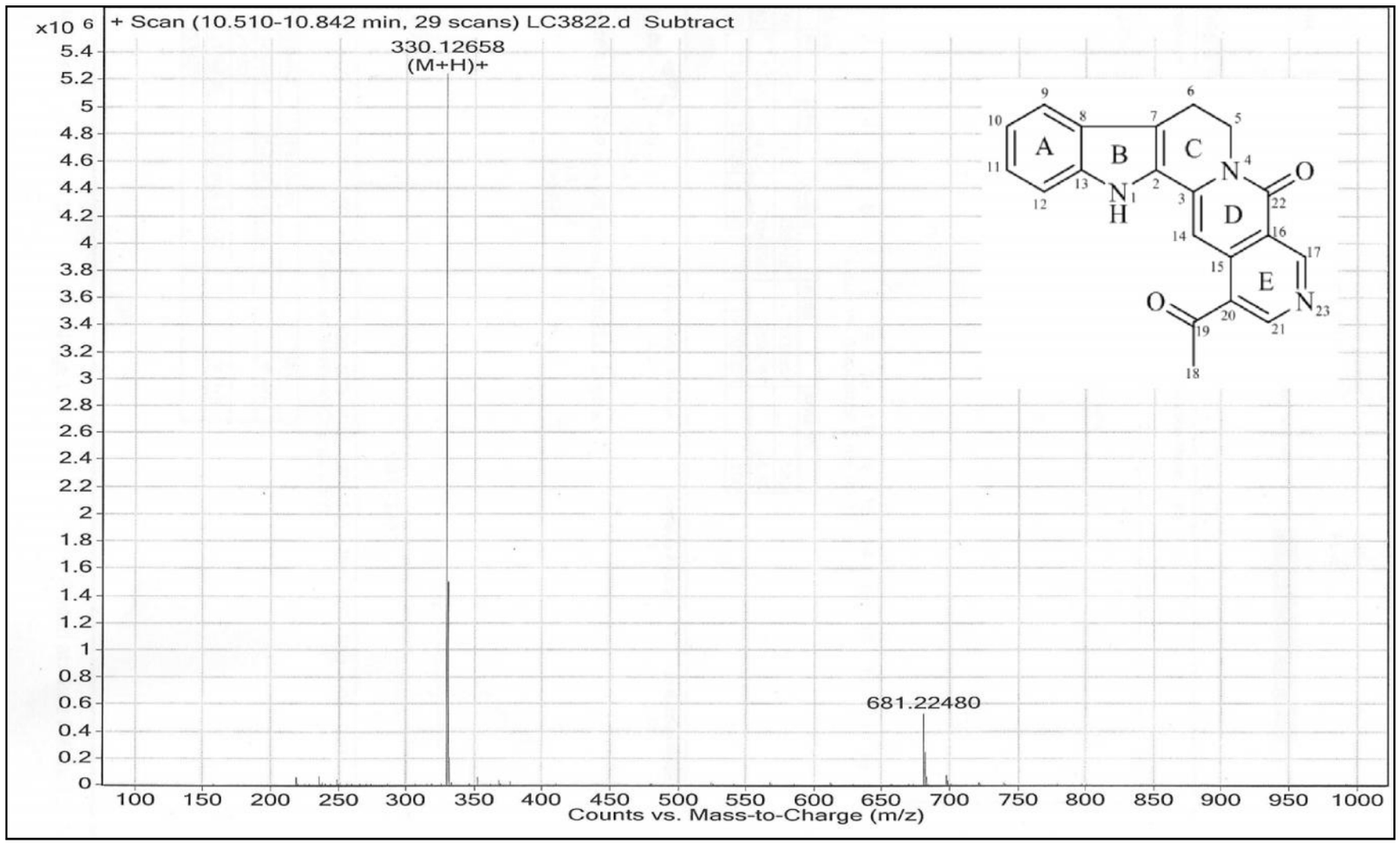

Figure 3.19: LCMS Spectrum of Naucletine **61**

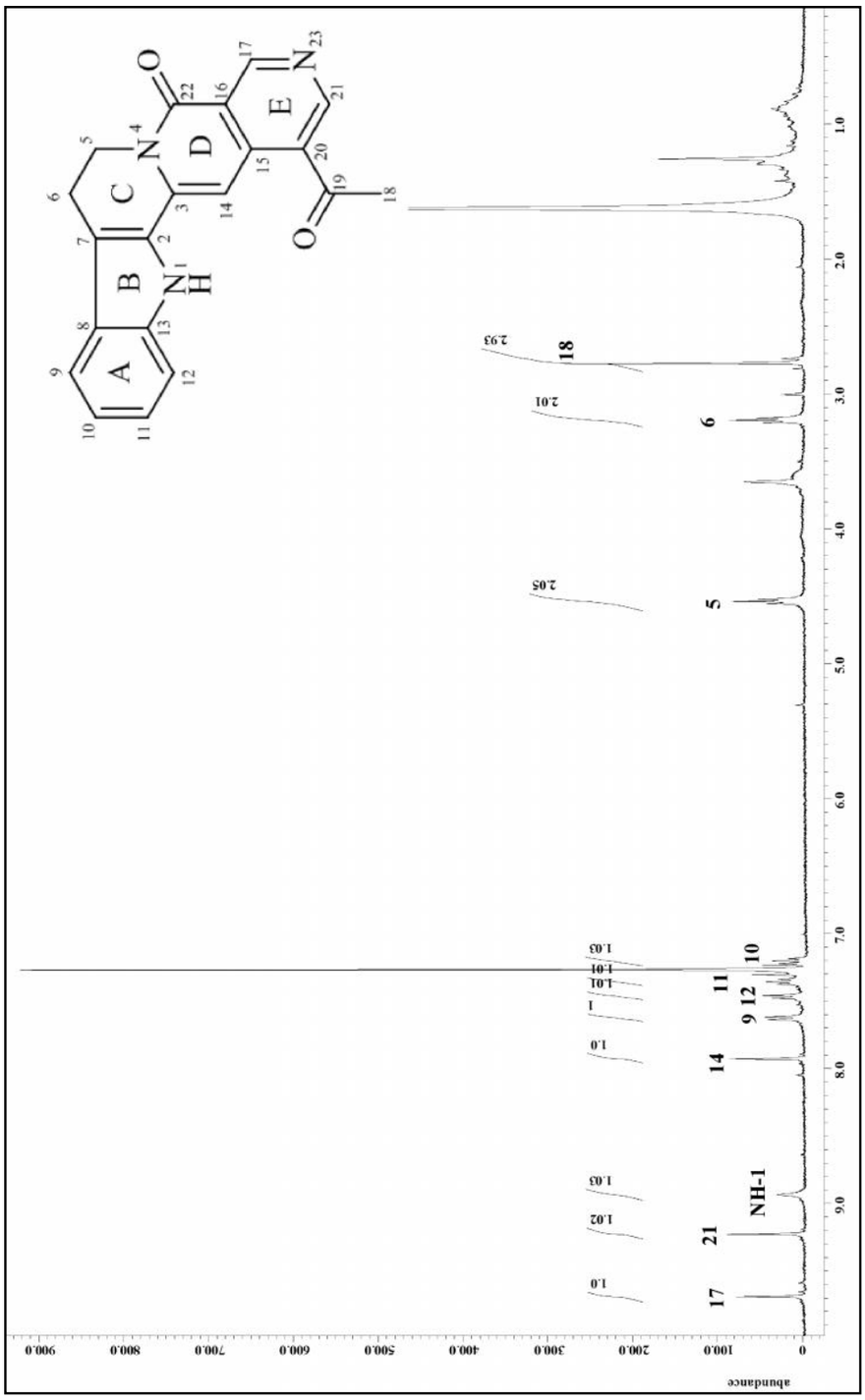

Figure 3.20: ^{1}H NMR Spectrum of Naucletine **61**

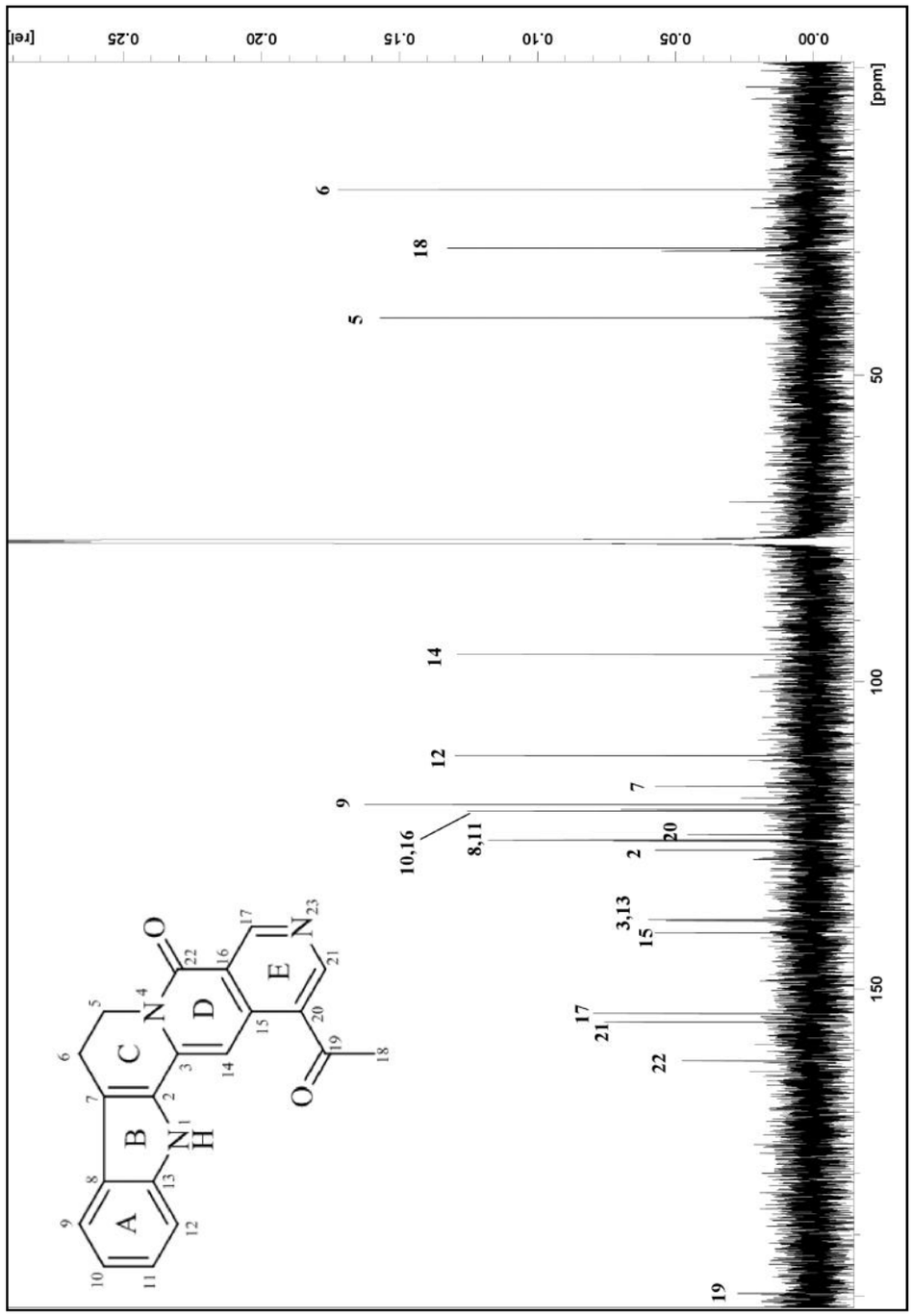

Figure 3.21: ^{13}C NMR Spectrum of Naucletine **61**

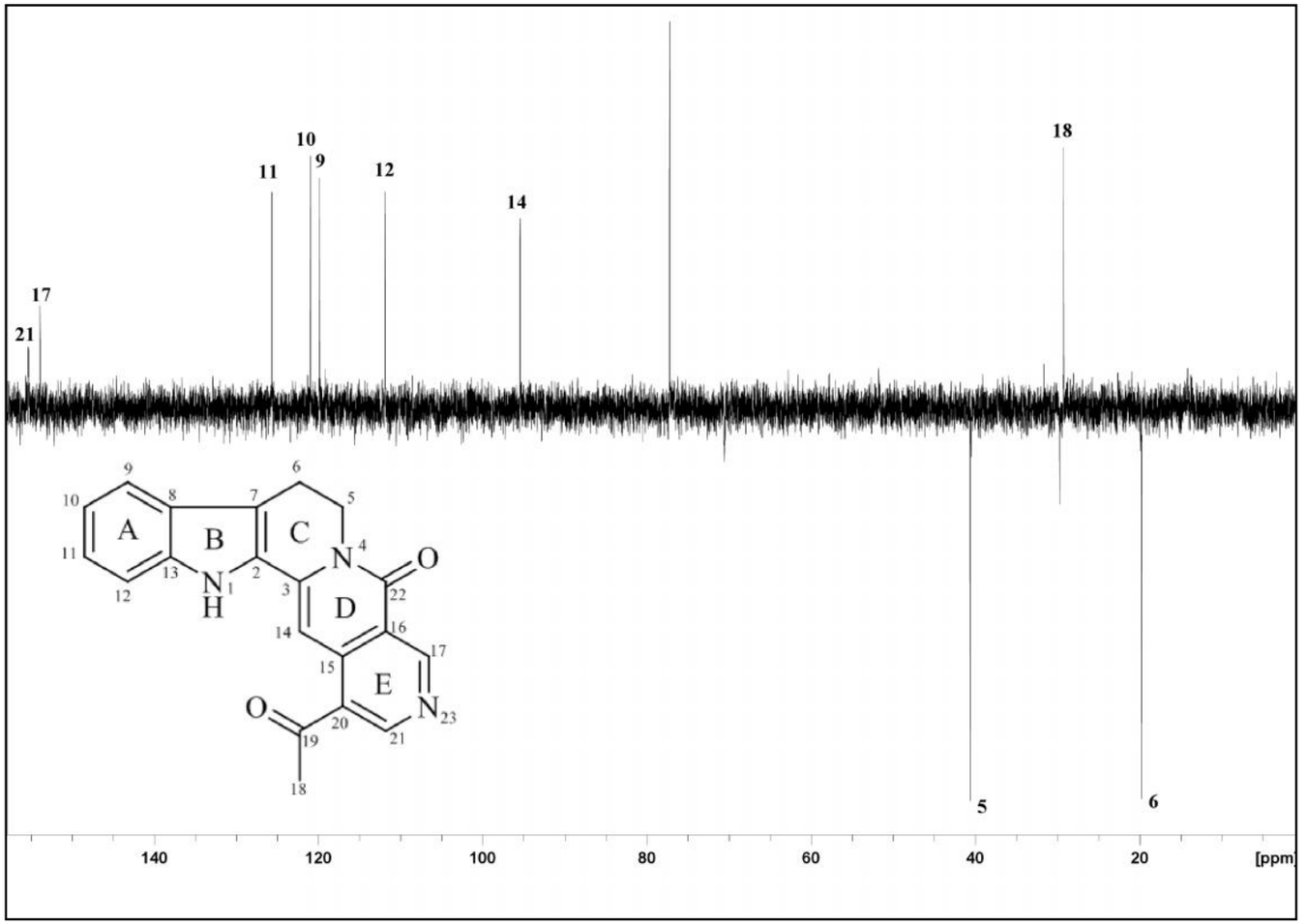

Figure 3.22: DEPT 135 Spectrum of Naucletine **61**

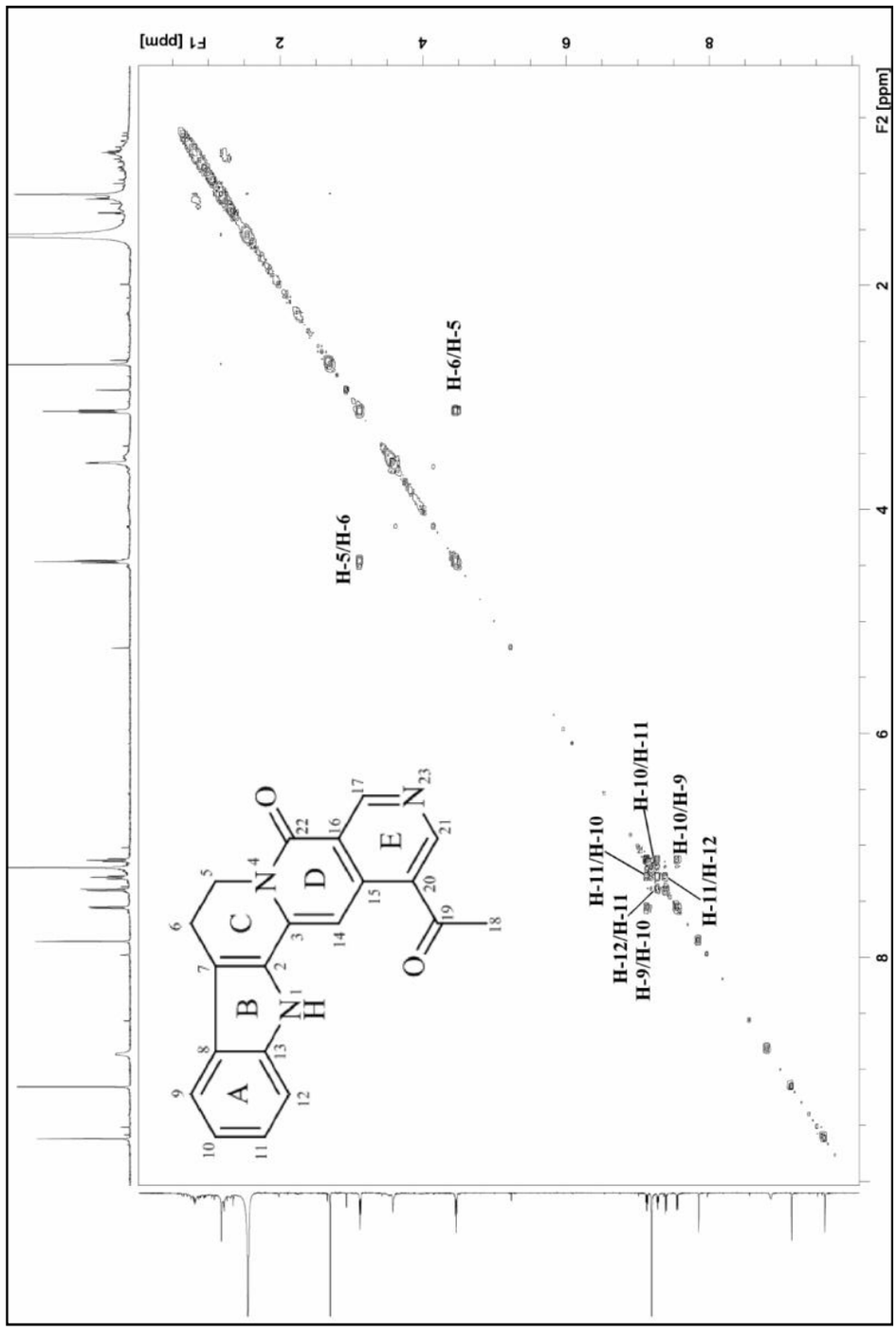

Figure 3.23: COSY Spectrum of Naucletine **61**

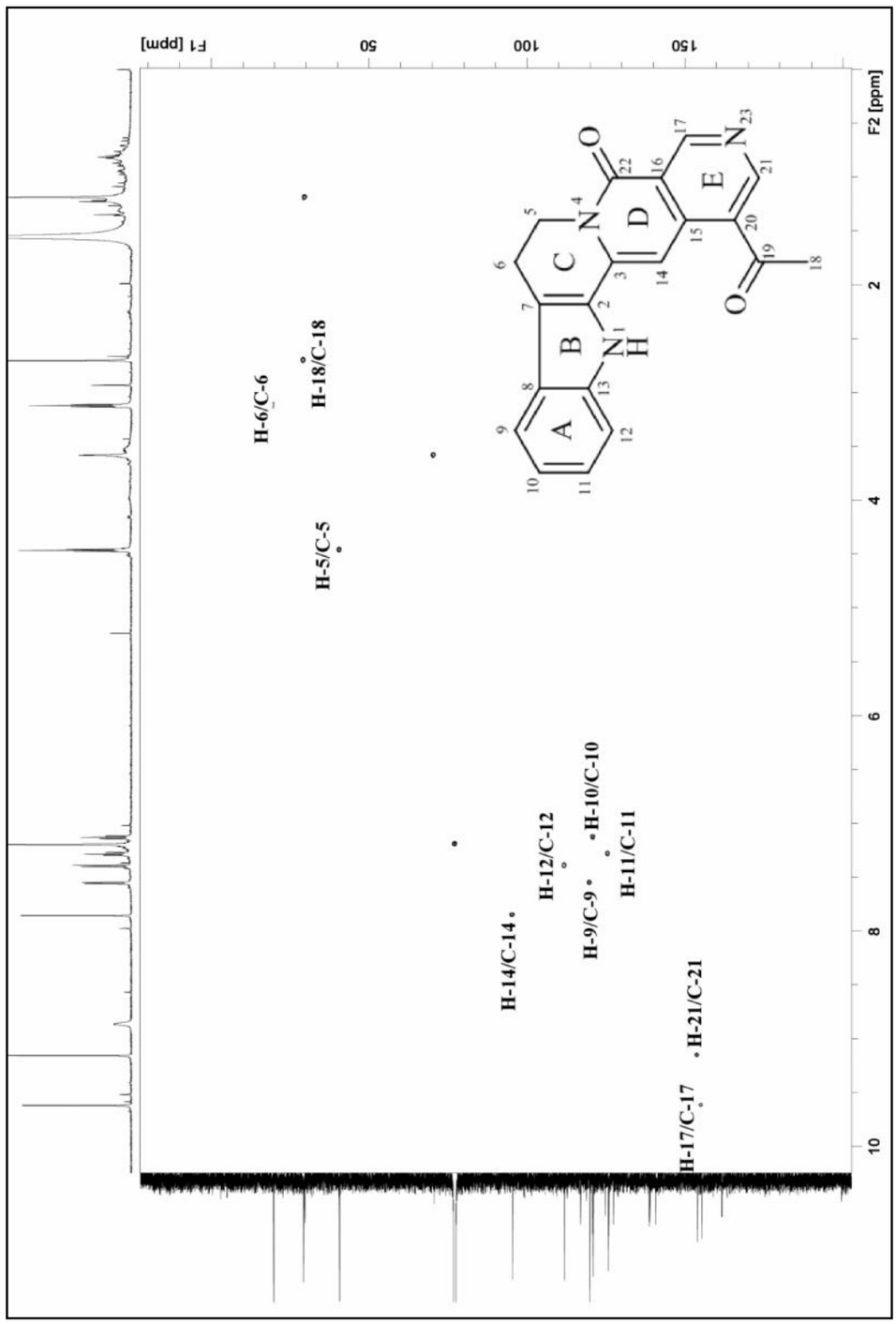

Figure 3.24: HSQC Spectrum of Naucletine **61**

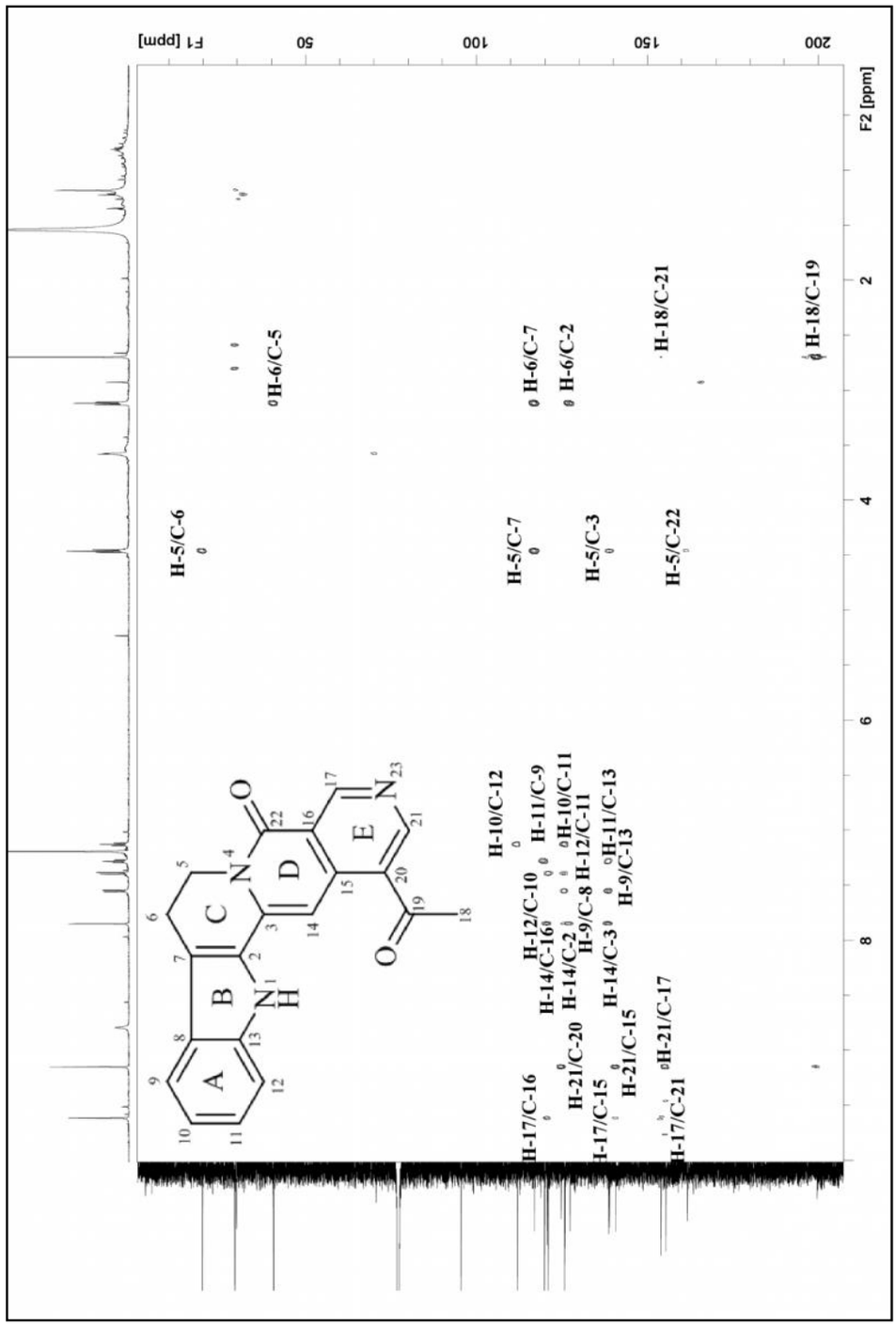

Figure 3.25: HMBC Spectrum of Naucletine **61**

3.2.4 Angustine 42

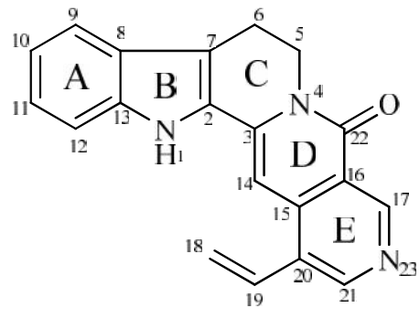

42

Angustine **42** was isolated as an orange amorphous solid. Its molecular formula was confirmed as $C_{20}H_{15}N_3O$ from the ESIMS (Figure 3.27) which revealed a pseudomolecular ion peak $[M+H]^+$ at *m/z* 314.1361 (calc. 314.1288). In the UV spectrum, absorption peaks at 399, 381, 305, 293 and 210 nm were observed.[15] In the IR spectrum, absorption bands were observed at 3425 and 1645 cm^{-1} indicated presence of N-H and conjugated lactam carbonyl functionalities respectively.[15]

The signals in ^1H and ^{13}C-NMR spectra for ring A, B, C and D were very similar to those of nauclefine **63** except the signals of ring E (fifth ring). In ^1H-NMR spectrum (Figure 3.28), H-21 (δ_H 8.75) resonated as a singlet implying that C-20 is substituted. In addition, three sets of downfield signals between δ_H 5.56-7.13 were observed; a *dd* (δ_H 7.09, 1H, *dd*, *J* = 17.2, 11.3 Hz, H-19) and two doublets (δ_H 5.56, 1H, *d*, *J* = 11.3 Hz, H-18a and δ_H 5.84, 1H, *d*, *J* = 17.2 Hz, H-18b). These signals signify the presence of a vinyl group (-CH=CH_2) which correlated to C-18 (δ_C 119.6) and C-19 (δ_C 130.5).

The ^{13}C-NMR spectrum (Figure 3.29) of angustine **42** indicated a total of twenty carbon signals; three methylenes, eight methines, eight quaternary carbons and one carbonyl carbon. HMBC correlations of H-14 (δ_H 6.76) to C-16 (δ_C 119.7), H-17 (δ_H 9.50) to C-15 (δ_C 139.3) and C-16, H-21 (δ_H 8.75) to C-15, indicated that the δ lactam ring (ring D) is fused to pyridine (ring E) through C-15 and C-16. In addition, the HMBC spectrum showed correlations of H_2-18 to C-20 (δ_C 127.6) and H-19 to C-21 (δ_C

148.3), suggesting the vinyl group is linked to pyridine forming a 3-vinylpyridine unit (Figure 3.26).

Complete ^{1}H and ^{13}C-NMR assignments (Table 3.5) were established by thorough analysis of COSY, HMBC and HSQC data as well as reported data,[15,72,73] thus the structure of angustine **42** was established. This indole alkaloid was the major compound in the three samples.

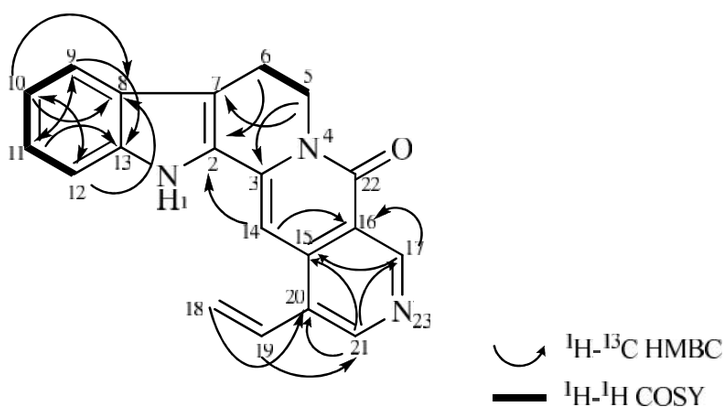

Figure 3.26: Selected COSY and HMBC Correlations of Angustine **42**

Table 3.5: ^{1}H-NMR (400 MHz) and ^{13}C-NMR (100 MHz) Spectral Data of Angustine **42** in $CDCl_3$.

Position	**^{1}H**		**^{13}C**	
	δ_H (multiplicity, *J* in Hz)		**δ_C**	
	Experimental ($CDCl_3$)	**Reference* ($CDCl_3$: CD_3OD -4:1)**	**Experimental ($CDCl_3$)**	**Reference* ($CDCl_3$: CD_3OD -4:1)**
NH-1	8.68 (*br s*)	-	-	-
2	-	-	127.6	127.3
3	-	-	136.6	137.1
5	4.54 (*t*, 6.5)	4.52 (*t*, 6.5)	40.7	40.5
6	3.18 (*t*, 6.5)	3.18 (*t*, 8.0)	19.9	19.3
7	-	-	116.6	115.0
8	-	-	126.2	125.2
9	7.63 (*d*, 8.1)	7.60 (*d*, 8.0)	119.9	119.1
10	7.21 (*dd*, 8.1, 7.0)	7.13 (*t*, 8.0)	121.1	119.8
11	7.34 (*dd*, 7.0, 8.4)	7.30 (*t*, 8.0)	125.5	124.4
12	7.45 (*d*, 8.4)	7.46 (*d*, 8.0)	111.8	111.5
13	-	-	138.6	138.7
14	6.76 (*s*)	7.16 (*s*)	93.7	94.1
15	-	-	139.3	139.8
16	-	-	119.7	118.8
17	9.50 (*s*)	9.34 (*s*)	150.8	149.3
18a	5.56 (*d*, 11.3)	5.61 (*d*, 12.0)	119.6	118.8
18b	5.84 (*d*, 17.2)	5.89 (*d*, 18.0)		
19	7.09 (*dd*, 17.2, 11.3)	7.17 (*dd*, 18.0, 12.0)	130.5	129.6
20	-	-	127.6	127.9
21	8.75 (*s*)	8.66 (*s*)	148.3	146.4
22	-	-	162.0	161.9

*Literature values from Erdelmeier et al. (1992).

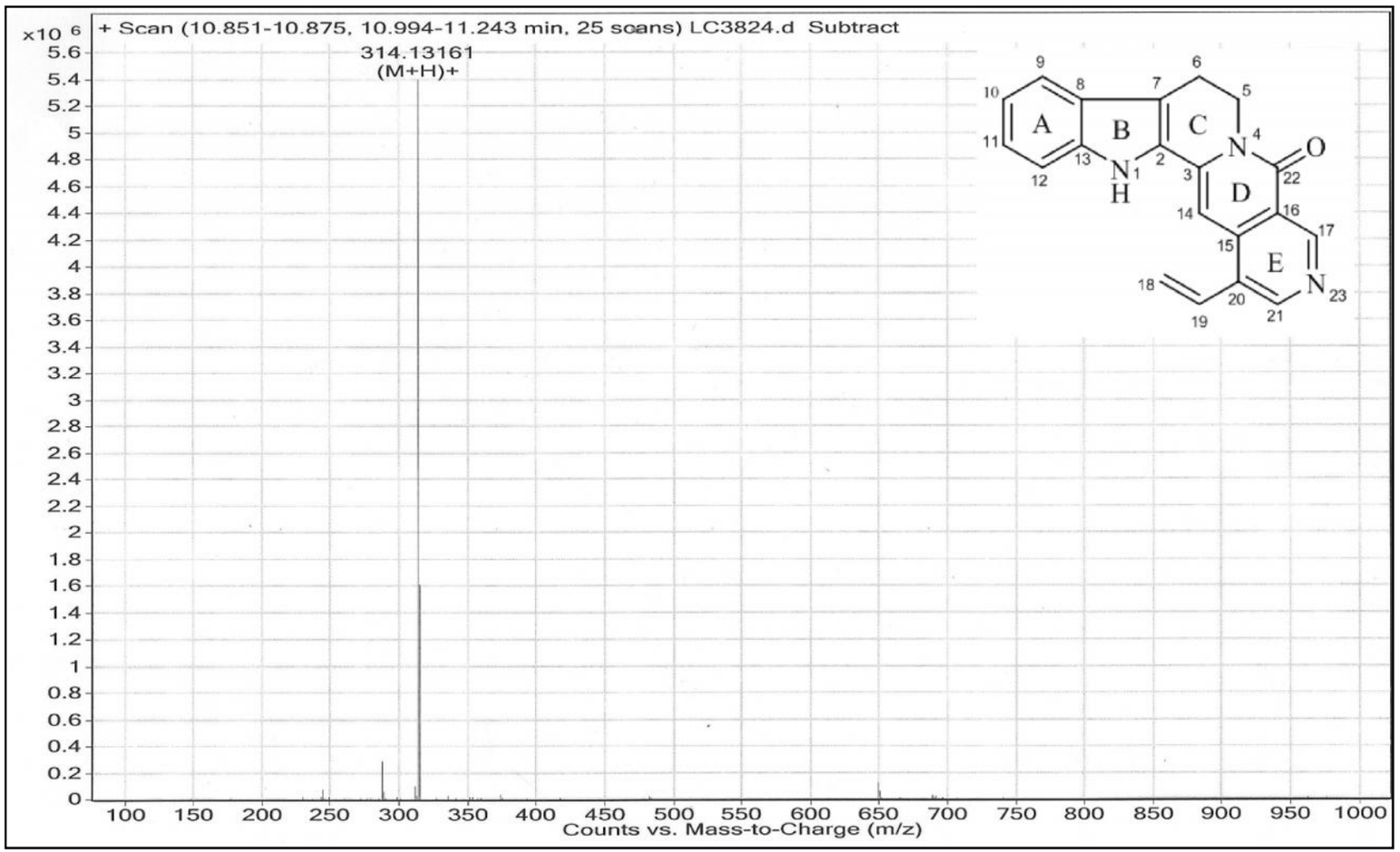

Figure 3.27: LCMS Spectrum of Angustine **42**

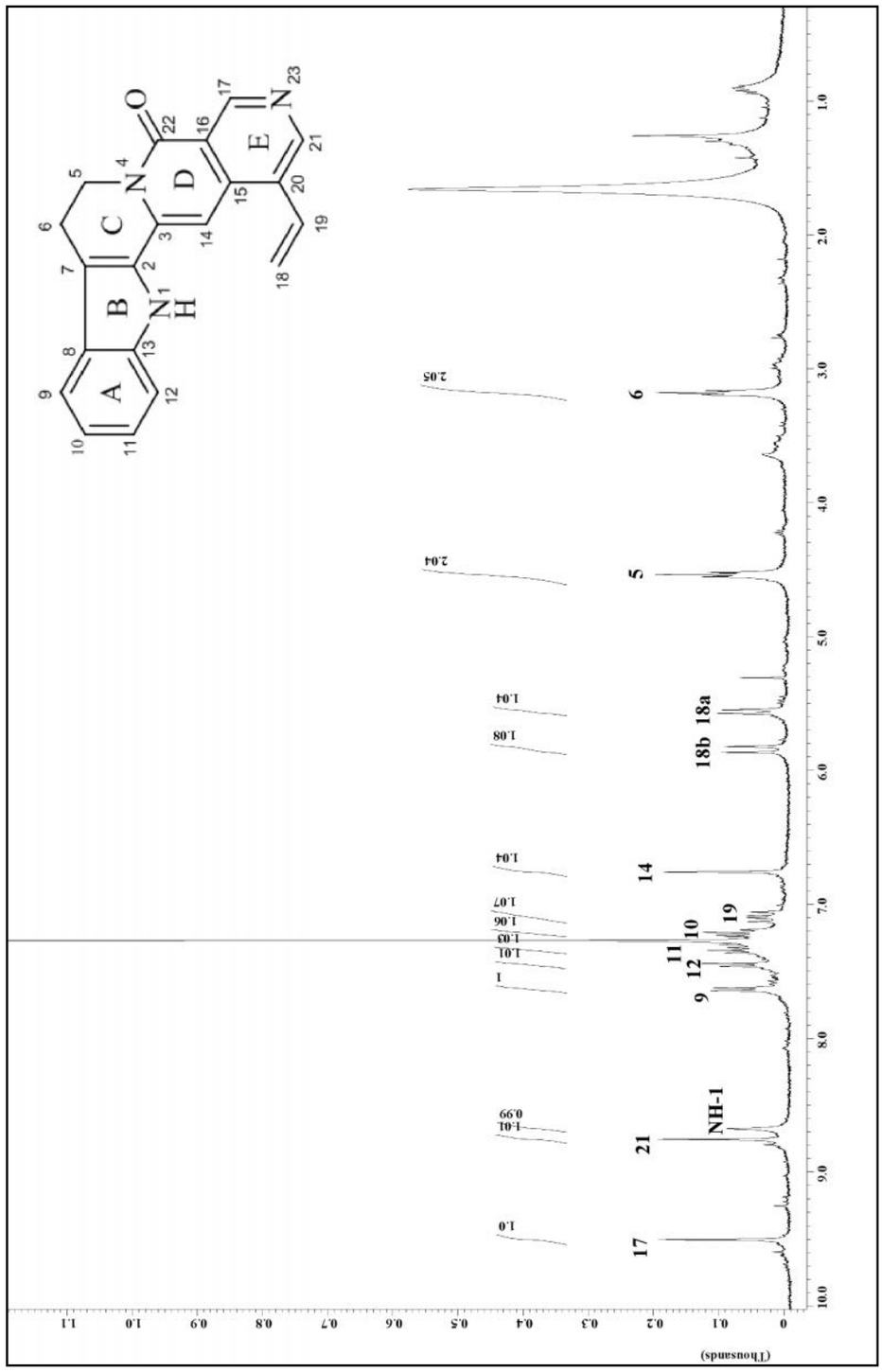

Figure 3.28: ^{1}H NMR Spectrum of Angustine **42**

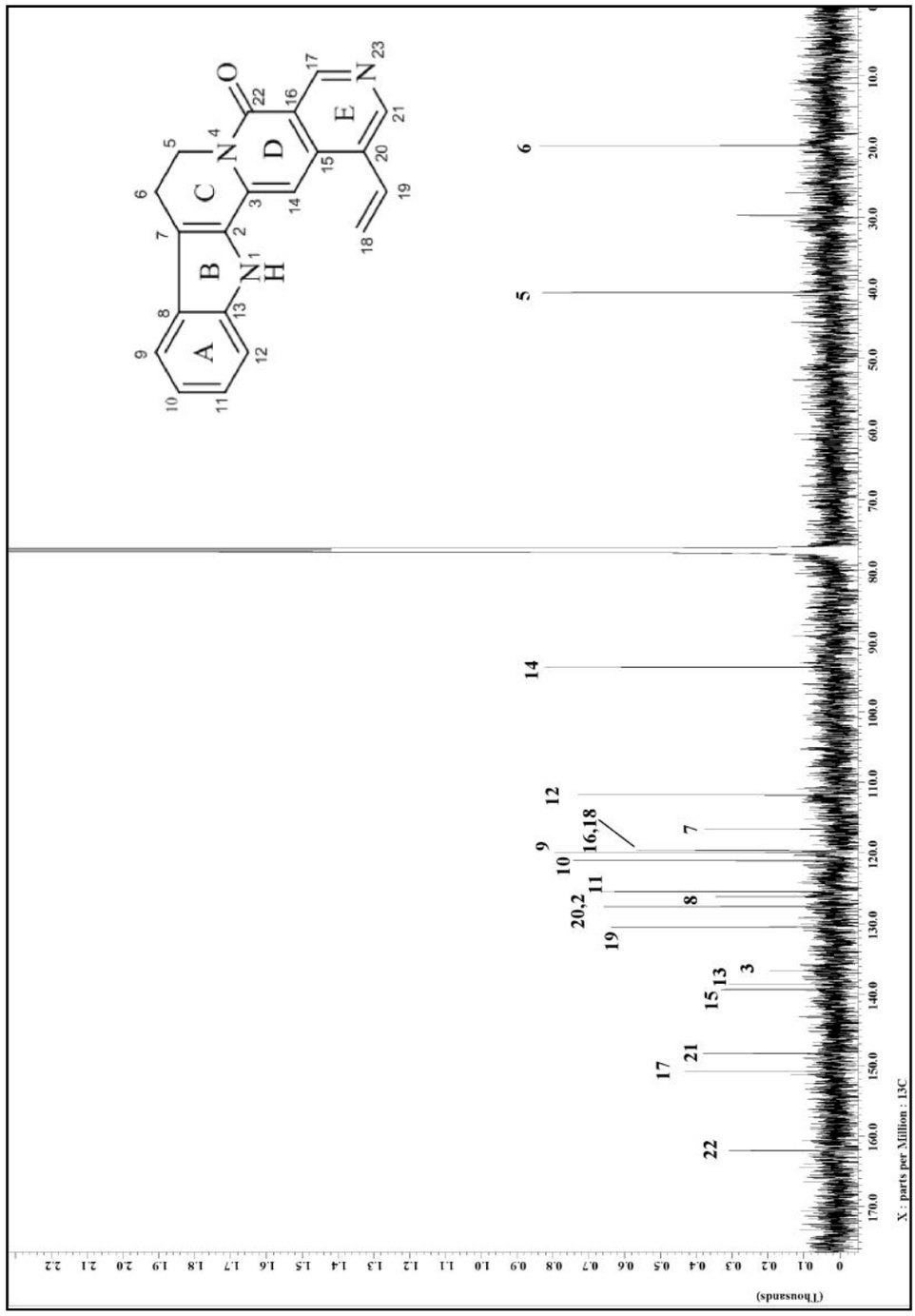

Figure 3.29: ^{13}C NMR Spectrum of Angustine **42**

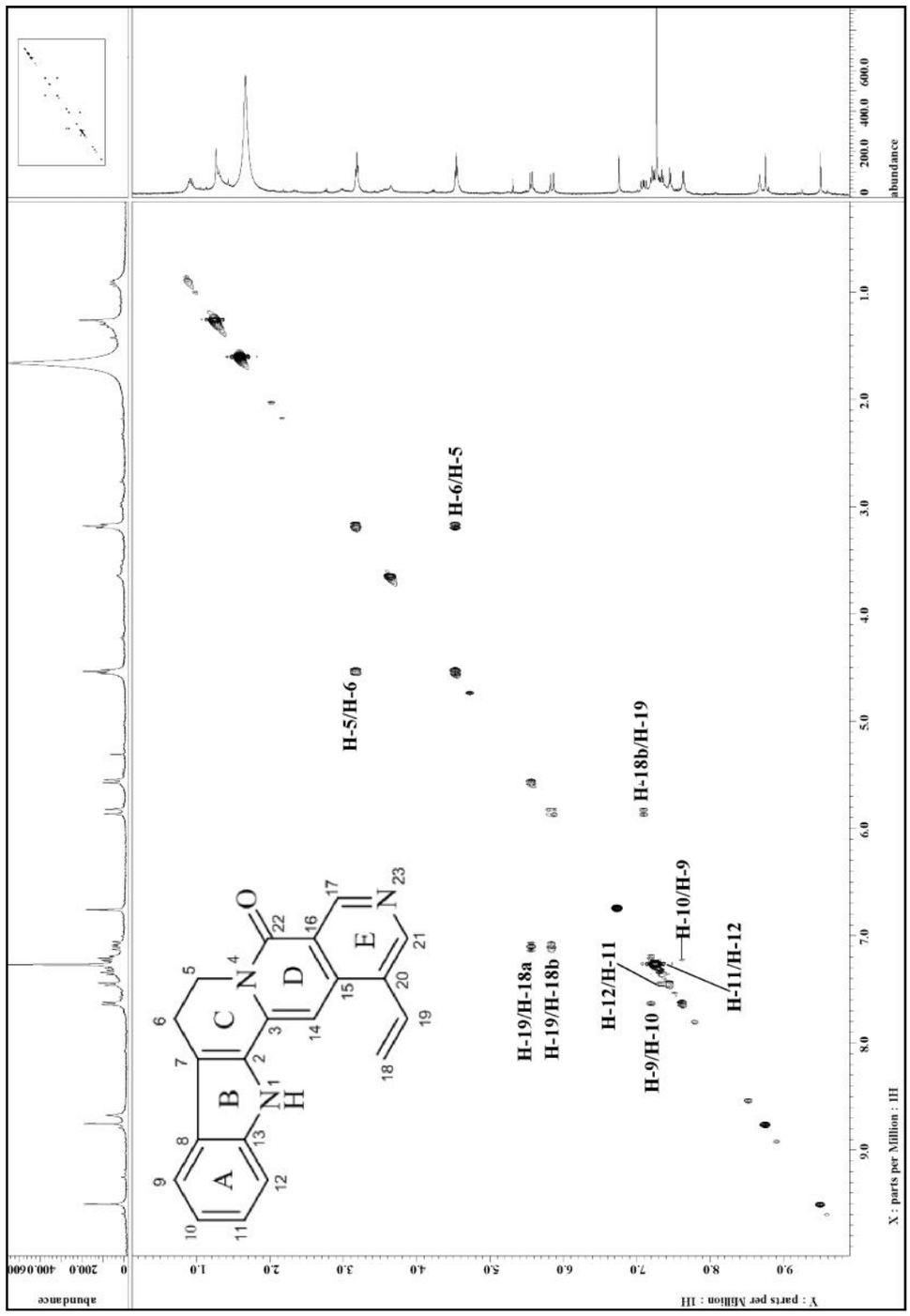

Figure 3.30: COSY Spectrum of Angustine **42**

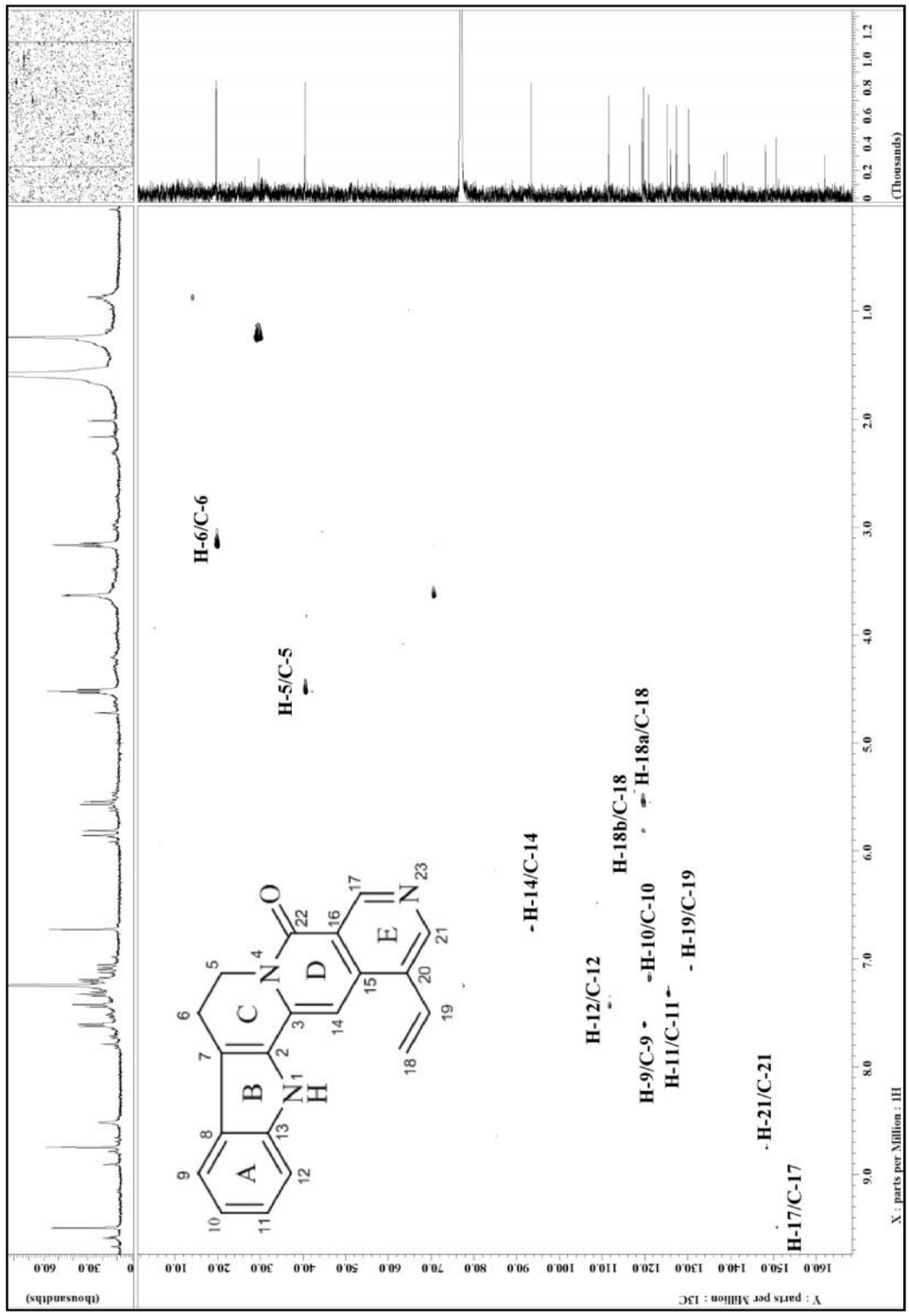

Figure 3.31: HSQC Spectrum of Angustine **42**

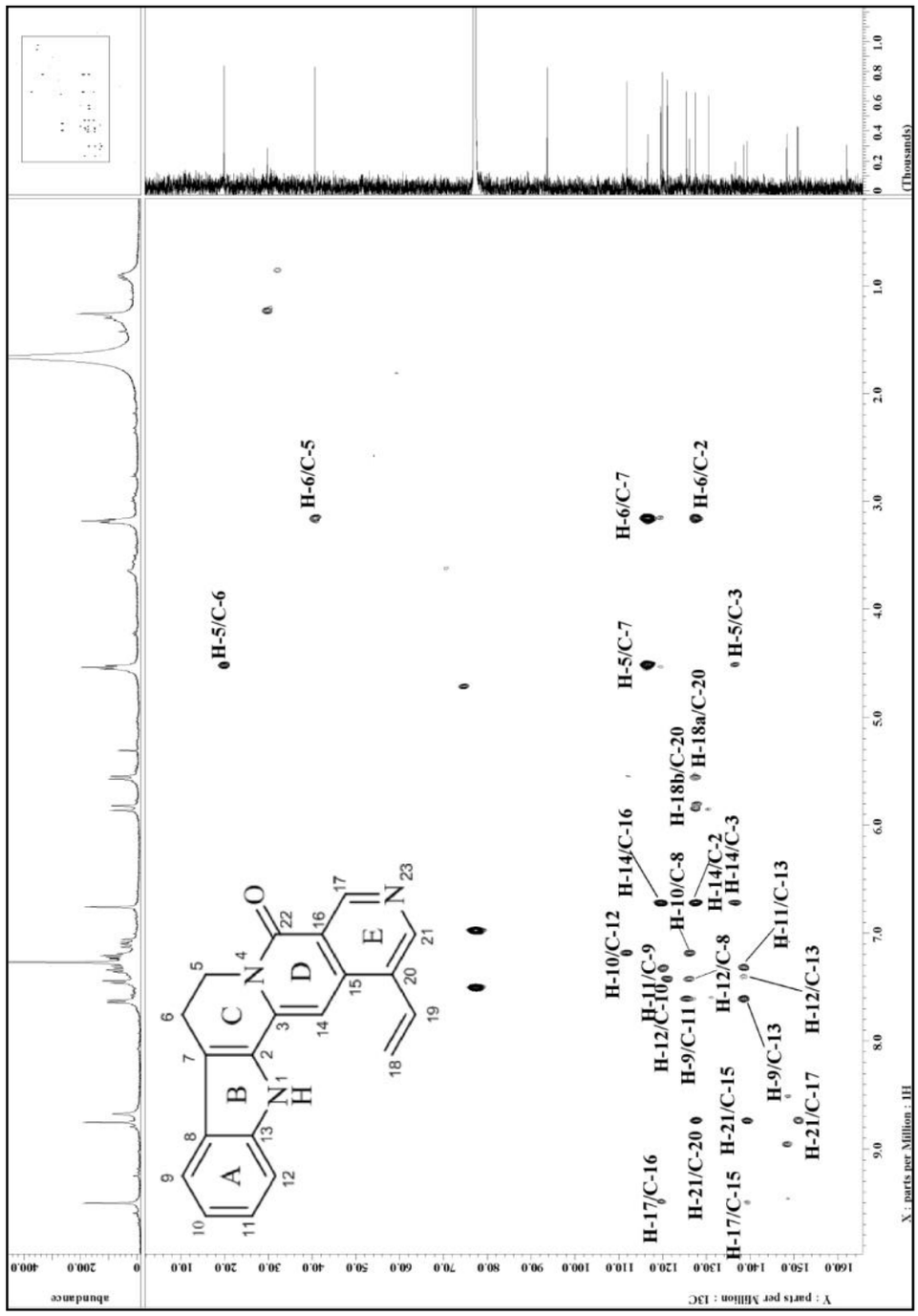

Figure 3.32: HMBC Spectrum of Angustine **42**

3.2.5 Angustoline 43

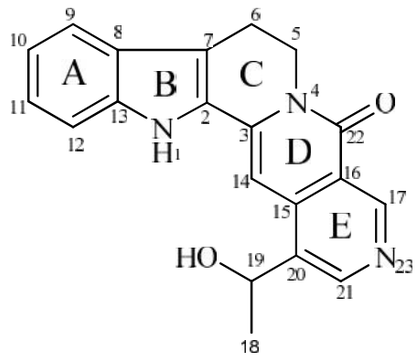

43

Angustoline **43** $[\alpha]_D^{23}$ -72.7 (*c* 0.11, $CHCl_3$) was obtained as an orange amorphous solid. It has a molecular formula of $C_{20}H_{17}N_3O_2$ as deduced from the LCMS-IT-TOF spectrum (Figure 3.34) which showed a pseudomolecular ion peak at *m/z* $[M+H]^+$ 332.1096 (calc. 332.1394). The UV spectrum showed absorption bands at 394, 375 and 210 nm.[15] IR spectrum revealed absorption bands at 3282, 1653 and 1103 cm^{-1} suggesting the presence of O-H group, conjugated lactam carbonyl and C-O functionalities respectively.[15]

The ^1H and ^{13}C-NMR spectra (Figure 3.35 and Figure 3.36) of angustoline **43** is reminiscent with those of nauclefine **63** especially for ring A, B, C and D. The difference is the substitution at C-20. A doublet of proton signal was observed in the shielded region at δ_H 1.44 (3H, *d*, *J* = 6.4 Hz, H_3-18) and a quartet of proton signal at δ_H 5.21 (1H, *q*, *J* = 6.4 Hz, H-19) which correlated with the carbon signals at δ_C 25.0 (C-18) and δ_C 65.0 (C-19) respectively in the HSQC spectrum, thus implying the presence of hydroxyethyl moiety [–CH(OH)-CH_3].

The ^{13}C-NMR and DEPT (Figure 3.37) spectra of angustoline **43** showed a total of twenty carbon signals; one methyl, two methylenes, eight methines, eight quaternary carbons and one carbonyl carbon. The deshielded C-3 which is vicinally located to N-4 gave its signal at δ_C 137.0. The lactam carbon (C-22) resonated downfield at δ_C 162.0.

H-17 and H-21 gave singlets at δ_H 9.90 and δ_H 9.26 respectively. The HMBC spectrum showed correlations between H_3-18 and C-19, H_3-18 and C-20 (δ_C 134.8), H-19 and C-20, H-21 and C-20 suggesting that the hydroxyethyl group is linked to pyridine (ring E) through C-20 (Figure 3.33).

From the analysis of the spectroscopic data obtained (Table 3.6) and comparison with the literature values,[15,72,78] the structure of angustoline **43** was confirmed without doubt.

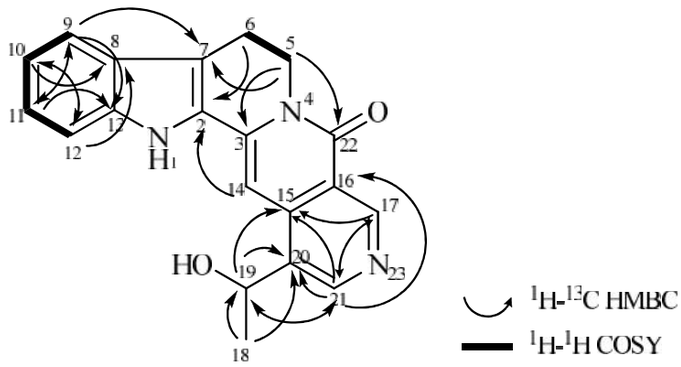

Figure 3.33: Selected COSY and HMBC Correlations of Angustoline **43**

Table 3.6: ^{1}H-NMR (400 MHz) and ^{13}C-NMR (100 MHz) Spectral Data of Angustoline **43** in C_5D_5N.

Position	**^{1}H δ_H (multiplicity, *J* in Hz)**		**^{13}C δ_C**	
	Experimental (C_5D_5N)	**Reference* ($CDCl_3$:CD_3OD-4:1)**	**Experimental (C_5D_5N)**	**Reference* ($CDCl_3$:CD_3OD-4:1)**
NH-1	-	-	-	-
2	-	-	128.9	127.5
3	-	-	137.0	137.4
5	4.53 (*t*, 6.4)	4.51 (*t*, 6.6)	40.6	41.0
6	3.02 (*t*, 6.4)	3.19 (*t*, 6.6)	19.8	20.0
7	-	-	115.1	115.5
8	-	-	126.3	129.9
9	7.69 (*d*, 8.2)	7.61 (*d*, 8.0)	119.9	119.8
10	7.21 (*dt*, 8.2, 1.0)	7.16 (*t*, 7.5)	120.3	120.5
11	7.30 (*dt*, 8.2, 1.0)	7.31 (*t*, 7.5)	124.6	125.1
12	7.42 (*d*, 8.2)	7.46 (*d*, 8.0)	112.2	112.1
13	-	-	139.7	139.3
14	7.20 (*s*)	7.22 (*s*)	94.5	95.0
15	-	-	139.1	140.5
16	-	-	120.0	120.0
17	9.90 (*s*)	9.38 (*s*)	150.4	150.3
18	1.44 (*d*, 6.4)	1.67 (*d*, 6.6)	25.0	23.8
19	5.21 (*q*, 6.4)	5.45 (*q*, 6.6)	65.0	66.2
20	-	-	134.8	134.2
21	9.26 (*s*)	8.60 (*s*)	148.3	146.4
22	-	-	162.0	162.8

*Literature values from Erdelmeier et al. (1992).

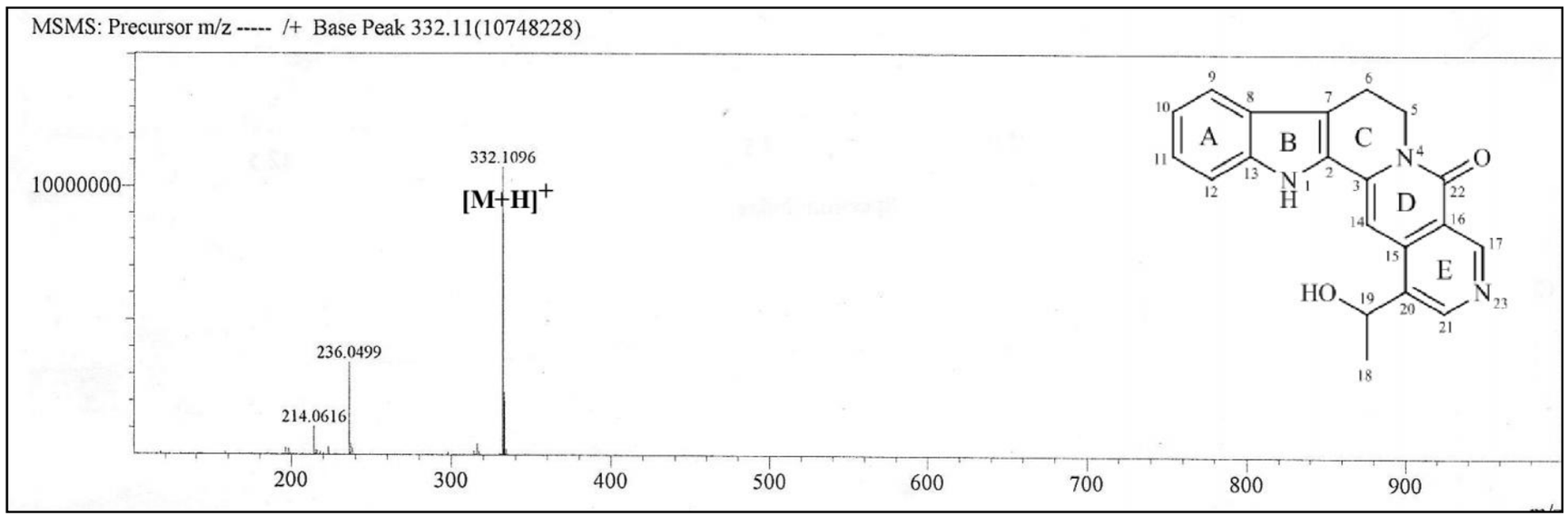

Figure 3.34: LCMS Spectrum of Angustoline **43**

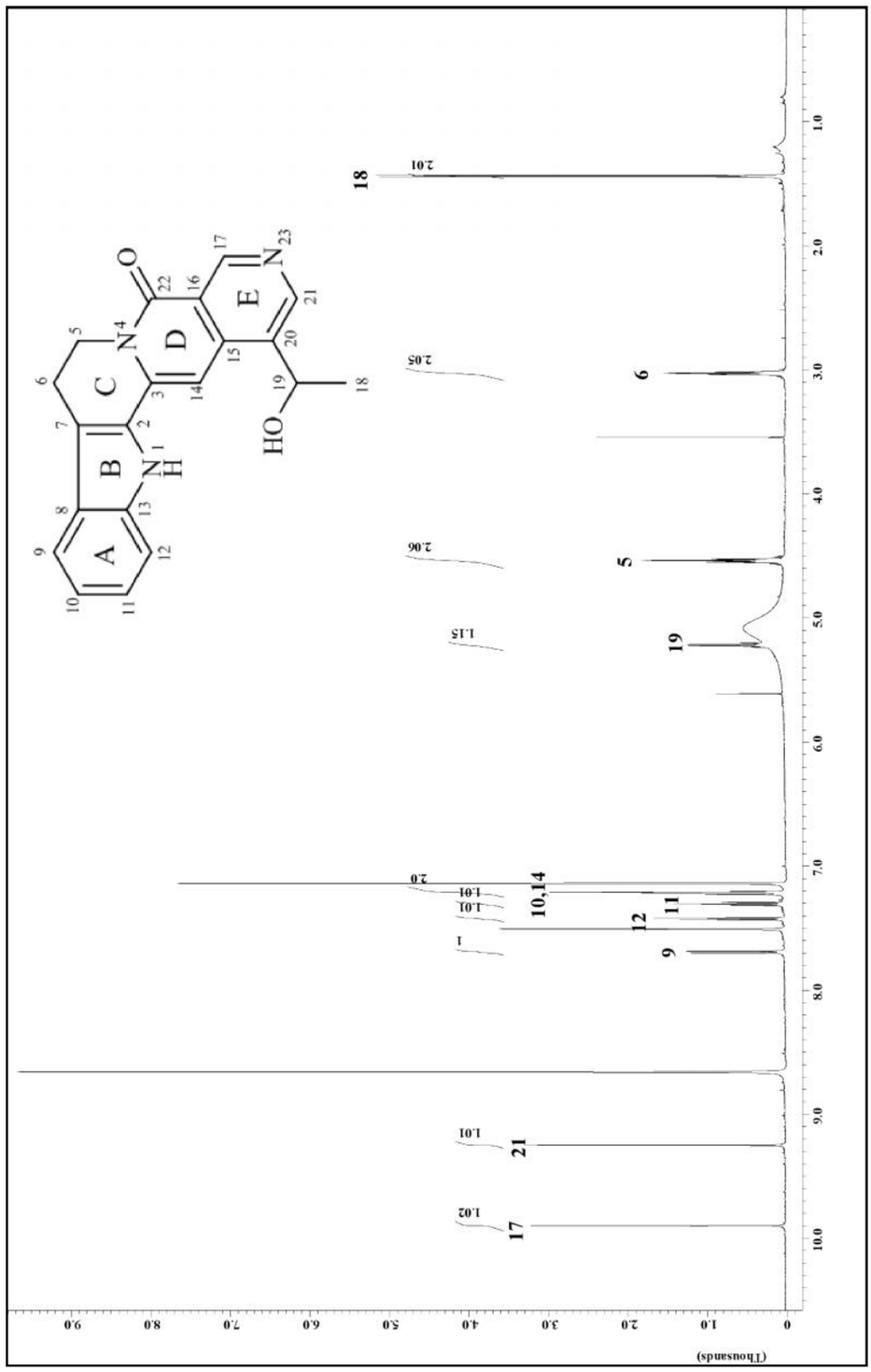

Figure 3.35: ^{1}H NMR Spectrum of Angustoline **43**

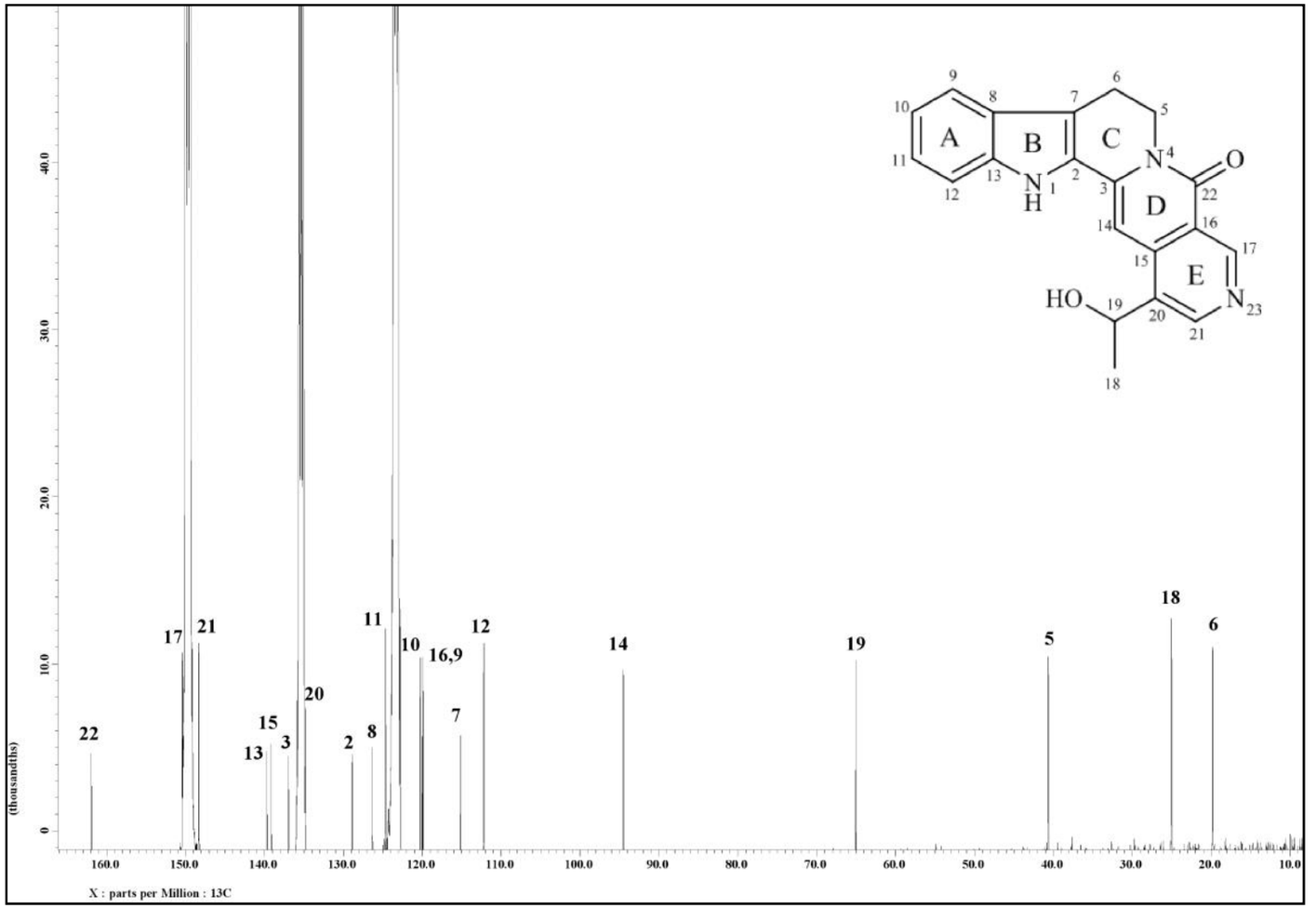

Figure 3.36: ^{13}C NMR Spectrum of Angustoline **43**

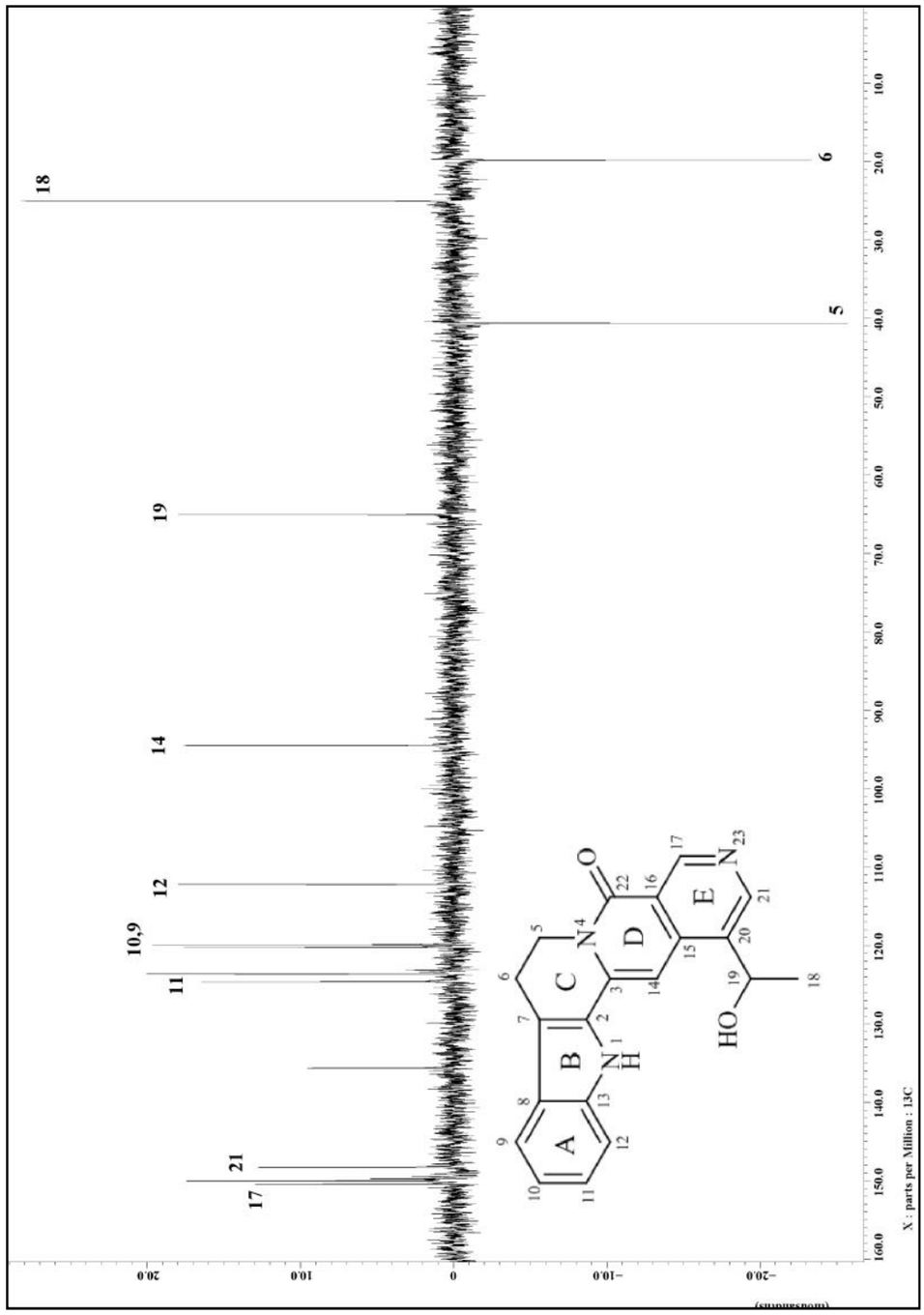

Figure 3.37: DEPT 135 Spectrum of Angustoline **43**

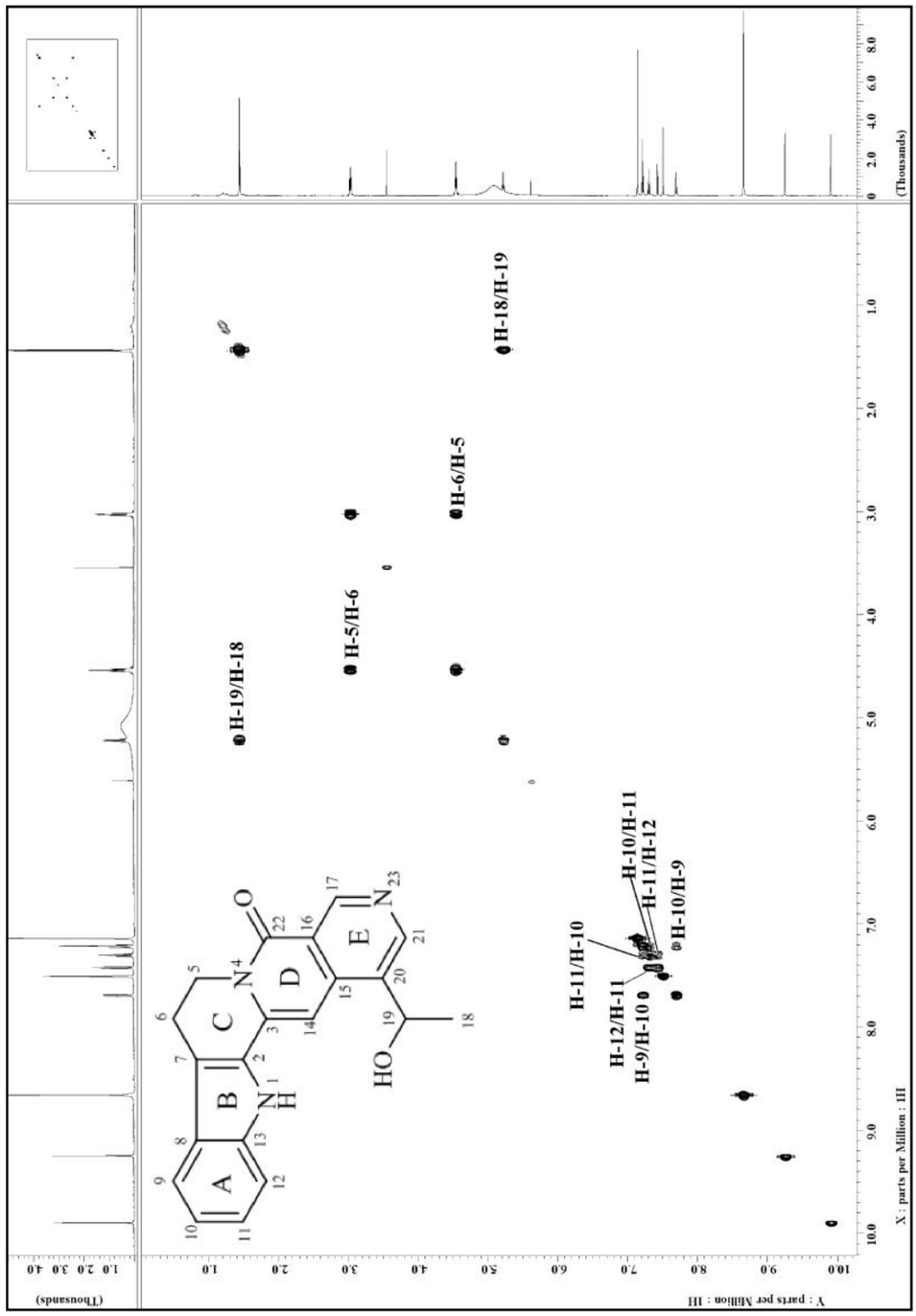

Figure 3.38: COSY Spectrum of Angustoline **43**

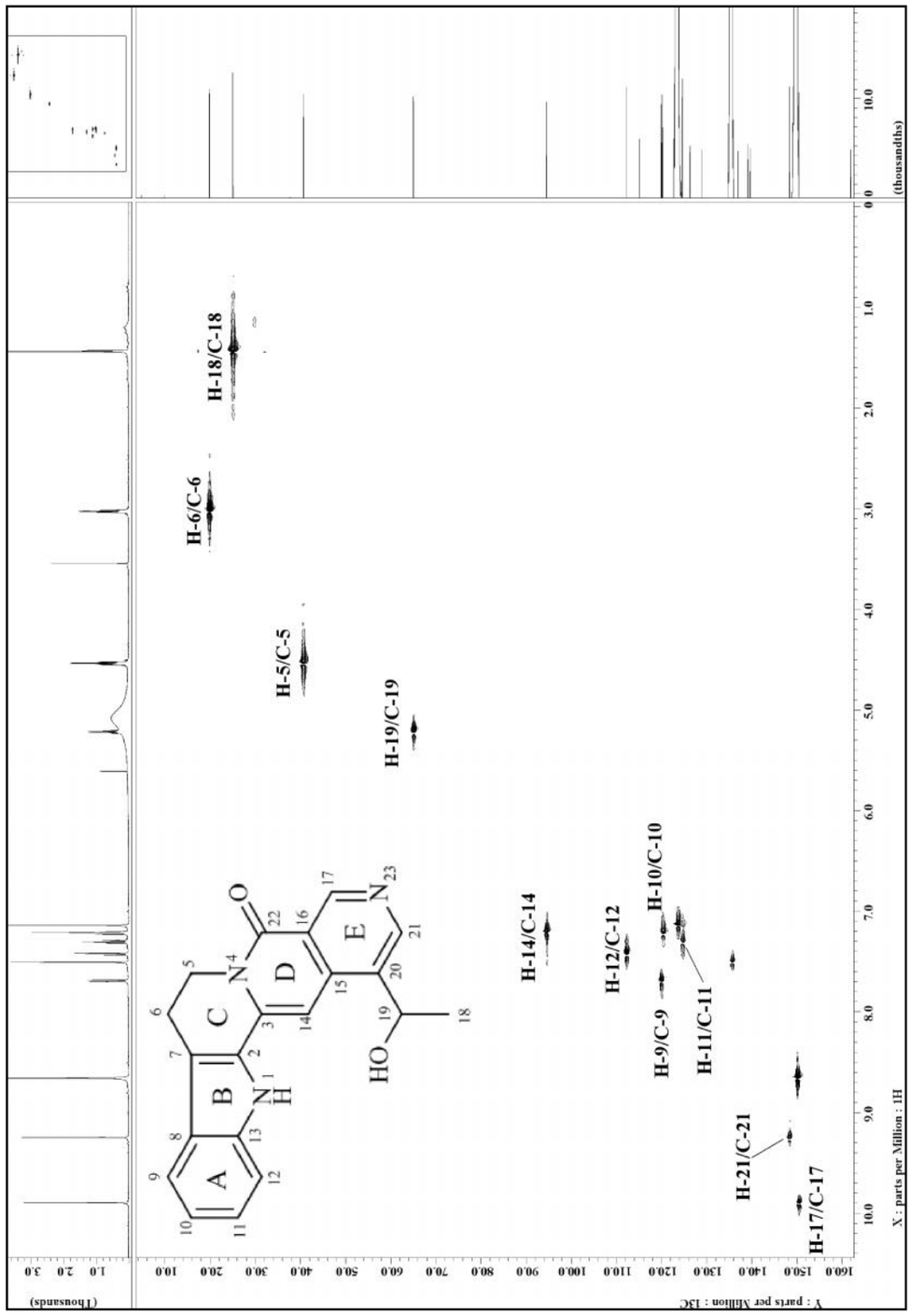

Figure 3.39: HSQC Spectrum of Angustoline **43**

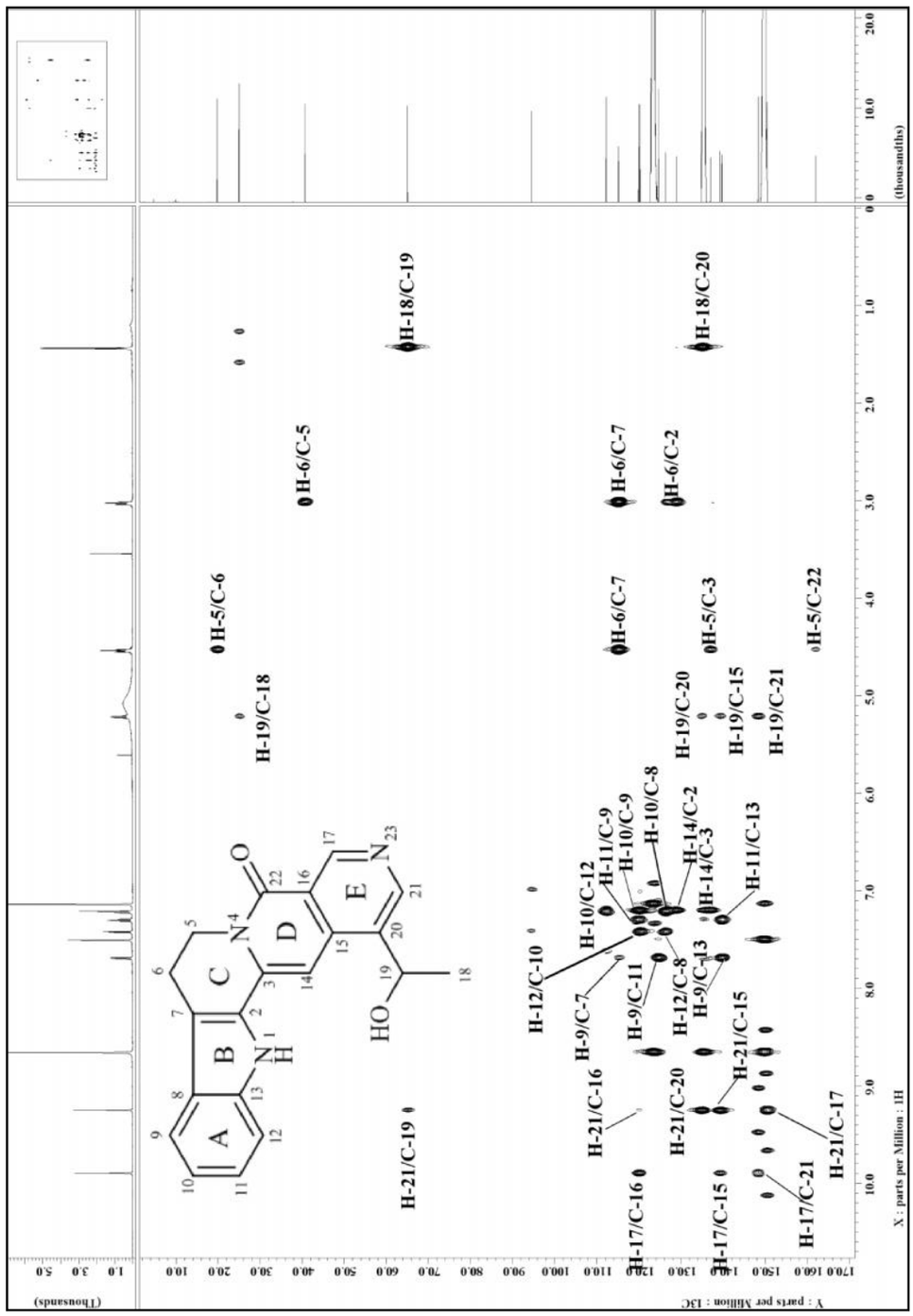

Figure 3.40: HMBC Spectrum of Angustoline **43**

3.2.6 3,14-dihydroangustoline 68

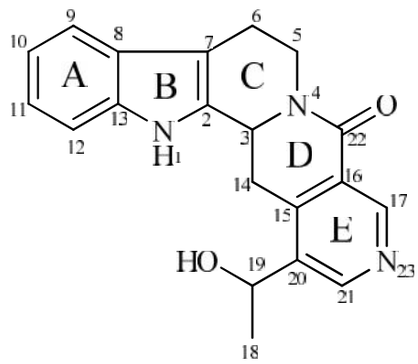

68

3,14-dihydroangustoline **68** $[\alpha]_D^{23}$ -88.9 (*c* 0.09, $CHCl_3$) was isolated as a yellowish amorphous solid. The LCMS-IT-TOF spectrum (Figure 3.42) displayed a pseudomolecular ion peak at *m/z* $[M+H]^+$ 334.1267, corresponding to the molecular formula of $C_{20}H_{19}N_3O_2$ (calc. 334.1550) with thirteen degrees of unsaturation which consisted eight double bonds and five rings. Its UV spectrum exhibited absorption peaks at 393, 375 and 219 nm.[15] Absorption bands at 3279, 1640 and 1101 cm^{-1} were observed in IR spectrum which were due to O-H, conjugated lactam carbonyl and C-O stretching vibration.[15]

Upon comparison of the ^1H and ^{13}C-NMR spectra (Figure 3.43 and Figure 3.44) of 3,14-dihydroangustoline **68** with angustoline **43**, a marked similarity was observed except for the signals at C-3 and C-14. A broad doublet of H-3 at δ_H 4.95 (1H, *br d*, *J* = 12.3 Hz, H-3) and a two doublet of doublets at δ_H 2.81 (1H, *dd*, *J* = 16.7, 12.3 Hz, H-14a) and at δ_H 3.80 (1H, *dd*, *J* = 16.7, 3.7 Hz, H-14b) which belong to two geminal protons at C-14 were observed. Besides, the two geminal protons of H_2-5 are not equivalent and resulted in appearance of a multiplet of H-5a (δ_H 2.90-2.97) and a broad doublet of H-5b (δ_H 5.11).

The ^{13}C-NMR and DEPT (Figure 3.45) spectra of this alkaloid indicated a total of twenty carbon signals; one methyl, three methylenes, eight methines, seven quaternary

carbons and one carbonyl carbon. A carbonyl signal of a δ lactam ring was observed at δ_C 163.5 (C-22). The HMBC spectrum showed correlations of H-14a with C-15 (δ_C 143.0), H-17 (δ_H 9.06) with C-15 and C-16 (δ_C 124.7), H-21 (δ_H 8.72) with C-15 suggesting the connectivity of ring D with ring E through C-15 and C-16. In addition, HMBC correlation of H-18 (δ_H 1.47) with C-19 (δ_C 65.0) and C-20 (δ_C 137.2) indicated that an hydroxyethyl group is connected to pyridine (ring E) (Figure 3.41).

The spectroscopic data obtained (Table 3.7) were consistent with those found in the literature,[15] thus confirming the identity of 3,14-dihydroangustoline **68**.

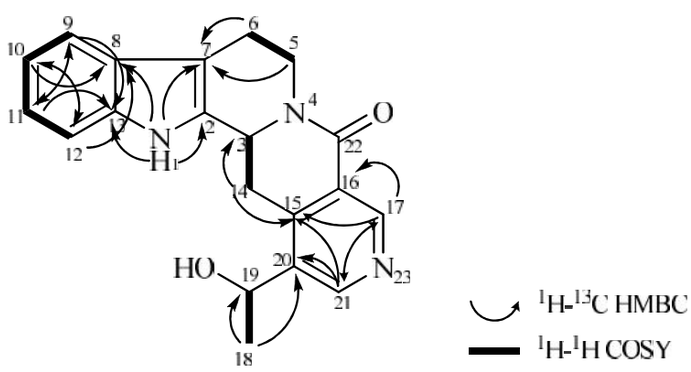

Figure 3.41: COSY and HMBC Correlations of 3,14-dihydroangustoline **68**

Table 3.7: ^{1}H-NMR (400 MHz) and ^{13}C-NMR (100 MHz) Spectral Data of 3,14-dihydroangustoline **68** in $CDCl_3$.

Position	**^{1}H δ_H (multiplicity, *J* in Hz)**		**^{13}C δ_C**	
	Experimental ($CDCl_3$)	**Reference* ($CDCl_3$: CD_3OD -4:1)**	**Experimental ($CDCl_3$)**	**Reference* ($CDCl_3$: CD_3OD -4:1)**
NH-1	9.54 (*br s*)	-	-	-
2	-	-	131.8	131.6
3	4.95 (*br d*, 12.3)	4.96 (*br*, ~13)	51.3	51.3
5a	2.90-2.97 (*m*,overlapped)	2.98 (*dt*, 12.6, 4.5)	39.6	39.5
5b	5.11 (*br d*, 12.8)	5.13 (*d*, *br*, 12.6)		
6	2.90-2.97 (*m*, overlapped)	2.92 (*m*)	20.9	20.9
7	-	-	109.4	109.6
8	-	-	126.5	126.5
9	7.52 (*d*, 7.7)	7.54 (*d*, 7.8)	118.6	118.6
10	7.11 (*t*, 7.7)	7.14 (*t*, 7.8)	119.9	119.9
11	7.18 (*t*, 7.7)	7.20 (*t*, 7.8)	122.5	122.5
12	7.35 (*d*, 7.7)	7.37 (*d*, 7.8)	111.3	111.2
13	-	-	136.8	137.1
14a	2.81 (*dd*, 16.7, 12.3)	2.86 (*dd*, 16.5, 13.0)	31.3	31.4
14b	3.78 (*dd*, 16.7, 3.7)	3.76 (*dd*, 16.5, 3.6)		
15	-	-	143.0	142.7
16	-	-	124.7	124.6
17	9.06 (*s*)	9.08 (*s*)	148.6	149.3
18	1.47 (*d*, 6.9)	1.51 (*d*, 6.7)	23.9	24.0
19	5.17 (*q*, 6.4)	5.20 (*q*, 6.7)	65.0	65.2
20	-	-	137.2	136.8
21	8.72 (*s*)	8.75 (*s*)	149.2	148.7
22	-	-	163.5	163.4

* Literature values from Erdelmeier et al. (1992).

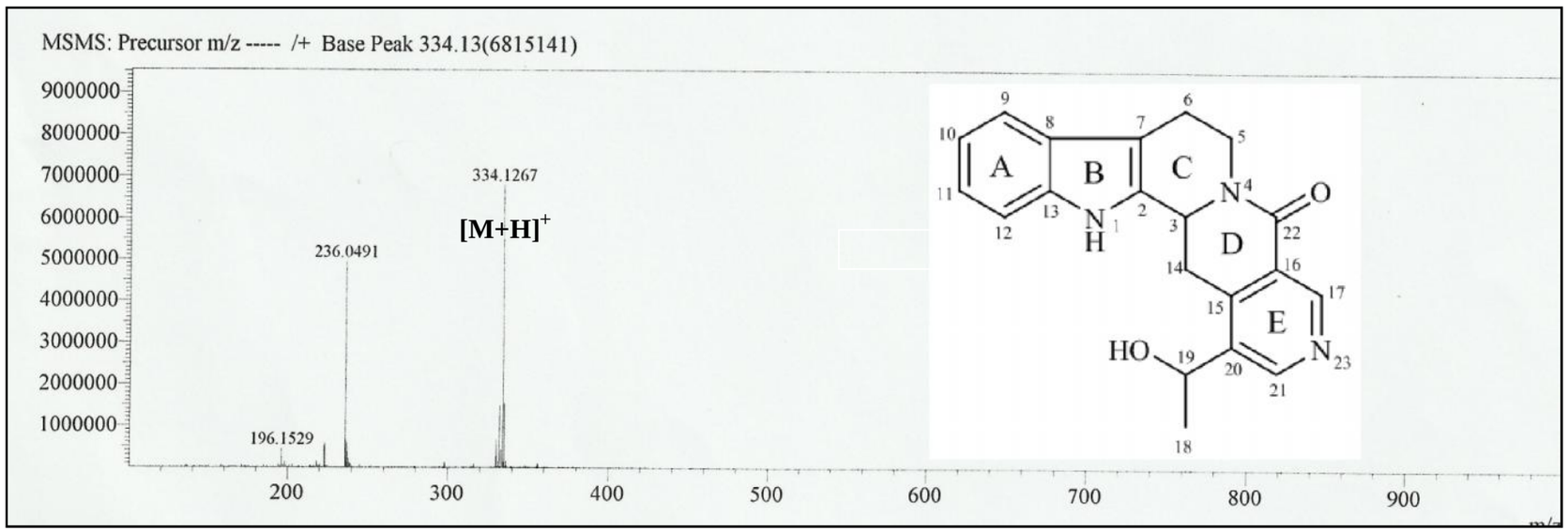

Figure 3.42: LCMS Spectrum of 3,14-dihydroangustoline **68**

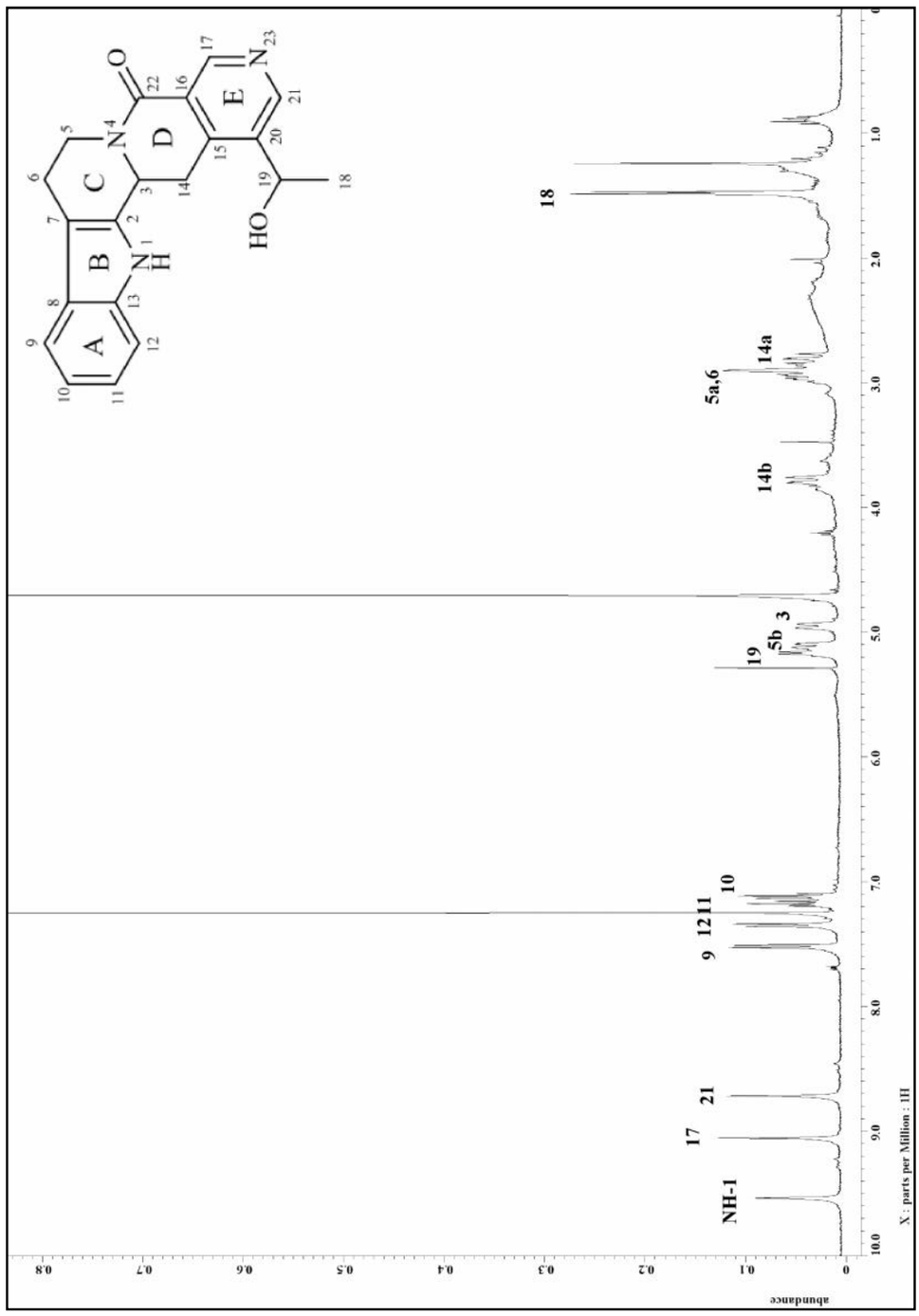

Figure 3.43: ^{1}H NMR Spectrum of 3,14 dihydroangustoline **68**

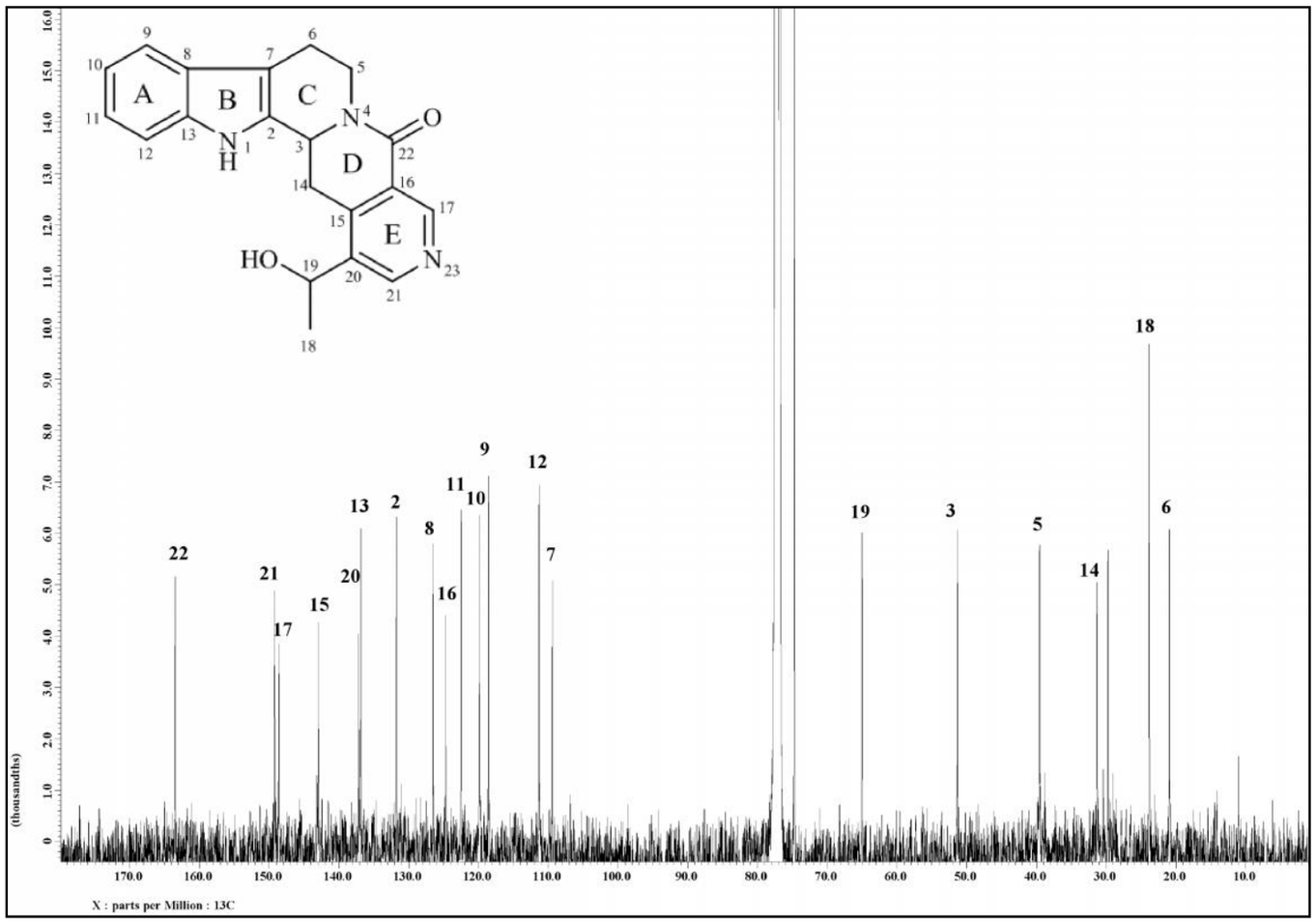

Figure 3.44: ^{13}C NMR Spectrum of 3,14-dihydroangustoline **68**

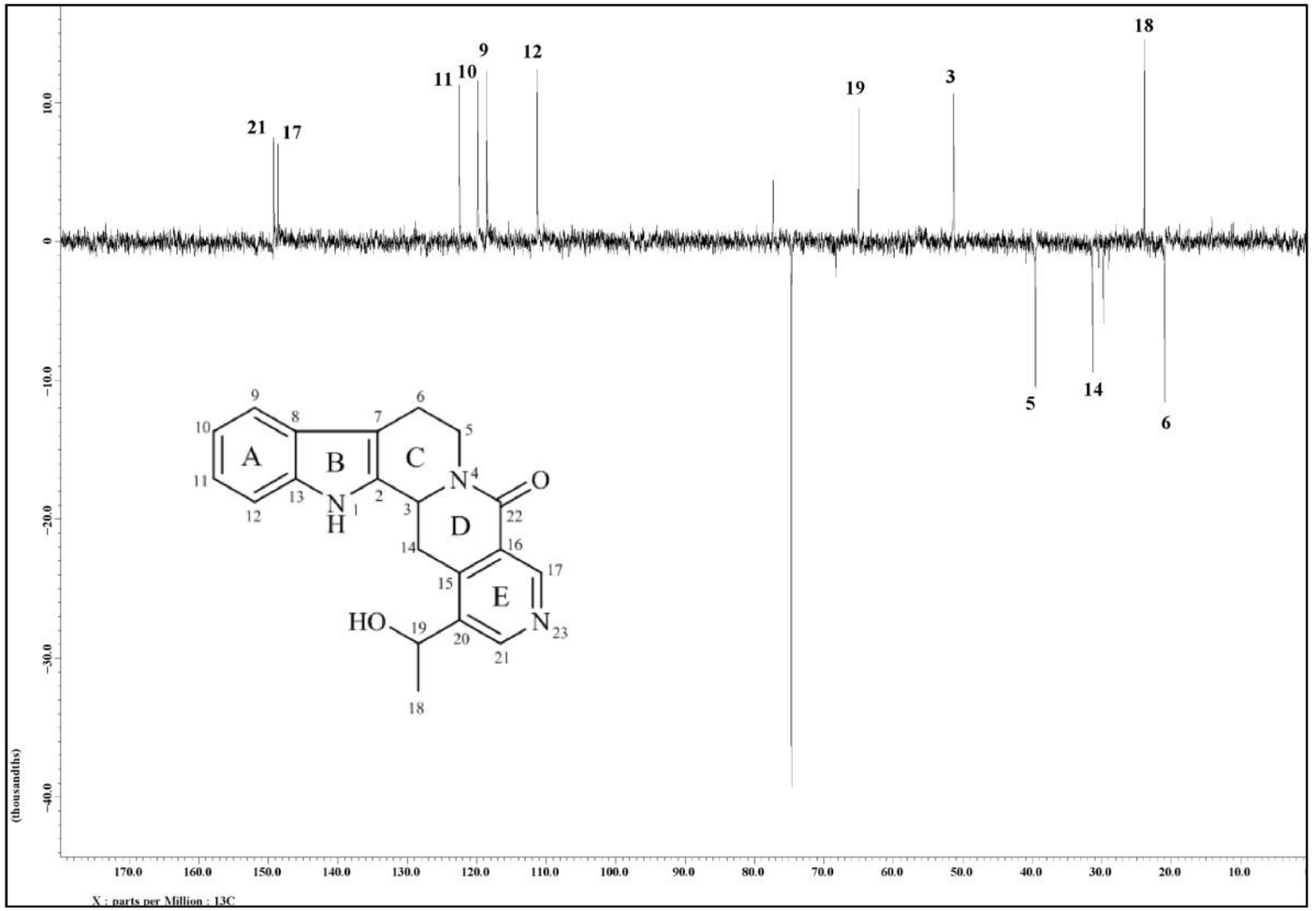

Figure 3.45: DEPT 135 Spectrum of 3,14-dihydroangustoline **68**

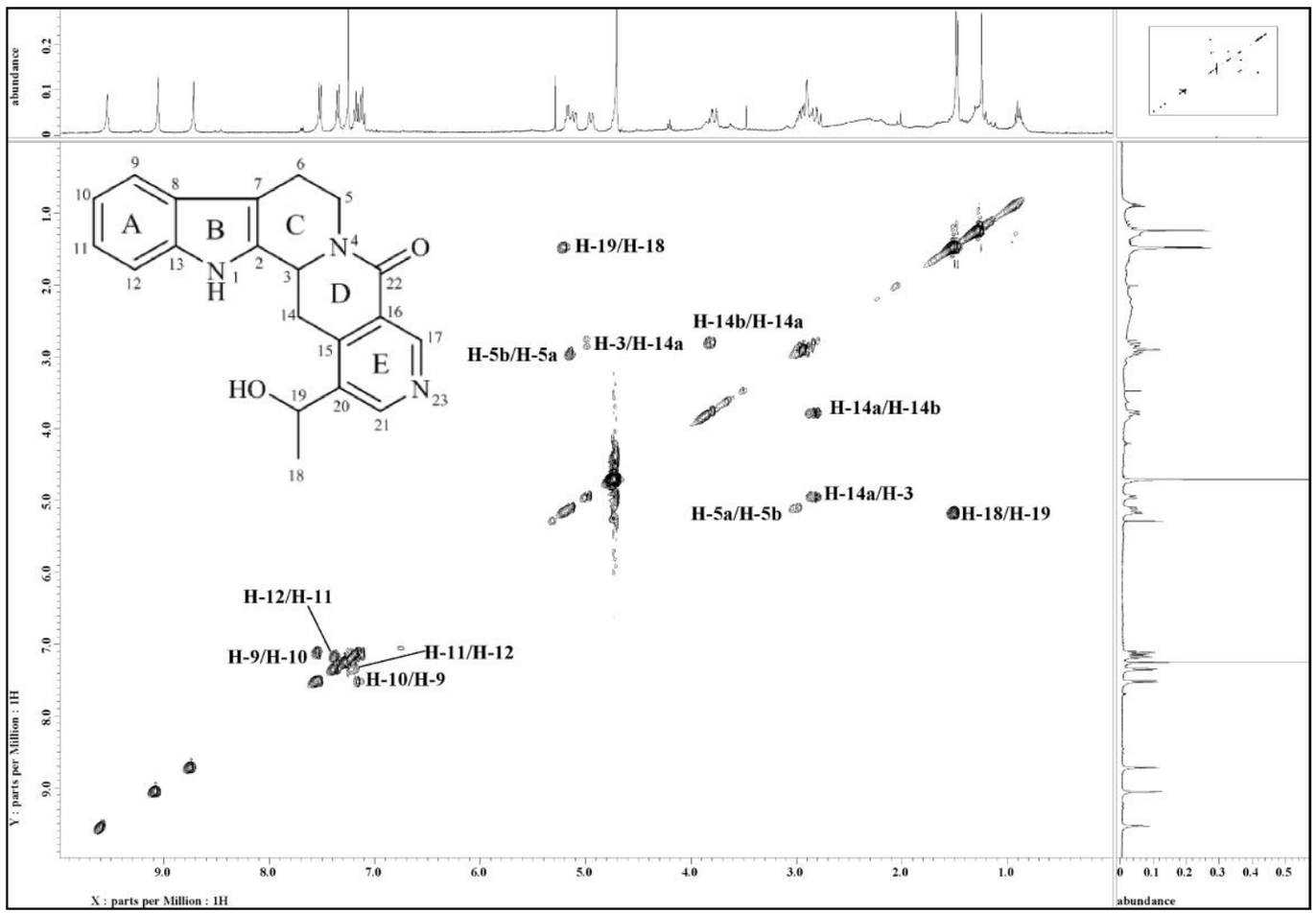

Figure 3.46: COSY Spectrum of 3,14-dihydroangustoline **68**

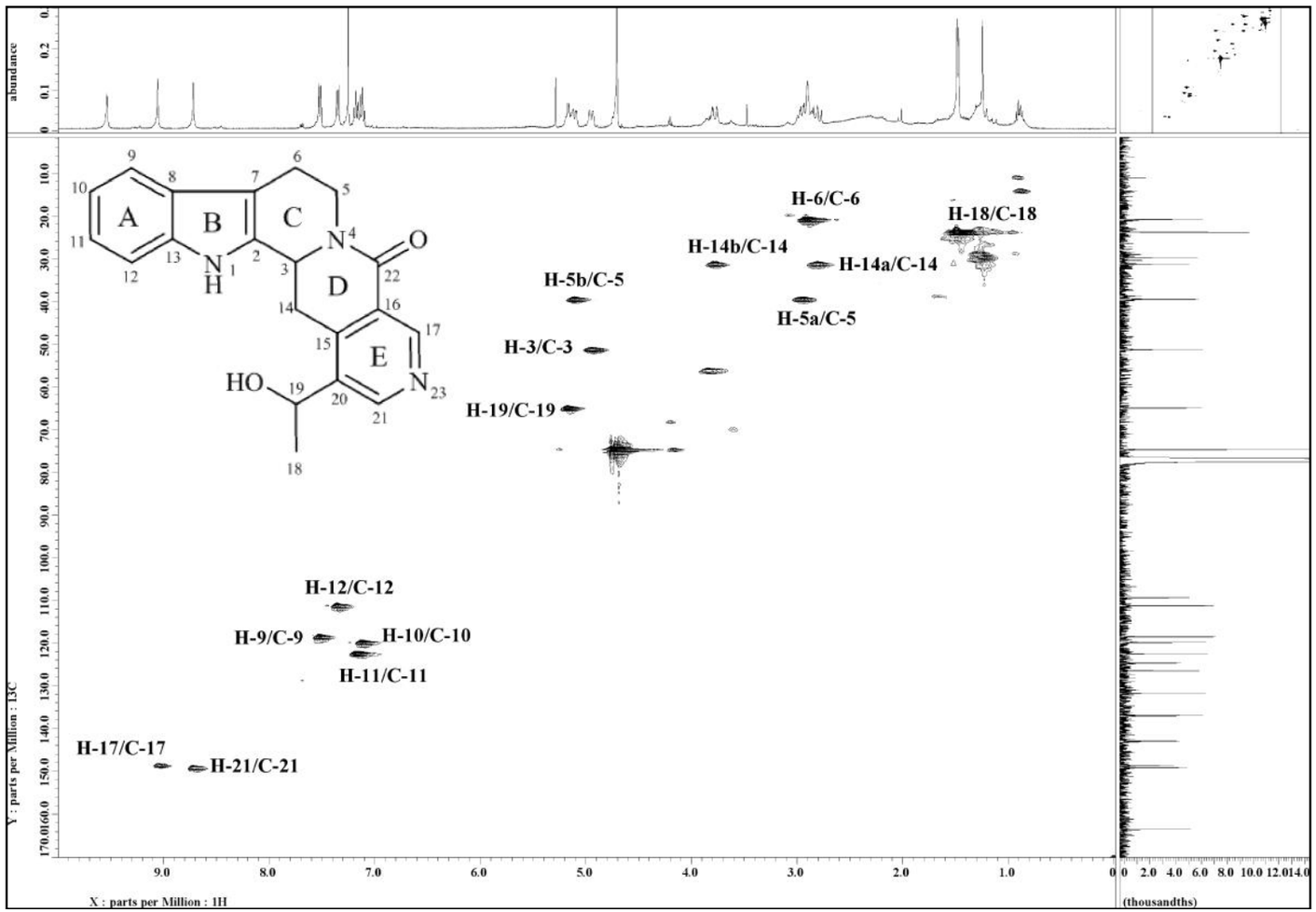

Figure 3.47: HSQC Spectrum of 3,14-dihydroangustoline **68**

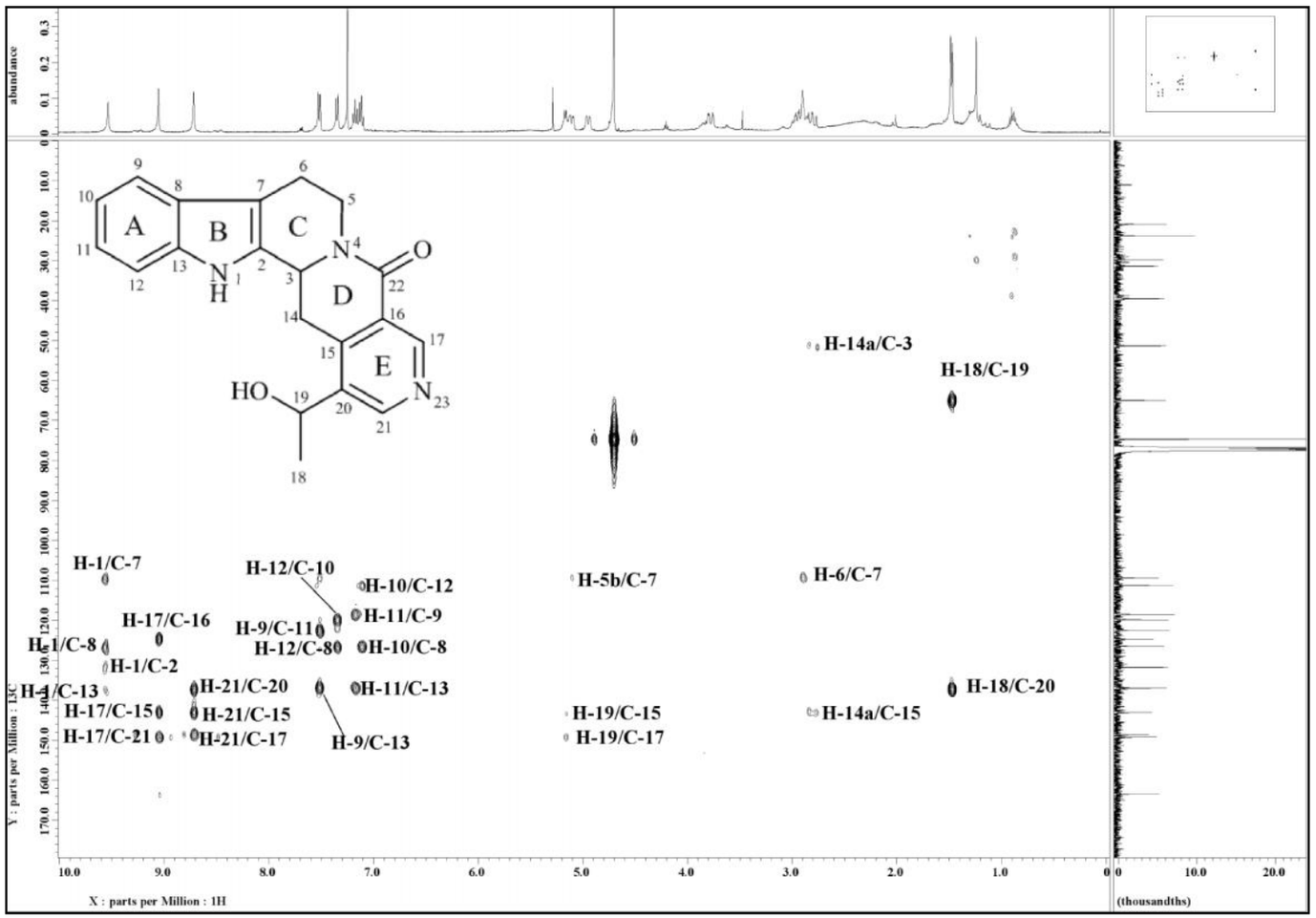

Figure 3.48: HMBC Spectrum of 3,14-dihydroangustoline **68**

3.2.7 Angustidine 44

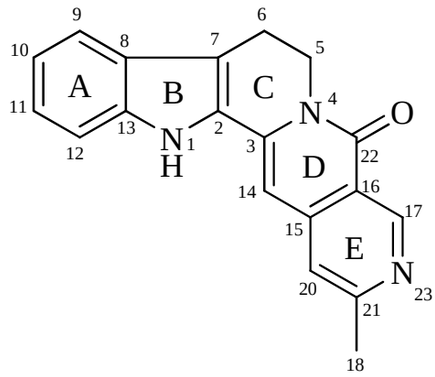

44

Angustidine **44** was obtained as an orange amorphous solid. Its molecular formula of $C_{19}H_{15}N_3O$ was determined through LCMS-IT-TOF spectrum (Figure 3.50) which showed a pseudomolecular ion peak $[M+H]^+$ at *m/z* 302.1317 (calc. 302.1288). In the UV spectrum, absorption maxima were observed at 391, 288 and 229 nm.[72] The IR spectrum revealed absorption bands at 3401 and 1644 cm^{-1} for stretching vibration of N-H and conjugated lactam carbonyl respectively.[80]

The ^1H and ^{13}C-NMR spectra (Figure 3.51 and Figure 3.52) of angustidine **44** and nauclefine **63** showed a significant resemblance except for the additional methyl singlet attached to C-21 was observed in the ^1H-NMR of angustidine **44**. Hence, a single proton signal was observed at δ_H 7.01 (1H, *s*, H-20) instead of a doublet in that of nauclefine **63**. Another downfield proton at δ_H 9.79 was assignable to H-17. A singlet was observed at highfield region, δ_H 2.47 which corresponded to carbon signal at δ_C 24.3 suggesting the presence of methyl group.

The ^{13}C-NMR and DEPT (Figure 3.53) spectra of angustidine **44** showed a total of nineteen carbon signals; one methyl, two methylenes, seven methines, eight quaternary carbons and one carbonyl. An upfield carbon signal at δ_C 24.3 was attributed to a methyl group of C-18. HMBC correlations of H_3-18 (δ_H 2.47) to C-20 (δ_C 117.3)

and C-21 (δ_C 161.8), H-20 with C-21 indicated that the methyl group is linked to pyridine (ring E) through C-21 forming a 2-methylpyridine unit (Figure 3.49).

Comprehensive study of the 1D and 2D-NMR spectral (Table 3.8) and comparison with the literature values[15,72] led to the conclusion that the investigated compound is indeed angustidine **44**.

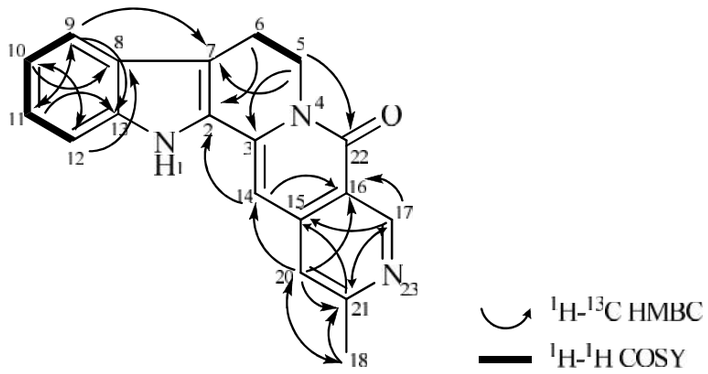

Figure 3.49: Selected COSY and HMBC Correlations of Angustidine **44**

Table 3.8: ^{1}H-NMR (400 MHz) and ^{13}C-NMR (100 MHz) Spectral Data of Angustidine **44** in C_5D_5N.

Position	**^{1}H**		**^{13}C**	
	δ_H (multiplicity, *J* in Hz)		**δ_C**	
	Experimental (C_5D_5N)	**Reference* ($CDCl_3$: CD_3OD-4:1)**	**Experimental (C_5D_5N)**	**Reference* ($CDCl_3$: CD_3OD -4:1)**
NH-1		11.82 (*s*)	-	-
2	-	-	128.7	127.7
3	-	-	137.4	137.0
5	4.49 (*t*, 6.9)	4.38 (*t*, 6.8)	40.6	40.3
6	2.98 (*t*, 6.9)	3.11 (t, 6.5)	19.8	19.3
7	-	-	115.0	114.6
8	-	-	126.3	125.5
9	7.67 (*d*, 8.0)	7.62 (*d*, 8.0)	119.9	119.7
10	7.21 (*t*, 8.0)	7.09 (*t*, 7.6)	120.3	119.9
11	7.31 (*t*, 8.0)	7.23 (*t*, 7.2)	124.6	124.4
12	7.55 (*d*, 8.0)	7.45 (*d*, 8.4)	112.3	112.0
13	-	-	139.6	138.5
14	6.94 (*s*)	6.94 (*s*)	97.4	97.0
15	-	-	142.5	141.9
16	-	-	118.3	119.9
17	9.79 (*s*)	9.21 (*s*)	151.0	150.2
18	2.47 (s)	2.58 (*s*)	24.3	24.3
20	7.01 (*s*)	7.35 (*s*)	117.3	117.2
21	-	-	161.8	160.2
22	-	-	160.3	**145.0

* Literature values from Erdelmeier et al. (1992).
** This value may be mistakenly written. All C=O shifts of lactam signal should be more than δ_C160. The assignment of C-22 of angustidine **44** was confirmed through 1D and 2D-NMR.

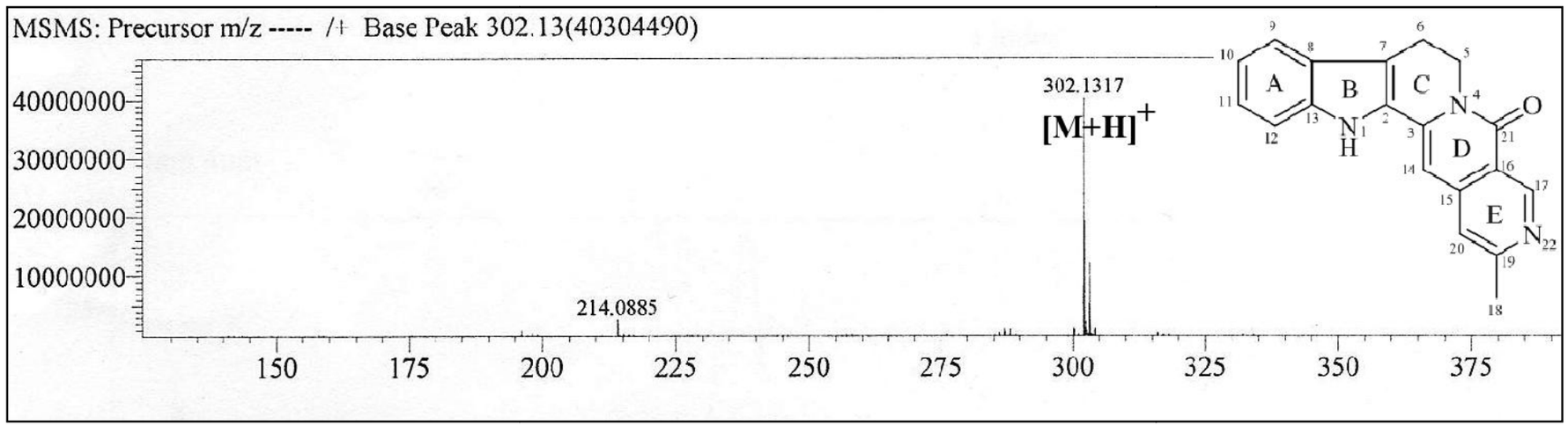

Figure 3.50: LCMS Spectrum of Angustidine **44**

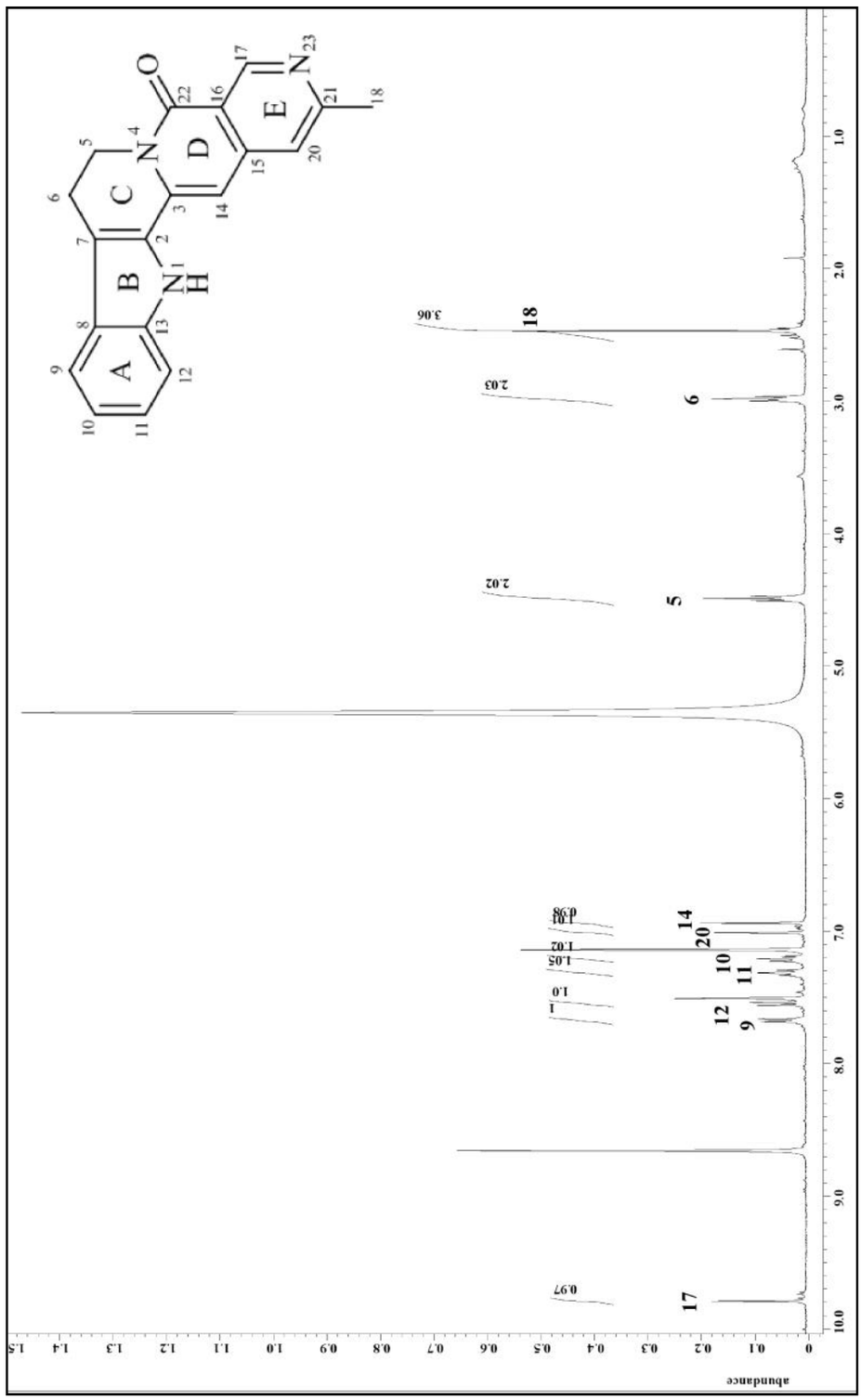

Figure 3.51: ^{1}H NMR Spectrum of Angustidine **44**

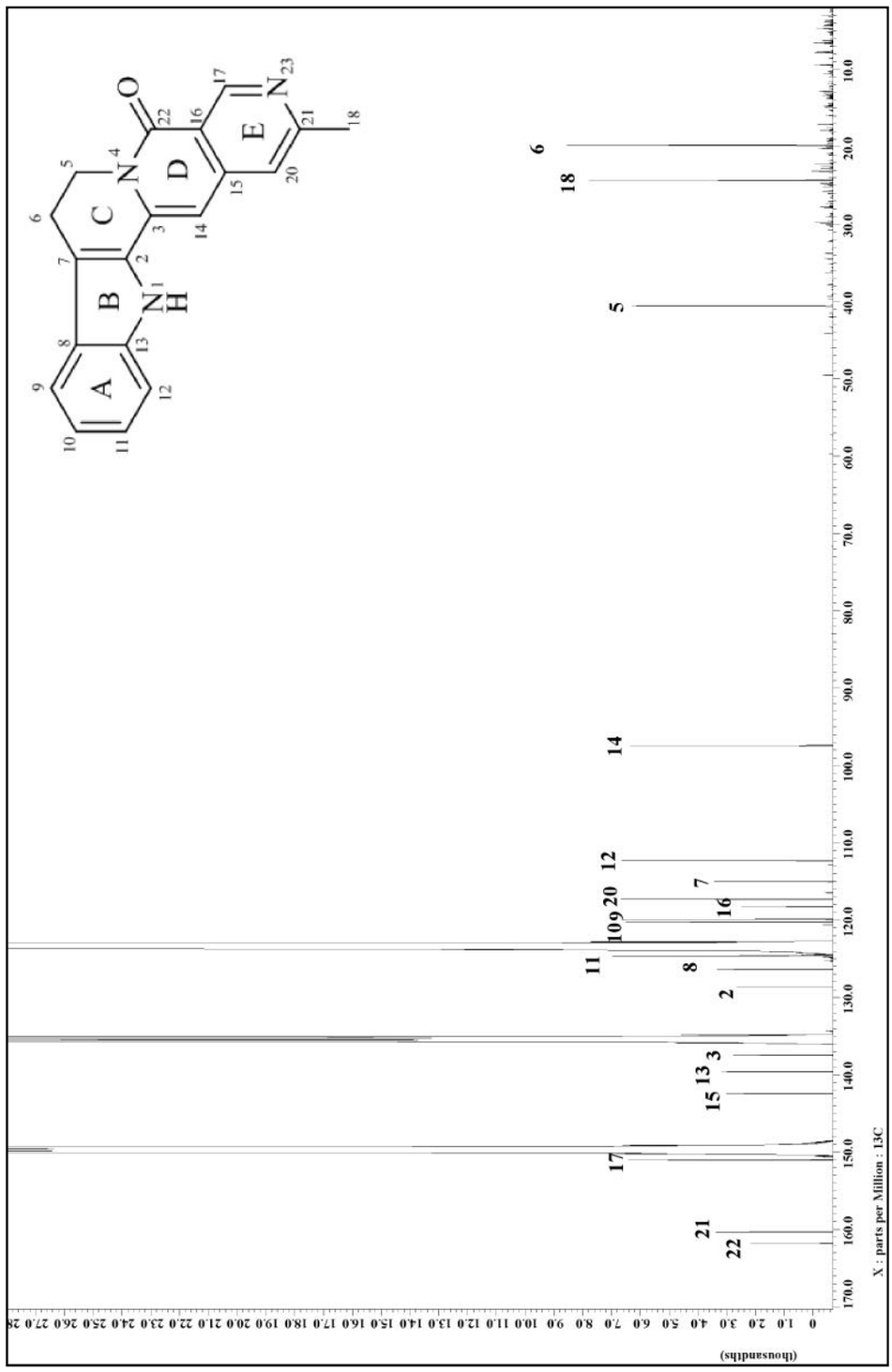

Figure 3.52: ^{13}C NMR Spectrum of Angustidine **44**

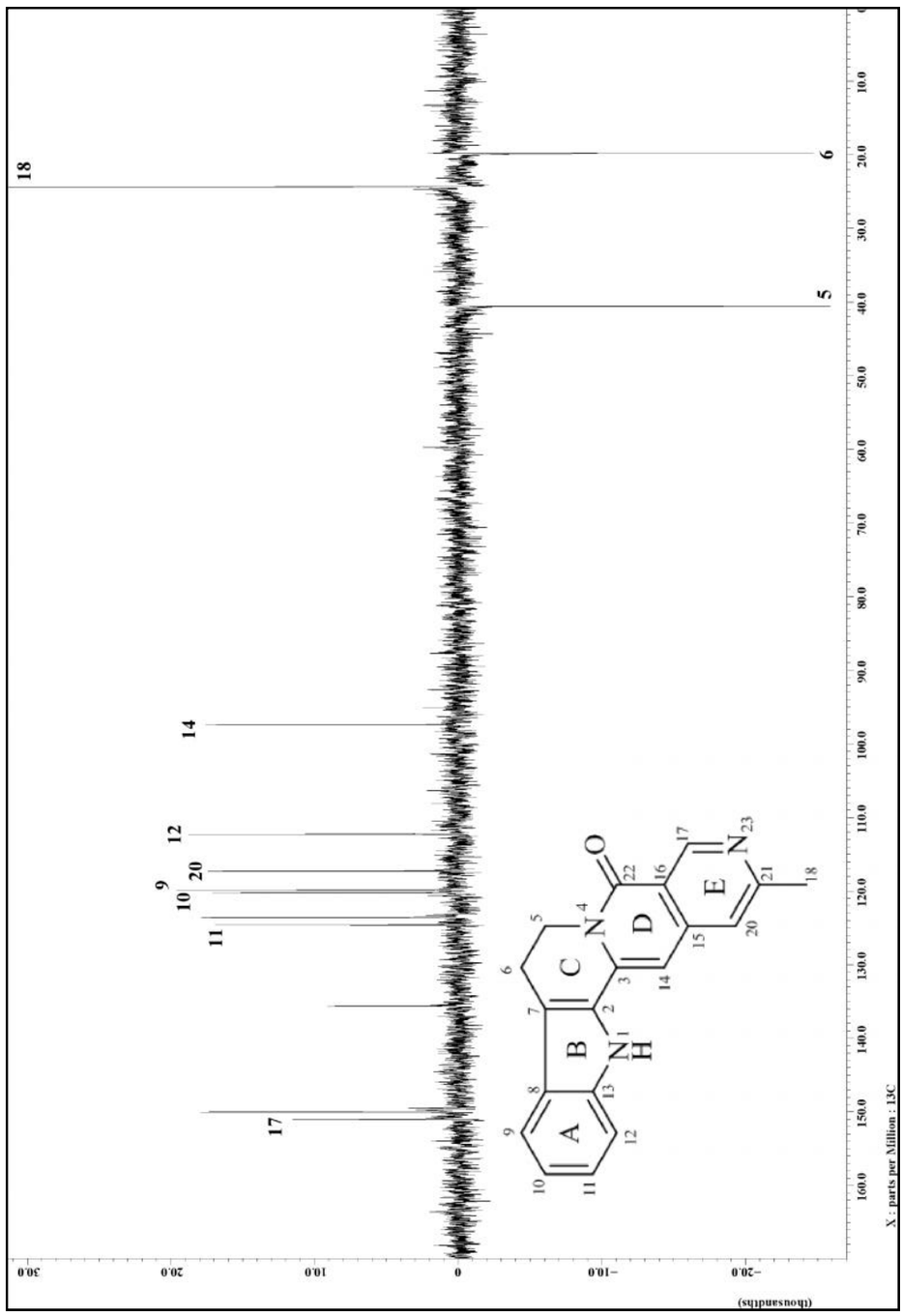

Figure 3.53: DEPT 135 Spectrum of Angustidine **44**

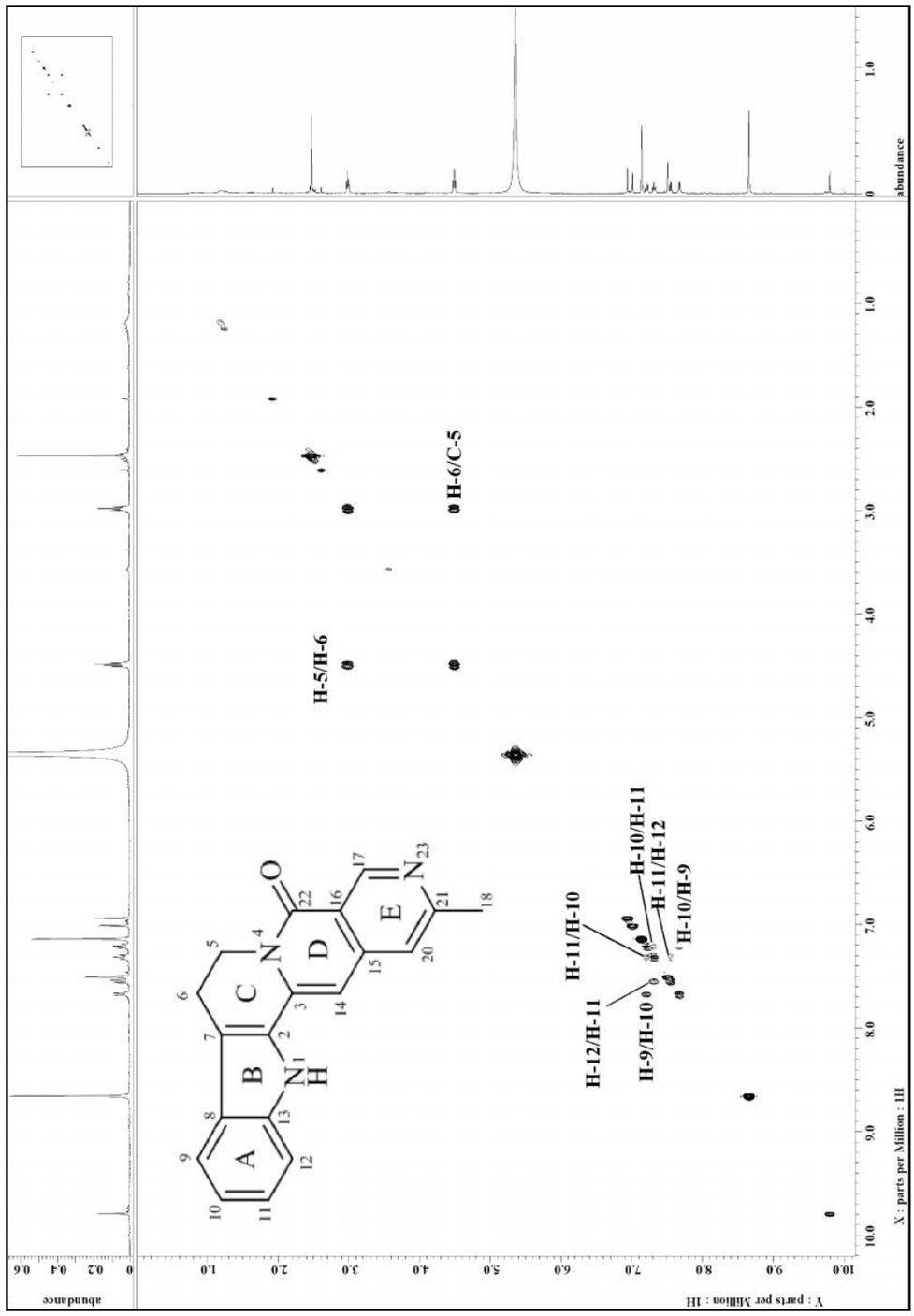

Figure 3.54: COSY Spectrum of Angustidine **44**

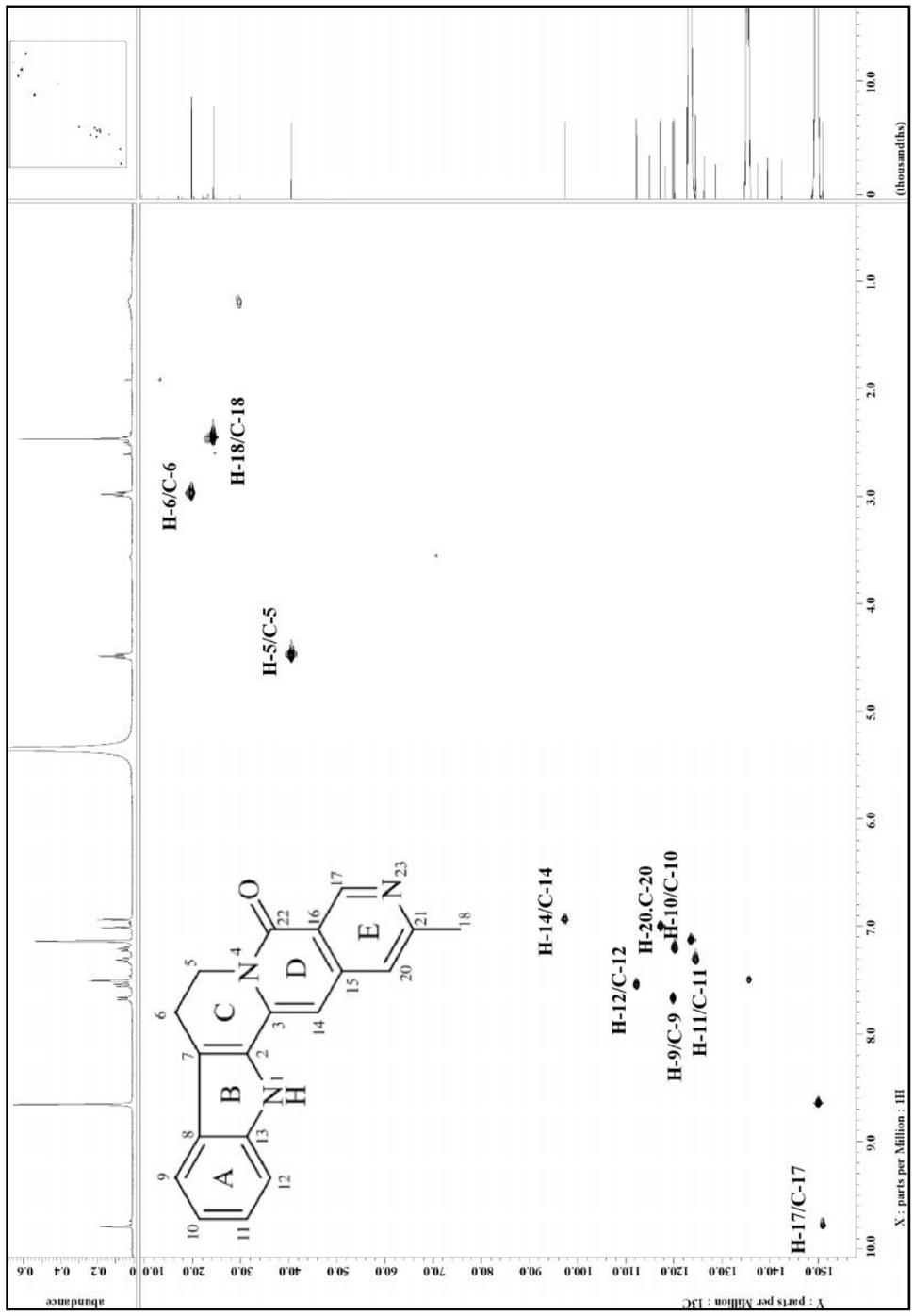

Figure 3.55: HSQC Spectrum of Angustidine **44**

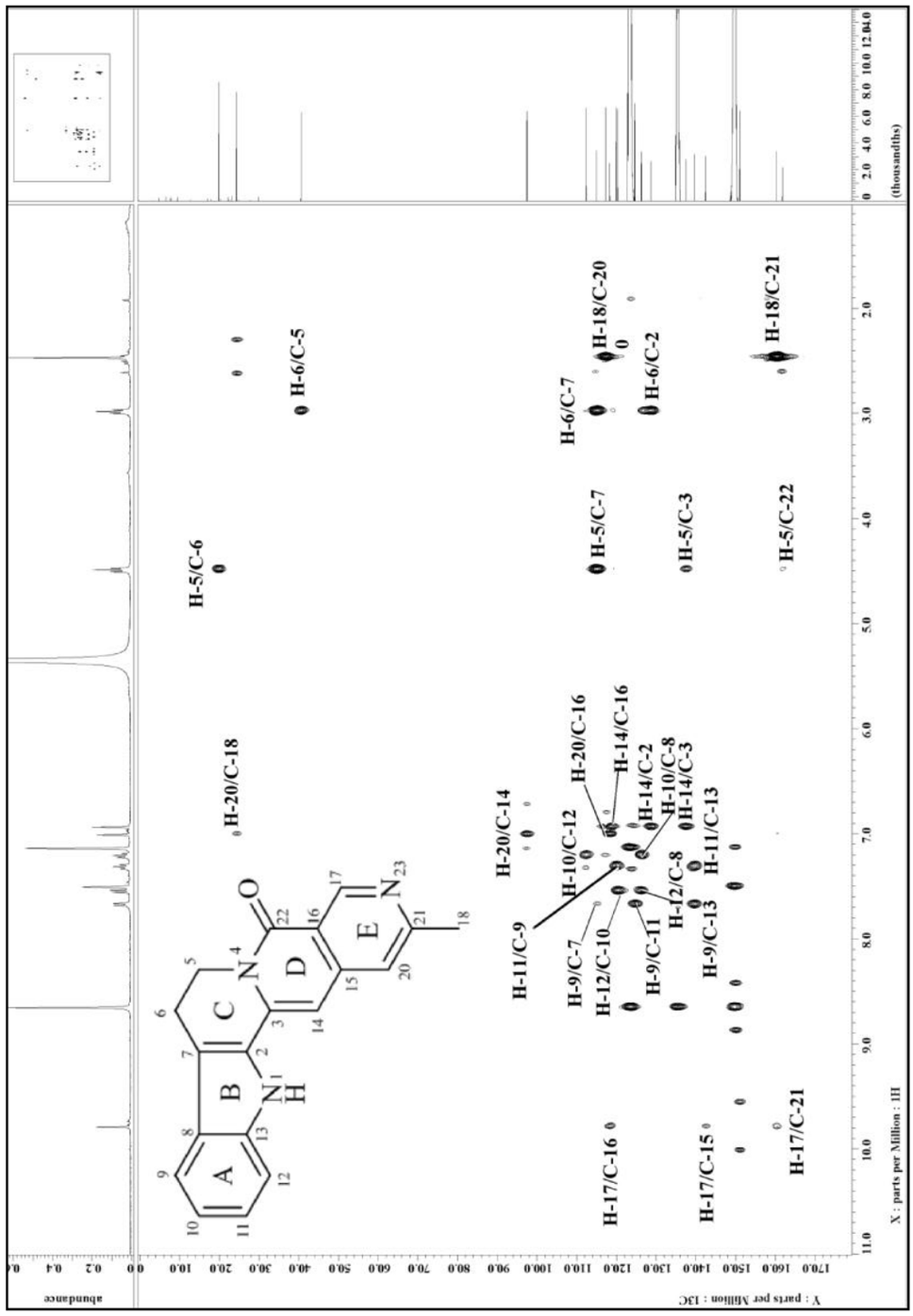

Figure 3.56: HMBC Spectrum of Angustidine **44**

3.2.8 Subditine 72

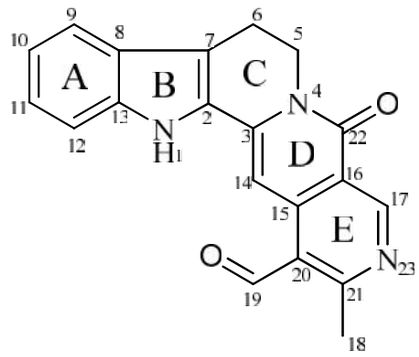

72

Subditine **72** was yielded as a yellowish amorphous solid. The LCMS-IT-TOF spectrum (Figure 3.58) revealed a pseudomolecular ion peak $[M+H]^+$ at *m/z* 330.1018, corresponding to the molecular formula of $C_{20}H_{15}N_3O_2$ (calc. 330.1237). The UV spectrum revealed absorptions at 393, 377 and 210 nm. The IR spectrum of subditine **72** showed absorption bands at 3305, 1651 and 1645 cm^{-1} suggested the existence of N-H, -HC=O and conjugated -NC=O functionality.[15]

In the ^{1}H-NMR spectrum (Figure 3.59), two doublets at δ_H 7.62 (1H, *d*, *J* = 7.8 Hz, H-9) and δ_H 7.47 (1H, *d*, *J* = 8.2 Hz, H-12), two *dd* at δ_H 7.34 (1H, *dd*, *J* = 8.2, 7.1 Hz, H-11) and δ_H 7.19 (1H, *dd*, *J* = 7.8, 7.1 Hz, H-10), two methylenes at δ_H 4.51 (2H, *t*, *J* = 6.9, H_2-5) and δ_H 3.16 (2H, *t*, *J* = 6.9, H_2-6) were observed and this suggested a naucleamide derivative with substitution pattern in ring A and C.[35] Furthermore, this tetrahydro-*β*-carboline skeleton (ring A, B and C)[75] was indicated with HMBC correlations of H_2-5 with C-3 (δ_C 139.4) and C-7 (δ_C 117.1), H_2-6 with C-2 (δ_C 127.3) and C-7, H-9 and H-11 with C-13 (δ_C 138.7) (Figure 2). A broad singlet at δ_H 8.94 implied the presence of an NH unit.

The ^{13}C-NMR and DEPT spectra (Figure 3.60 and Figure 3.61) of subditine **72** indicated a total of twenty carbon signals; one methyl, two methylene, six methine, nine

quaternary carbon and two carbonyl. The carbonyl of the lactam ring resonated at δ_C 161.7 (C-22). In addition, the HMBC spectrum showed correlation between H-14 (δ_H 7.97) and C-3, H-14 and C-16 (δ_C 119.3), thus supporting the presence of a δ lactam ring. Furthermore, HMBC correlations of H-14 with C-16 and C-20 (δ_C 127.6), H-17 (δ_H 9.57) with C-15 (δ_C 141.1) and C-16, H_3-18 (δ_H 2.98) with C-21 (δ_C 165.9), H-19 (δ_H 10.72) with C-20 (δ_C 127.6) indicated that ring D is connected to a nicotinaldehyde ring (ring E) with a methyl group forming a 2-methylnicotinaldehyde unit (Figure 3.57). Subditine **72** is very similar to the known compound, angustidine **44** except that the former has an additional carbonyl group at C-19.

Complete ^{1}H and ^{13}C-NMR assignments (Table 3.9) were established by thorough analysis of COSY, HMBC, HSQC and NOESY data. Subditine **72** is a new corynanthe indole alkaloid isolated from the bark of *N. subdita*. A proposed biogenesis pathway for subditine **72** was shown in Scheme 3.2.

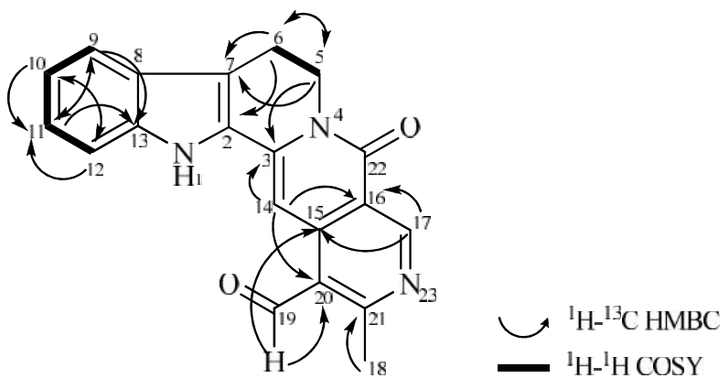

Figure 3.57: COSY and HMBC Correlations of Subditine **72**

Table 3.9: ^{1}H-NMR (400 MHz) and ^{13}C-NMR (100 MHz) Spectral Data of Subditine **72** in $CDCl_3$.

Position	**^{1}H (multiplicity, *J* in Hz)**	**^{13}C (δ_C)**
NH-1	8.94 (*br s*)	-
2	-	127.3
3	-	139.4
5	4.51 (*t*, 6.9)	40.5
6	3.16 (*t*, 6.9)	19.7
7	-	117.1
8	-	125.8
9	7.62 (*d*, 7.8)	119.9
10	7.19 (*dd*, 7.8, 7.1)	120.9
11	7.34 (*dd*, 7.1, 8.2)	125.7
12	7.47 (*d*, 8.2)	111.9
13	-	138.7
14	7.97 (*s*)	94.7
15	-	141.1
16	-	119.3
17	9.57 (*s*)	155.2
18	2.98 (*s*)	22.6
19	10.72 (*s*)	192.6
20	-	127.6
21	-	165.9
22	-	161.7

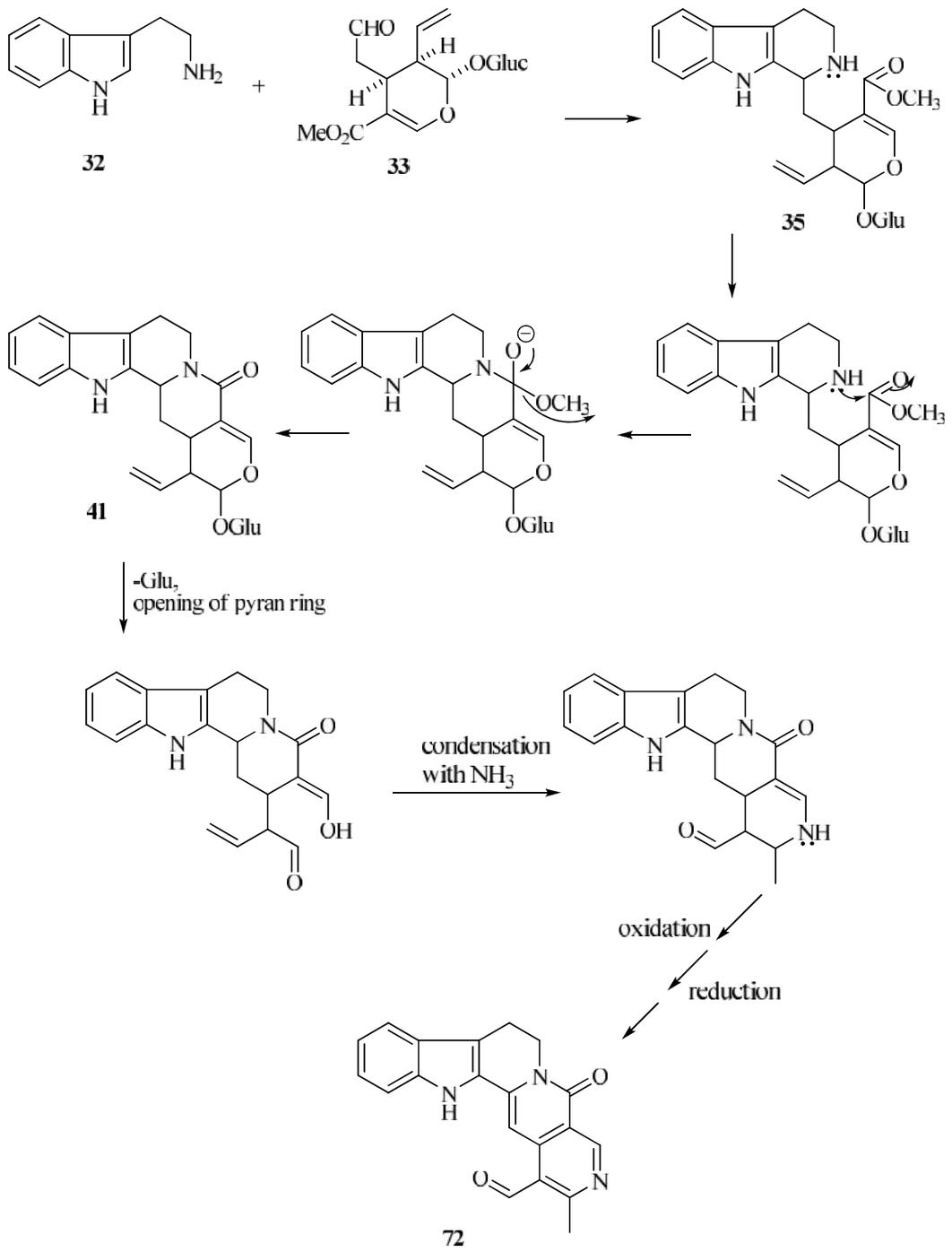

Scheme 3.2: Proposed biogenesis pathway for subditine **72**.

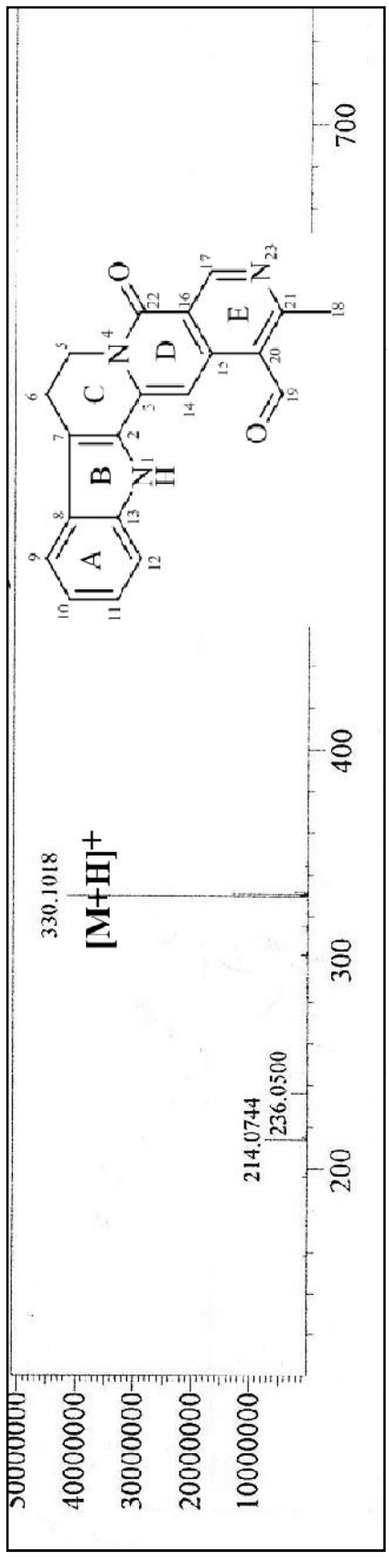

Figure 3.58: LCMS Spectrum of Subditine **72**

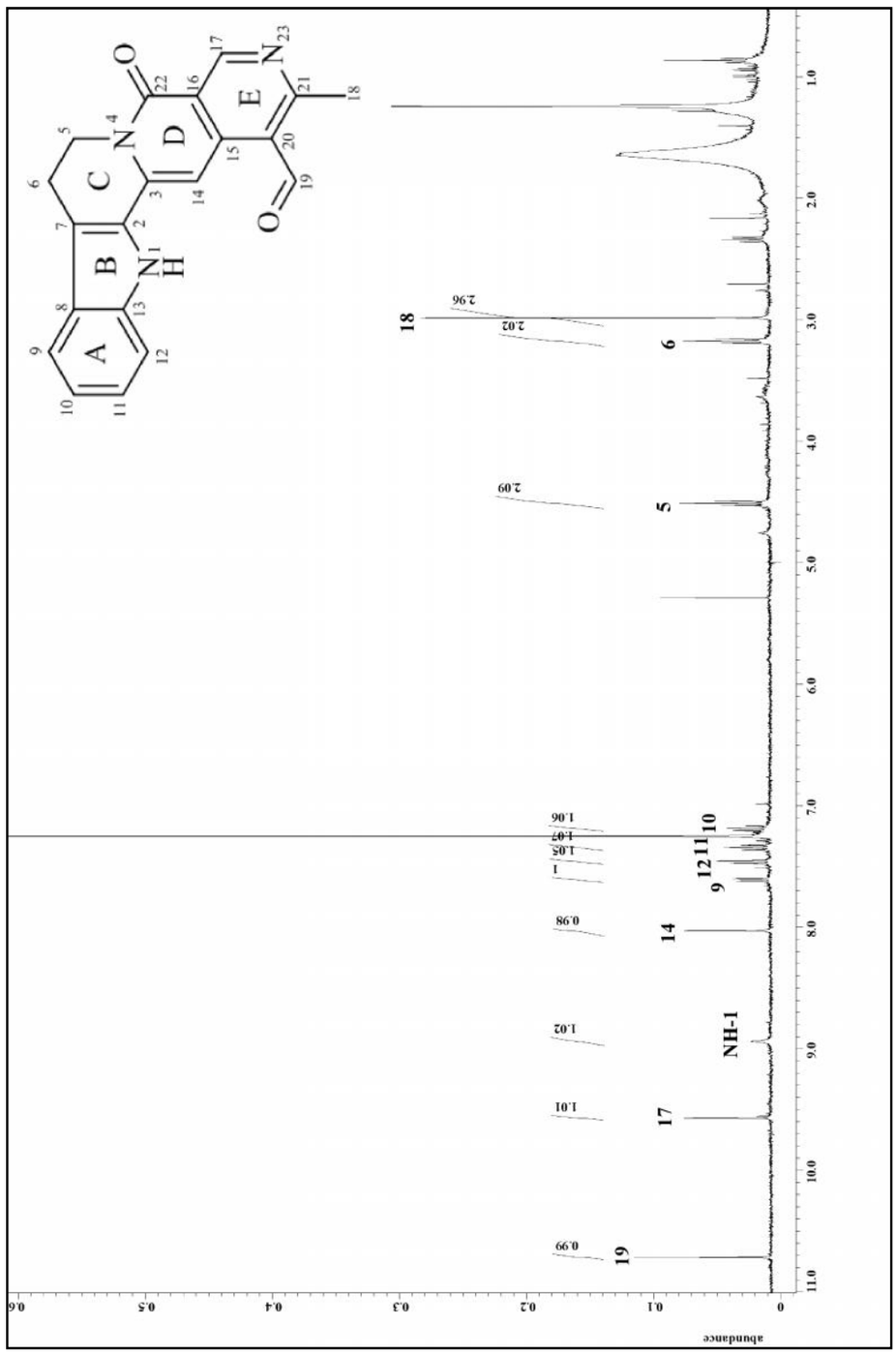

Figure 3.59: ^{1}H NMR Spectrum of Subditine **72**

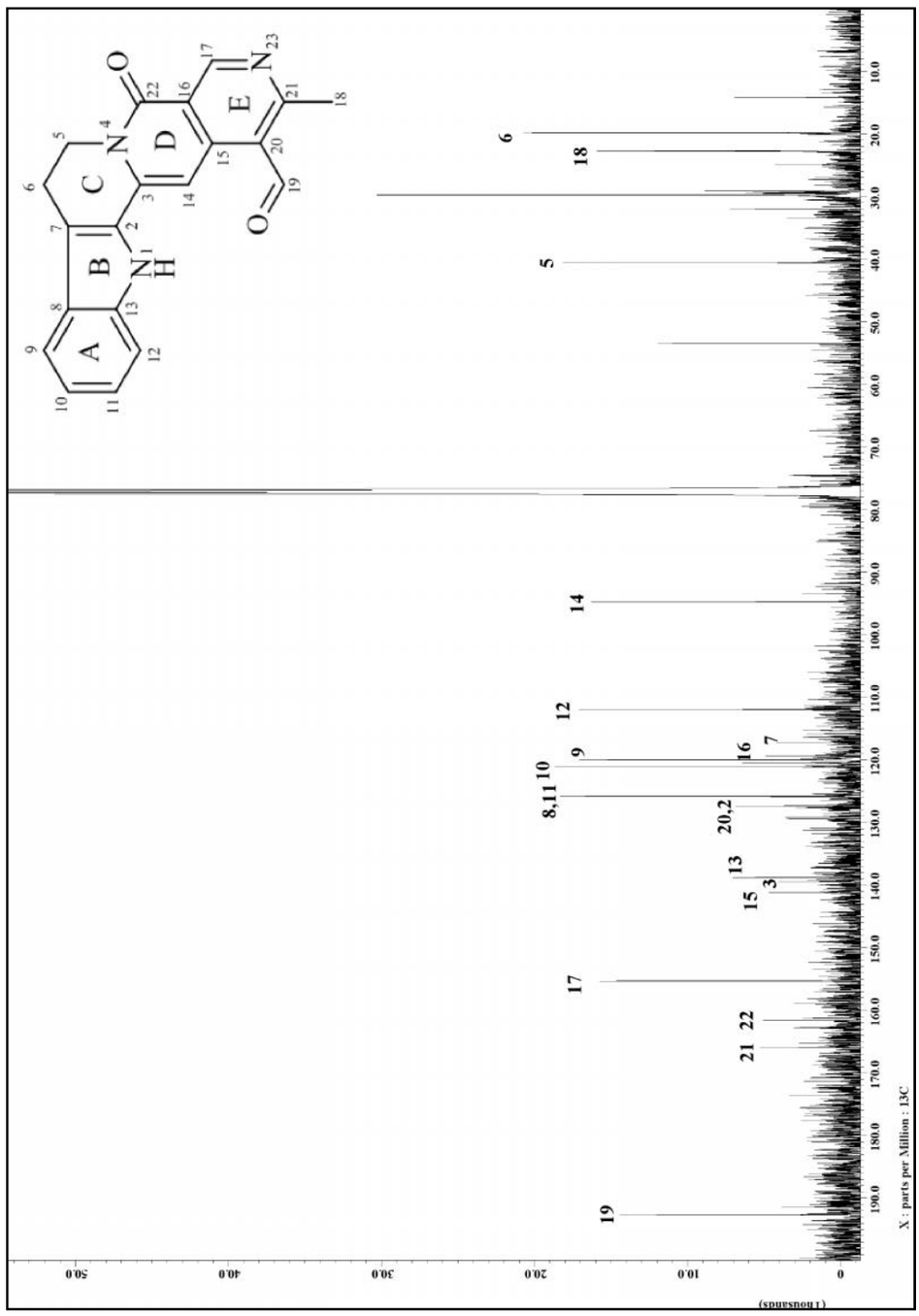

Figure 3.60: ^{13}C NMR Spectrum of Subditine **72**

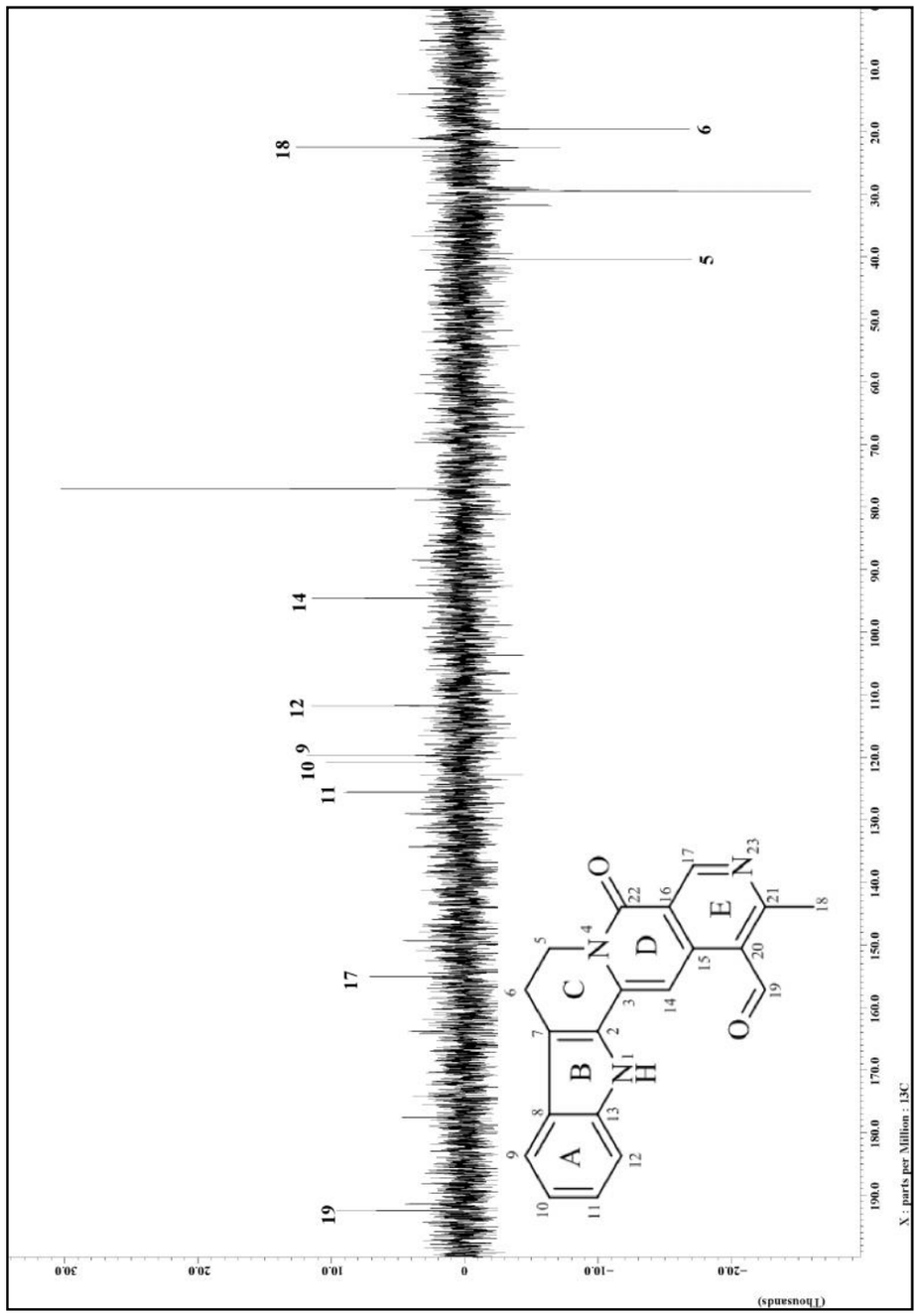

Figure 3.61: DEPT 135 Spectrum of Subditine **72**

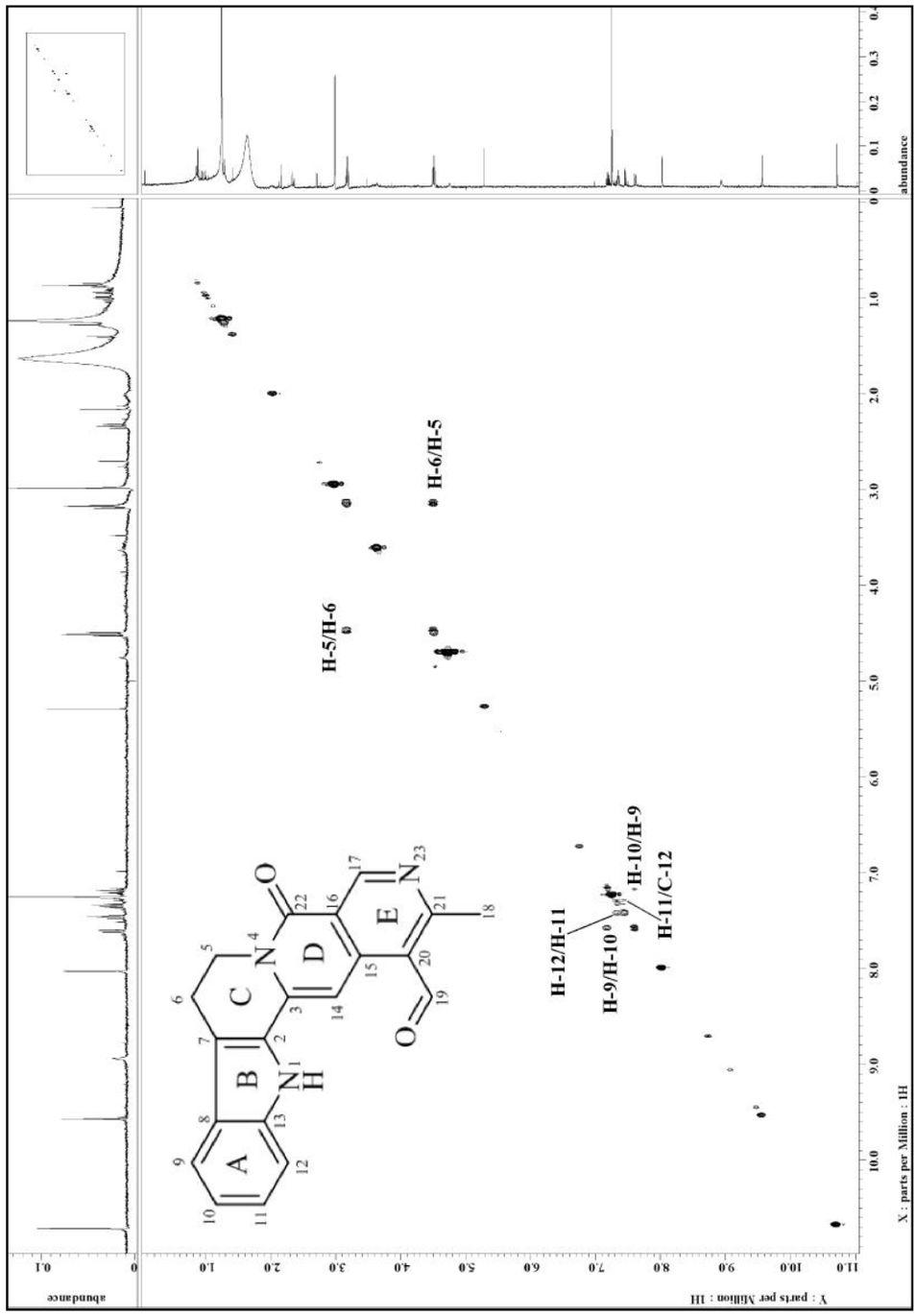

Figure 3.62: COSY Spectrum of Subditine **72**

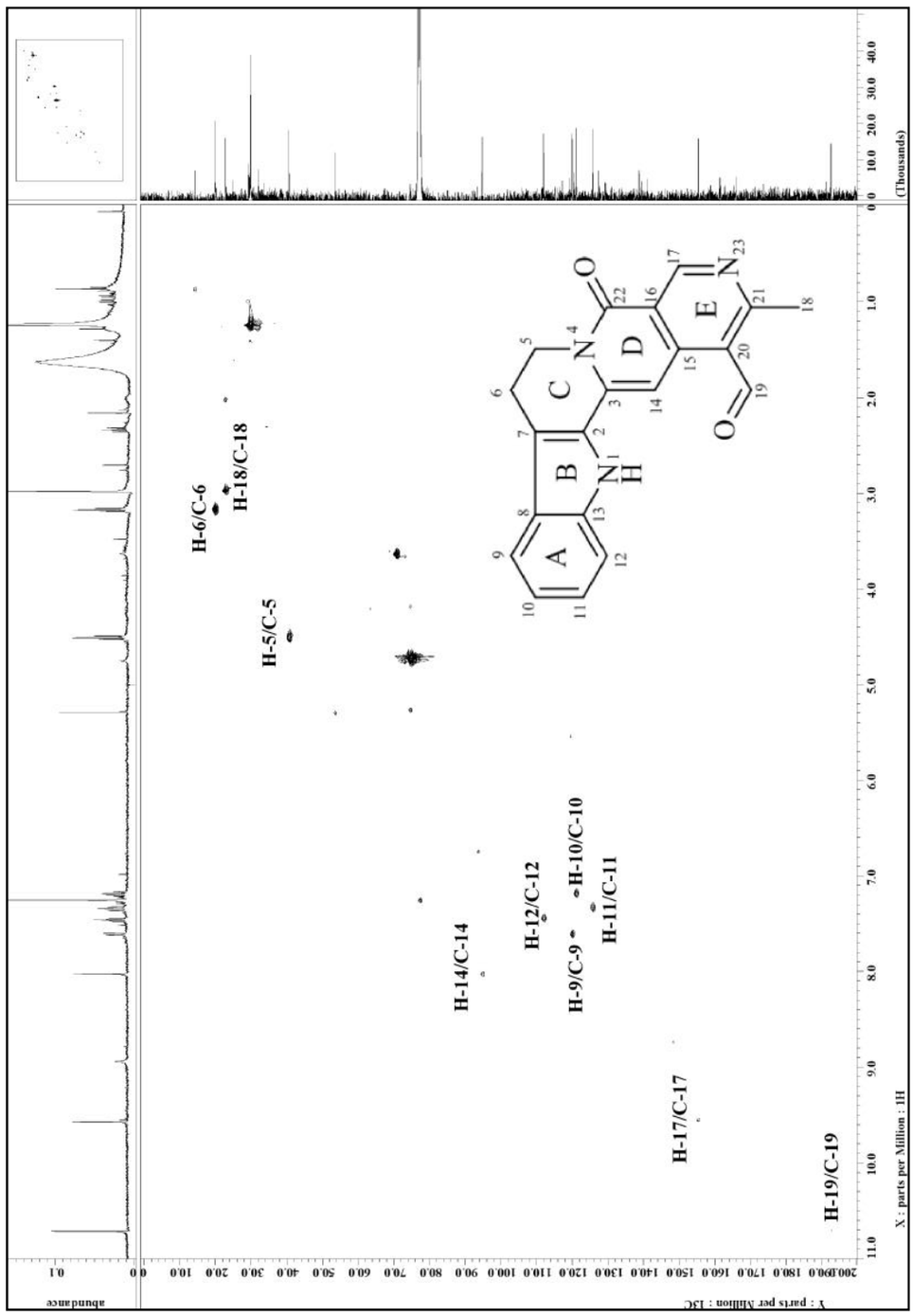

Figure 3.63: HSQC Spectrum of Subditine **72**

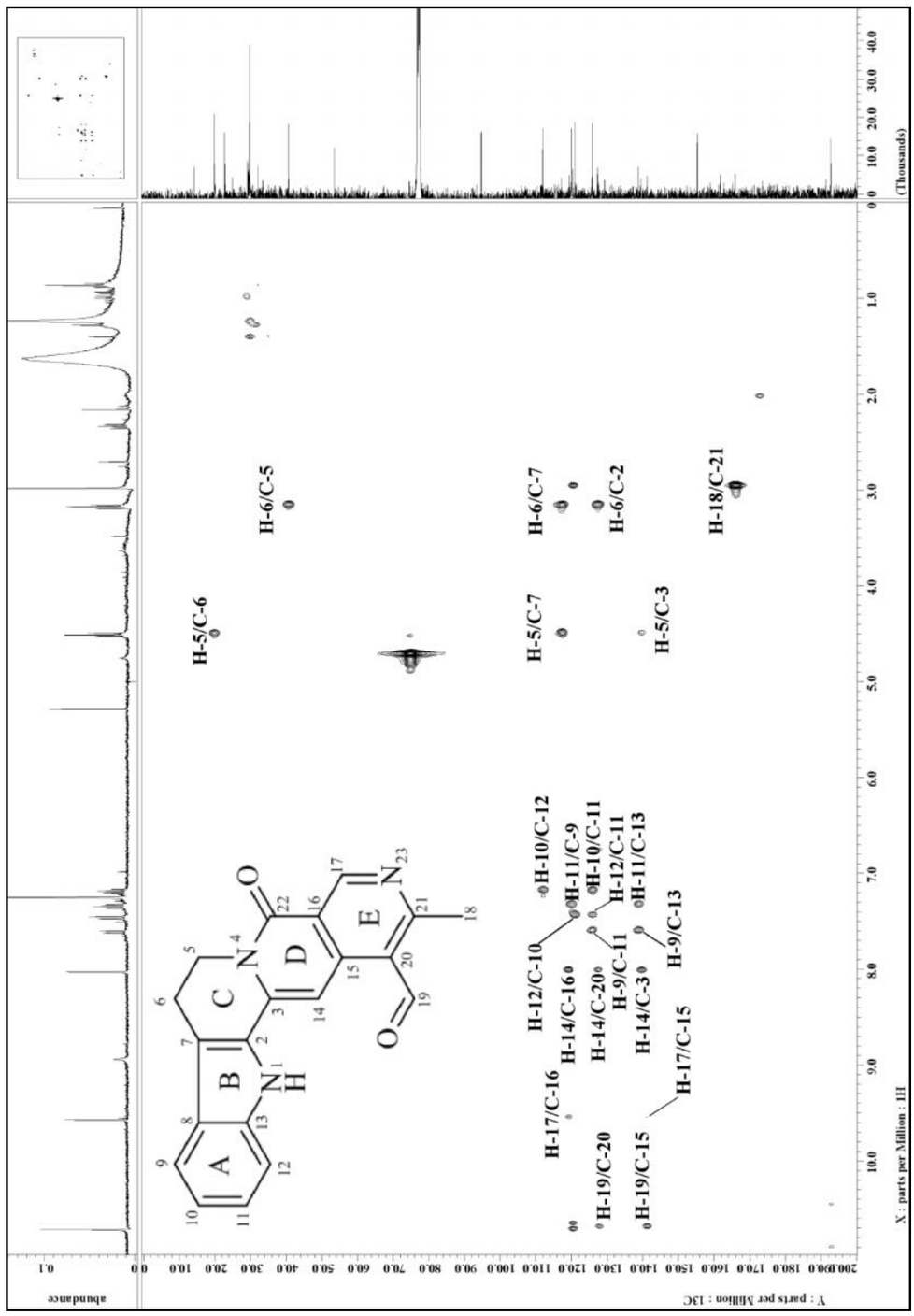

Figure 3.64: HMBC Spectrum of Subditine **72**

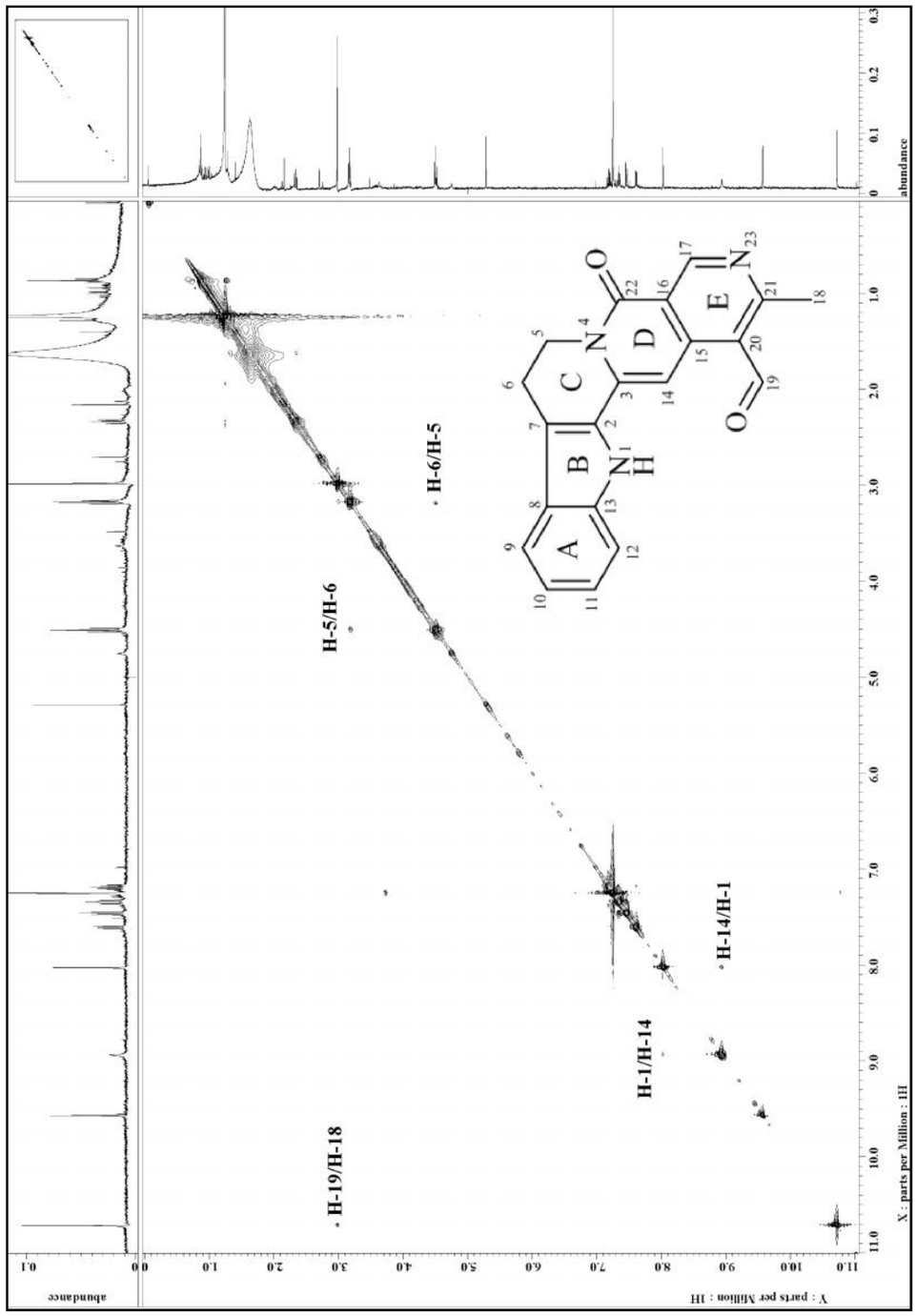

Figure 3.65: NOESY Spectrum of Subditine **72**

3.2.9 Strictosamide 70

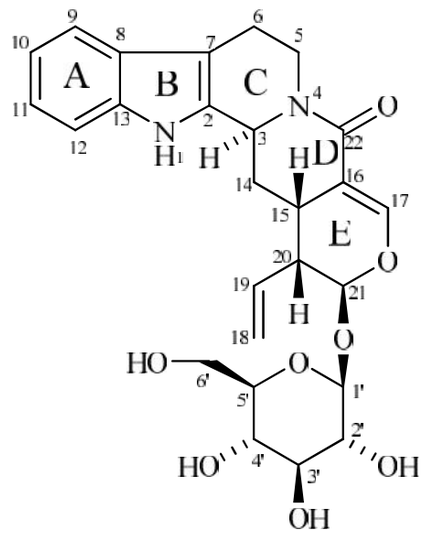

70

Strictosamide **70** $[\alpha]_D^{23}$ -40.0º (*c* 0.1, MeOH) was isolated as a light yellowish amorphous solid. The ESIMS (Figure 3.67) revealed a pseudomolecular ion peak $[M+Na]^+$ at *m/z* 521.1875, corresponding to the molecular formula of $C_{26}H_{30}N_2O_8$ (calc. 521.1894). The UV spectrum showed absorption bands at 387, 328, 225 and 203 nm.[83] Stretching of conjugated lactam carbonyl and C-O groups were observed at 1653 and 1050 cm^{-1} respectively in its IR spectrum.[83]

The ^{1}H-NMR and ^{13}C-NMR spectra (Figure 3.68 and Figure 3.69) of this alkaloid also showed a similar pattern with that of 3,14-dihydroangustoline **68** in aromatic region and also the presence of two methylenes which indicating the presence of a tetrahydro-*β*-carboline skeleton (ring A, B and C).[75] Besides, this alkaloid showed the presence of a δ lactam ring (ring D) with carbonyl group at position C-22 which resonated at 167.1. From COSY spectrum (Figure 3.71), a broad doublet of methine proton, H-3, at δ_H 5.10 showed correlation with a pair of geminal methylene protons signal at δ_H 2.47-2.51 and δ_H 2.07 which were assignable to H-14a and H-14b respectively. These methylene protons also coupled with the methine proton, H-15, at δ_H 2.80-2.84. Furthermore, correlation of two *dd* at δ_H 5.40 and δ_H 5.35 (H-18a and H-18b respectively) with an

olefinic methine of H-19 at δ_H 5.68 can be observed from COSY spectrum. The geminal protons, H_2-18, showed HMBC correlation with an allylic methine carbon of C-20 at δ_C 44.8. H-19 also showed COSY correlation with the allylic proton H-20 (δ_H 2.72) which in turn also coupled with the methine proton, H-15.

The ^{13}C-NMR and DEPT spectra of strictosamide **70** indicated a total of twenty six carbon signals. The carbonyl carbon of the δ lactam ring appeared at downfield region at δ_C 167.1 (C-22). HMBC correlation of H-17 (δ_H 7.40) to C-15 (δ_C 25.0), C-16 (δ_C 109.3), C-21 (δ_C 98.1) and C-22, H-20 to C-15 and C-16 as well as H-21 to C-15 and C-17 (δ_C 149.2) indicating a 3,4-dihydro-2*H*-pyran ring (ring E) was attached to the δ lactam ring (ring D) (Figure 3.66). Besides, the ^{13}C-NMR spectrum displayed the signal of a glucose moiety. The anomeric carbon C-1' and H-1' signals were observed at δ_C 100.5 and δ_H 4.60 respectively. HMBC spectrum showed correlation of the acetal proton H-21 at δ_H 5.44 (1.7 Hz) with C-1' suggesting a glucose unit was attached to C-21 (δ_C 98.1).

Strictosamide **70** has similar structure with vincosamide[83]. The only difference is the stereochemistry at C-3 where strictosamide **70** has a C-3 α epimer while vincosamide has a C-3 β epimer.[84,85] The difference can be observed by comparison of the reported data in which the chemical shift at C-5 and C-14 where it can be affected by the coupling of H-3. C-5 and C-14 of strictosamide **70** were at δ_C 44.8 and δ_C 27.4 while those of vincosamide were at δ_C 41.3 and δ_C 32.7 respectively.[84] In addition, the configuration of C-21 was deduced to be β by the coupling constant of 7.9 Hz between anomeric proton H-1' and H-21.[84,86,85] For an α configuration, the coupling constant value will be around 1.2 Hz due to the difference in the dihedral angles between both isomers.[87]

From the analysis of the spectroscopic data obtained (Table 3.10) and comparison with the literature values[83,84,85], the structure of strictosamide **70** was established without doubt.

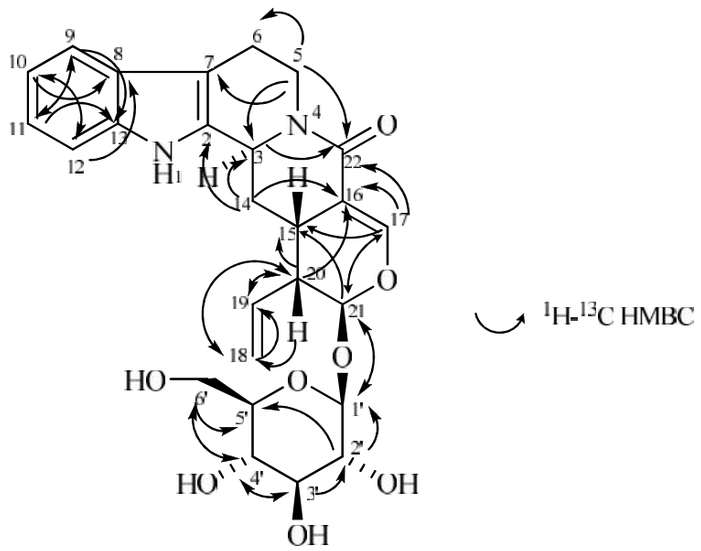

Figure 3.66: Selected HMBC Correlations of Strictosamide **70**

Table 3.10: ^{1}H-NMR (600 MHz) and ^{13}C-NMR (150 MHz) Spectral Data of Strictosamide **70** in CD_3OD.

Position	**^{1}H** δ_H **(multiplicity, *J* in Hz)**		**^{13}C** δ_C	
	Experimental (CD_3OD)	**Reference* (CD_3OD)**	**Experimental (CD_3OD)**	**Reference* (CD_3OD)**
NH-1	-	-	-	-
2	-	-	134.8	134.8
3	5.10 (*br d*)	5.03 (*m*)	55.1	55.1
5a	4.98 (*dd*, 5.6, 12.5)	4.93 (*dd*, 5.0, 12.0)	44.8	44.7
5b	3.14 (*dt*, 4.6, 12.5)	3.07 (*dt*, 4.0, 12.0)		
6a	2.95-2.97 (*m*)	2.93 (*m*)	22.1	22.1
6b	2.69-2.72 (*m*)	2.53-2.69 (*m*)		
7	-	-	110.3	110.3
8	-	-	128.7	128.7
9	7.41 (*d*, 8.1)	7.37 (*d*, 8.1)	118.7	118.7
10	7.03 (*dt*, 8.1, 1.0)	6.99 (*dt*, 8.1, 1.0)	120.2	120.1
11	7.12 (*dt*, 8.1, 1.0)	7.07 (*dt*, 8.1, 1.0)	122.5	122.5
12	7.35 (*d*, 8.1)	7.32 (*d*, 8.1)	112.3	112.3
13	-	-	137.8	137.8
14a	2.47-2.51 (*m*)	2.44 (*m*)	27.4	27.3
14b	2.07 (*ddd*, 13.9, 13.9, 5.9)	2.02 (*ddd*, 13.8, 13.8, 6.0)		
15	2.80-2.84 (*m*)	2.79 (*m*)	25.0	24.9
16	-	-	109.3	109.2
17	7.40 (*s*)	7.36 (*s*)	149.2	149.1
18a	5.40 (*dd*, 17.1, 1.7)	5.38 (*dd*, 16.0, 2.0)	120.5	120.5
18b	5.35 (*dd*, 10.2, 1.7)	5.33 (*dd*, 10.0, 2.0)		
19	5.68 (*ddd*, 17.2, 10.2, 10.2)	5.64 (*ddd*, 17.0, 10.0, 10.0)	134.4	134.4
20	2.69-2.72 (*m*)	2.63-2.69 (*m*)	44.8	44.7
21	5.44 (*d*, 1.7)	5.29 (*d*, 2.0)	98.1	98.1
22	-	-	167.1	167.1
1’	4.60 (*d*, 7.9)	4.56 (*d*, 7.9)	100.5	100.5
2’	2.96-2.99 (*m*)	2.96 (*m*)	74.3	74.3
3’	3.26-3.30 (*m*, overlapped)	3.16-3.34 (*m*)	78.3	78.2
4’	3.19-3.22 (*m*)		71.4	71.4
5’	3.26-3.30 (*m*, overlapped)		78.0	77.9
6a’	3.88 (*dd*, 11.9, 2.1)	3.85 (*dd*, 12.0, 1.9)	62.6	62.6
6b’	3.65 (*dd*, 11.9, 6.1)	3.62 (*dd*, 12.0, 5.7)		

* Literature values from Fan et al. (2010)

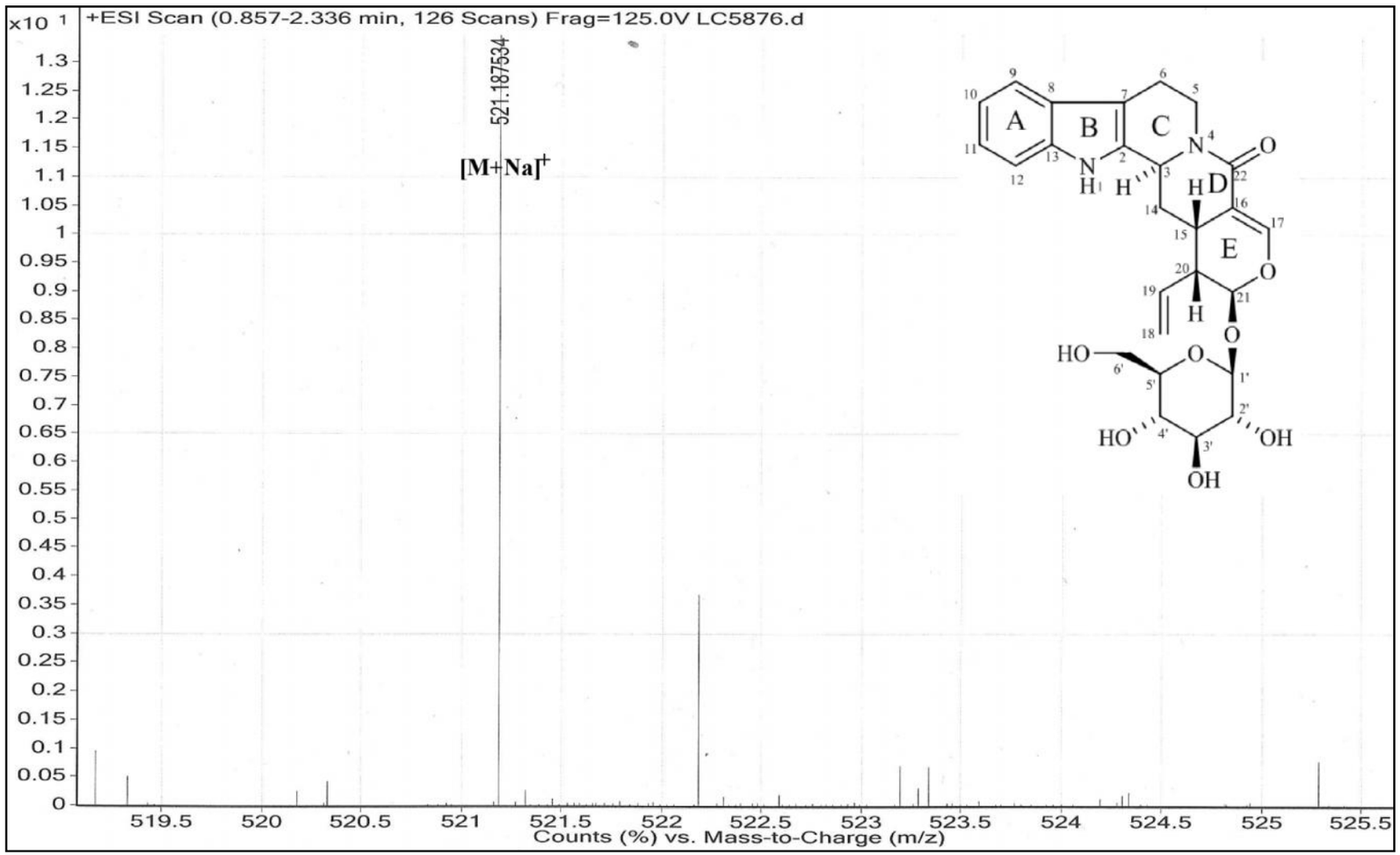

Figure 3.67: LCMS Spectrum of Strictosamide **70**

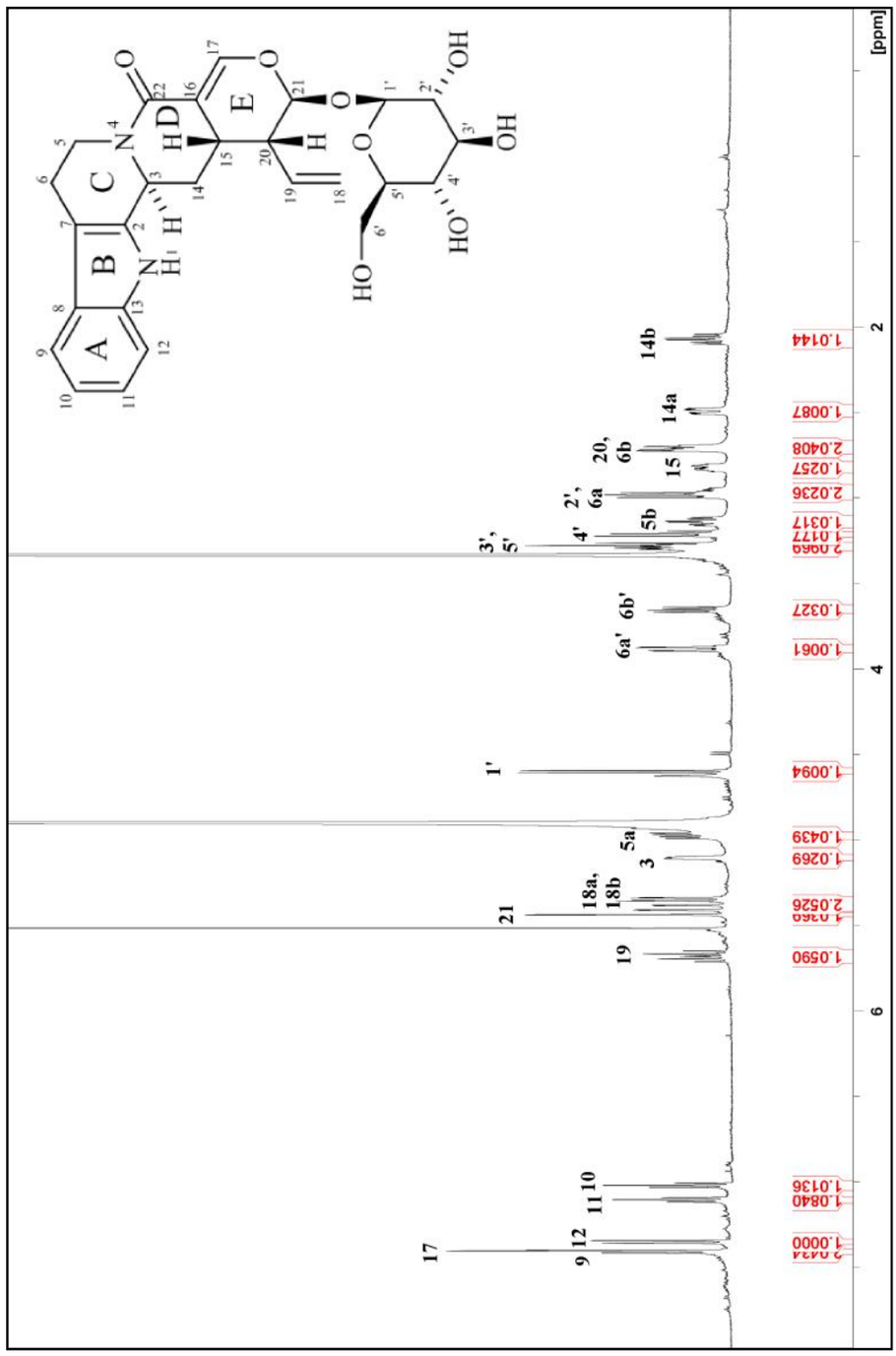

Figure 3.68: ^{1}H NMR Spectrum of Strictosamide **70**

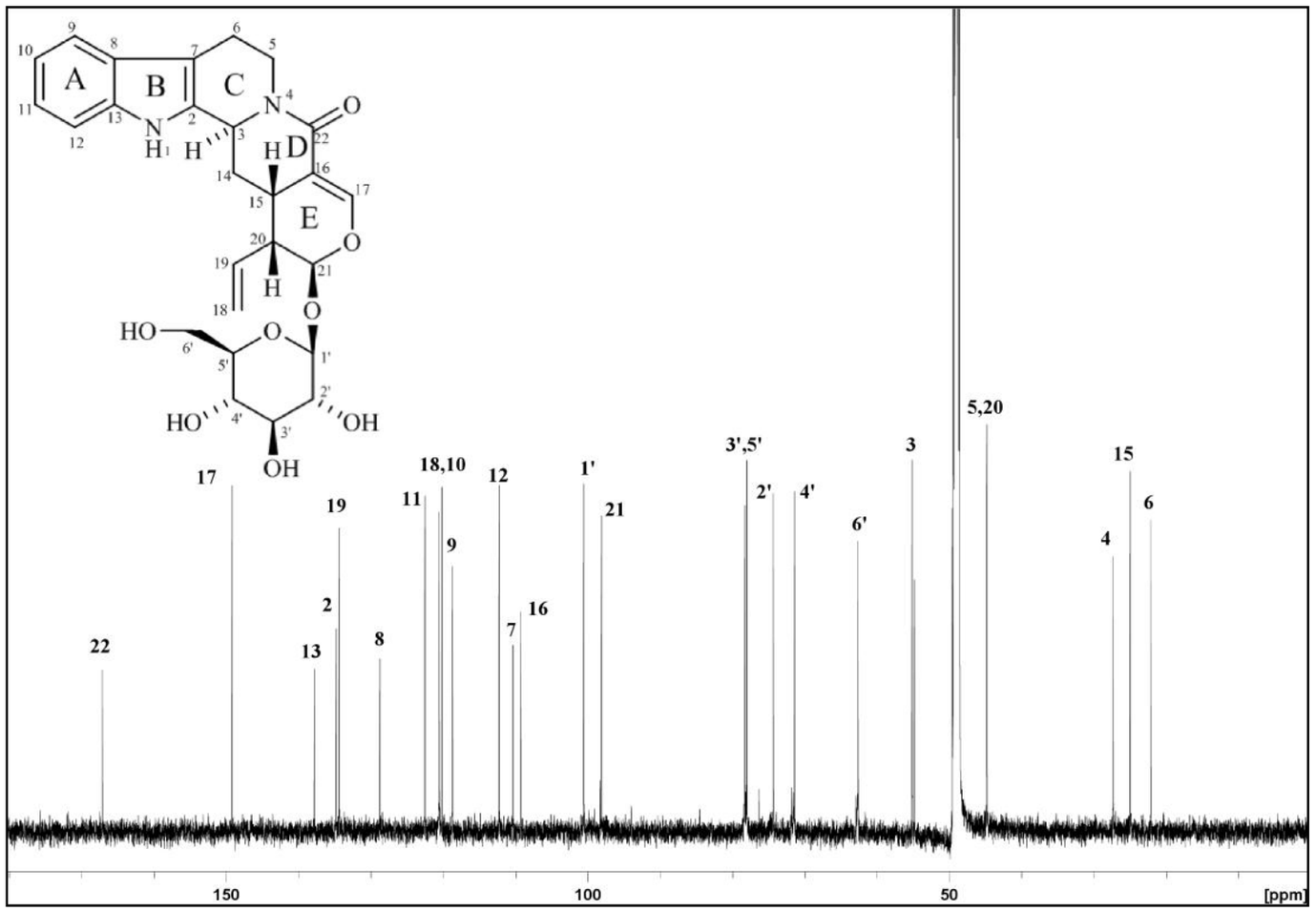

Figure 3.69: ^{13}C NMR Spectrum of Strictosamide **70**

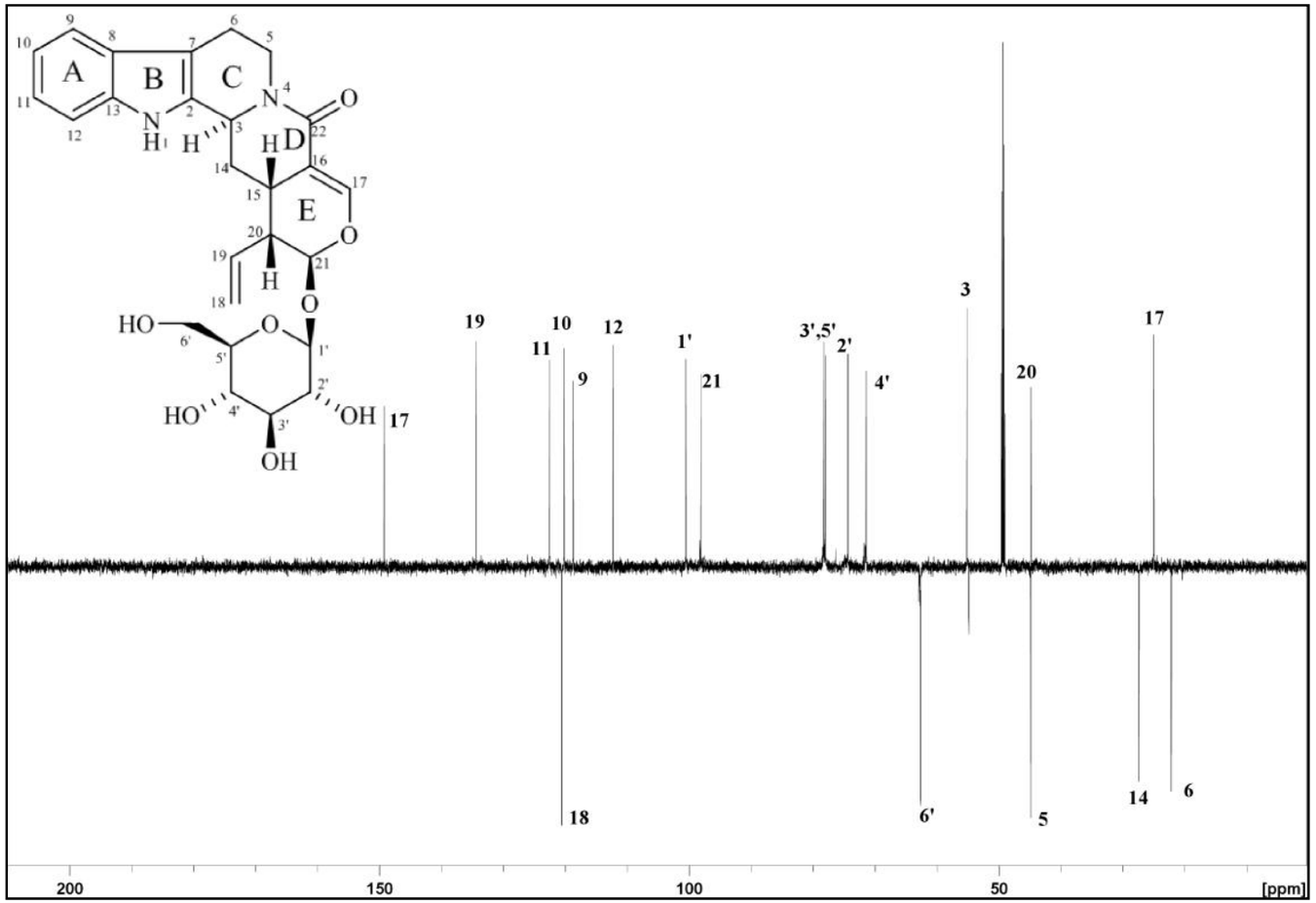

Figure 3.70: DEPT 135 NMR Spectrum of Strictosamide **70**

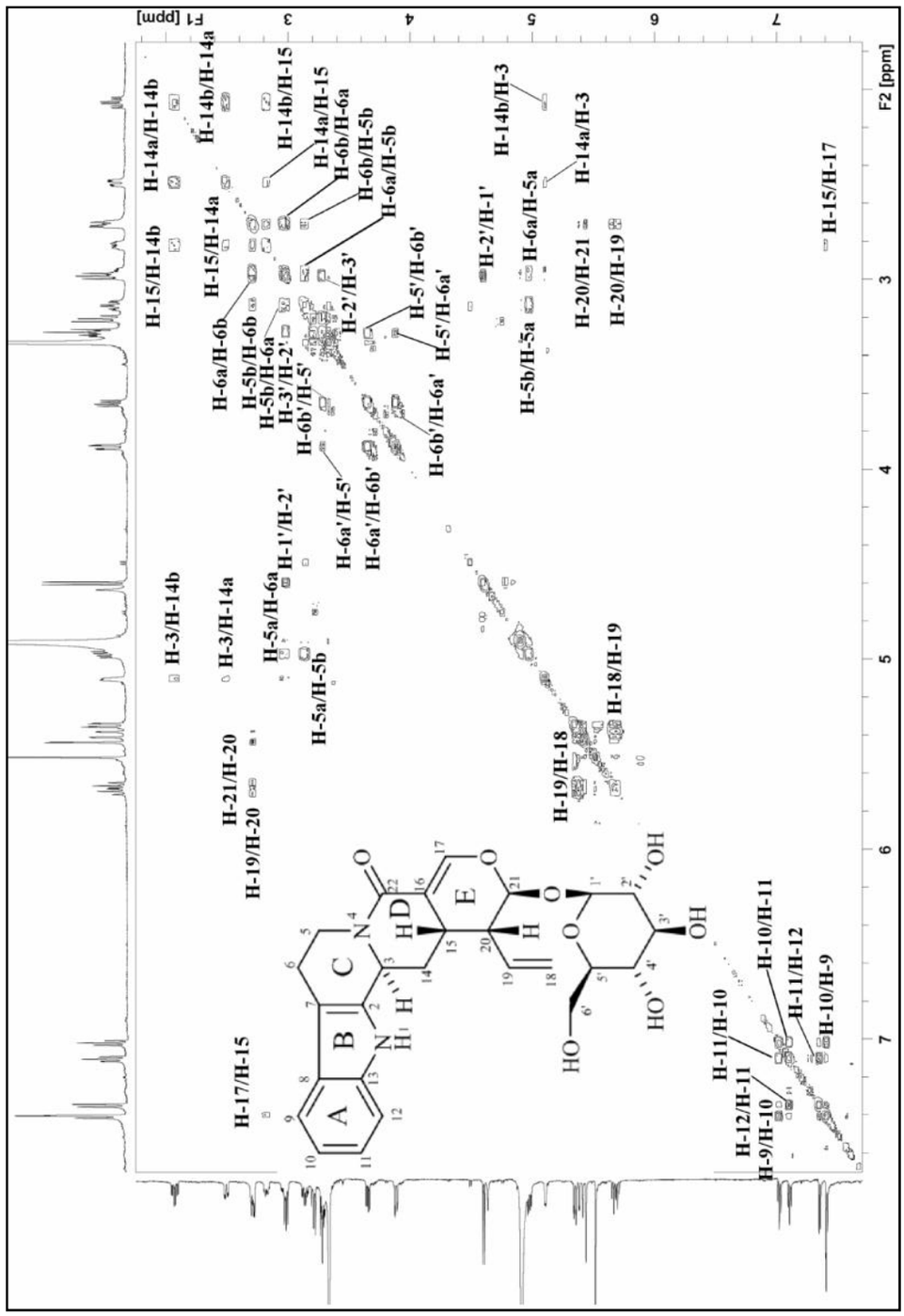

Figure 3.71: COSY Spectrum of Strictosamide **70**

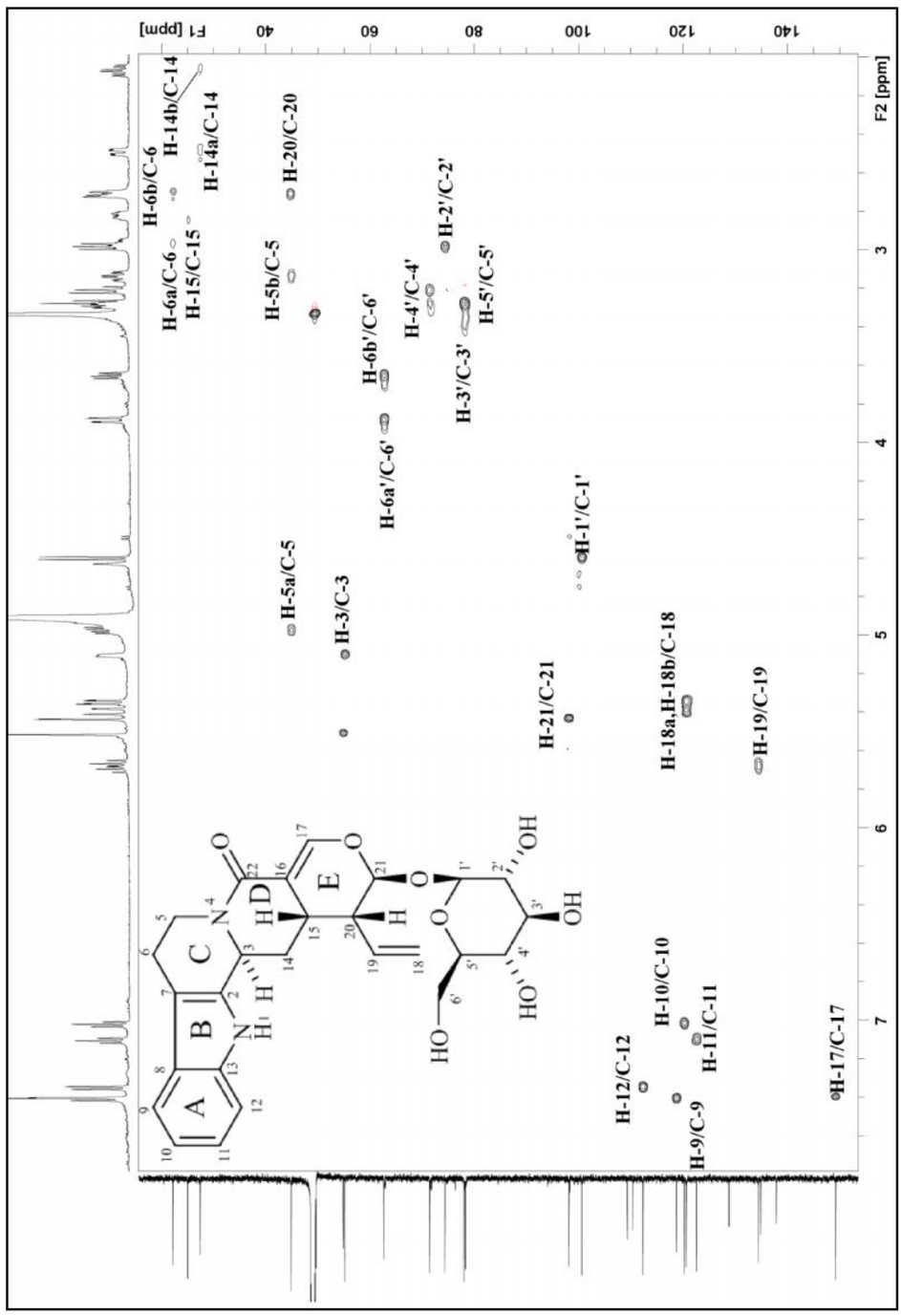

Figure 3.72: HSQC Spectrum of Strictosamide **70**

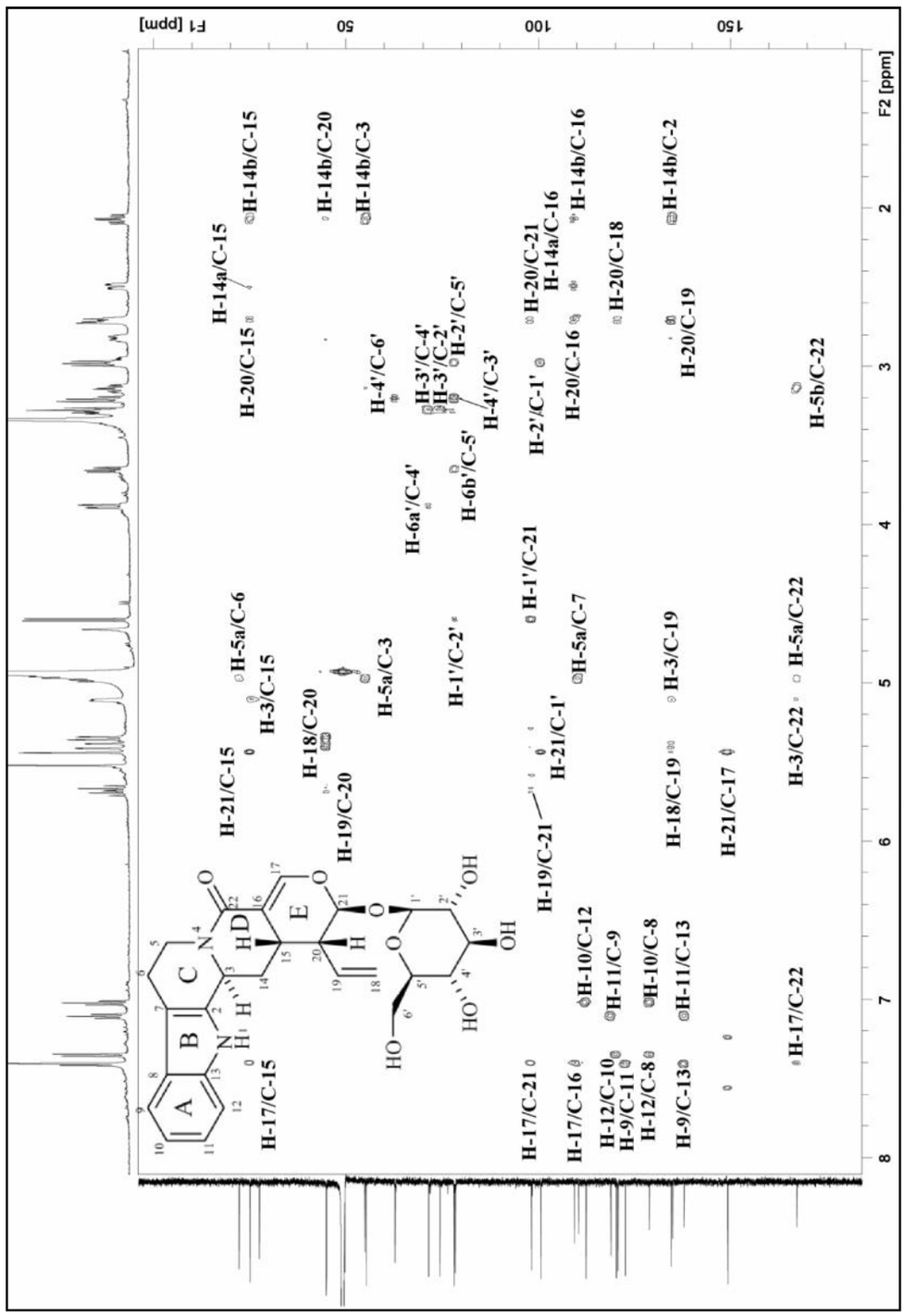

Figure 3.73: HMBC Spectrum of Strictosamide **70**

3.2.10 Pumiloside 69

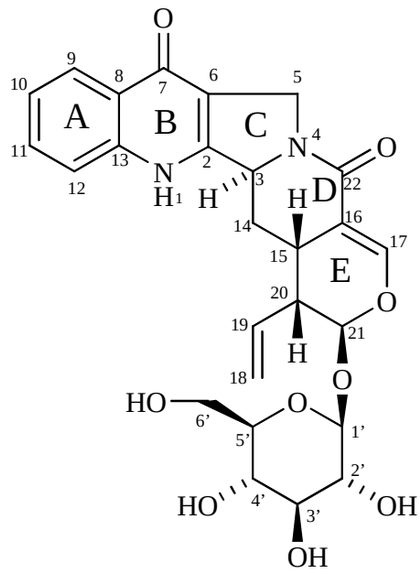

69

Pumiloside **69** $[\alpha]_D^{24}$ -93.5º (*c* 0.31, MeOH) was afforded as a light yellowish amorphous solid. The ESIMS (Figure 3.75) displayed a pseudomolecular ion peak $[M+Na]^+$ at *m/z* 535.1649 which was in agreeable to the molecular formula of $C_{26}H_{28}N_2O_9$ (calc. 535.1687) with fourteen degree of unsaturation which consisted of eight double bonds and six rings. Interestingly, the mass of pumiloside **69** showed an increase of 28 mass unit as compared to strictosamide **70** thus indicative the possible presence of a carbonyl group. The UV spectrum showed absorption bands at 328, 314, 244 and 210 nm.[83] The IR spectrum of pumiloside **69** showed absorption peaks at 3415 and 1653 cm^{-1} which indicated N-H and conjugated –NC=O stretching respectively.[83]

The ^{1}H-NMR and ^{13}C-NMR spectra (Figure 3.76 and Figure 3.77) of this alkaloid showed very similar profile with that of strictosamide **70** including its stereochemistry. However, in ^{13}C-NMR spectrum, a slight difference were observed in the signals of C-6 and C-3 and the presence of an extra C=O signal at δ_C 173.3 (C-7). In addition, in the ^{1}H-NMR spectrum, the presence of two *d* at δ_H 8.25 (1H, *d*, *J* = 8.1 Hz, H-9) and δ_H 7.71 (1H, *d*, *J* = 8.1 Hz, H-12), two *dt* at δ_H 7.63 (1H, *dt*, *J* = 8.1, 1.2 Hz, H-11) and δ_H

7.35 (1H, *dt*, *J* = 8.1, 1.2 Hz, H-10) indicating the existence of aromatic system of ring A. However, there was only one methylene at δ_H 4.62 (1H, *dd*, *J* = 14.2, H-5a) and δ_H 4.45 (1H, *dd*, *J* = 14.2, H-5b) was observed and HMBC spectrum showed correlation of this methylene signal with C-2 (δ_C 151.5), C-3 (δ_C 60.3) and C-6 (δ_C 113.4), suggesting that ring C was a five membered ring instead of six membered ring in strictodsamide **70**.

The ^{13}C-NMR spectrum of pumiloside **69** indicated a total of twenty six carbon signals. The carbonyl of lactam ring resonated at downfield region, δ_C 164.5 (C-22). HMBC spectrum showed correlation of H-9 and H-12 with another carbonyl signal C-7 suggesting the presence of quinolone unit of ring A and B (Figure 3.74).

From the analysis of the spectroscopic data obtained (Table 3.11) and comparison with the literature values,[83,84,85] the structure of pumiloside **69** was established by possessing a quinoline instead of indole skeleton compared with strictosamide **70**.

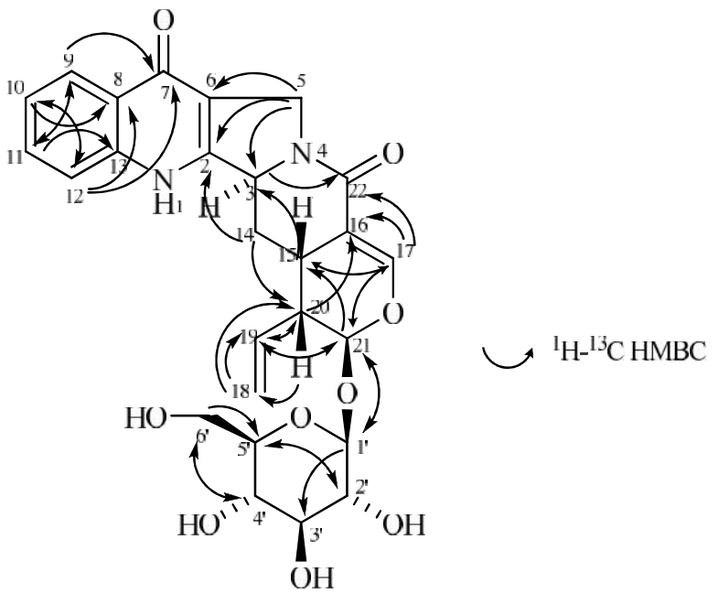

Figure 3.74: Selected HMBC Correlations of Pumiloside **69**

Table 3.11: ^{1}H-NMR (600 MHz) and ^{13}C-NMR (150 MHz) Spectral Data of Pumiloside **69** in DMF-d_7.

Position	^{1}H		^{13}C	
	δ_H (multiplicity, *J* in Hz)		δ_C	
	Experimental (DMF-d_7)	**Reference* (CD_3OD)**	**Experimental (DMF-d_7)**	**Reference* (CD_3OD)**
NH-1	-	-	-	-
2	-	-	151.5	149.7
3	4.83 (*br d*, 12.1)	4.77 (*d*, 12.0)	60.3	59.4
5a	4.62 (*dd*, 14.2)	4.48 (*dd*, 14, 2.5)	47.8	47.4
5b	4.45 (*dd*, 14.2)	4.33 (*d*, 14)		
6	-	-	113.4	113.0
7	-	-	173.3	173.0
8	-	-	126.2	125.3
9	8.25 (*d*, 8.1)	8.12(*d*, 8.1)	125.1	124.7
10	7.35 (*dt*, 8.1, 1.2)	7.35(*td*, 8.1, 1.3)	123.1	123.2
11	7.63 (*dt*, 8.1, 1.2)	7.66(*td*, 8.1, 1.3)	131.3	131.6
12	7.71 (*d*, 8.1)	7.60 (*d*, 8.1)	119.7	118.3
13	-	-	142.2	140.4
14a	2.62-2.64 (*m*, overlapped)	2.50 (*m*)	29	28.1
14b	2.07 (*q*, 13.4)	2.02 (*q*, 12.0)		
15	3.28-3.33 (*m*, overlapped)	3.29 (*m*)	24.4	23.7
16	-	-	109.7	108.9
17	7.09 (*d*, 2.7)	7.05 (*d*, 2.6)	145.4	145.1
18a	5.40 (*dd*, 17.1)	5.48(*dd*, 17, 1.5)	120.1	120.5
18b	5.30 (*dd*, 10.3)	5.35(*dd*, 10, 1.5)		
19	5.82-5.87 (*m*)	5.81 (*dt*, 17, 10)	133.2	132.5
20	2.62-2.64 (*m*, overlapped)	2.66 (*dd*, 9, 5)	44.7	43.6
21	5.46 (*d*, 1.5)	5.40 (*d*, 2.0)	95.9	94.8
22	-	-	164.5	163.9
1’	4.72 (*d*, 7.9)	4.55 (*d*, 7.9)	98.9	97.8
2’	3.21-3.24 (*m*)	2.97-3.07 (*m*)	74.2	73.1
3’	3.34-3.37 (*m*)	3.16-3.21 (*m*)	78.1	77.3
4’	3.28-3.33 (*m*, overlapped)	2.97-3.07 (*m*)	71.2	70.1
5’	3.41-3.43 (*m*)	3.16-3.21 (*m*)	77.6	76.5
6a’	3.89 (*dd*, 11.9)	3.70(*dd*, 11, 5.7)	62.2	61.1
6b’	3.65 (*q*, 11.9)	3.44 (*m*)		

* Literature values from Fan et al. (2010).

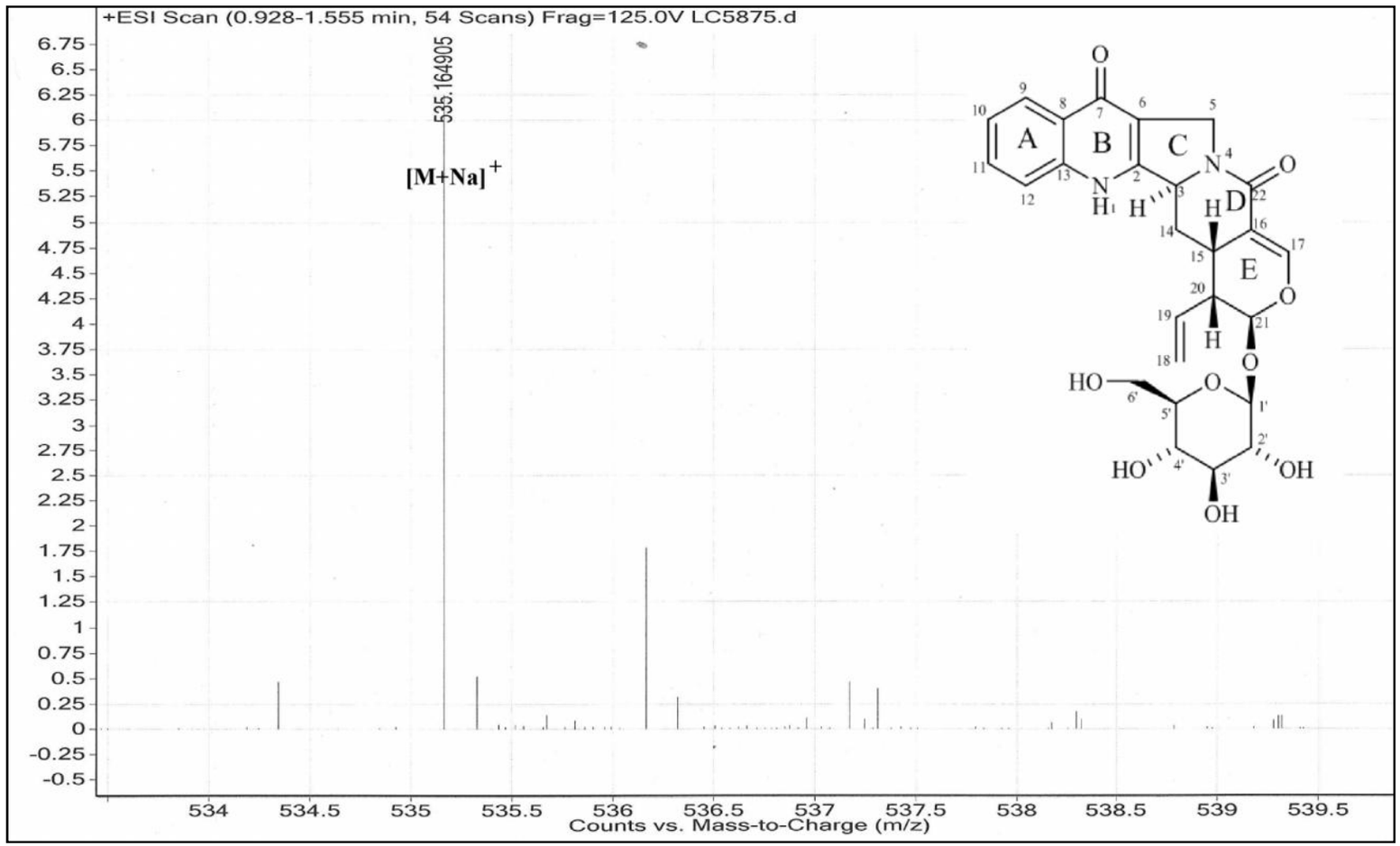

Figure 3.75: LCMS Spectrum of Pumiloside **69**

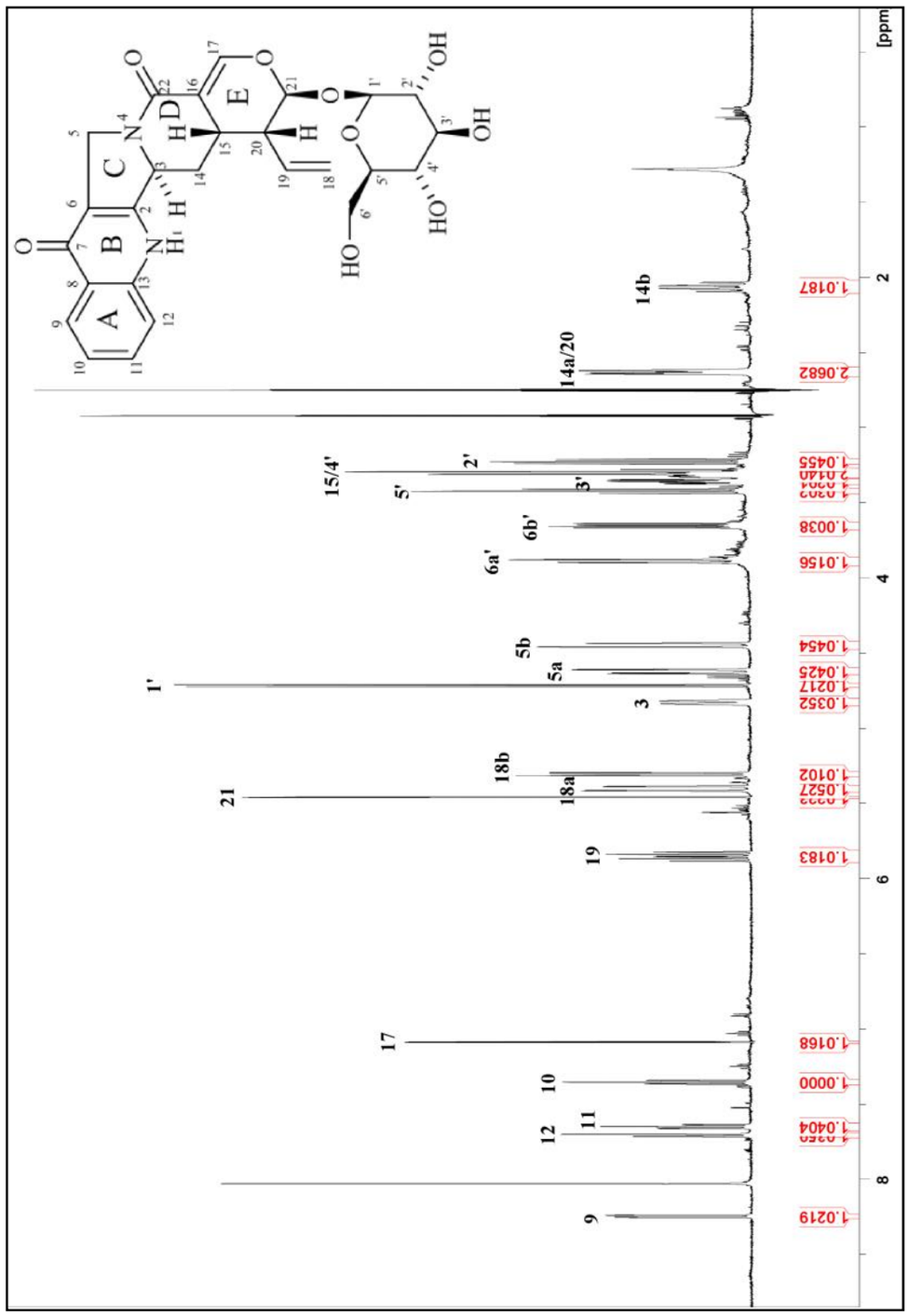

Figure 3.76: ^{1}H NMR Spectrum of Pumiloside **69**

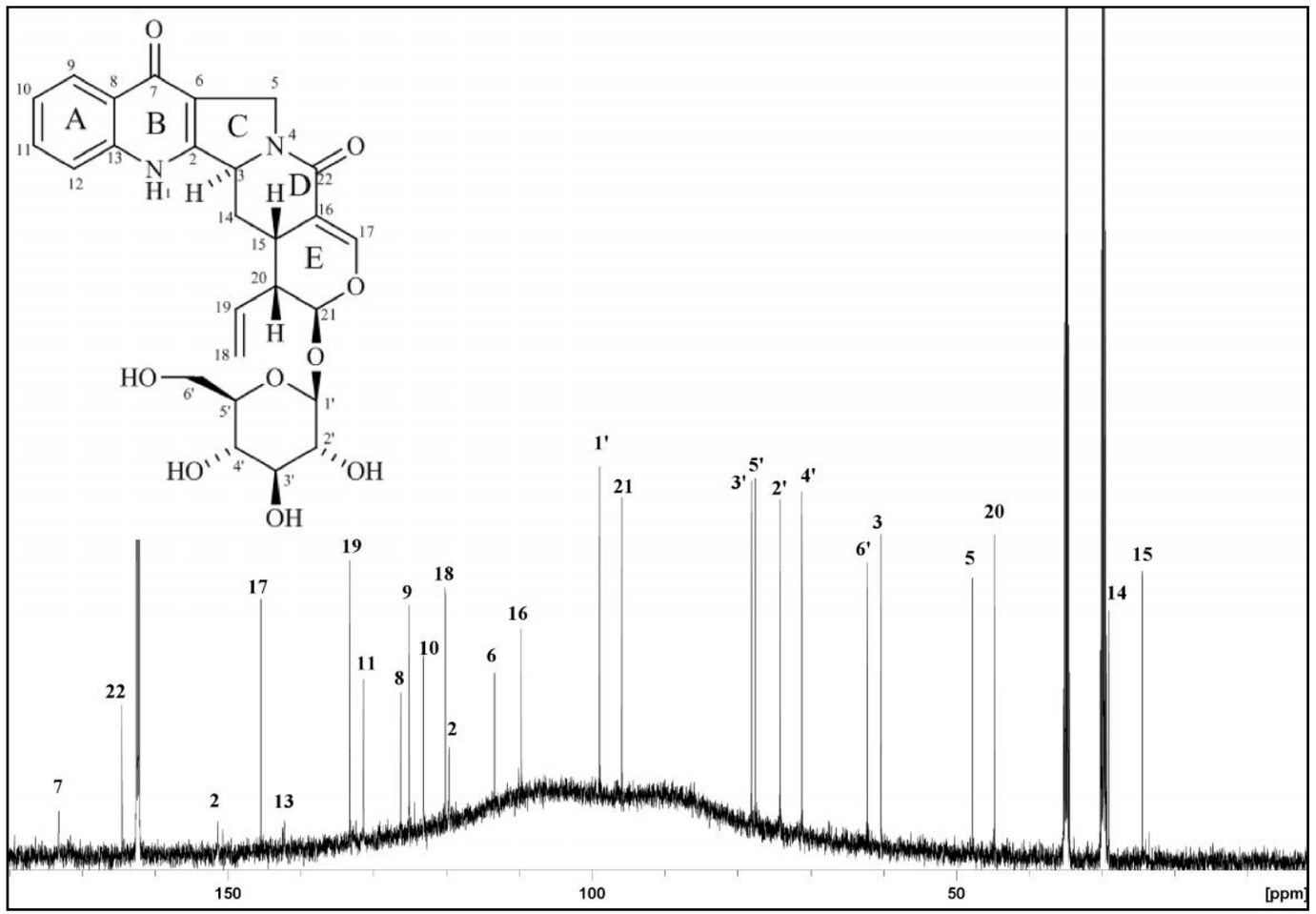

Figure 3.77: ^{13}C NMR Spectrum of Pumiloside **69**

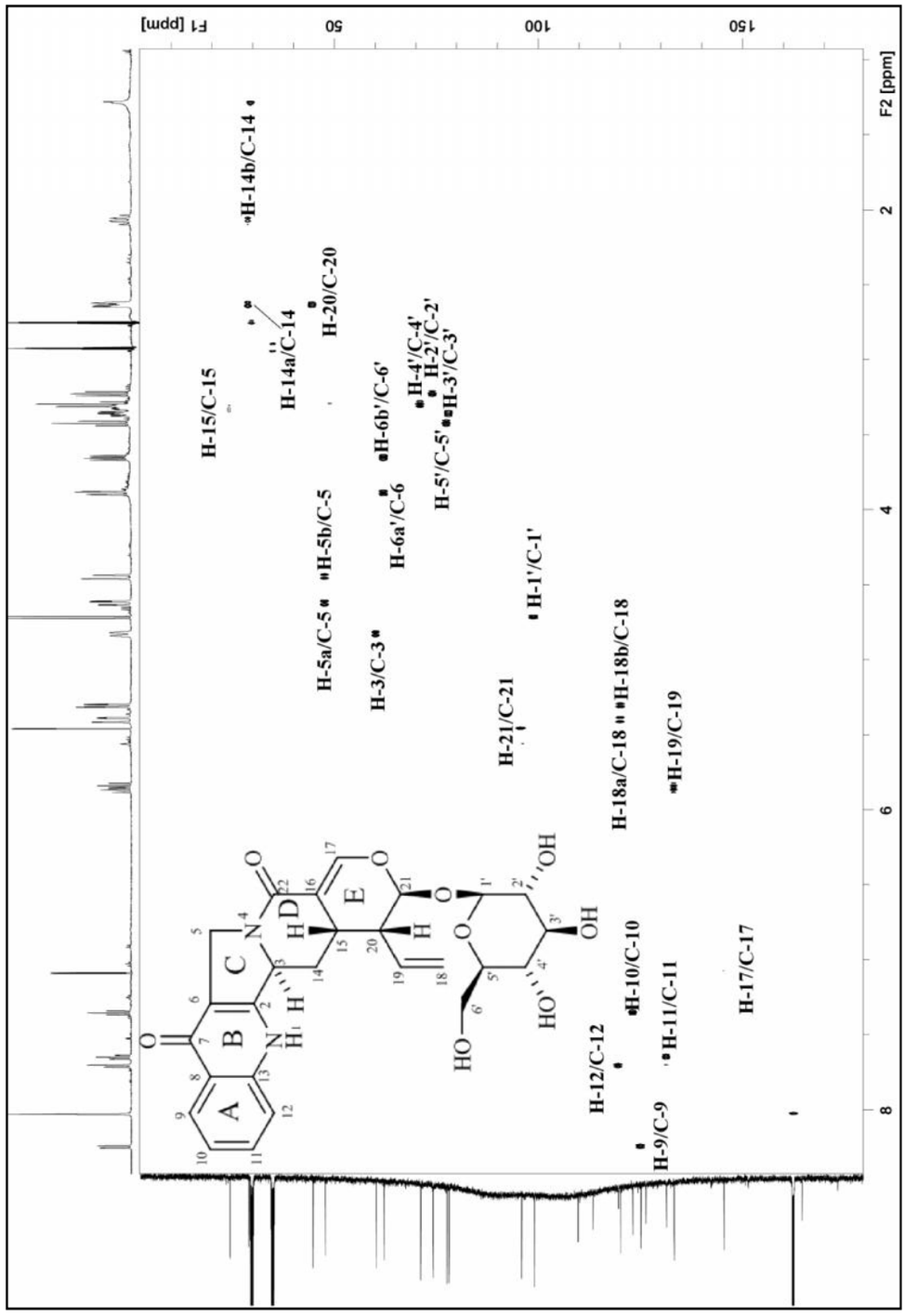

Figure 3.78: HSQC Spectrum of Pumiloside **69**

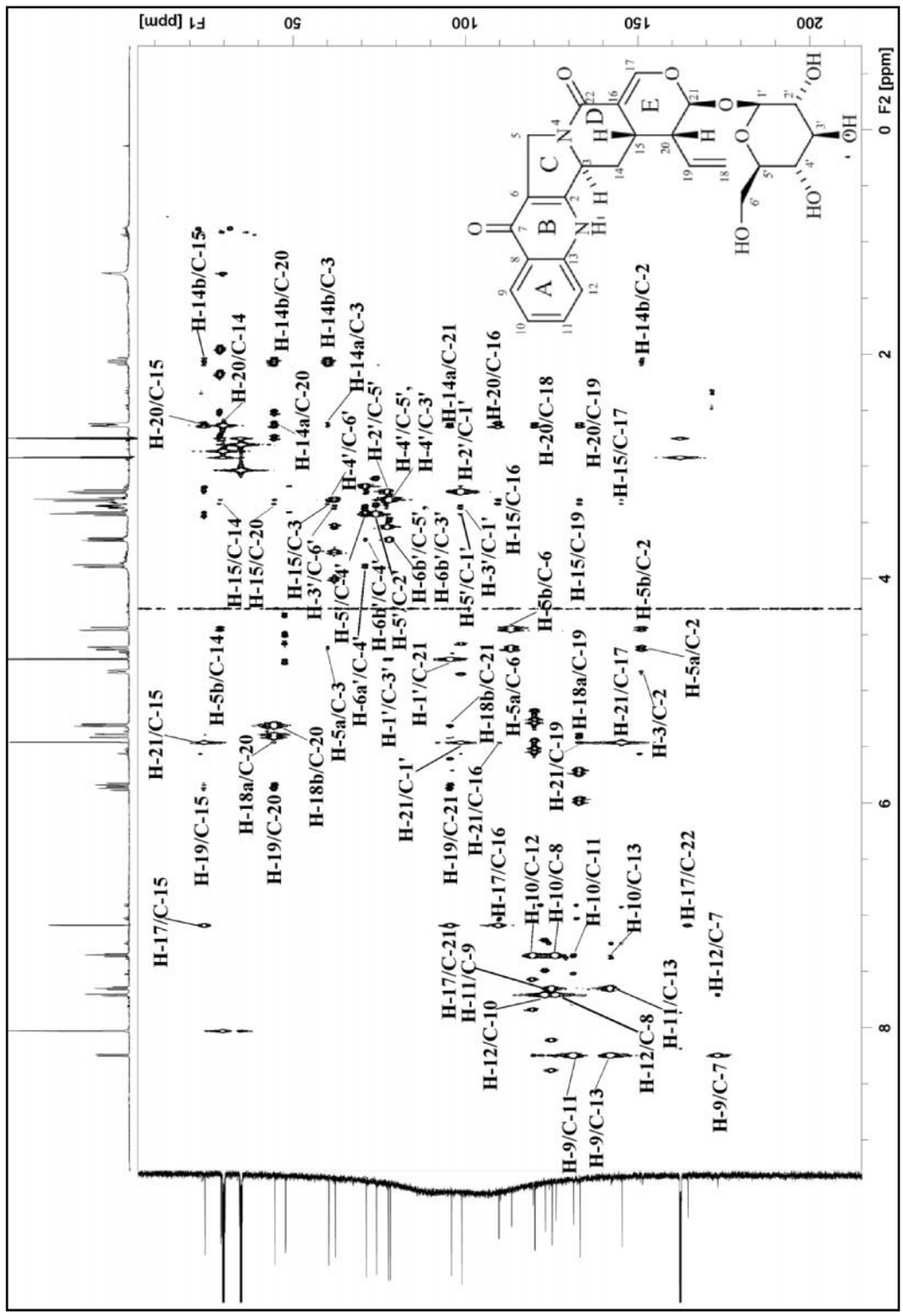

Figure 3.79: HMBC NMR Spectrum of Pumiloside **69**

3.2.11 Naucleficine 64

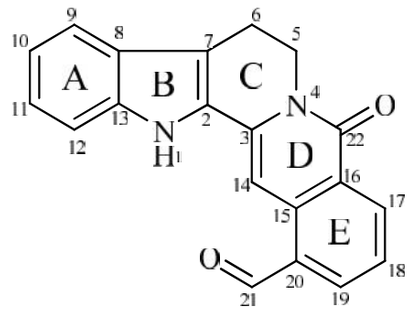

64

Naucleficine **64** was obtained as an orange amorphous solid. It molecular formula was confirmed as $C_{20}H_{14}N_2O_2$ from the ESIMS (Figure 3.81) which showed a pseudomolecular ion peak $[M+H]^+$ at *m/z* 315.1126 (calc. 315.1128). In UV spectrum, absorption maxima were observed at 379, 364, 298, 263 and 229 nm.[74] The IR spectrum of naucleficine **64** showed absorption peaks at 3271, 1676 and 1642 cm^{-1}, indicating the existence of N-H, conjugated HC=O and conjugated –NC=O stretching vibrations.[74]

Analysis of ^{1}H-NMR and ^{13}C-NMR spectra (Figure 3.82 and Figure 3.83) of naucleficine **64** showed a similar pattern with that of nauclefine **63** in the aromatic region (two doublets and two triplets) and also the presence of two methylenes which suggesting a tetrahydro-*β*-carboline skeleton (ring A, B and C).[75] Both compounds also possess the δ lactam ring D. Two other aromatic protons at δ_H 8.71 (1H, *d*, *J* = 7.3 Hz, H-17), δ_H 7.55 (1H, *t*, *J* = 7.3 Hz, H-18) and δ_H 8.05 (1H, *d*, *J* = 7.3 Hz, H-19) could be assigned to H-17 and H-19 of ring E. A broad NH singlet can be seen at δ_H 8.90 in ^{1}H-NMR spectrum.

The ^{13}C-NMR and DEPT (Figure 3.84) spectra of naucleficine **64** indicated a total of twenty carbon signals; two methylenes, eight methines, eight quaternary carbons and two carbonyl carbons (Table 1). Two downfield carbon signals at δ_C 161.9 (C-22) and δ_C 193.6 (C-21) could be assigned to carbonyl group of a δ lactam ring and an aldehyde unit respectively. In the HMBC spectrum, correlation of H-14 (δ_H 8.17) to C-3

(δ_C 135.3), H-5 (δ_H 4.54) to C-3 and C-22 (δ_C 161.9) can be observed, thus supporting the connectivity of ring C with ring D (δ lactam ring). HMBC correlations of H-14 to C-16 (δ_C 126.4), H-17 to C-22, H-18 to C-15 (δ_C 129.5) and C-16 indicating connectivity of the δ lactam ring D with benzene ring (ring E) through C-15 and C-16. Furthermore, the HMBC spectrum showed correlation of H-19 to C-21, H-21 (δ_H 10.23) to C-20 suggesting that the aldehydic moiety is linked to ring E through C-20 (Figure 3.80).

Complete ^{1}H and ^{13}C-NMR assignments (Table 3.12) were established by thorough analysis of COSY, HMBC and HSQC data. From the analysis of the spectroscopic data obtained and comparison with the literature values,[74,88,89] the identity of naucleficine **64** was ensured.

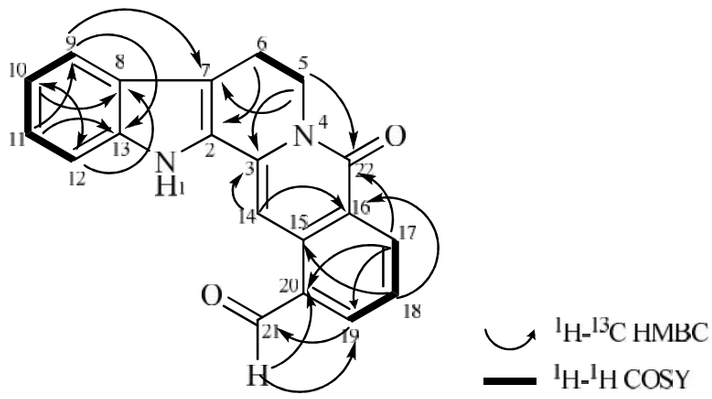

Figure 3.80: Selected COSY and HMBC Correlations of naucleficine **64**

Table 3.12: ^{1}H-NMR (400 MHz) and ^{13}C-NMR (100 MHz) Spectral Data of Naucleficine **64** in $CDCl_3$.

Position	**^{1}H δ_H (multiplicity, *J* in Hz)**		**^{13}C δ_C**	
	Experimental ($CDCl_3$)	**Reference* (DMSO-d_6)**	**Experimental ($CDCl_3$)**	**Reference* (DMSO-d_6)**
NH-1	8.90 (*br s*)	11.76 (*br s*)	-	-
2	-	-	128.0	127.8
3	-	-	135.3	135.0
5	4.54 (*t*, 6.9)	4.42 (*t*, 6.6)	40.9	40.4
6	3.16 (*t*, 6.9)	3.12 (*t*, 6.6)	19.9	19.1
7	-	-	115.2	114.0
8	-	-	126.1	125.4
9	7.57 (*d*, 7.8)	7.60 (*d*, 7.2)	119.6	119.3
10	7.17 (*t*, 7.8)	7.08 (*t*, 7.8)	120.7	119.6
11	7.31 (*t*, 7.8)	7.24 (*t*, 7.7)	125.0	124.0
12	7.46 (*d*, 7.8)	7.48 (*d*, 8.1)	111.8	111.9
13	-	-	138.4	138.5
14	8.17 (*s*)	8.11 (*s*)	96.1	94.8
15	-	-	129.5	129.5
16	-	-	126.4	125.5
17	8.71 (*d*, 7.3)	8.53 (*d*, 7.5)	134.9	134.2
18	7.55 (*t*, 7.3)	7.62(*t*, 7.2)	125.3	125.9
19	8.05 (*d*, 7.3)	8.24 (*d*, 7.5)	141.6	138.4
20	-	-	135.8	135.5
21	10.23 (*s*)	10.43 (*s*)	193.6	192.6
22	-	-	161.9	160.7

*Literature values from Donfack et al. (2012).

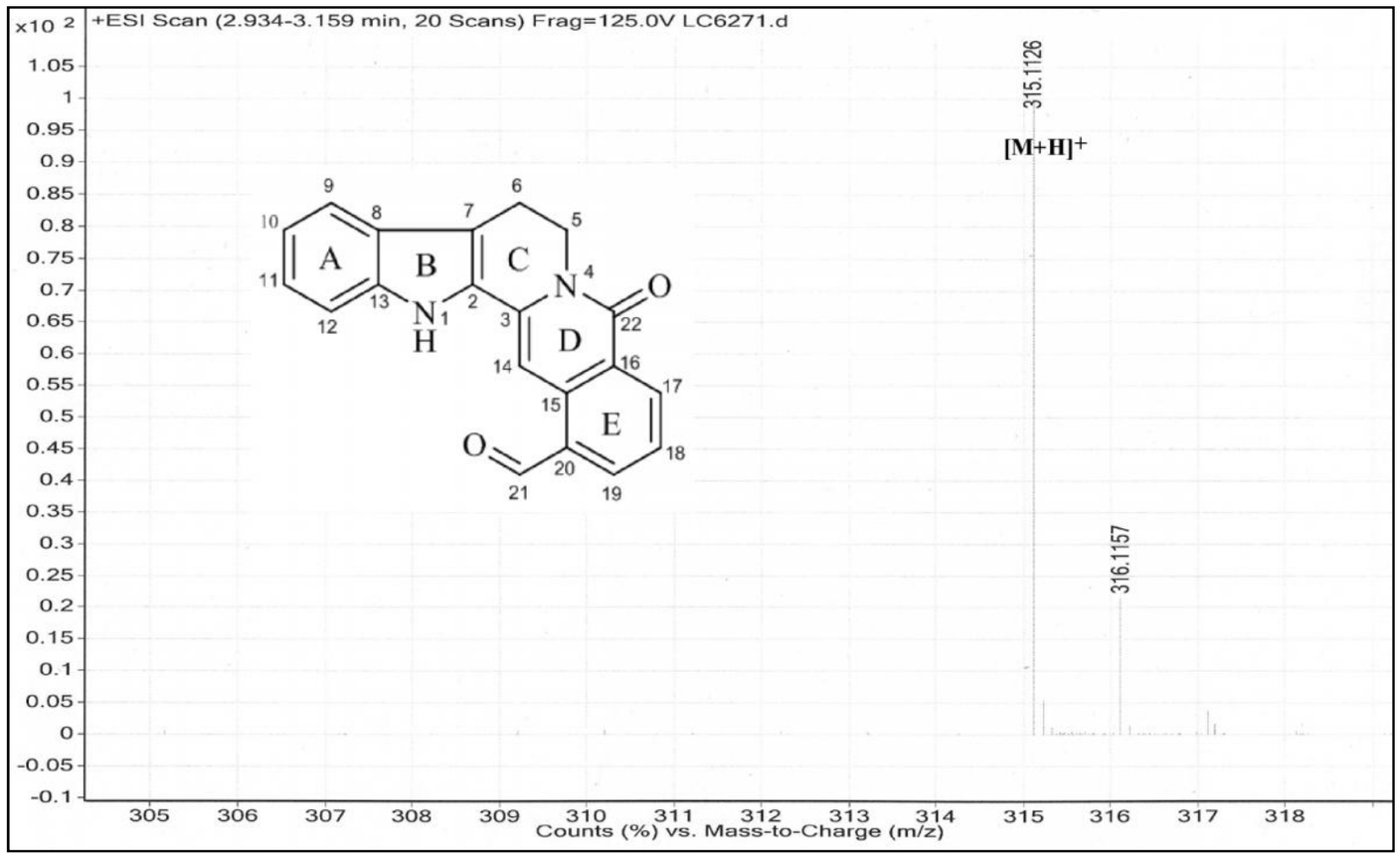

Figure 3.81: LCMS Spectrum of Naucleficine **64**

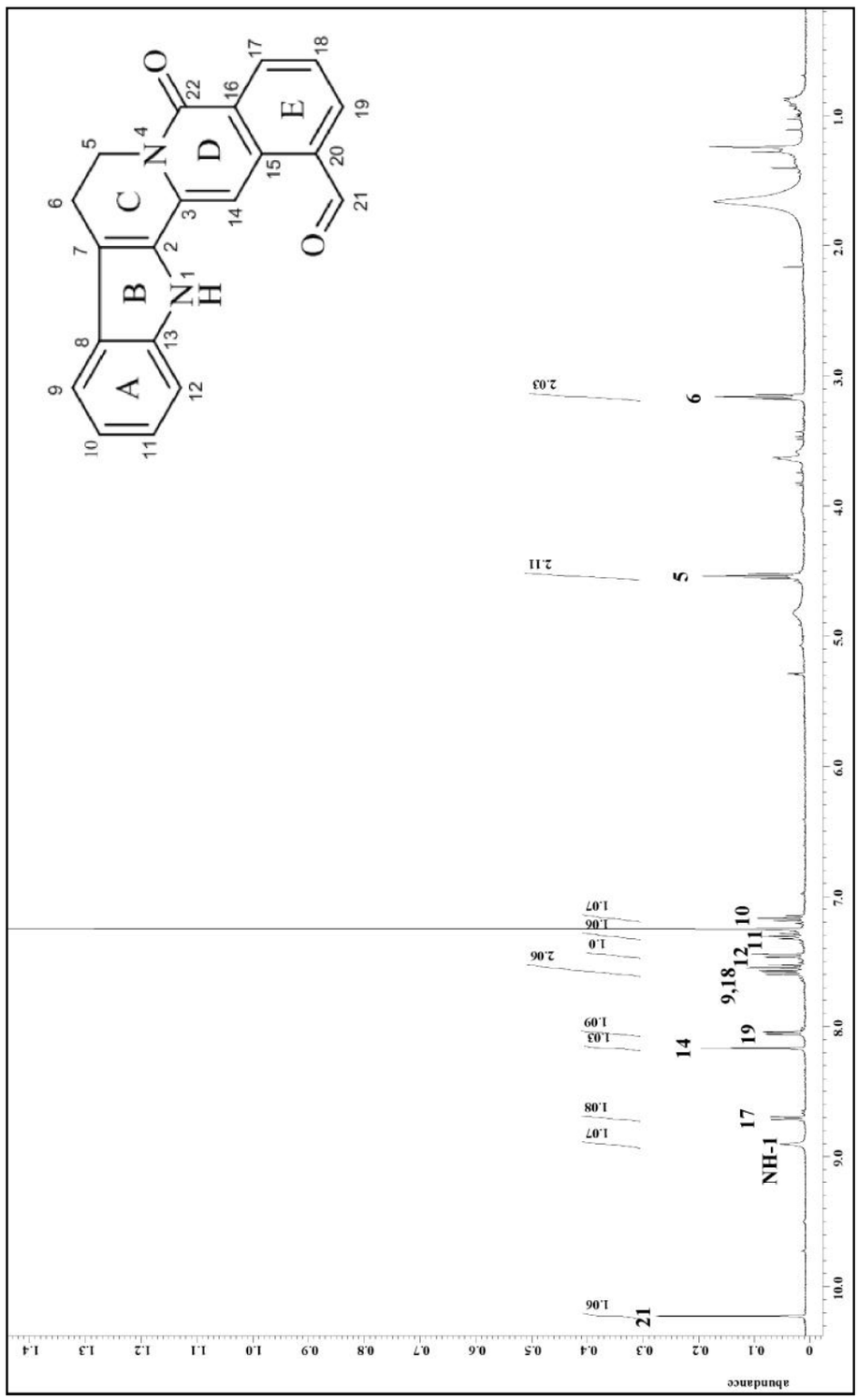

Figure 3.82: ^{1}H NMR Spectrum of Naucleficine **64**

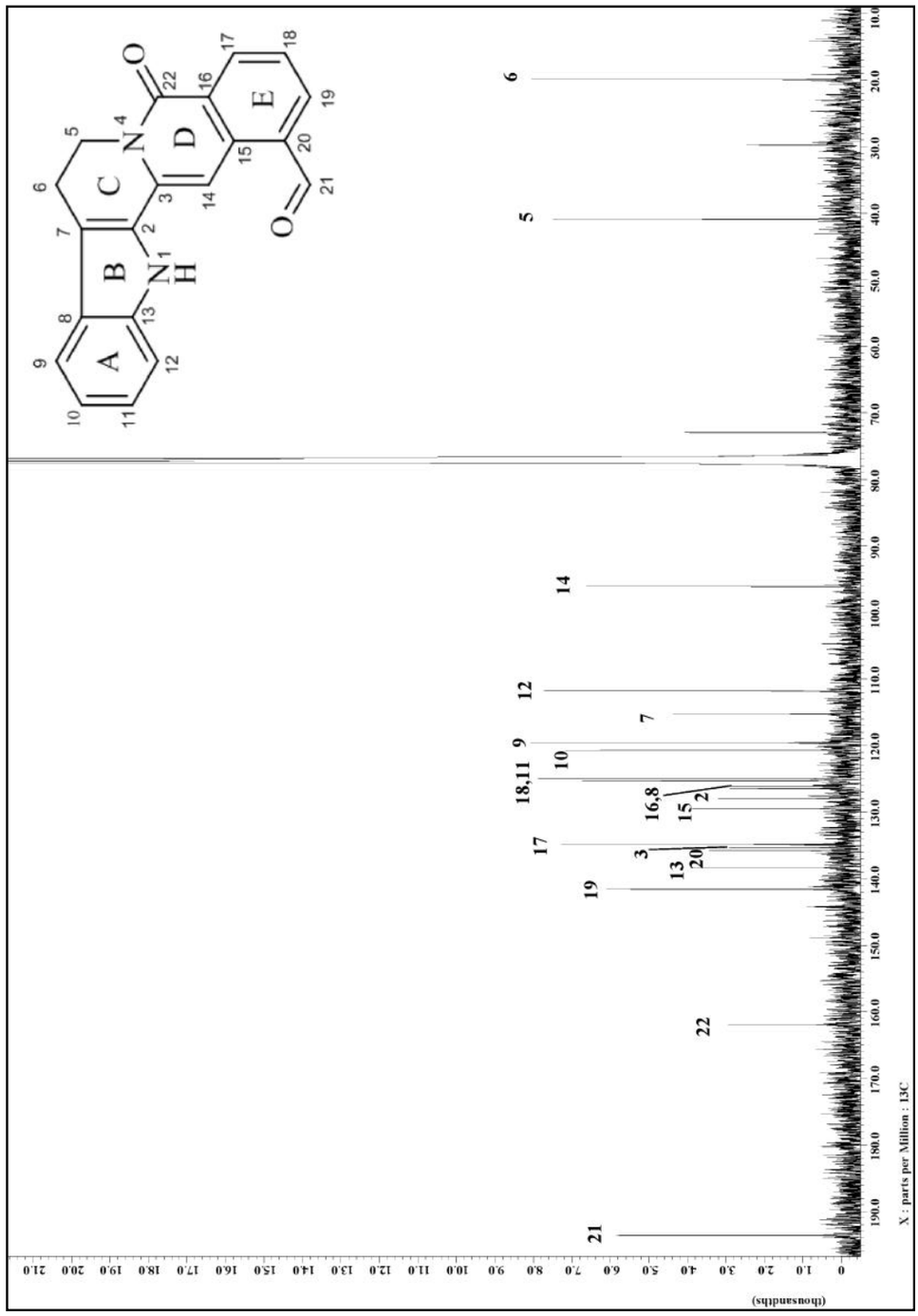

Figure 3.83: ^{13}C NMR Spectrum of Naucleficine **64**

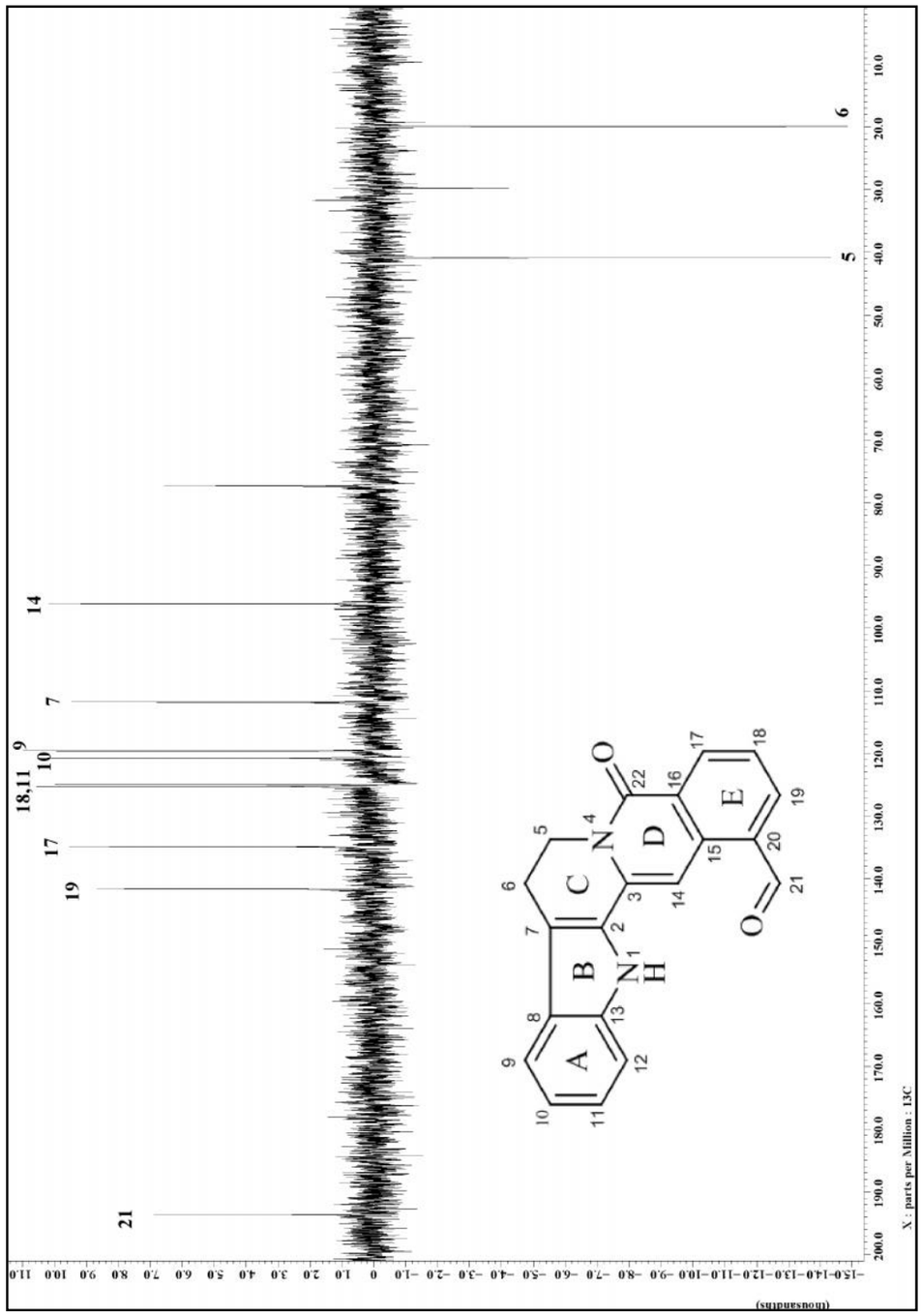

Figure 3.84: DEPT 135 Spectrum of Naucleficine **64**

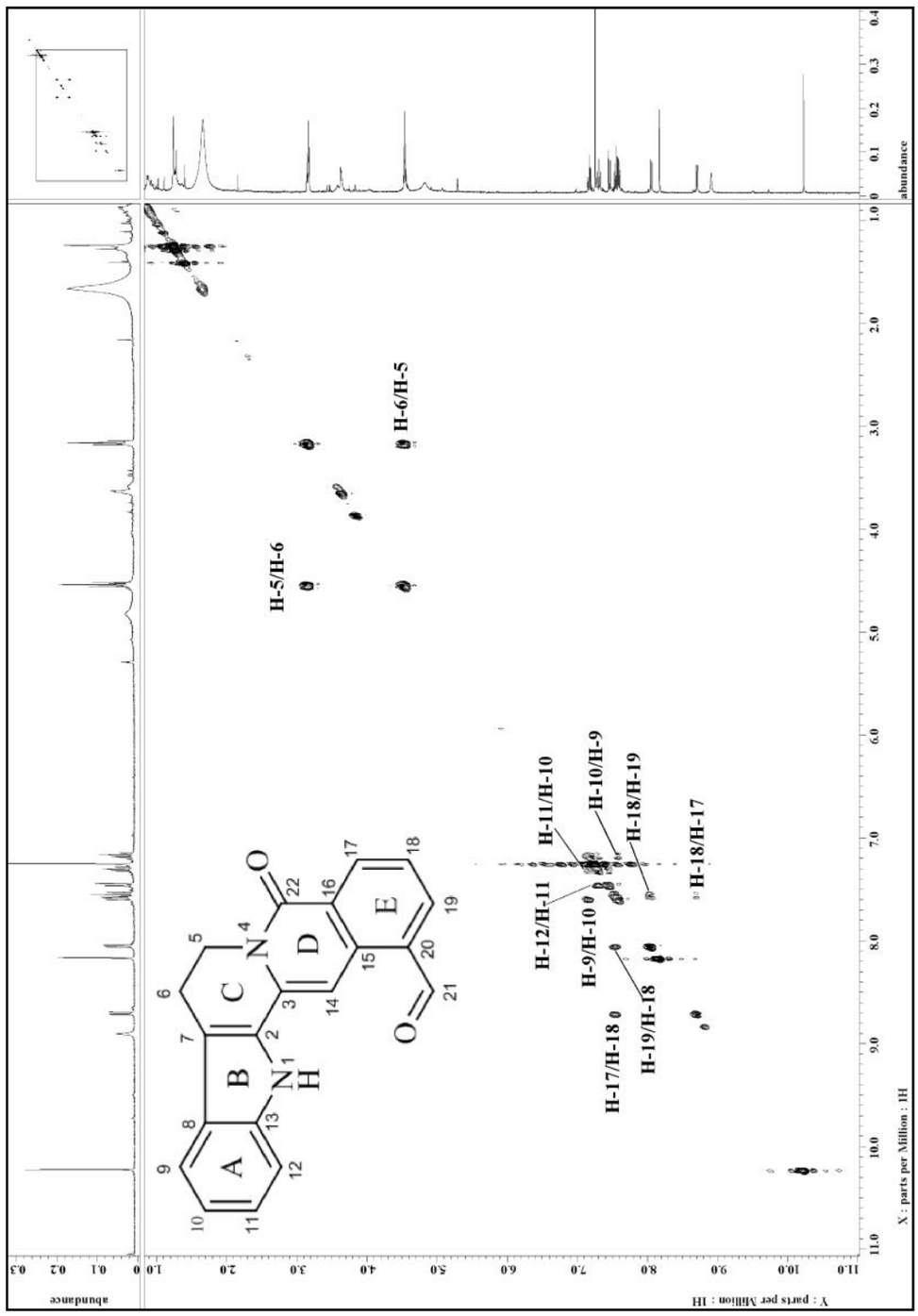

Figure 3.85: COSY Spectrum of Naucleficine **64**

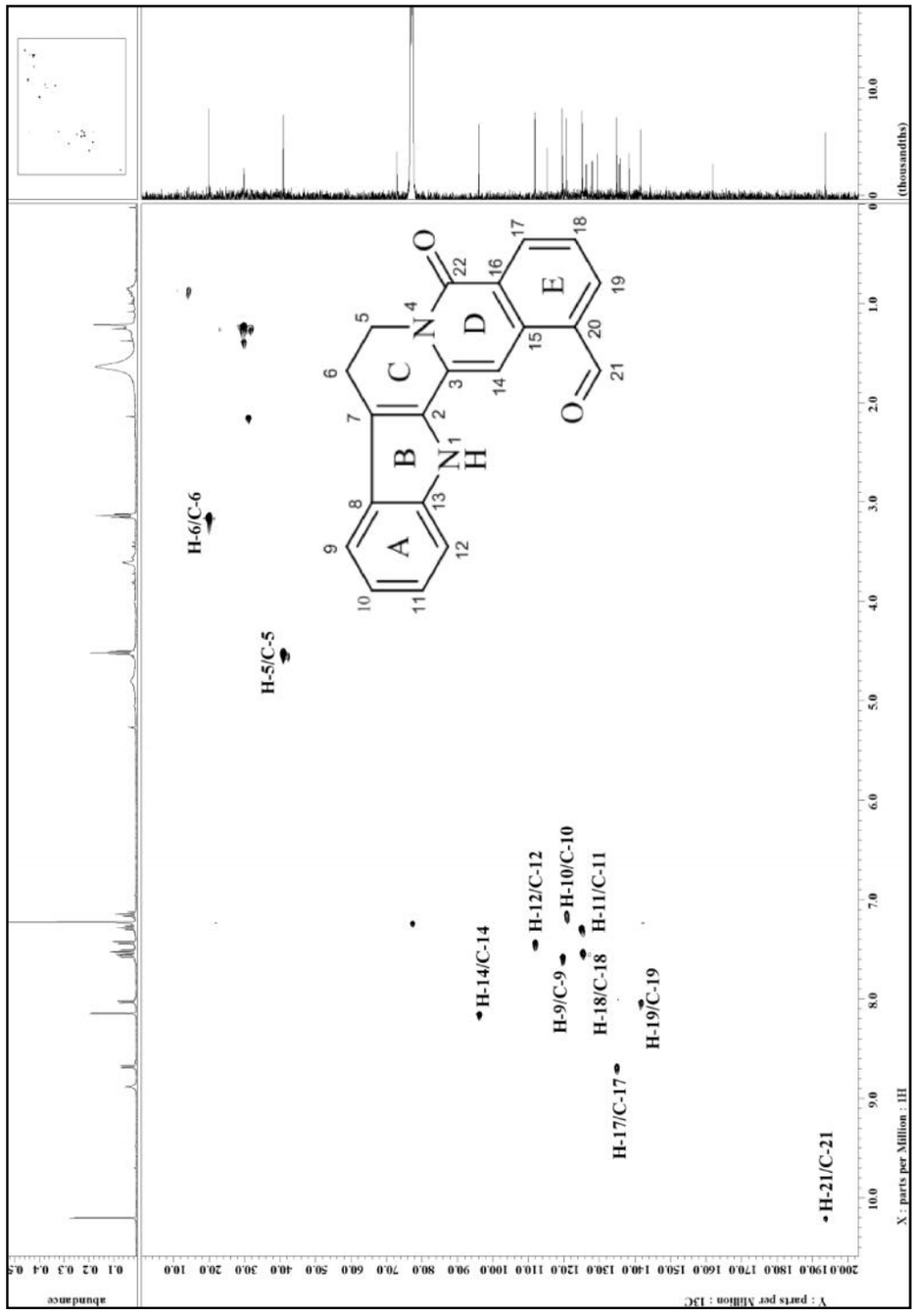

Figure 3.86: HSQC Spectrum of Naucleficine **64**

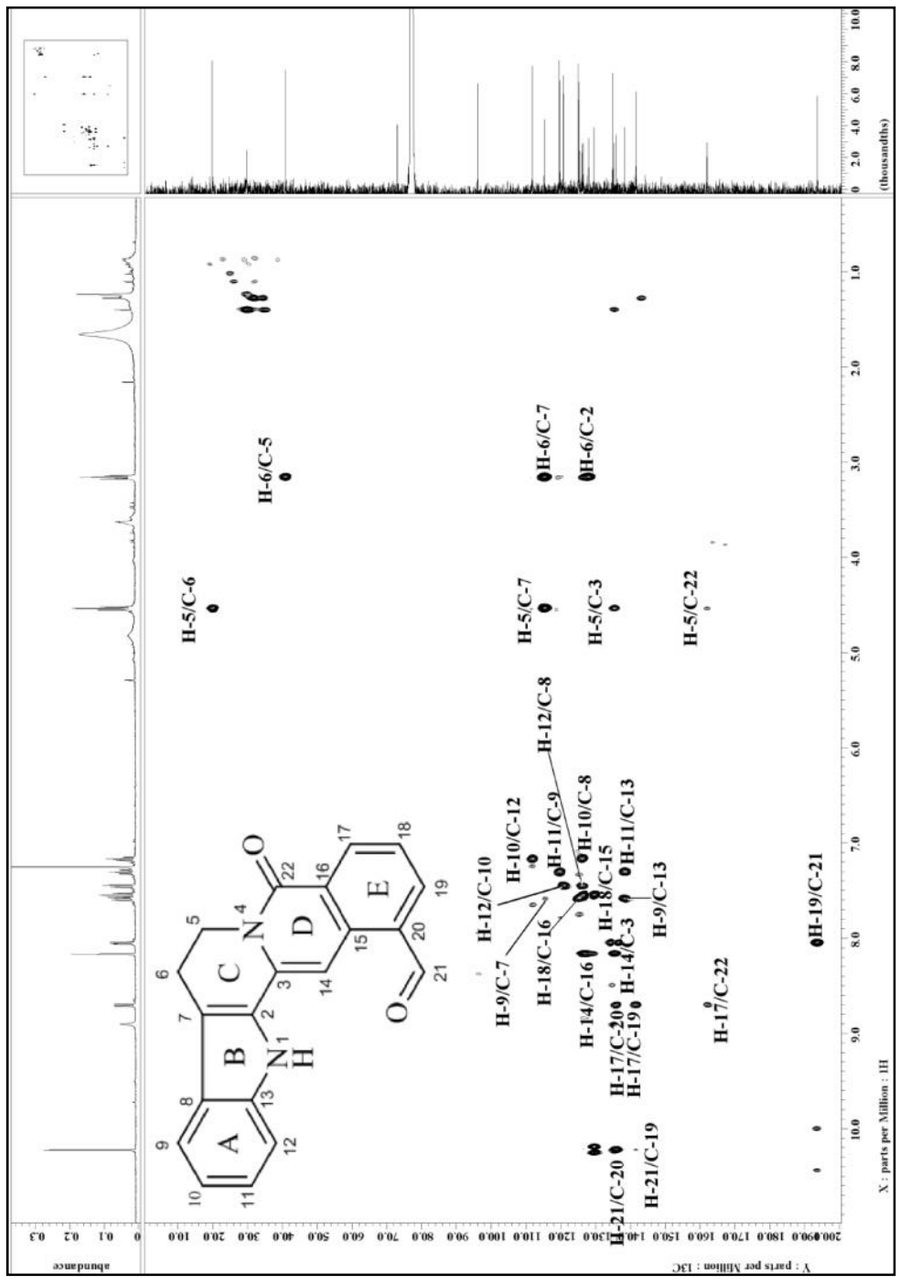

Figure 3.87: HMBC Spectrum of Naucleficine **64**

3.2.12 Naucleactonin C 65

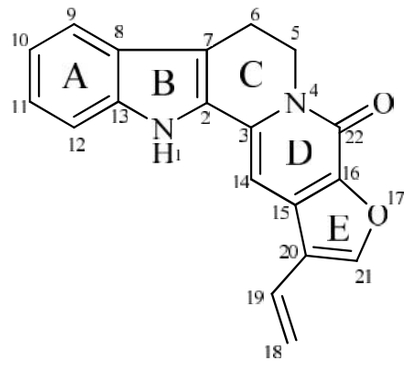

65

Naucleactonin C **65** was yielded as a yellowish amorphous solid. The ESIMS (Figure 3.89) displayed a pseudomolecular ion peak $[M+H]^+$ at *m/z* 303.1127, corresponding to the molecular formula of $C_{19}H_{14}N_2O_2$ (calc. 303.1128). Absorption peaks at 368, 353 and 211 nm were observed in UV spectrum.[83] In the IR spectrum of naucleactonin C **65**, absorption peaks at 3281 and 1653 cm^{-1} were revealed due to N-H and conjugated -NC=O stretching vibrations respectively.[83]

In the ^{1}H-NMR spectrum (Figure 3.90), two sets of doublets and triplets at δ_H 7.58 (1H, *d*, *J* = 8.0 Hz, H-9), δ_H 7.42 (1H, *d*, *J* = 8.0 Hz, H-12), δ_H 7.17 (1H, *t*, *J* = 8.0 Hz, H-10) and δ_H 7.30 (1H, *t*, *J* = 8.0 Hz, H-11) which represented an ortho-disubstituted aromatic ring system together with the presence of two methylenes at δ_H 4.55 (2H, *t*, *J* = 6.9 Hz, H_2-5) and δ_H 3.11 (2H, *t*, *J* = 6.9 Hz, H_2-6), suggesting a tetrahydro-*β*-carboline skeleton (ring A, B and C).[75] In addition, two doublets and one *dd* were apparent at δ_H 5.76 (1H, *d*, *J* = 17.9 Hz, H-18a), δ_H 5.40 (1H, *d*, *J* = 11.5 Hz, H-18b) and δ_H 6.68 (1H, *dd*, *J* = 17.9, 11.5 Hz, H-19) respectively were attributed to C-18 (δ_C 116.4) and C-19 (δ_C 125.6), indicating the presence of a vinyl group (-CH=CH_2). A broad singlet of NH can be observed at δ_H 8.46.

The ^{13}C-NMR spectrum (Figure 3.91) of naucleficine **64** indicated a total of nineteen carbon signals; three methylenes, seven methines, eight quaternary carbons and

one carbonyl carbon. A downfield carbon signal was observed at δ_C 153.6 which could be assigned to carbonyl group of a δ lactam ring (C-22). The proof that H-21 belongs to the deshielded five membered furan ring is from the ^{13}C signal of C-21 due to the electronegative effect of the vicinal O-17. However, H-21 resonated at higher field due to steric hindrance effect which is confirmed in many furan system.[90] HMBC correlations of H-14 (δ_H 6.78) to C-16 (δ_C 143.5), H-21 (δ_H 7.74) to C-15 (δ_C 130.3) and C-16 indicated that ring D is connected to the furan ring (ring E). In addition, the attachment of the vinyl group with the furan ring forming a vinylfuran unit through C-20 was suggested by the HMBC correlation of H_2-18 to C-20 (Figure 3.88).

Based on the available spectral data (Table 3.13) and investigation of the literature values,[83] the structure of naucleactonin C **65** was confirmed.

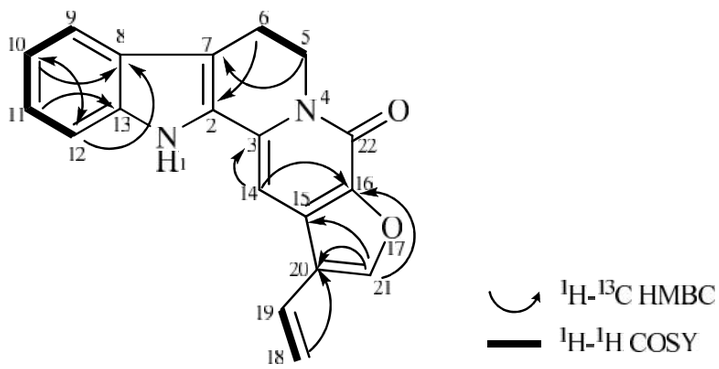

Figure 3.88: Selected COSY and HMBC Correlations of Naucleactonin C **65**

Table 3.13: ^{1}H-NMR (400 MHz) and ^{13}C-NMR (100 MHz) Spectral Data of Naucleactonin C **65** in $CDCl_3$.

Position	**^{1}H δ_H (multiplicity, *J* in Hz)**		**^{13}C δ_C**	
	Experimental ($CDCl_3$)	**Reference* (DMSO-d_6)**	**Experimental ($CDCl_3$)**	**Reference* (DMSO-d_6)**
NH-1	8.46 (*br s*)	11.67 (*s*)	-	-
2	-	-	128.3	128.5
3	-	-	133.5	133.6
5	4.55 (*t*, 6.9)	4.40 (*t*, 6.7)	40.8	40.1
6	3.11 (*t*, 6.9)	3.07 (*t*, 6.7)	19.9	19.1
7	-	-	113.9	111.9
8	-	-	126.3	125.4
9	7.58 (*d*, 8.0)	7.59 (*d*, 8.0)	119.5	119.1
10	7.17 (*t*, 8.0)	7.07 (*td*, 8.0, 1.0)	120.8	119.4
11	7.30 (*t*, 8.0)	7.22 (*td*, 8.0, 1.0)	124.4	123.4
12	7.42 (*d*, 8.0)	7.42 (*d*, 8.0)	111.6	111.5
13	-	-	137.9	137.8
14	6.78 (*s*)	7.33 (*s*)	93.2	93.3
15	-	-	130.3	129.7
16	-	-	143.5	142.5
18a	5.76 (*d*, 17.9)	5.97 (*d*, 18.0)	116.4	116.1
18b	5.40 (*d*, 11.5)	5.47 (*d*, 11.0)		
19	6.68 (*dd*, 17.9, 11.5)	6.80 (*dd*, 18.0, 11.0)	125.6	125.9
20	-	-	120.6	119.9
21	7.74 (*s*)	8.23 (*s*)	146.2	147.5
22	-	-	153.6	152.4

* Literature values from Fan et al. (2010).

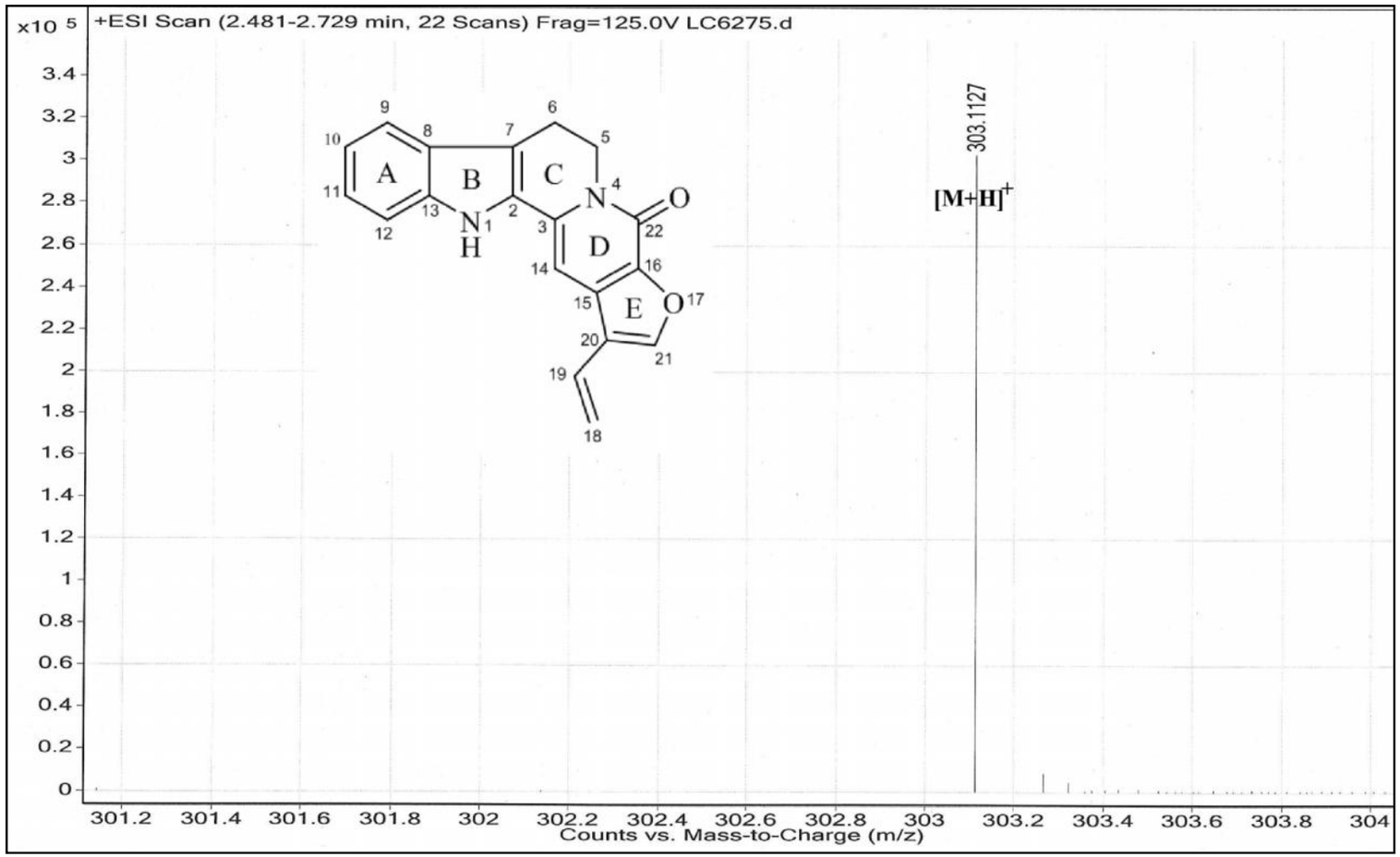

Figure 3.89: LCMS Spectrum of Naucleactonin C **65**

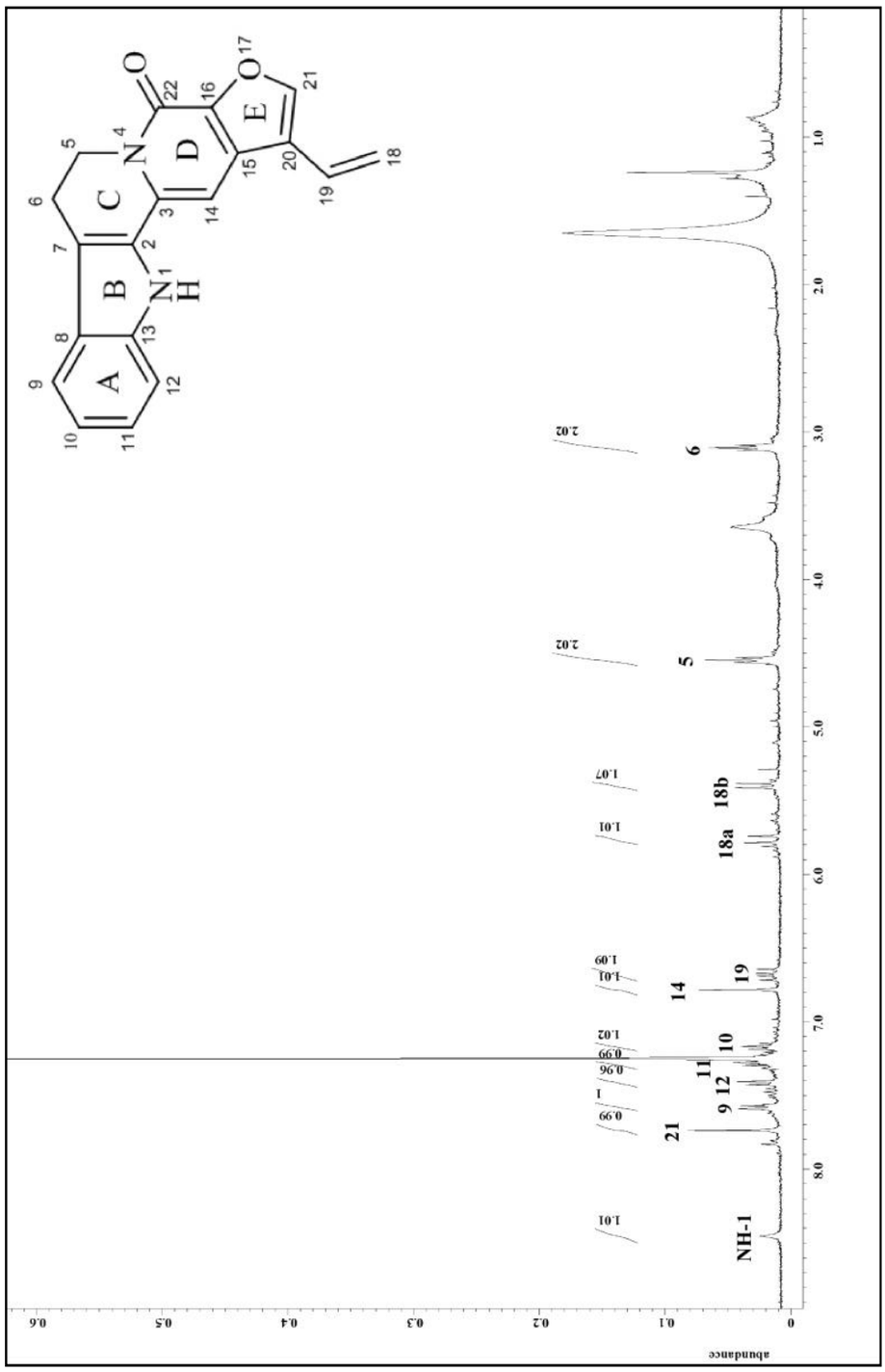

Figure 3.90: ^{1}H NMR Spectrum of Naucleactonin C **65**

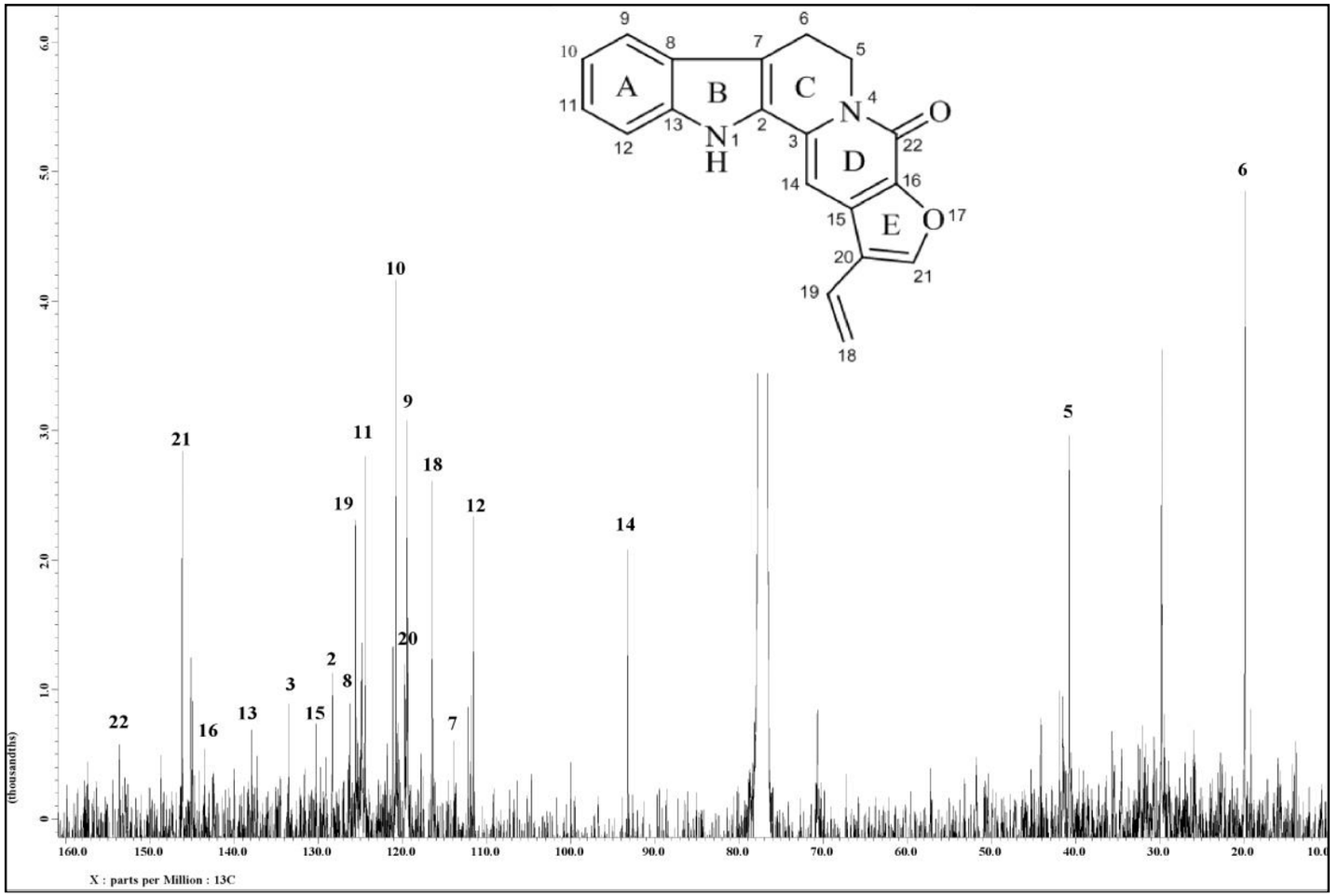

Figure 3.91: ^{13}C NMR Spectrum of Naucleactonin C **65**

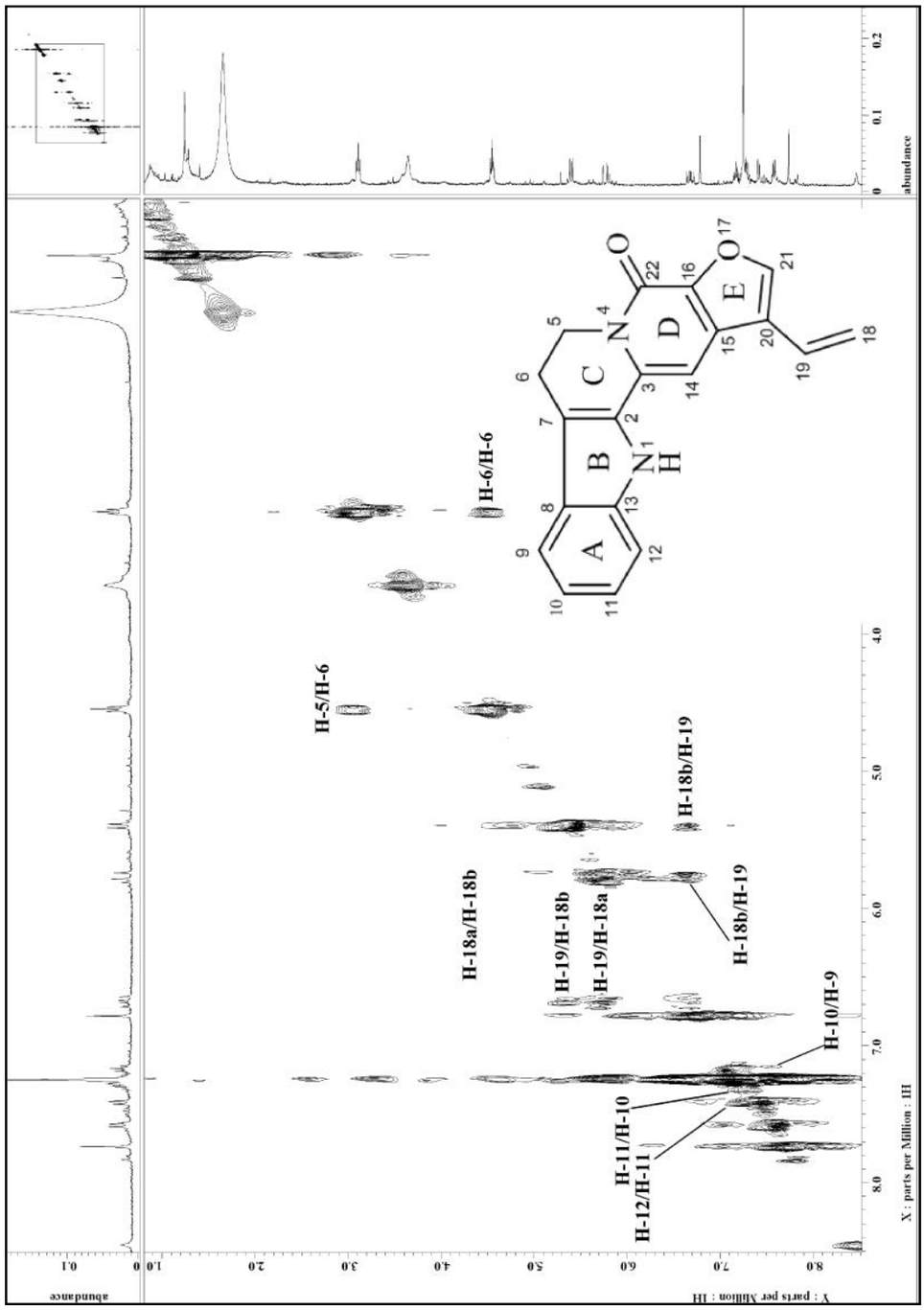

Figure 3.92: COSY Spectrum of Naucleactonin C **65**

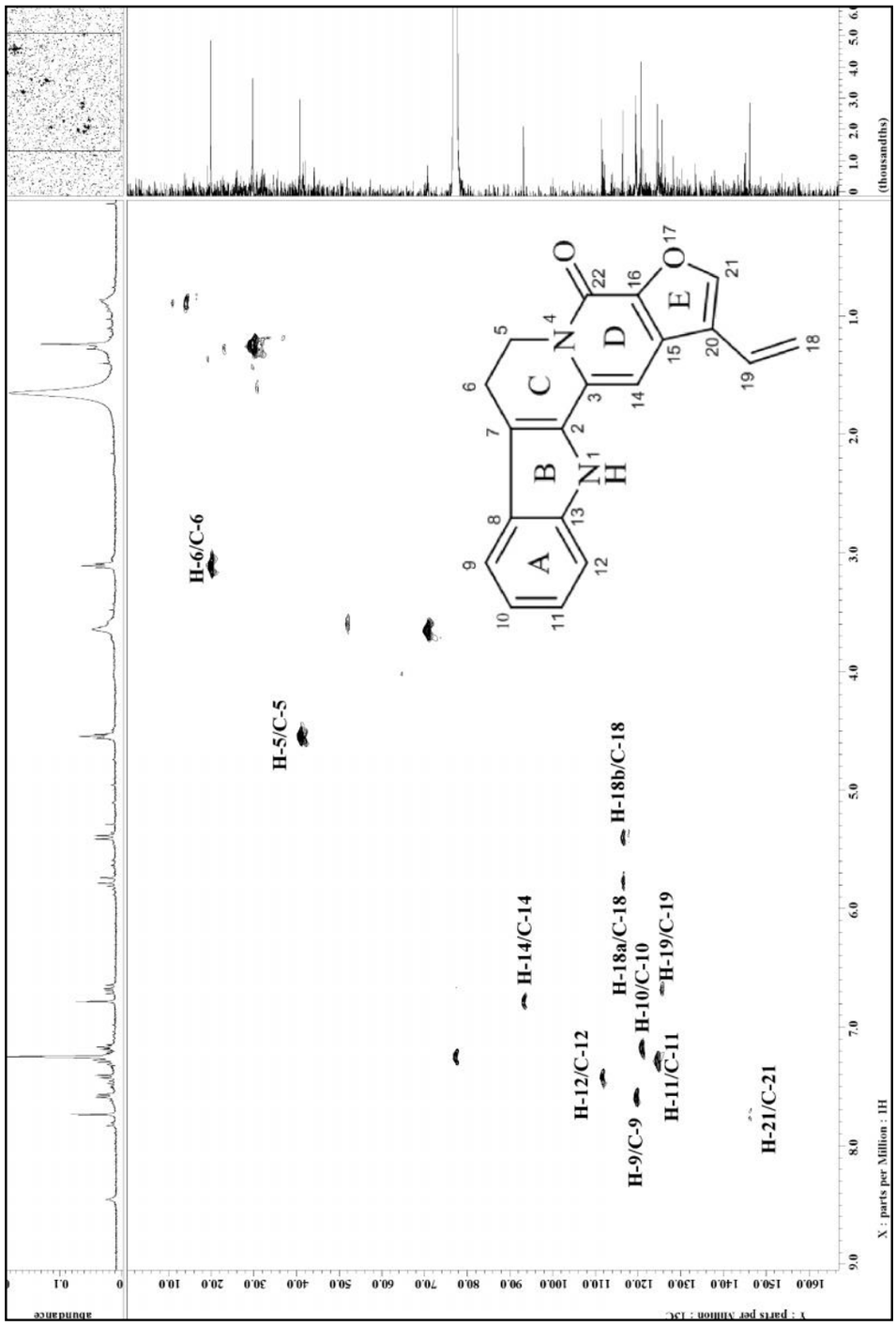

Figure 3.93: HSQC Spectrum of Naucleactonin C **65**

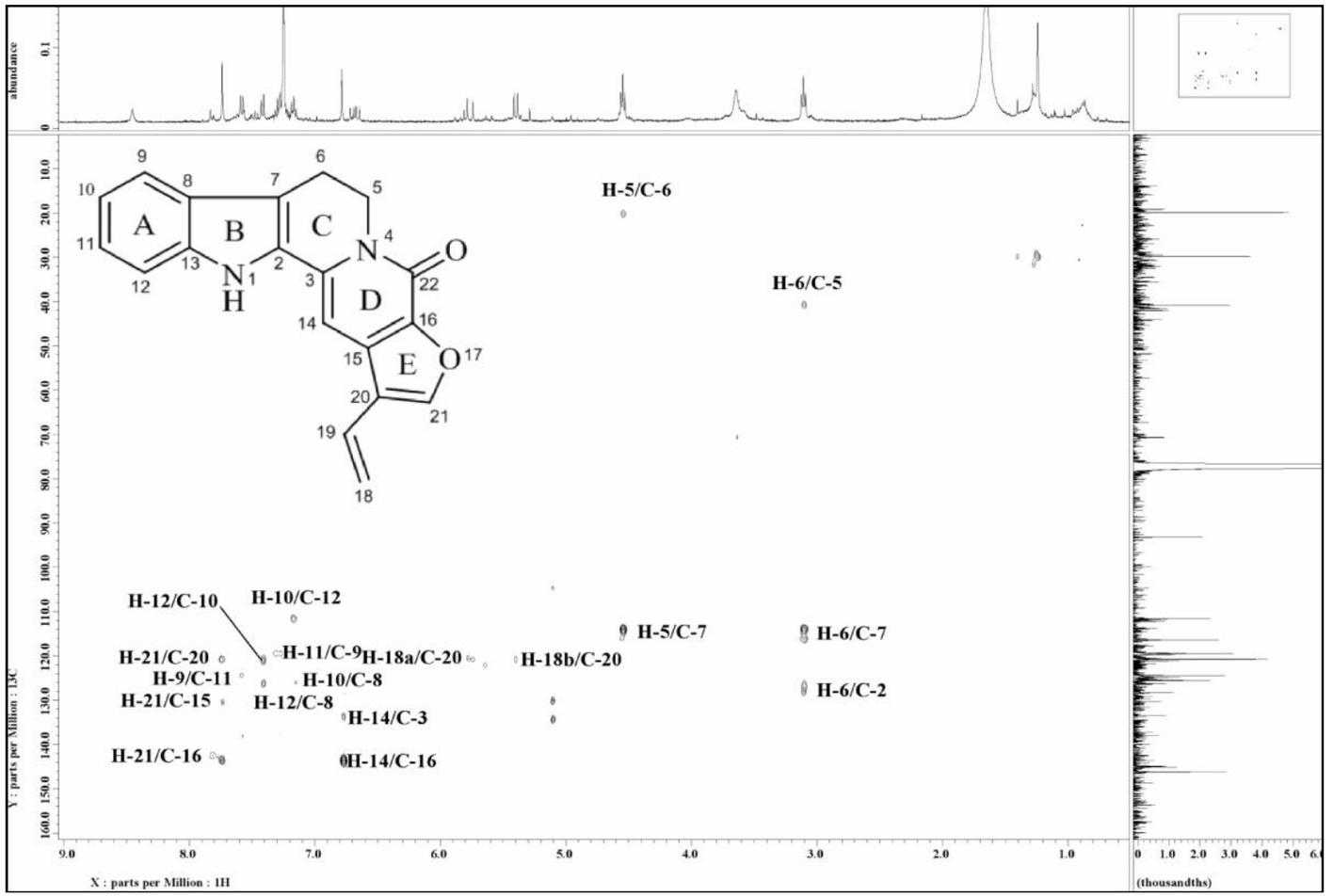

Figure 3.94: HMBC Spectrum of Naucleactonin C **65**

3.2.13 Harmane 67

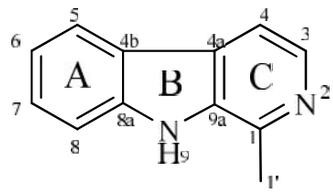

67

Harmane **67** was isolated as a brownish amorphous solid. It has a molecular formula of $C_{12}H_{10}N_2$ as deduced from the ESIMS (Figure 3.96) which showed a pseudomolecular ion peak at *m/z* $[M+H]^+$ 183.0942 (calc.183.0917). In UV spectrum, the absorption peaks at 348, 288, 233 nm were observed.[91] The IR spectrum of harmane **67** showed a broad absorption band at 3145 cm^{-1} indicated the presence of N-H group of indole alkaloid.

In the ^{1}H-NMR spectrum (Figure 3.97), proton signals at the aromatic regions of δ_H 8.10 (1H, *d*, *J* = 8.0 Hz, H-5), δ_H 7.52-7.57 (1H, *m*, overlapped, H-8), δ_H 7.52-7.57 (1H, *m*, overlapped, H-7), δ_H 7.27 (1H, *m*, H-6) and two downfield methine signals at δ_H 8.34 (1H, *t*, *J* = 5.4, H-3) and δ_H 7.81 (1H, *t*, *J* = 5.4, H-4), suggesting the presence of β-carboline skeleton.[92] COSY correlation between H-3 and H-4, H-5 and H-6, H-7 and H-6 were observed. A broad singlet at δ_H 8.80 could be assigned to NH.

The ^{13}C-NMR and DEPT spectra (Figure 3.98 and Figure 3.99) of harmane **67** indicated a total of twelve carbon signals; one methyl, six methines and five quaternary carbons. An upfield methyl signal of H_3-1' at δ_H 2.81 correlated with two quaternary carbon of C-9a (δ_C 134.7) and C-1 (δ_C 141.8), indicating a methyl unit was attached to the β-carboline skeleton (Figure 3.95).

From the analysis of the spectroscopic data obtained (Table 3.14) and comparison with the literature values,[92,93] the structure of harmane **67** was confirmed.

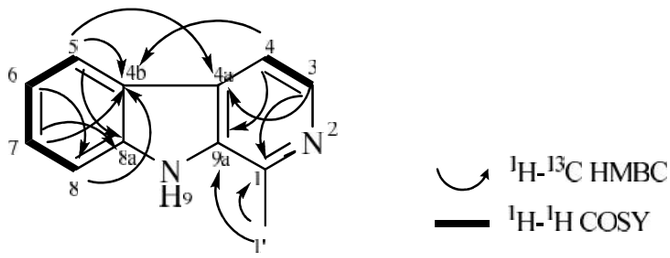

Figure 3.95: Selected COSY and HMBC Correlations of Harmane **67**

Table 3.14: ^{1}H-NMR (400 MHz) and ^{13}C-NMR (100 MHz) Spectral Data of Harmane **67** in $CDCl_3$.

Position	**^{1}H**		**^{13}C**	
	δ_H (multiplicity, *J* in Hz)		**δ_C**	
	Experimental ($CDCl_3$)	**Reference* ($CDCl_3$)**	**Experimental ($CDCl_3$)**	**Reference* ($CDCl_3$)**
1	-	-	141.8	141.8
3	8.34 (*d*, 5.4)	8.37 (*d*, 5.2)	138.4	138.8
4	7.81 (*d*, 5.4)	7.83 (*d*, 5.5)	113.1	112.9
4a	-	-	128.5	128.3
4b	-	-	122.0	122.1
5	8.10 (*d*, 8.0)	8.12 (*d*, 8.0)	121.9	121.8
6	7.27 (*m*)	7.29 (*dt*, 6.9, 2.2)	120.0	120.2
7	7.52-7.57 (*m*, overlapped)	7.54 (*m*)	128.4	128.2
8	7.52-7.57 (*m*, overlapped)	7.54 (*m*)	111.7	111.6
8a	-	-	140.3	140.1
NH-9	8.80 (*br s*)	8.62 (*br s*)	-	-
9a	-	-	134.7	134.6
1’	2.81 (*s*)	2.84 (*s*)	20.2	20.4

*Literature value from Seki et al. (1993).

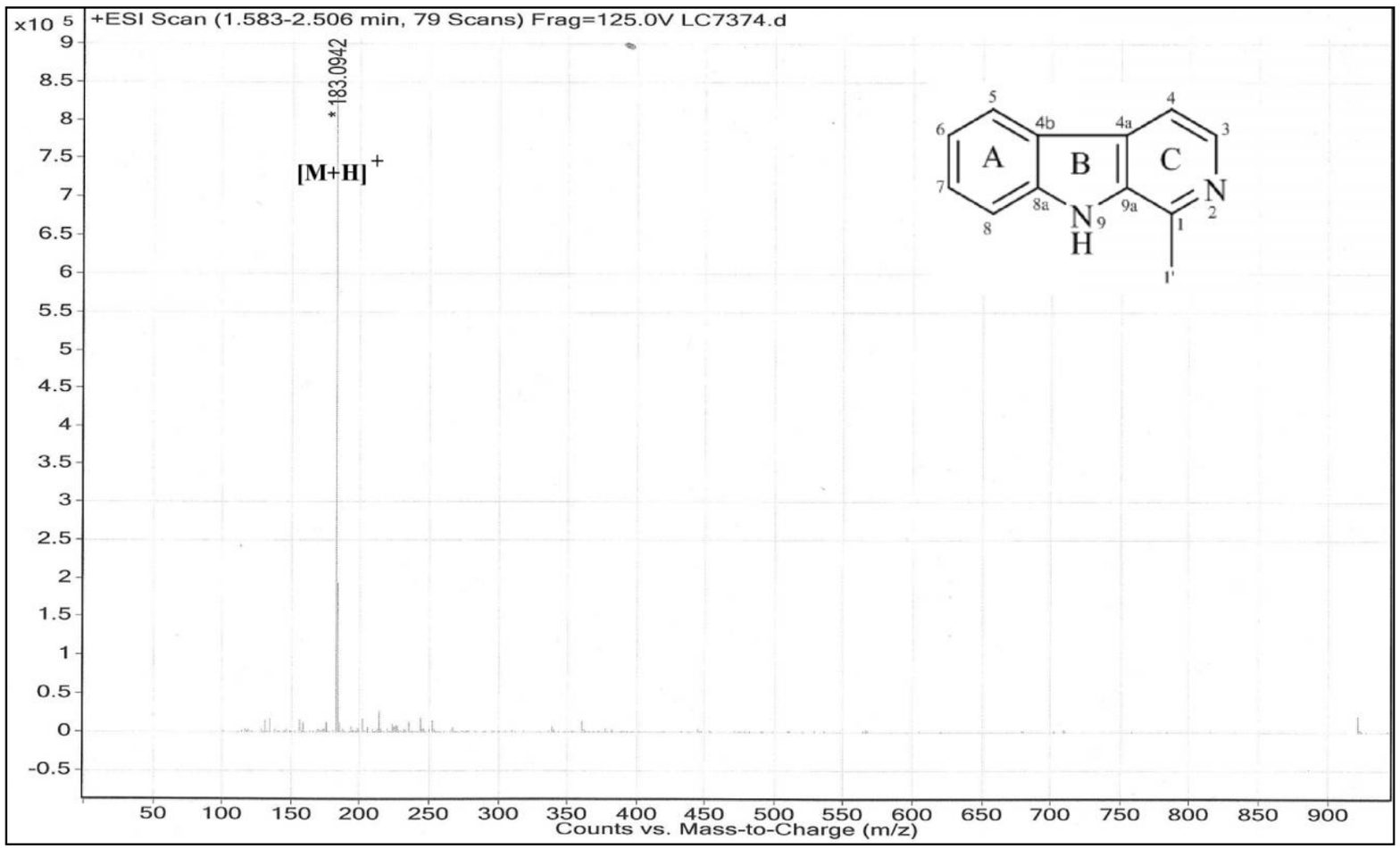

Figure 3.96: LCMS Spectrum of Harmane **67**

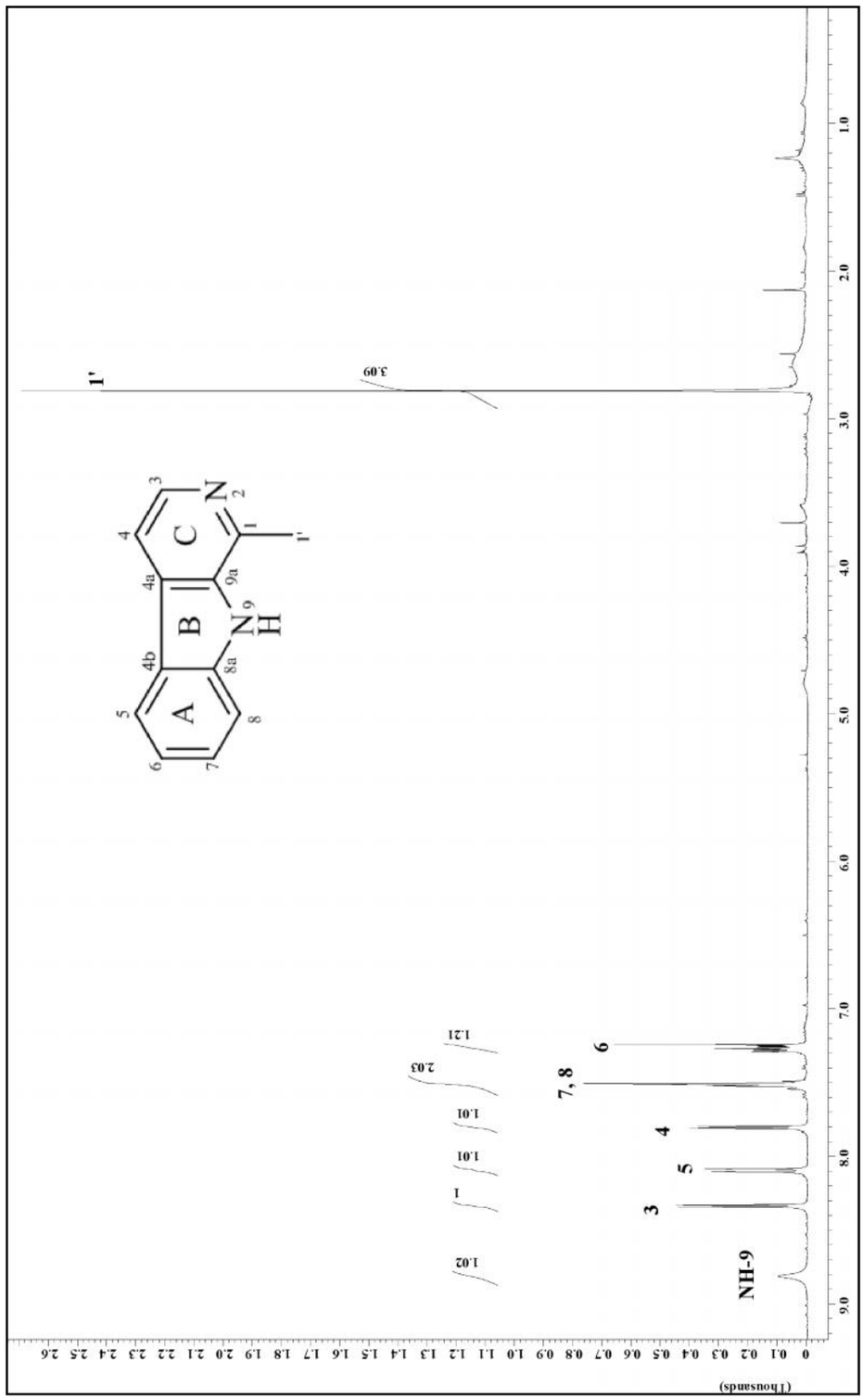

Figure 3.97: ^{1}H NMR Spectrum of Harmane **67**

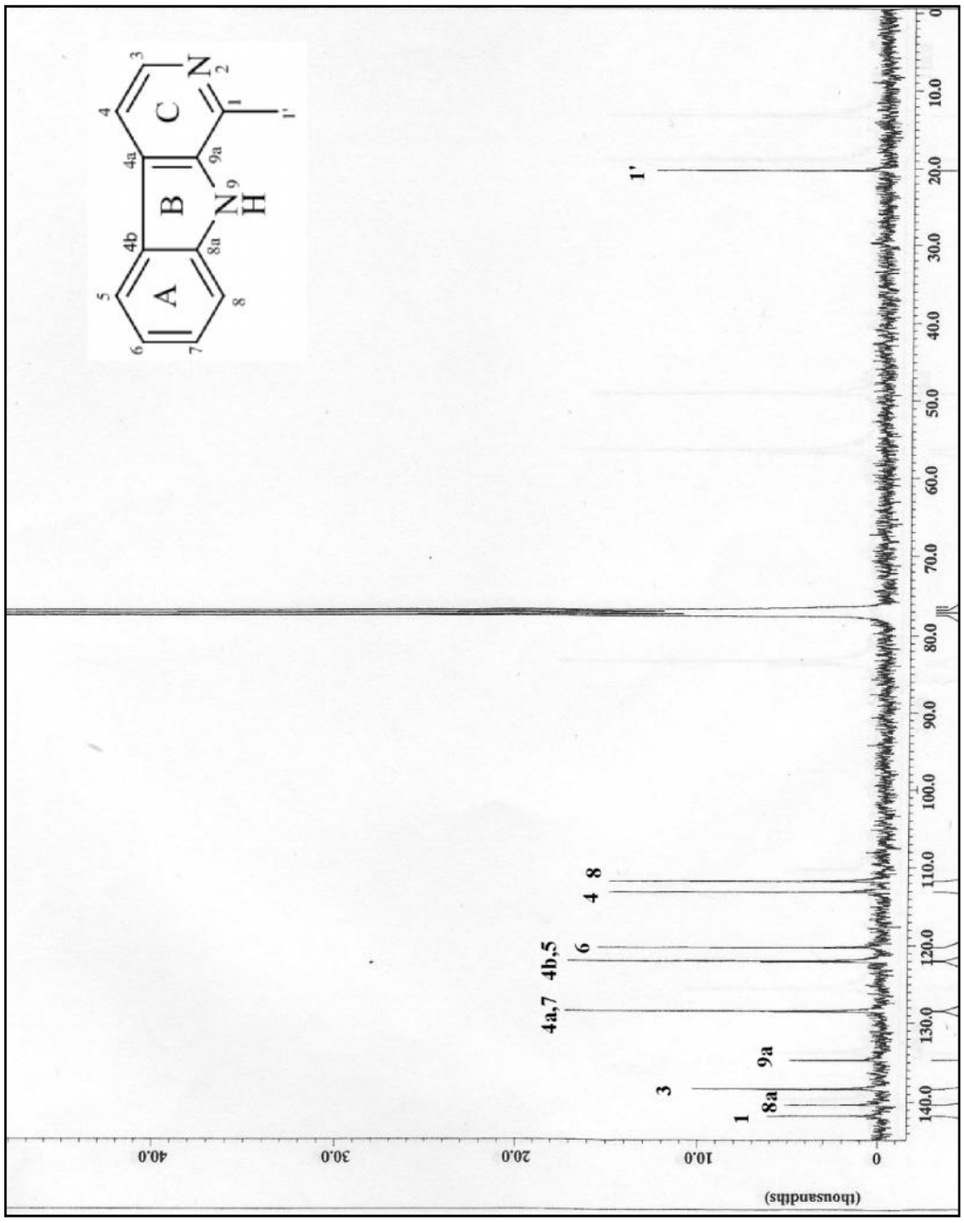

Figure 3.98: ^{13}C NMR Spectrum of Harmane **67**

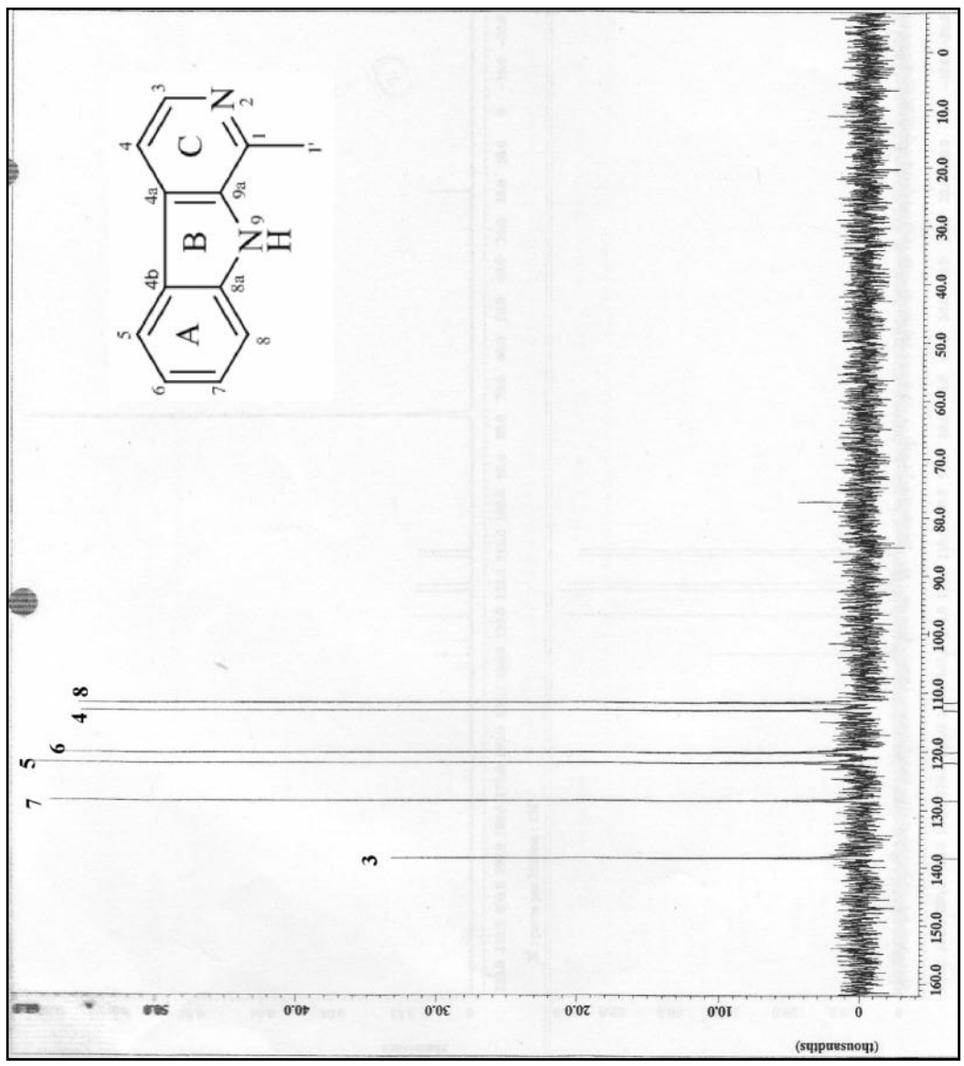

Figure 3.99: DEPT 90 Spectrum of Harmane **67**

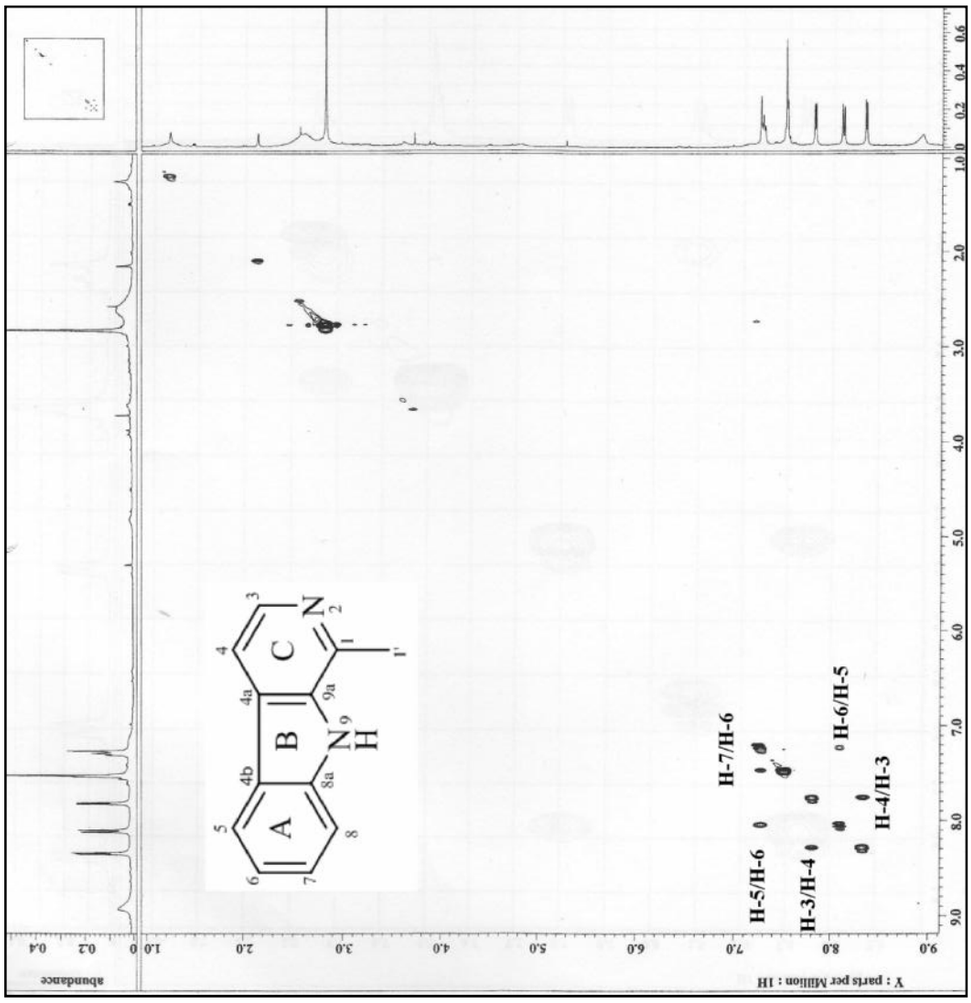

Figure 3.100: COSY Spectrum of Harmane **67**

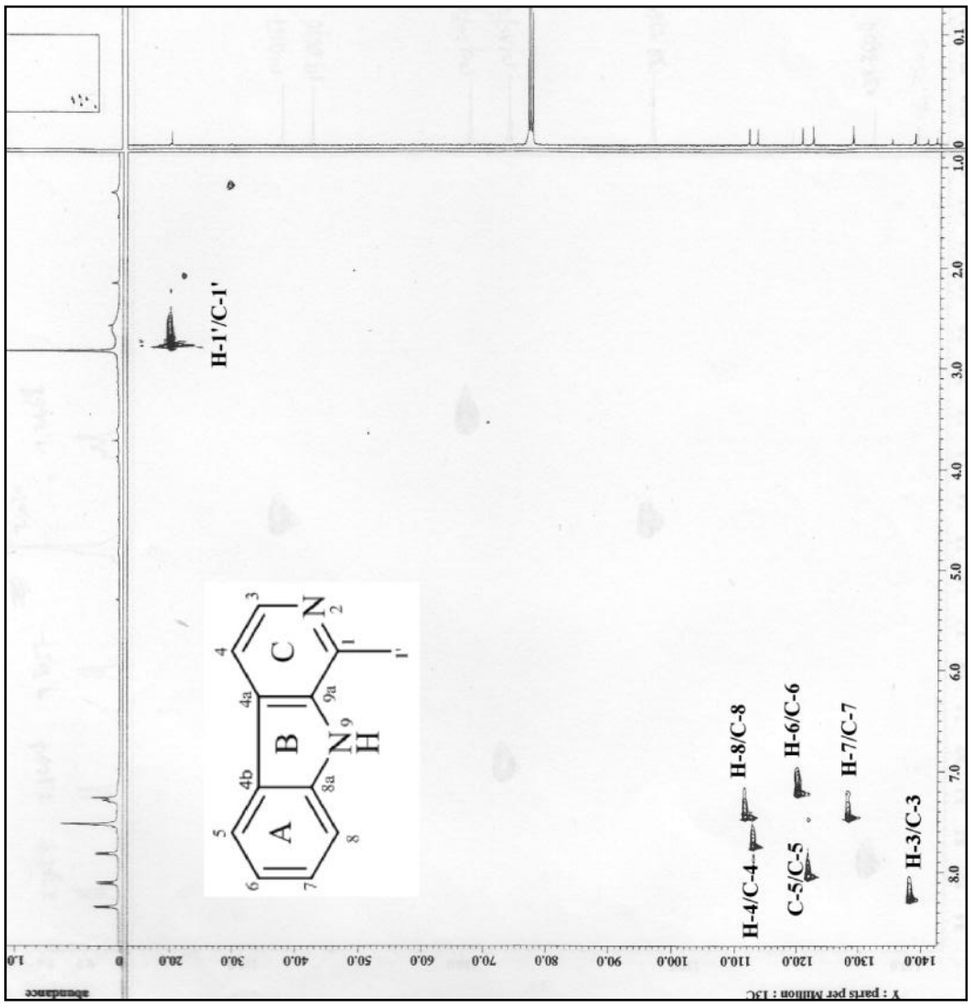

Figure 3.101: HSQC NMR Spectrum of Harmane **67**

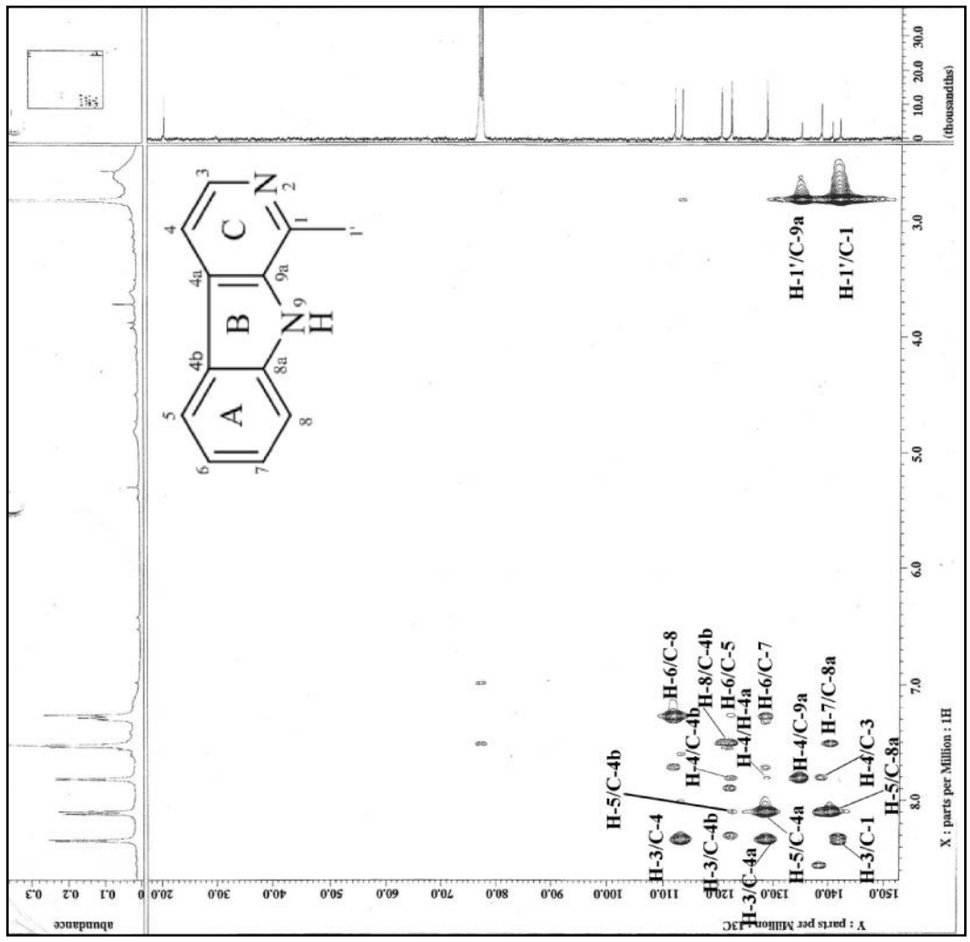

Figure 3.102: HMBC NMR Spectrum of Harmane **67**

3.2.14 1,2,3,4-tetrahydro-1-oxo-β-carboline 60

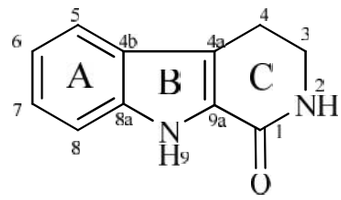

60

1,2,3,4-tetrahydro-1-oxo-β-carboline **60** was afforded as a brownish amorphous solid. The LCMS-IT-TOF spectrum (Figure 3.104) displayed a pseudomolecular ion peak $[M+H]^+$ at *m/z* 187.9447, corresponding to the molecular formula of $C_{11}H_{10}N_2O$ (calc. 187.0866). In UV spectrum, absorption maxima of this alkaloid at 298 and 240 nm were observed.[94] In IR spectrum, absorption peaks at 3415 and 1734 cm^{-1} were observed due to N-H and C=O stretching respectively.[94]

In the ^{1}H-NMR spectrum (Figure 3.105), the presence of two doublets at δ_H 7.61 (1H, *d*, *J* = 8.2 Hz, H-5) and δ_H 7.45 (1H, *d*, *J* = 8.2 Hz, H-8), two *dt* at δ_H 7.33 (1H, *dt*, *J* = 8.2, 0.9 Hz, H-7) and δ_H 7.17 (1H, *dt*, *J* = 8.2, 0.9 Hz, H-6), two methylenes at δ_H 3.73 (1H, *dt*, *J* = 2.6, 7.1 Hz, H-3) and δ_H 3.68 (1H, *t*, *J* = 7.1, 14.0 Hz, H-4), suggesting a tetrahydro-*β*-carboline skeleton (ring A, B and C)[75]. This skeleton can also be indicated by HMBC correlations of H-4 to C-4b (δ_C 119.9) and C-9a (δ_C 126.2), H-5 to C-7 (δ_C 125.3) and C-8a (δ_C 137.1), H-7 to C-8a (Figure 3.103). Two broad singlet can be observed at δ_H 9.11 and δ_H 5.66 which were assigned to NH-9 and NH-2 respectively.

The ^{13}C-NMR spectrum (Figure 3.106) of 1,2,3,4-tetrahydro-1-oxo-β-carboline **60** indicated a total of eleven carbon signals; two methylenes, four methines, four quaternary carbons and one carbonyl carbon. A downfield carbonyl signal resonated at δ_C 162.8 (C-1). HMBC correlation of H-3 to this carbonyl signal suggesting the presence of oxo-β-carboline skeleton.

Based on the spectral data obtained (Table 3.15) and comparison with literature values,[94] the structure of 1,2,3,4-tetrahydro-1-oxo-β-carboline **60** was confirmed without doubt.

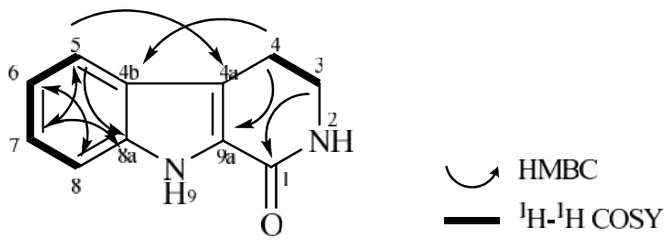

Figure 3.103: Selected COSY and HMBC Correlations of 1,2,3,4-tetrahydro-1-oxo-β-carboline **60**

Table 3.15: ^{1}H-NMR (400 MHz) and ^{13}C-NMR (100 MHz) Spectral Data of 1, 2, 3, 4-tetrahydro-1-oxo-β-carboline **60** in $CDCl_3$.

Position	**^{1}H δ_H (multiplicity, *J* in Hz)**		**^{13}C δ_C**	
	Experimental ($CDCl_3$)	**Reference* ($CDCl_3$)**	**Experimental ($CDCl_3$)**	**Reference* ($CDCl_3$)**
1	-	-	162.8	163.1
NH-2	5.66 (*br s*)	5.76 (*s*)	-	-
3	3.73 (*dt*, 2.6, 7.1)	3.71 (*dt*, 2.7, 7.3)	42.2	42.3
4	3.08 (*t*, 7.1, 14.0)	3.06 (*t*, 6.8, 14.2)	20.8	20.9
4a	-	-	125.3	126.2
4b	-	-	119.9	120.0
5	7.61 (*d*, 8.2)	7.45 (*d*, 8.2)	120.4	120.4
6	7.17 (*dt*, 8.2,0.9)	7.15 (*dt*, 0.9, 7.2)	120.3	120.4
7	7.33 (*dt*, 8.2, 0.9)	7.31 (*dt*, 0.8, 6.9)	125.3	125.3
8	7.45 (*d*, 8.2)	7.58 (*d*, 8.2)	112.3	112.5
8a	-	-	137.1	137.2
NH-9	9.11 (b*r s*)	9.26 (*s*)	-	-
9a	-	-	126.2	126.2

*Literature value from Fadaeinasab et al. (2013).

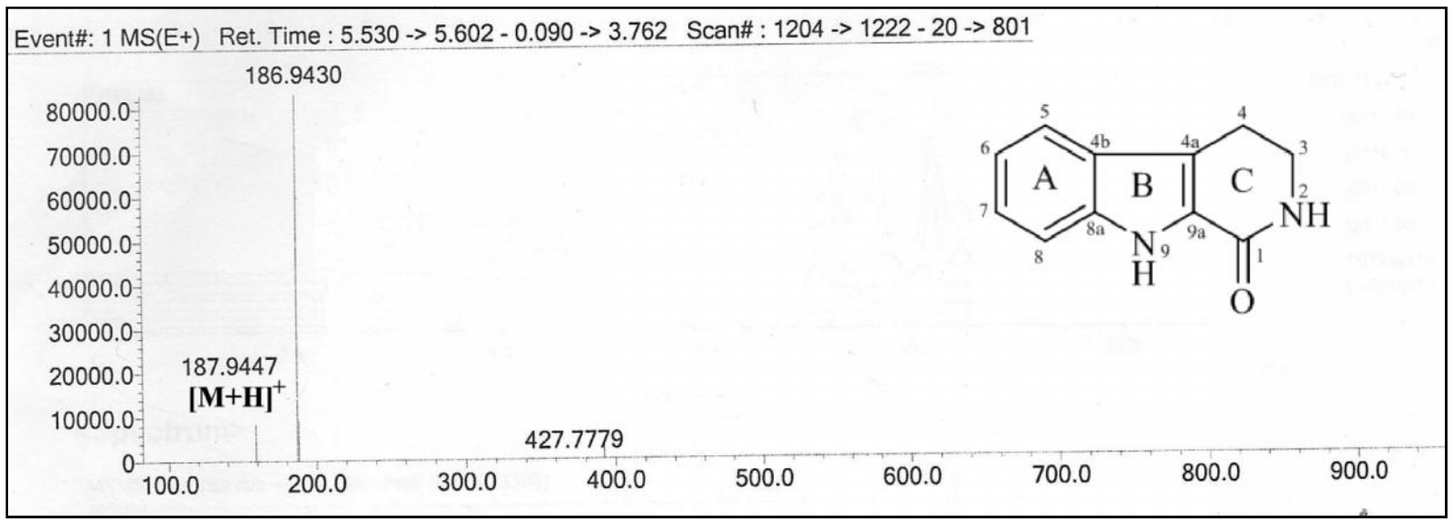

Figure 3.104: LCMS Spectrum of 1, 2, 3, 4-tetrahydro-1-oxo-β-carboline **60**

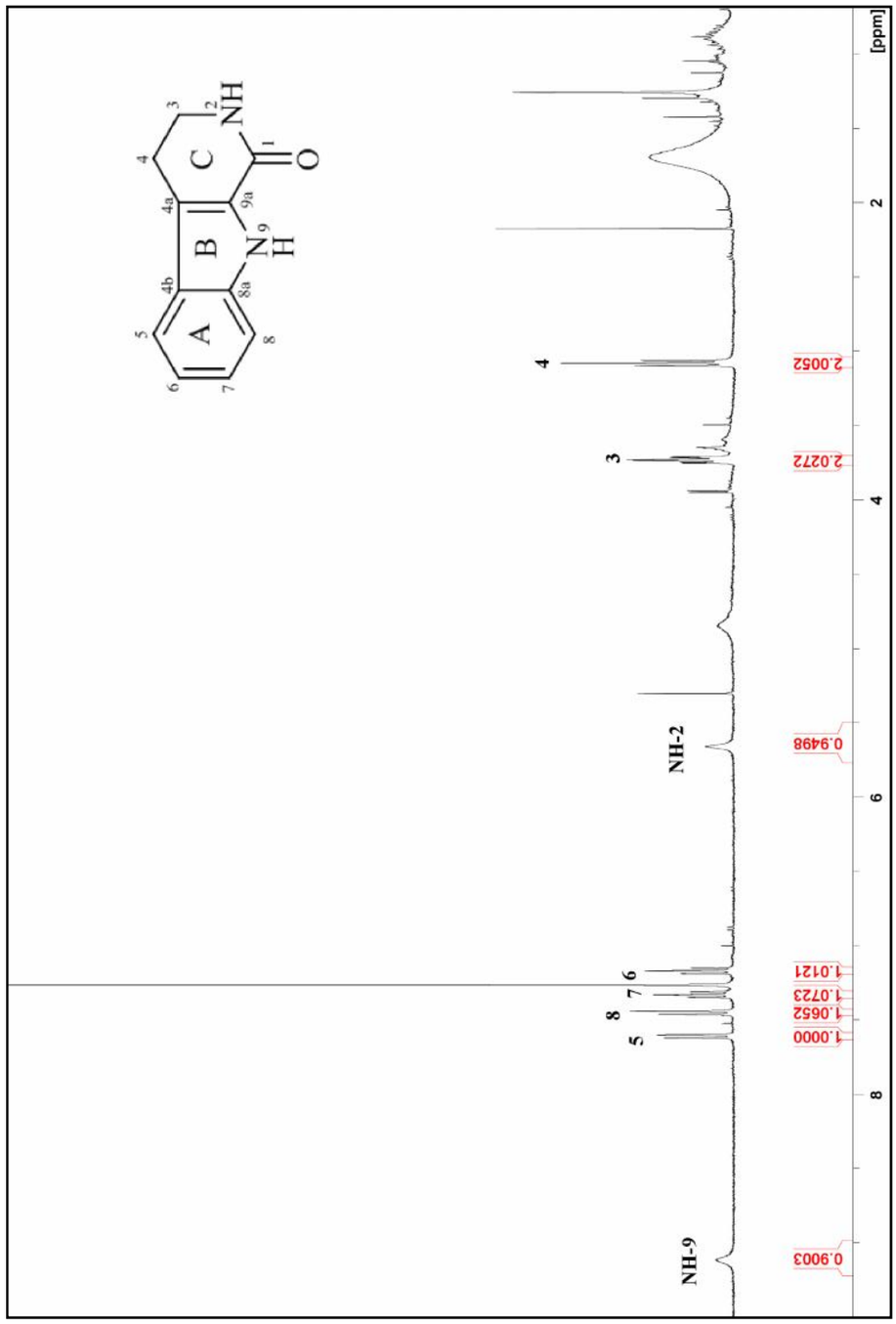

Figure 3.105: ^{1}H NMR Spectrum of 1, 2, 3, 4-tetrahydro-1-oxo-β-carboline **60**

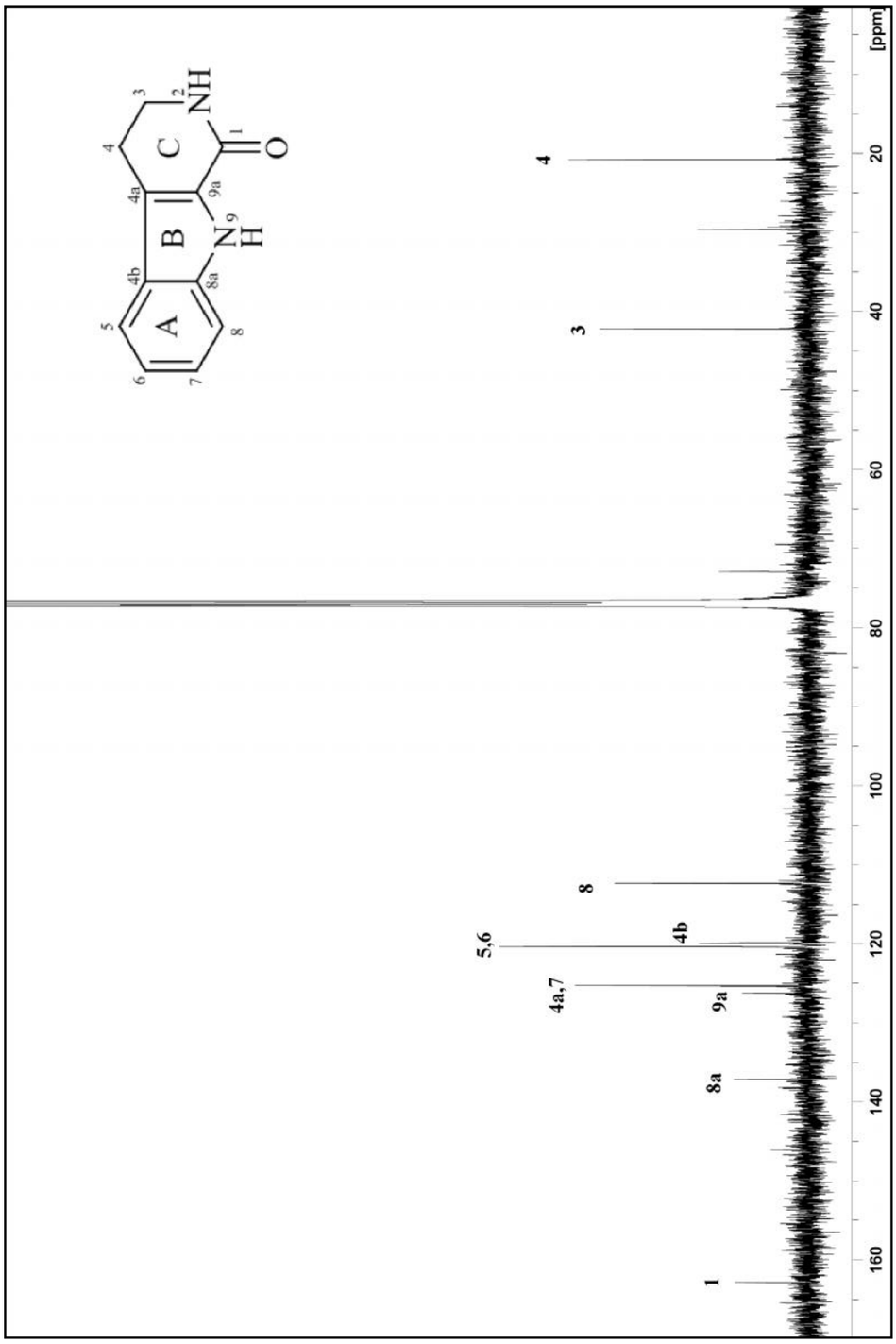

Figure 3.106: ^{13}C NMR Spectrum of 1, 2, 3, 4-tetrahydro-1-oxo-β-carboline **60**

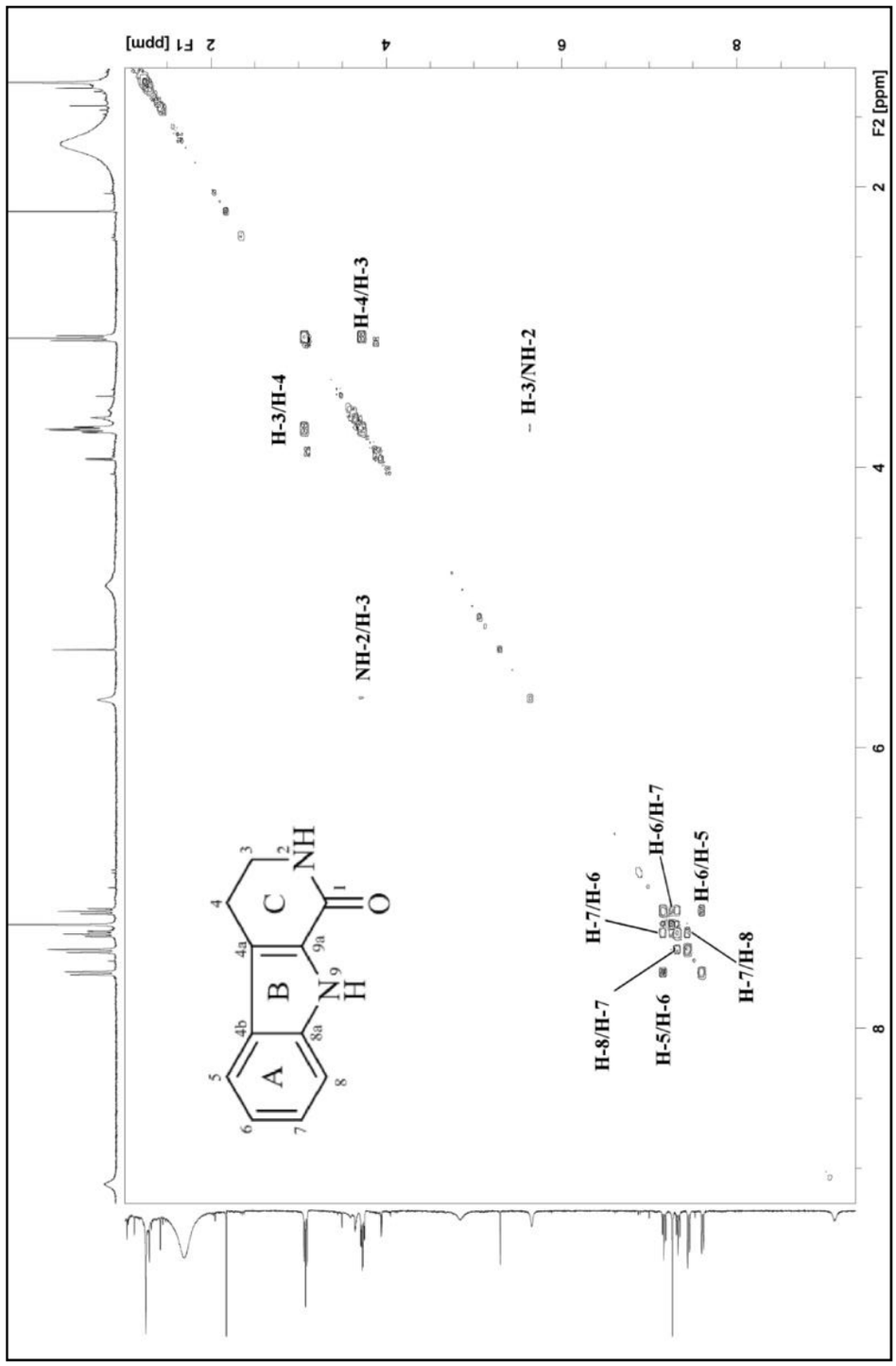

Figure 3.107: COSY Spectrum of 1, 2, 3, 4-tetrahydro-1-oxo-β-carboline **60**

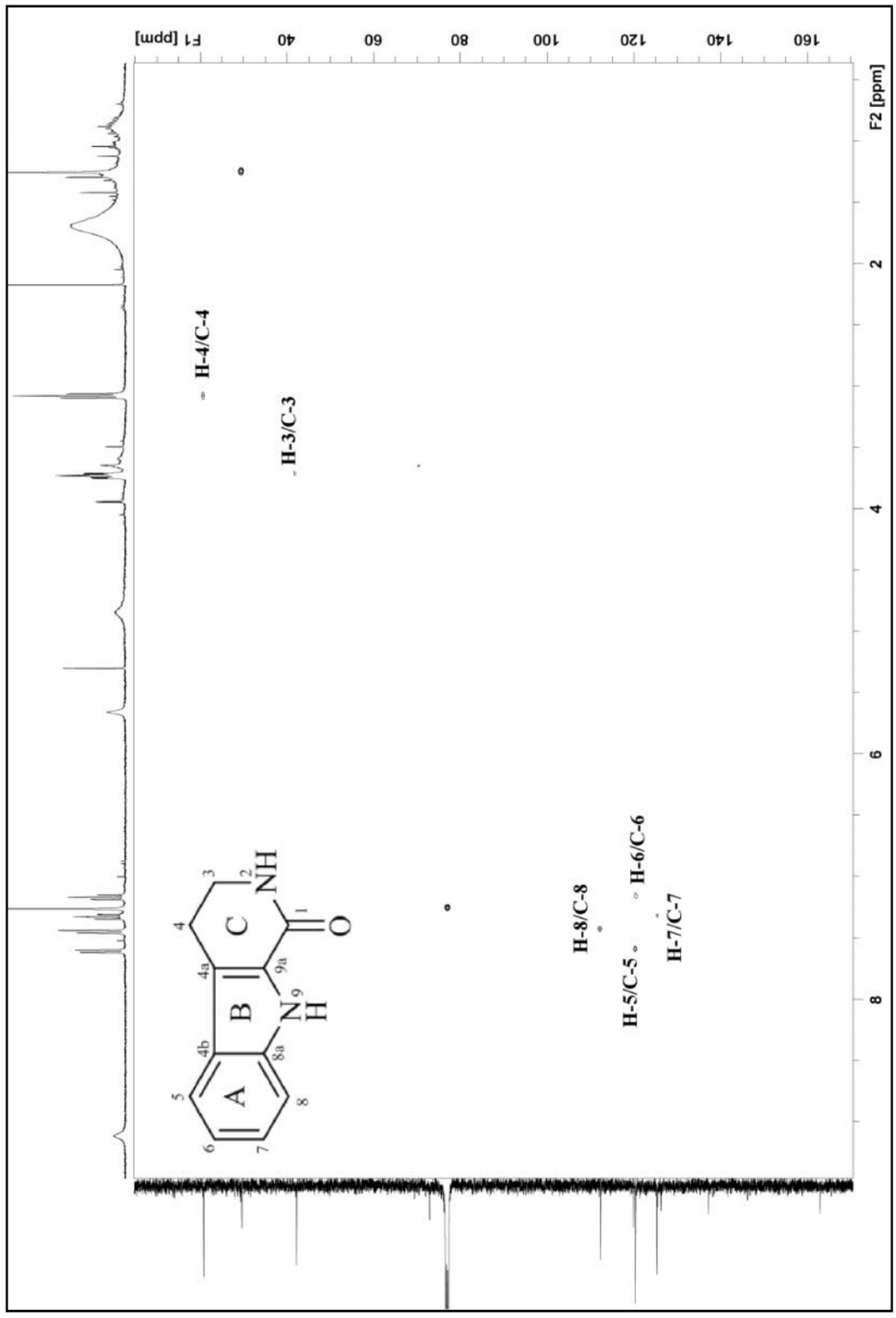

Figure 3.108: HSQC Spectrum of 1, 2, 3, 4-tetrahydro-1-oxo-β-carboline **60**

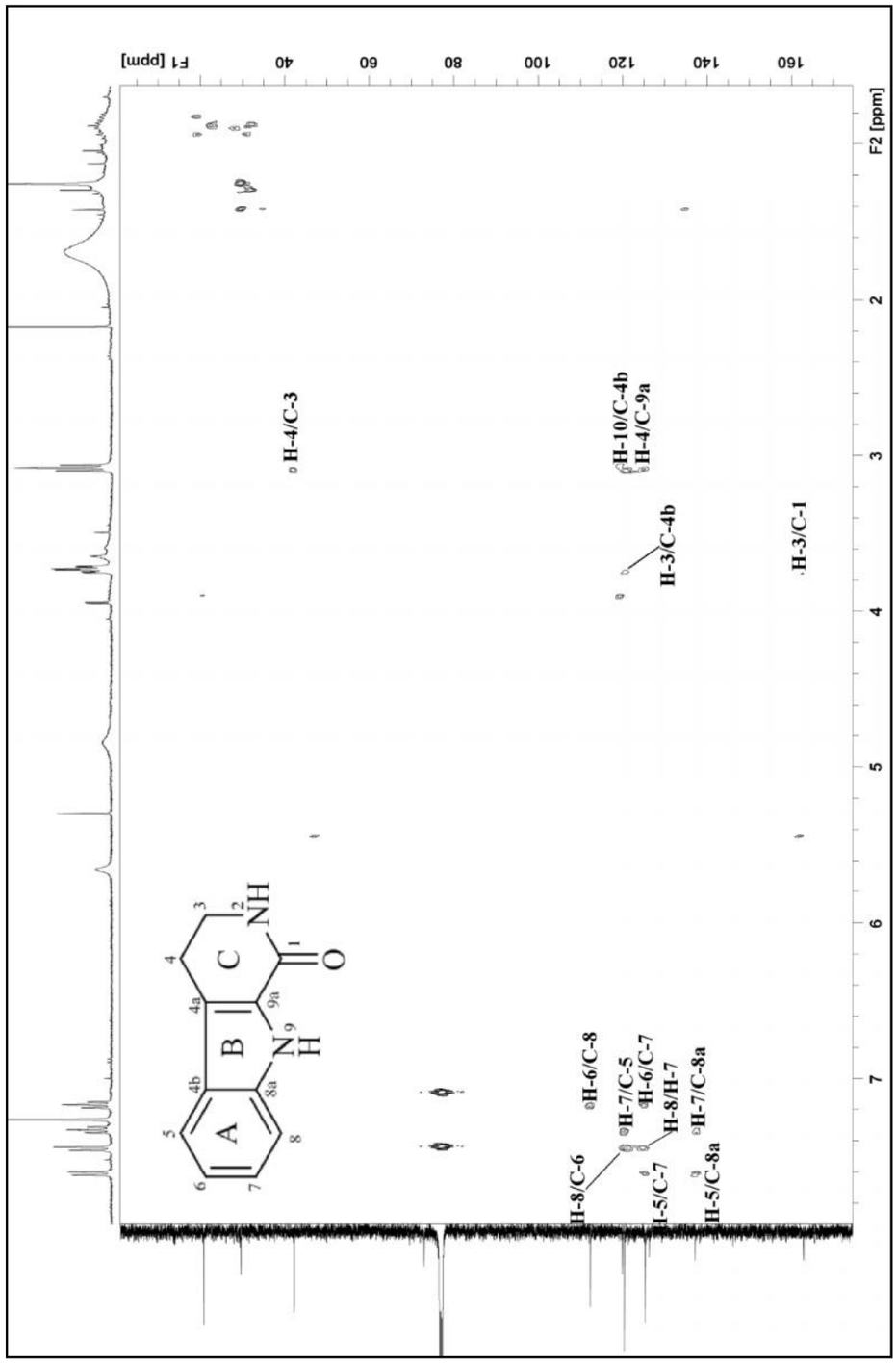

Figure 3.109: HMBC Spectrum of 1, 2, 3, 4-tetrahydro-1-oxo-β-carboline **60**

3.2.15 Benzamide 62

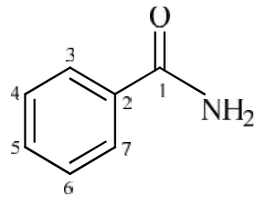

62

Benzamide **62** was obtained as light yellowish amorphous solid. Its molecular formula was confirmed as C_7H_7NO from the ESIMS (Figure 3.111) which revealed a pseudomolecular ion peak $[M+H]^+$ at *m/z* 122.0601 (calc. 122.0600). In its UV spectrum, absorption bands of this compound at 222 nm were observed.[95] The IR spectrum showed absorption peaks at 3390 and 3187 cm^{-1}, indicating the presence of NH_2 group. The peak at 1615 cm^{-1} indicated conjugated carbonyl stretching vibrations.[95,96]

In the ^{1}H-NMR spectrum (Figure 3.112), the overlapping proton signals in aromatic region were observed as two sets of doublets and three sets of triplets suggested the presence of mono-substituted aromatic ring. H-3 was overlapped with H-7 at δ_H 7.80-7.82 (2H, *d*, *J* = 7.4 Hz) and appeared as doublet peak while H-4 was overlapped with H-6 at δ_H 7.43-7.47 (2H, *t*, *J* = 7.4 Hz) and appeared as triplet peak. Doublet of H-5 resonated at δ_H 7.53 (1H, *d*, *J* = 7.4 Hz). Furthermore, a broad doublet was observed at δ_H 6.01 which attributed to NH_2 group.

The ^{13}C-NMR and DEPT spectral (Figure 3.113 and Figure 3.114) of benzamide **62** showed a total of seven carbon signals; five methines, one quaternary carbon and one carbonyl carbon. A carbonyl signal resonated at downfield region δ_C 169.7 (C-1). Overlapped carbon signals of C-4 and C-6, C3 and C-7 at δ_C 128.8 and δ_C 127.5 respectively were due to equivalent environment in the aromatic ring. Connectivity of

the aromatic ring with an amide group was shown through HMBC correlation of H-3 and H-7 with carbonyl group of C-1 (Figure 3.110).

From the analysis of the spectroscopic data obtained (Table 3.16) and comparison with the literature values,[96] the structure of benzamide **62** was confirmed.

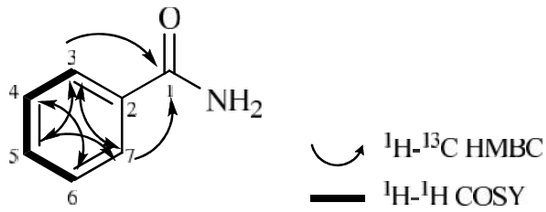

Figure 3.110: COSY and HMBC Correlations of Benzamide **62**

Table 3.16: ^{1}H-NMR (400 MHz) and ^{13}C-NMR (100 MHz) Spectral Data of Benzamide **62** in $CDCl_3$.

Position	**^{1}H δ_H (multiplicity, *J* in Hz)**		**^{13}C δ_C**	
	Experimental ($CDCl_3$)	**Reference* ($CDCl_3$)**	**Experimental ($CDCl_3$)**	**Reference* ($CDCl_3$)**
NH_2	6.01 (*br d*)	-	-	-
1	-		169.7	169.9
2	-	-	132.9	133.3
3	7.80-7.82 (*d*, 7.4)	**7.39-7.43 (*m*)	127.5	**128.5
4	7.43-7.47 (*t*, 7.4)	**7.78-7.80 (*m*)	128.8	**127.3
5	7.53 (*t*, 7.4)	7.47-7.51 (*m*)	132.3	132.0
6	7.43-7.47 (*t*, 7.4)	**7.78-7.80 (*m*)	128.8	**127.3
7	7.80-7.82 (*d*, 7.4)	**7.39-7.43 (*m*)	127.5	**128.5

* Literature value from Saidi (2010).
** The chemical shifts were interchangeable. Experimental values were confirmed through 1D and 2D-NMR.

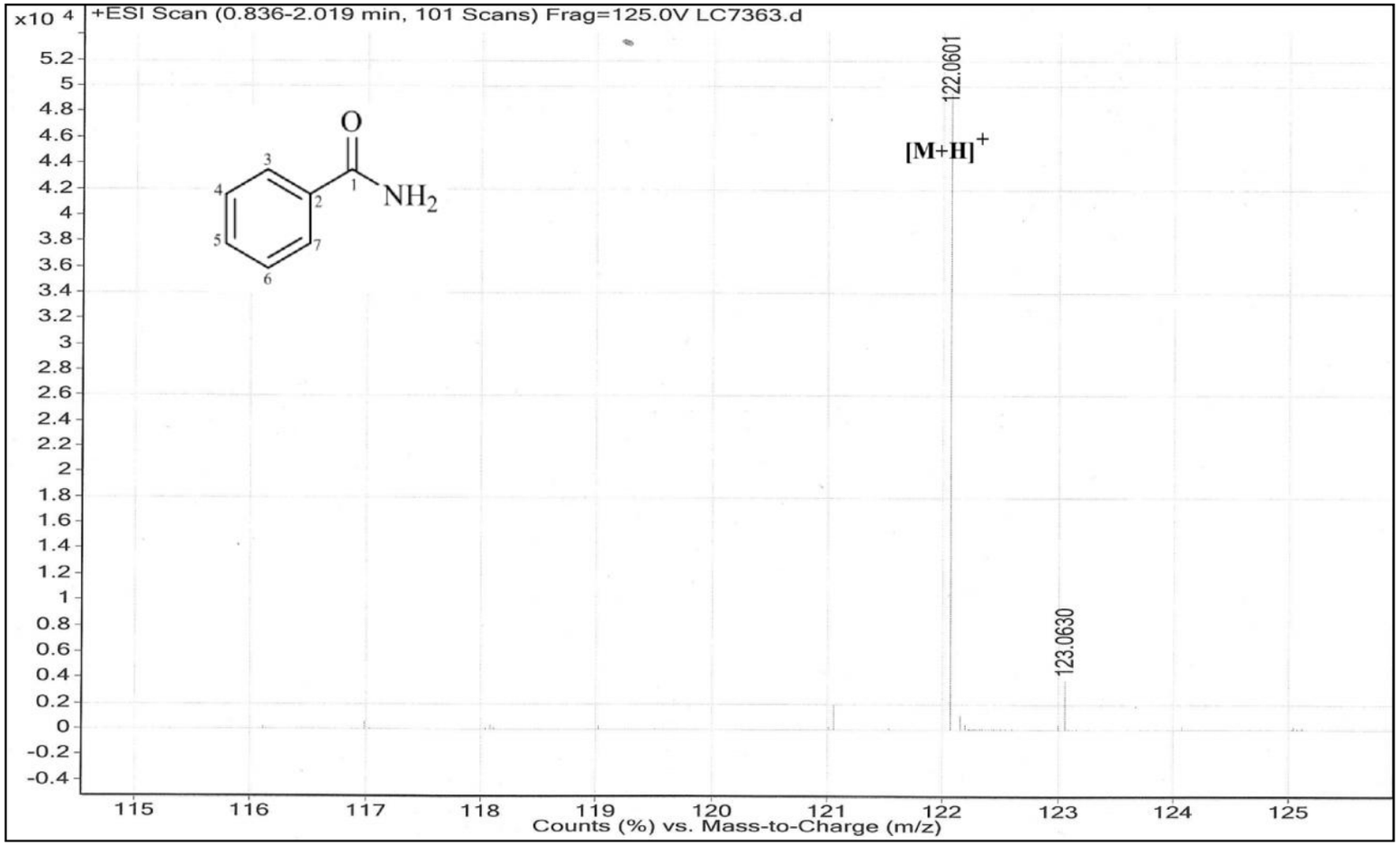

Figure 3.111: LCMS Spectrum of Benzamide **62**

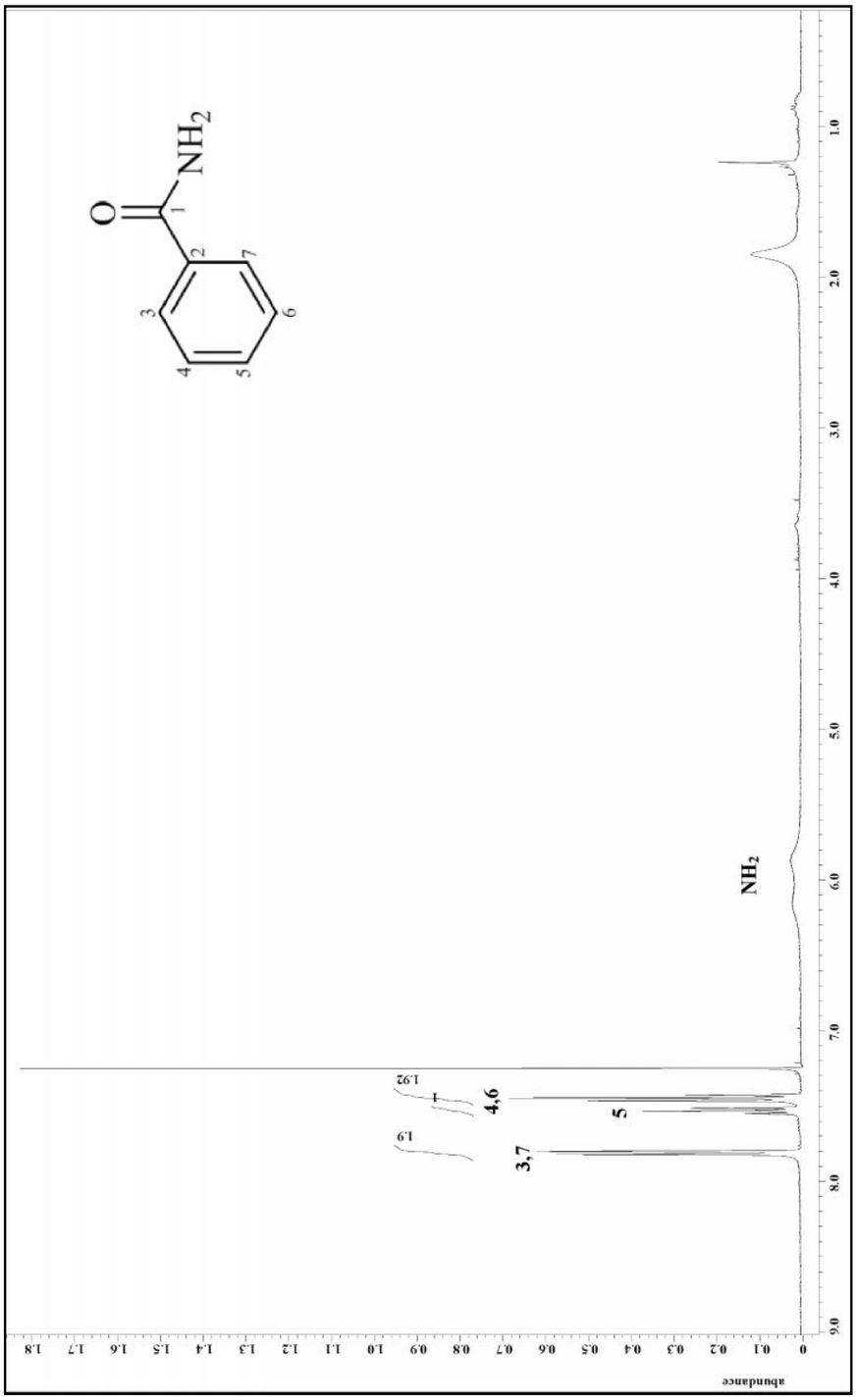

Figure 3.112: ^{1}H NMR Spectrum of Benzamide **62**

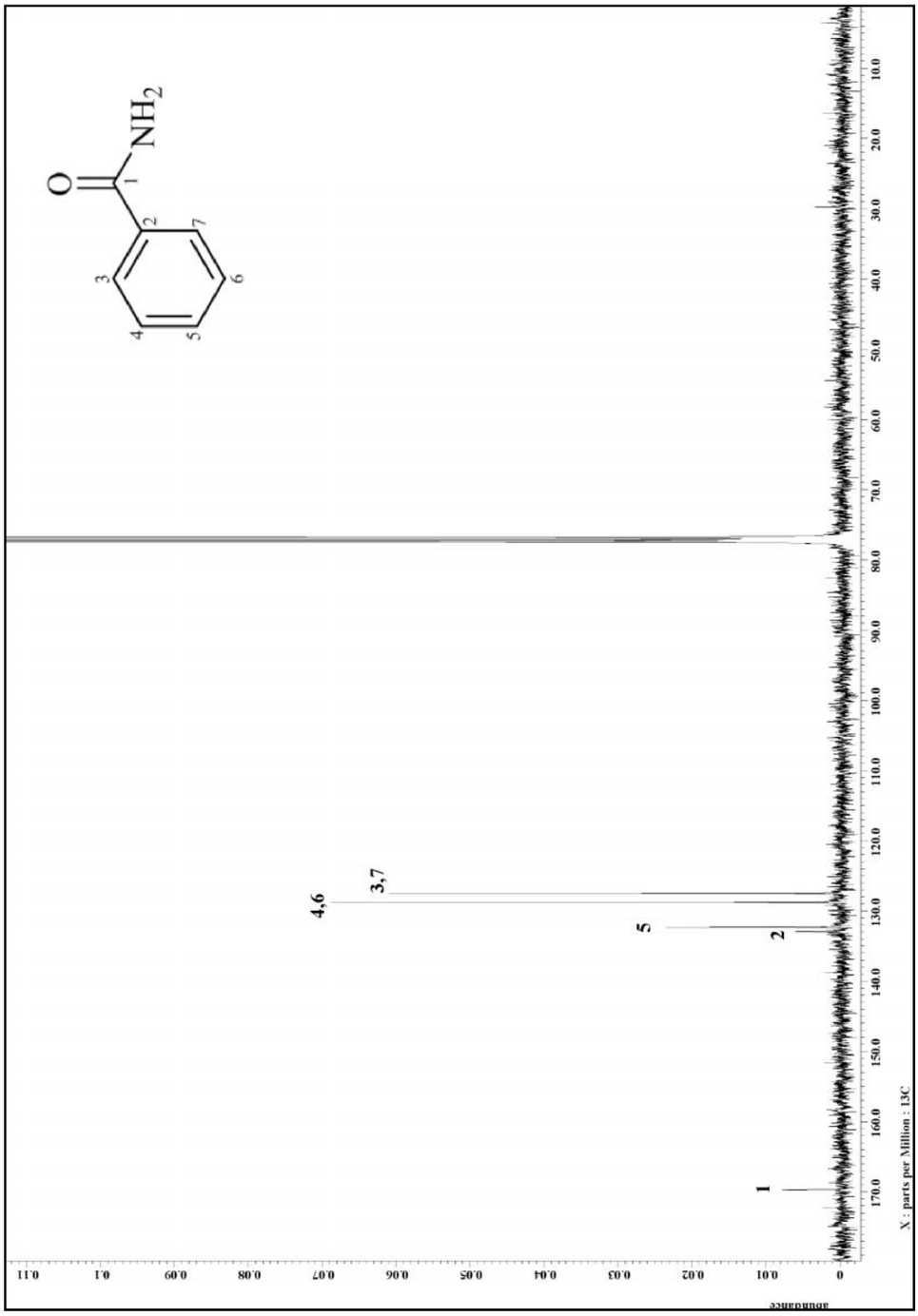

Figure 3.113: ^{13}C NMR Spectrum of Benzamide **62**

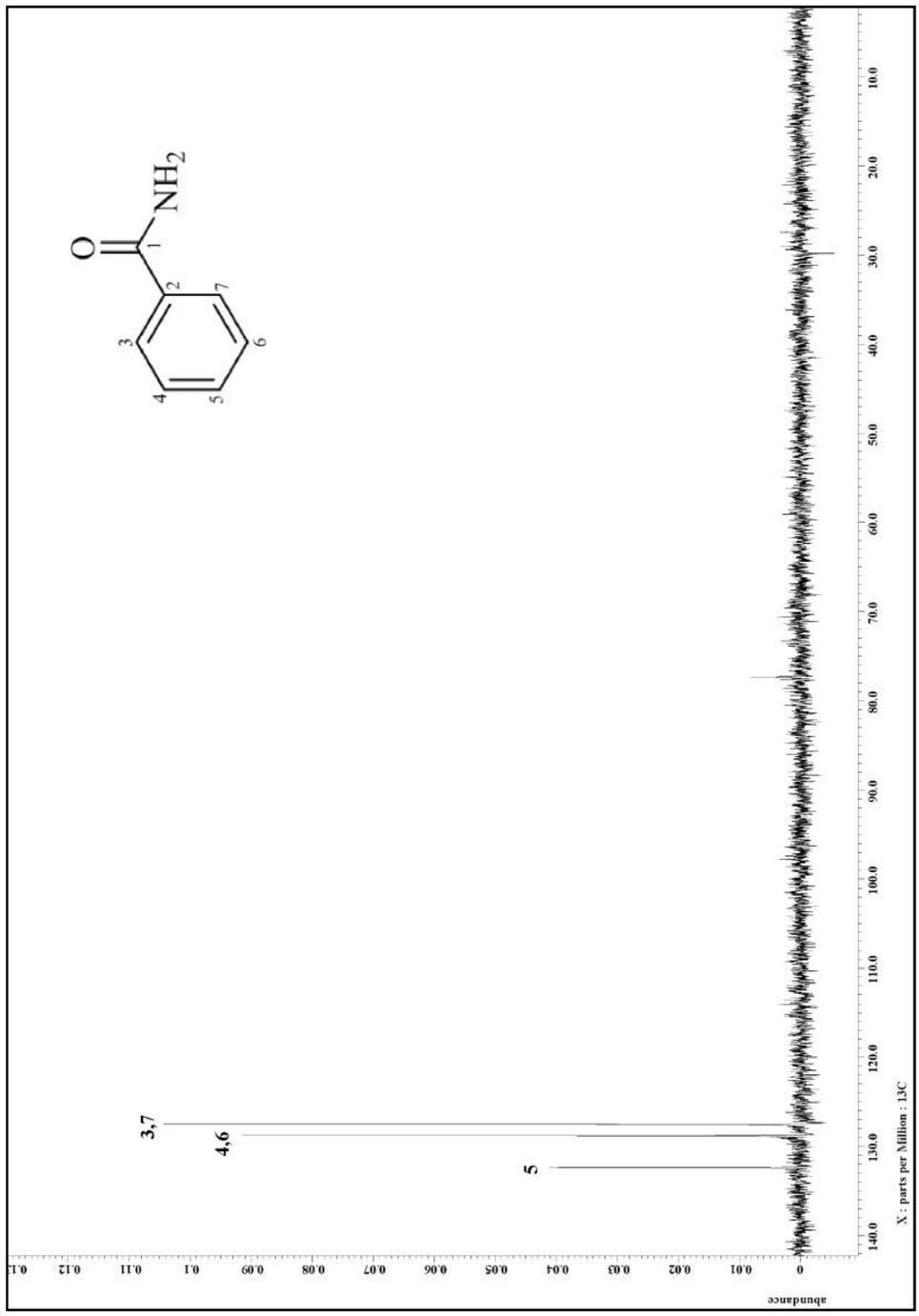

Figure 3.114: DEPT Spectrum of Benzamide **62**

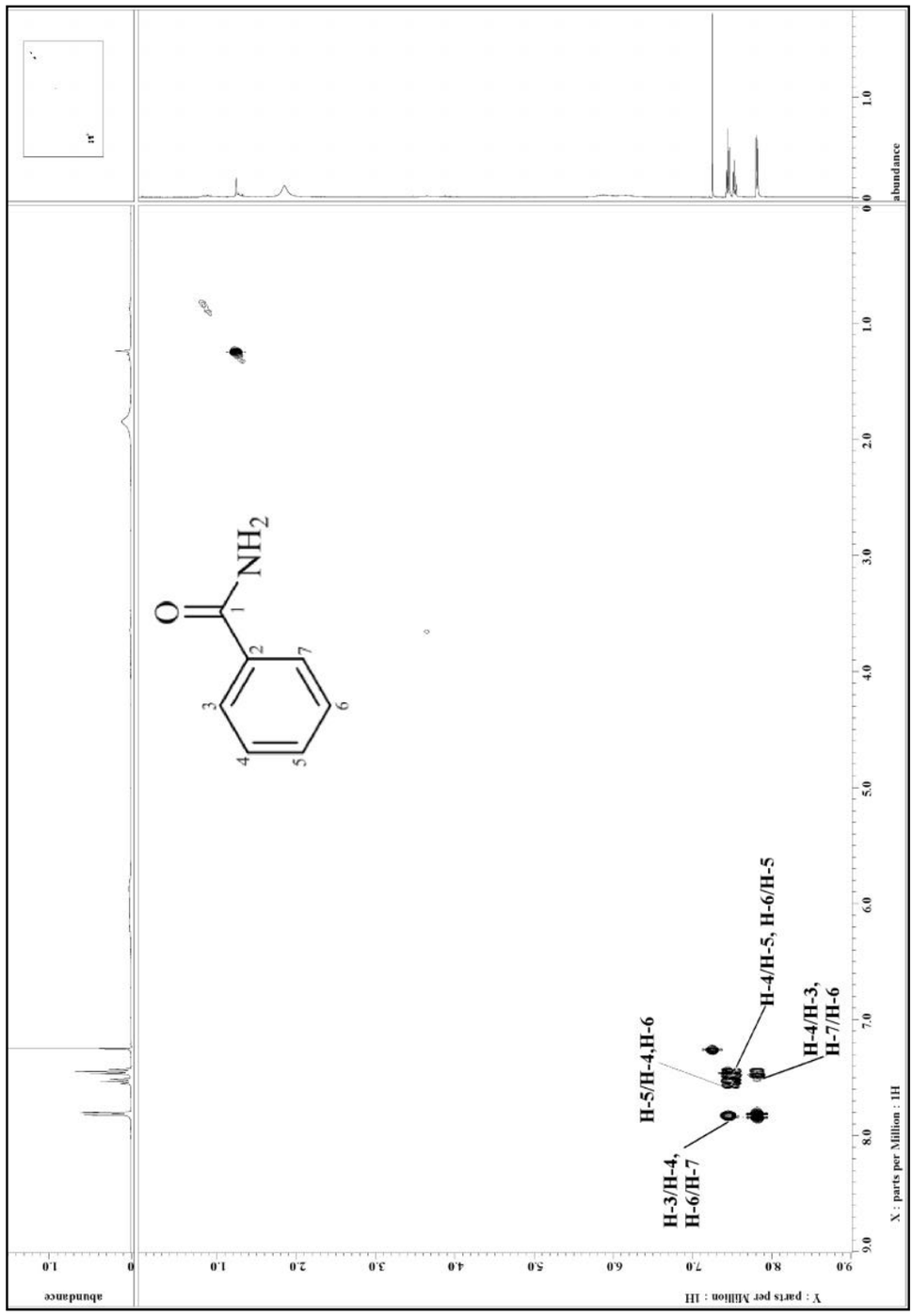

Figure 3.115: COSY Spectrum of Benzamide **62**

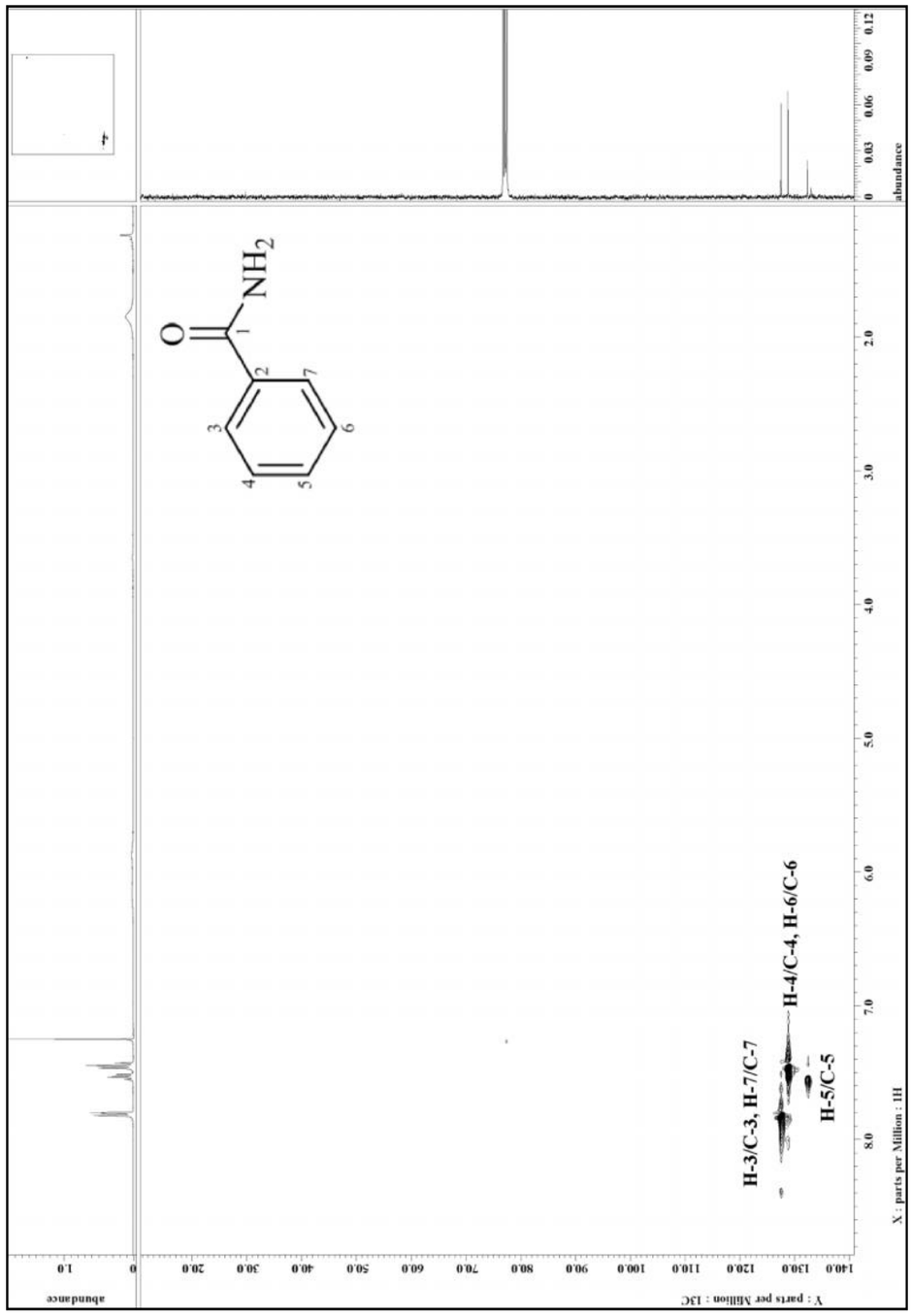

Figure 3.116: HSQC Spectrum of Benzamide **62**

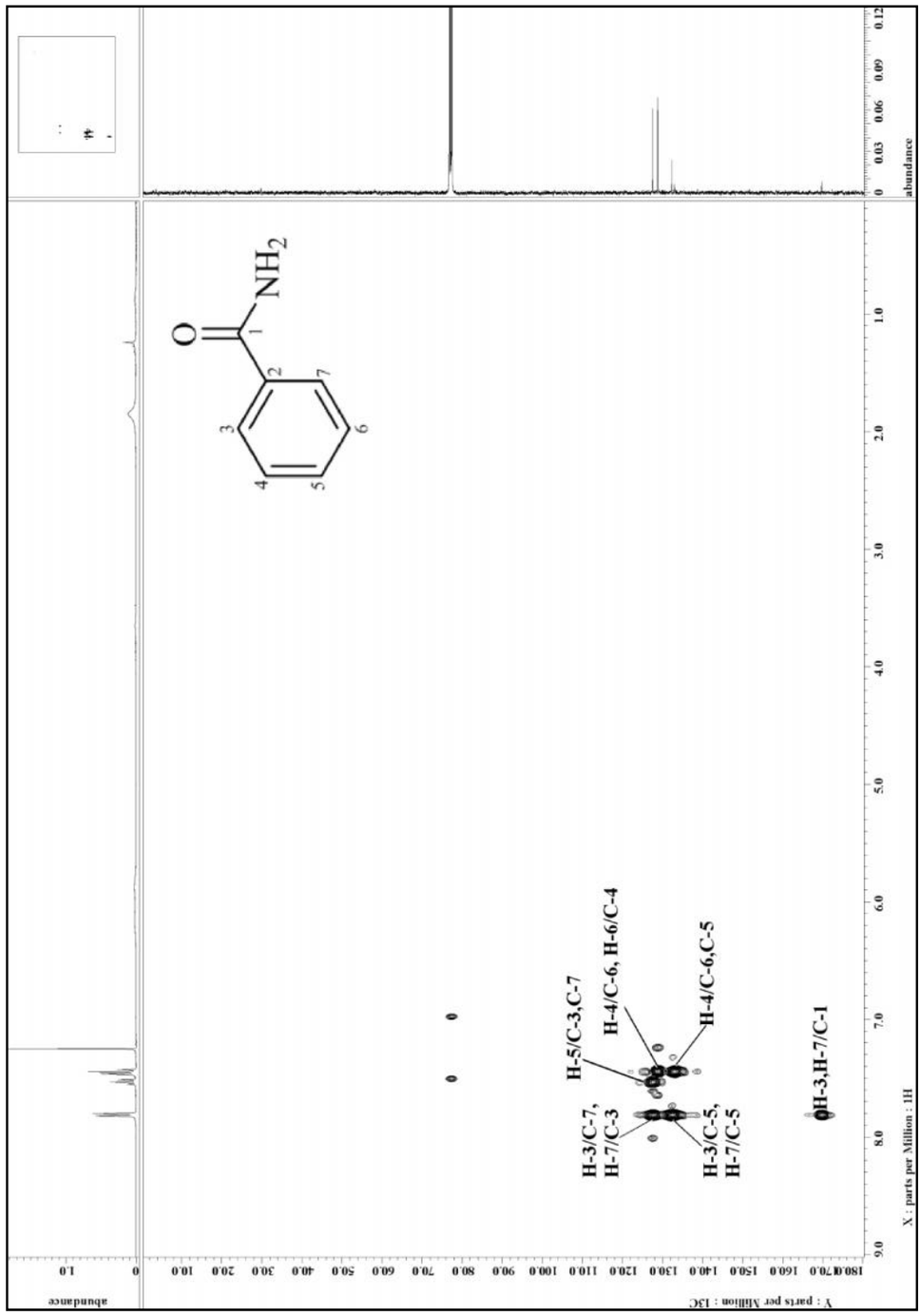

Figure 3.117: HMBC Spectrum of Benzamide **62**

3.2.16 Cinnamide 59

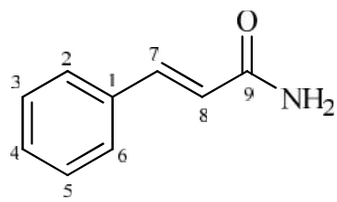

59

Cinnamide **59** was yielded as a light yellowish amorphous solid. The ESIMS (Figure 3.118) showed a pseudomolecular ion peak $[M+H]^+$ at *m/z* 148.0750, corresponding to the molecular formula of C_9H_9NO (calc. 148.0757). In UV spectrum, absorption bands of compound at 272 and 217 nm were observed. The IR spectrum of cinnamide **59** showed absorption peaks at 3369 and 3172 cm^{-1} indicating the presence of NH_2 group while 1655 cm^{-1} was due to carbonyl stretching vibrations.[96]

In the ^{1}H-NMR spectrum (Figure 3.119), the overlapped proton signals at δ_H 7.52-7.53 (2H, *m*, H-2 and H-6) and δ_H 7.38-7.39 (3H, *m*, H-3, H-4 and H-5) indicating the presence of mono-substituted aromatic ring. The doublets proton signals at δ_H 6.46 (1H, *d*, *J* = 15.7, H-7) and δ_H 7.66 (1H, *d*, *J* = 15.7, H-8) with coupling constant of 15.7 Hz suggesting the presence of a trans-substituted double bond.

The ^{13}C-NMR spectrum (Figure 3.120) of cinnamide **59** indicated a total of nine carbon signals; seven methines, one quaternary carbon and one carbonyl carbon. A downfield carbonyl signal resonated at δ_C 167.6 (C-9). The carbon signal for C-8 (δ_C 119.3) appeared more upfield than that C-7 (δ_C 142.7) due to the resonance effect caused by the vicinal C=O group.

From the analysis of the spectroscopic data obtained (Table 3.17) and comparison with the literature values,[96] the structure of cinnamide **59** was confirmed.

Table 3.17: ^{1}H-NMR (400 MHz) and ^{13}C-NMR (100 MHz) Spectral Data of Cinnamide **59** in $CDCl_3$.

Position	**^{1}H**		**^{13}C**	
	δ_H (multiplicity, *J* in Hz)		**δ_C**	
	Experimental ($CDCl_3$)	**Reference* ($CDCl_3$)**	**Experimental ($CDCl_3$)**	**Reference* ($CDCl_3$)**
1	5.56 (*br d*)	-	134.5	134.4
2	7.52-7.53 (*m*)	7.47-7.49 (*dd*, 9.2, 3.9)	127.9	127.8
3	7.38-7.39 (*m*)	7.33-7.34 (*m*)	128.9	128.7
4	7.38-7.39 (*m*, overlapped)	7.33-7.34 (*m*)	130.0	129.8
5	7.38-7.39 (*m*)	7.33-7.34 (*m*)	128.9	128.7
6	7.52-7.53 (*m*)	7.47-7.49 (*dd*, 9.2, 3.9)	127.9	127.8
7	7.66 (*d*, 15.7)	7.59-7.63 (d, 15.6)	142.7	**129.3
8	6.46 (*d*, 15.7)	6.47-6.49 (*d*, 15.6)	119.3	**142.2
9	-		167.6	168.8

* Literature value from Saidi (2010)
**The chemical shifts were interchangeable. Experimental values were confirmed through 1D and 2D-NMR

.

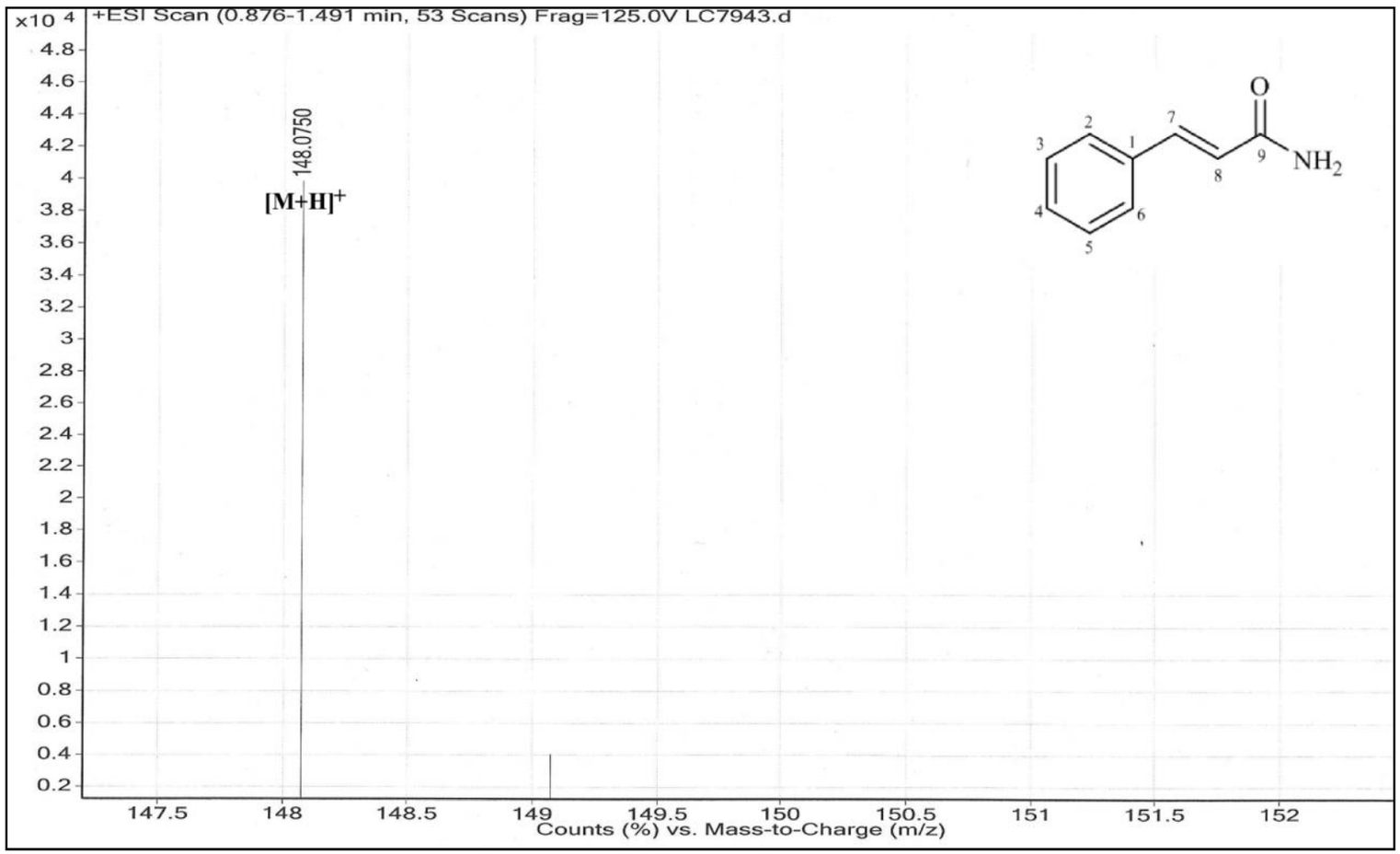

Figure 3.118: LCMS Spectrum of Cinnamide **59**

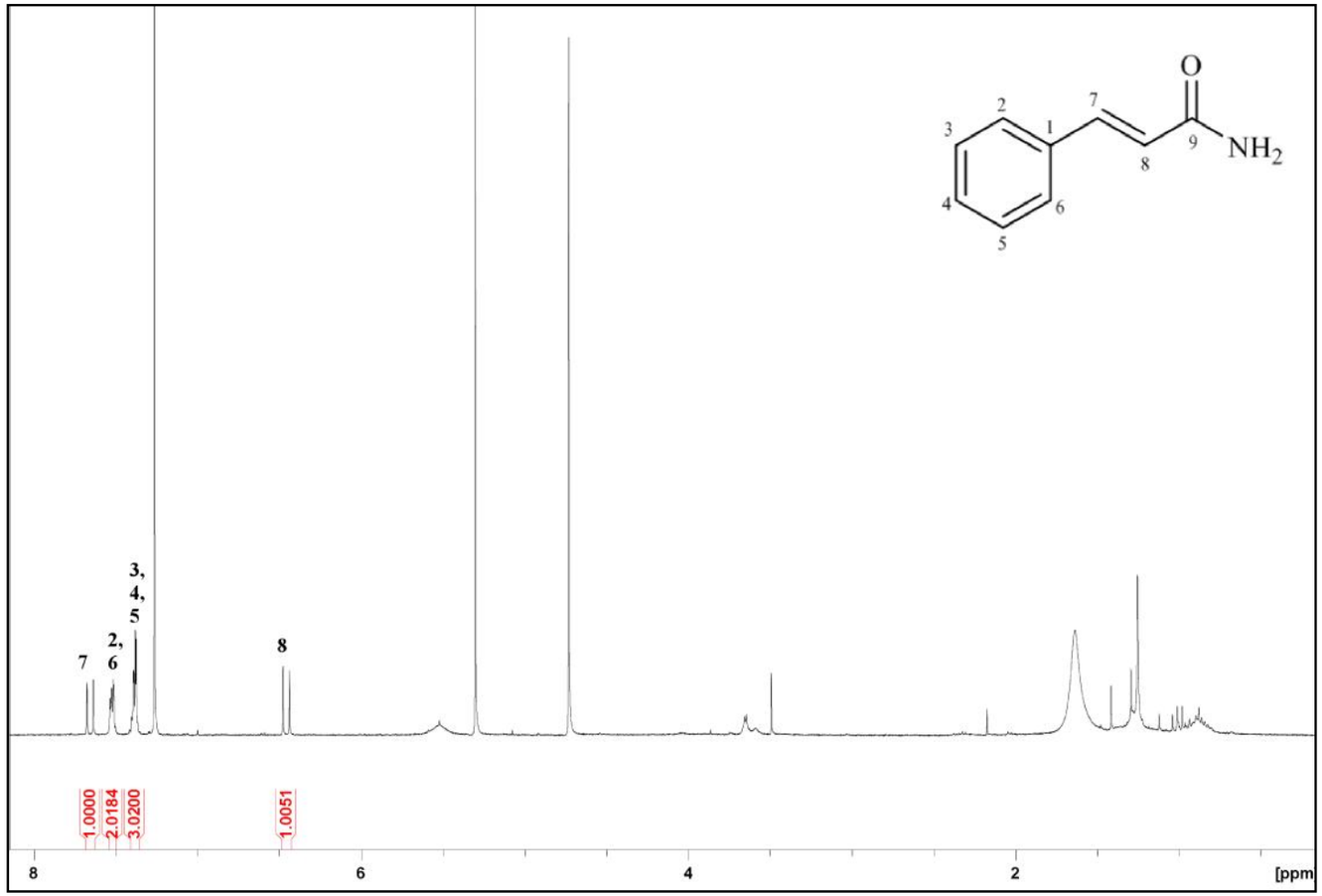

Figure 3.119: ^{1}H NMR Spectrum of Cinnamide **59**

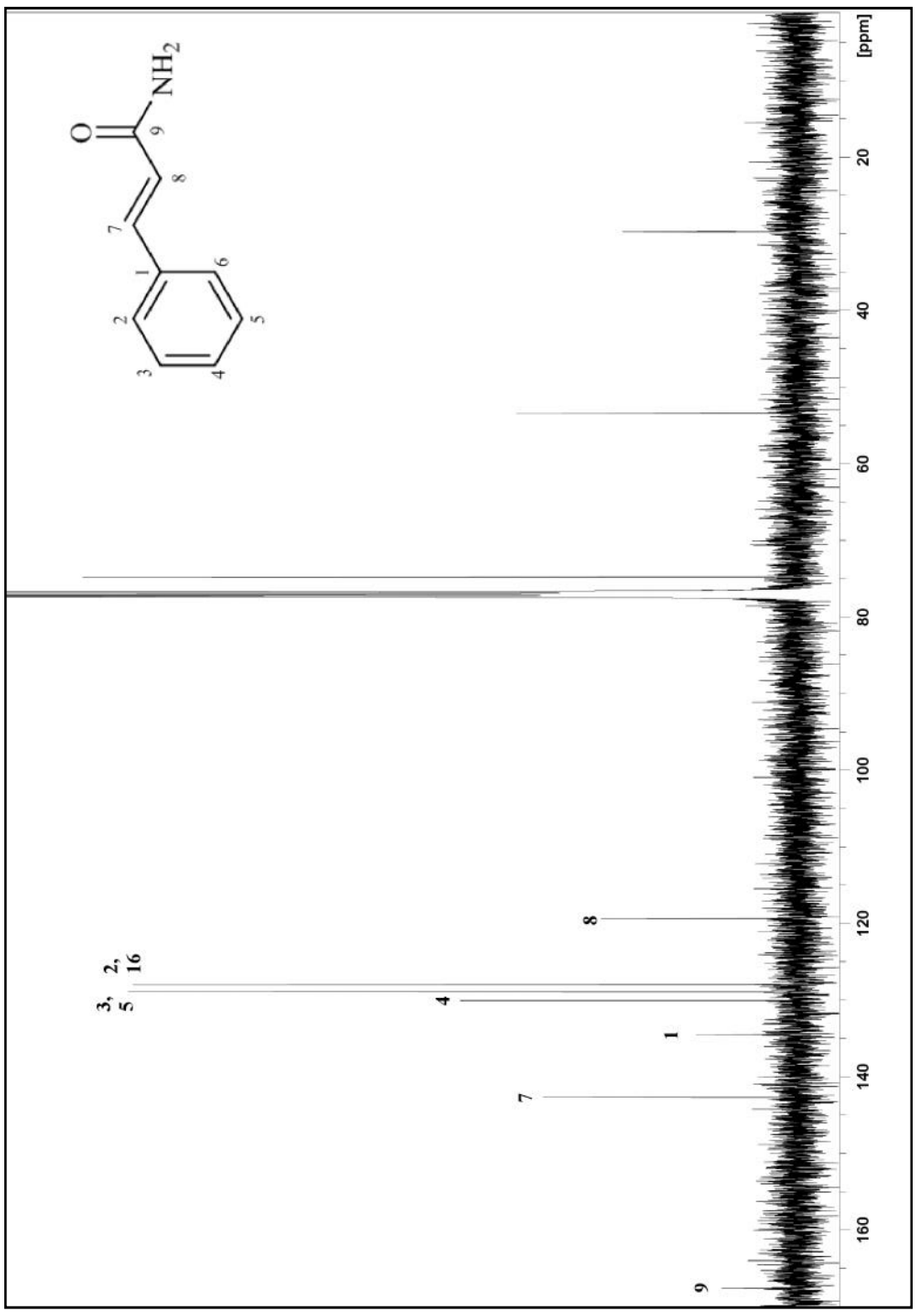

Figure 3.120: ^{13}C NMR Spectrum of Cinnamide **59**

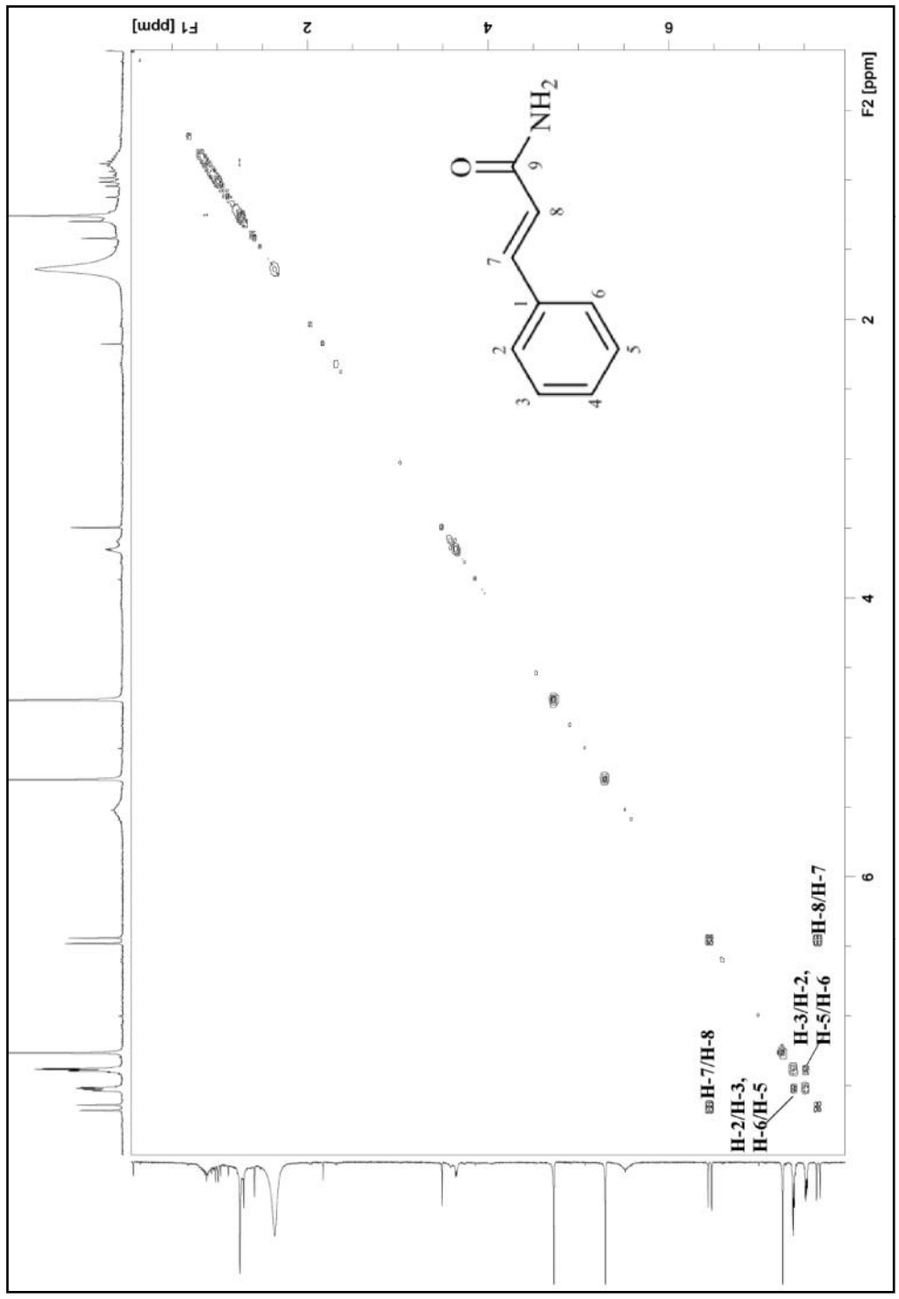

Figure 3.121: COSY Spectrum of Cinnamide **59**

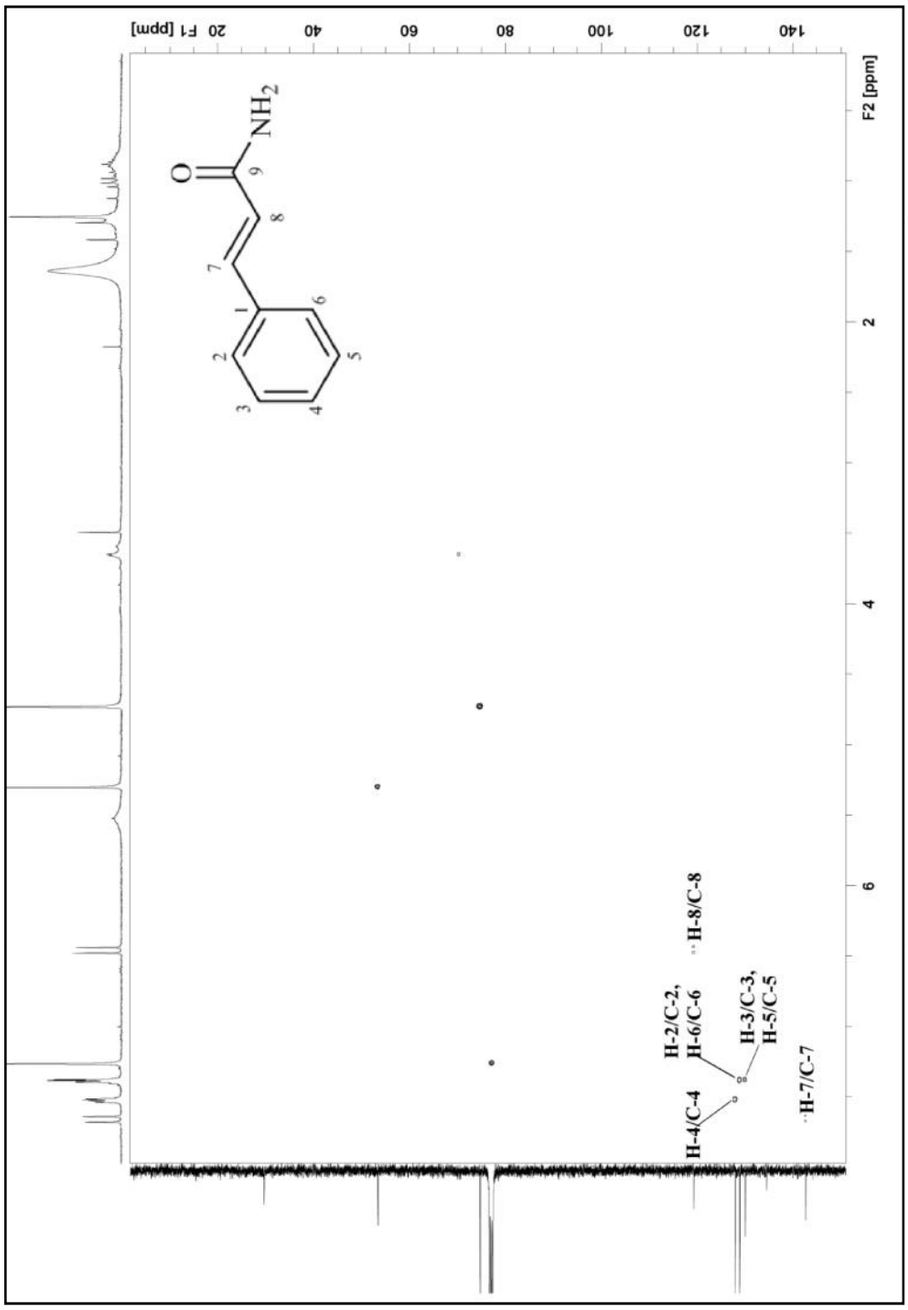

Figure 3.122: HSQC Spectrum of Cinnamide **59**

3.2.17 Blumenol B 71

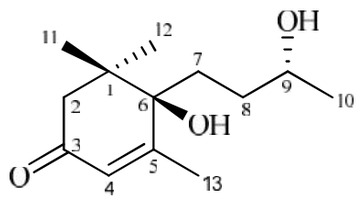

71

Blumenol B **71** $[\alpha]_D^{23}$ +36.4º (*c* 0.11, $CHCl_3$) was isolated as a white amorphous solid. It has a molecular formula of $C_{13}H_{22}O_3$ as deduced from the ESIMS (Figure 3.124) which displayed a pseudomolecular ion peak at *m/z* $[M+H]^+$ 227.1733 (calc. 227.1642). UV spectrum exhibited absorption maxima at 242 nm.[97] The IR spectrum of showed absorption peaks at 3401, 1651 and 1126 cm^{-1}, indicating the presence of OH, C=O and C-O stretching vibrations.[97]

In the ^{1}H-NMR spectrum (Figure 3.125), a methyl group resonated as a doublet at δ_H 1.22 (*J* = 6.0) which could be assigned to H-10. This methyl proton was coupled with H-9 which gave a signal as multiplet at δ_H 3.75-3.81. In addition, two singlets corresponding to six protons of two methyls (H_3-11 and H_3-12) appeared at δ_H 1.08 and δ_H 1.04 respectively. Furthermore, another methyl group (δ_H 2.04, H_3-13) attached to C-5 gave a fine doublet with a coupling constant of 0.9 Hz due to the long range coupling with H-4. One set of doublet (δ_H 2.33 and δ_H 2.48) and two sets of multiplets (δ_H 1.94-1.99 and δ_H 1.79-1.89, δ_H 1.58-1.67 and δ_H 1.47-1.56) may be attributed to the methylene groups H_2-2, H_2-7 and H_2-8 respectively.

The ^{13}C-NMR and DEPT spectra (Figure 3.126 and Figure 3.127) of blumenol B **71** showed a total of thirteen carbon signals; four methyl, three methylenes, two methines, three quaternary carbons and one carbonyl carbon which represented a C13 nor-isoprenoid skeleton.[98] A downfield carbon signal was observed at δ_C 198.1 which corresponded to the carbonyl group of C-3. The other two oxygenated carbons, C-6 and

C-9, gave signals at δ_C 77.9 and δ_C 68.8. The stereochemistry of this compound was confirmed through comparison with reported data[98]. There were two chiral centres in this compound; C-6 and C-9. According to literature review,[98] there are two diastereomers; (6*S*, 9*R*) and (6*R*, 9*R*) found in plants. The difference of chemical shift at C-7 could be used to distinguish between the diastereomers where 6*S* isomer (δ_H 1.84-1.99, δ_C 34.8) had downfield signals of ^{1}H and ^{13}C-NMR for C-7 compared with 6*R* isomer (δ_H 1.72-1.91, δ_C 33.5).[98] Hence, blumenol B **71** has stereochemistry of 6*S*, 9*R* by comparing with the reported ^{1}H and ^{13}C-NMR data. In addition, synthesis of blumenol B **71** has been done by Weiss, Koreeda and Nakanishi (1973) to study its stereochemistry.

Complete ^{1}H and ^{13}C-NMR assignments (Table 3.18) were established by thorough analysis of COSY, HMBC and HSQC data. From the analysis of the spectroscopic data obtained and comparison with the literature values,[98,100,101] the structure of blumenol B **71** was confirmed.

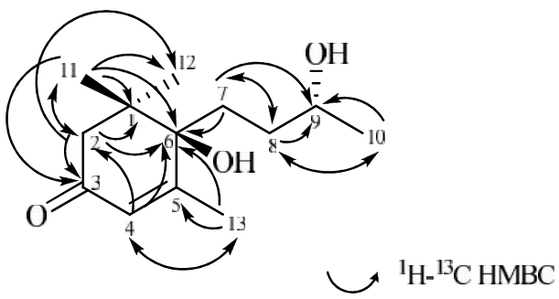

Figure 3.123: HMBC Correlation of Blumenol B **71**

Table 3.18: ^{1}H-NMR (400 MHz) and ^{13}C-NMR (100 MHz) Spectral Data of Blumenol B **71** in $CDCl_3$.

Position	**^{1}H**		**^{13}C**	
	δ_H (multiplicity, *J* in Hz)		**δ_C**	
	Experimental ($CDCl_3$)	**Reference* ($CDCl_3$)**	**Experimental ($CDCl_3$)**	**Reference* ($CDCl_3$)**
1	-	-	41.8	41.7
2β	2.48 (*d*, 18.3)	2.50 (*d*, 18.0)	50.1	50.0
2α	2.23 (*d*, 18.3)	2.25 (*d*, 18.0)		
3	-	-	198.1	198.0
4	5.84 (*br s*)	5.86 (*dq*, 1.4, 1.2)	126.1	126.1
5	-	-	168.3	168.1
6	-	-	77.9	77.8
7a	1.94-1.99 (*m*)	1.99 (*m*)	34.8	34.8
7b	1.79-1.89 (*m*)	1.84 (*m*)		
8a	1.58-1.67 (*m*)	1.64 (*m*)	33.6	33.3
8b	1.47-1.56 (*m*)	1.53 (*m*)		
9	3.75-3.81 (*m*)	3.79 (*m*)	68.8	68.8
10	1.22 (*d*, 6.0)	1.23 (*d*, 6.2)	24.3	24.2
11	1.08 (*s*)	1.09 (*s*)	23.8	23.8
12	1.04 (*s*)	1.06 (*s*)	24.0	23.9
13	2.04 (*d*, 0.9)	2.06 (*d*, 1.4)	21.8	21.7

*Literature value from Almeida et al. (2011).

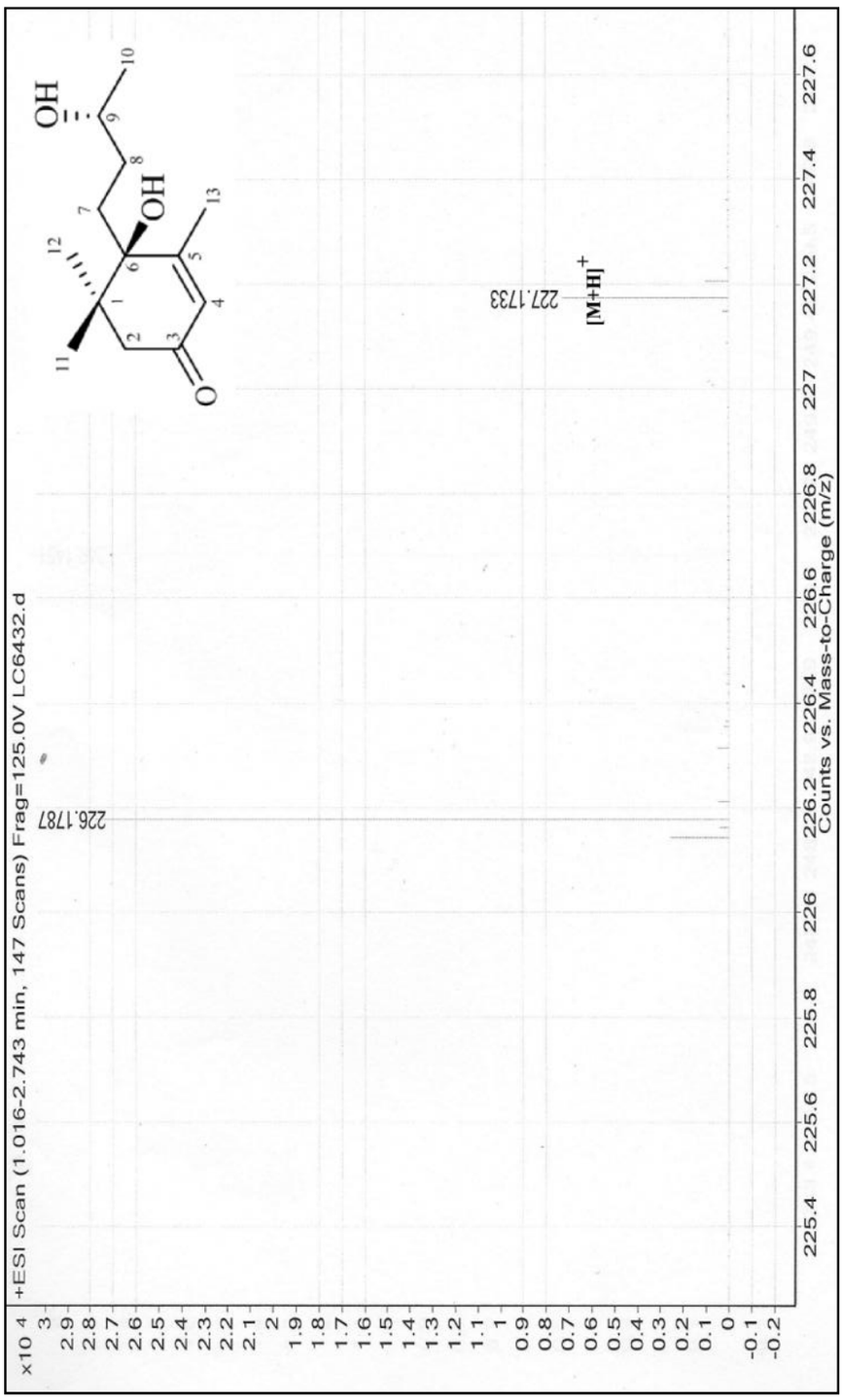

Figure 3.124: LCMS Spectrum of Blumenol B **71**

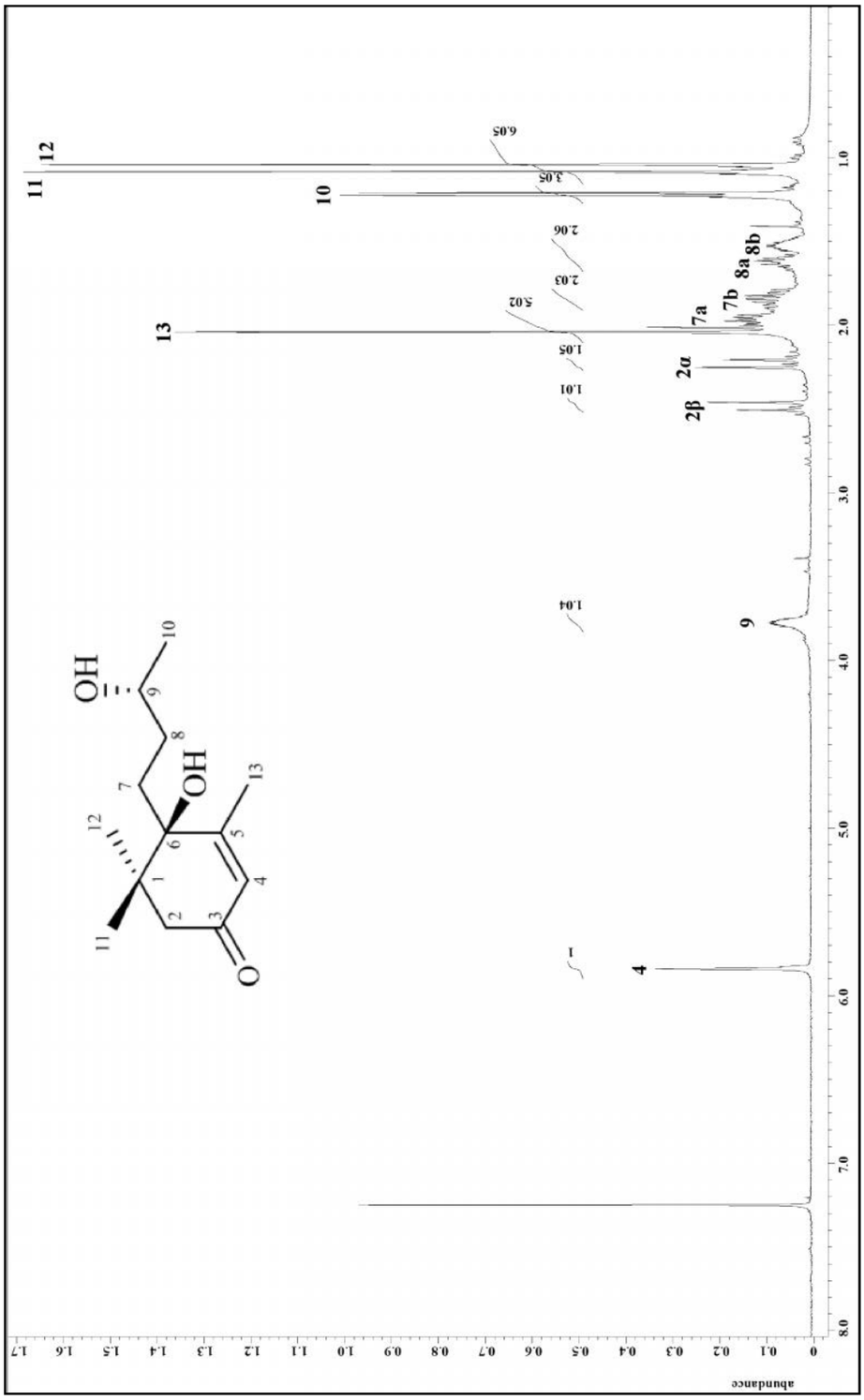

Figure 3.125: ^{1}H NMR Spectrum of Blumenol B **71**

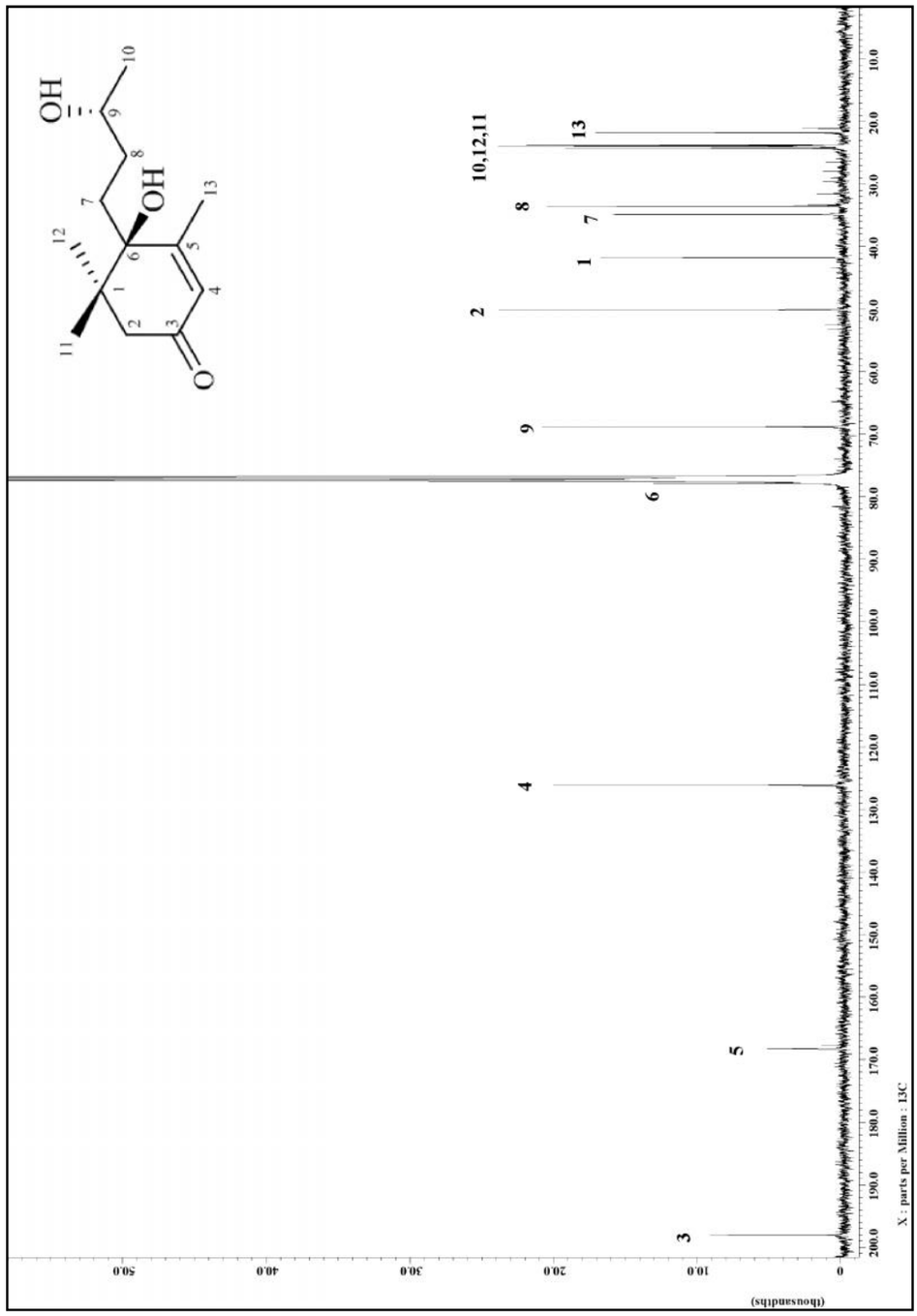

Figure 3.126: ^{13}C NMR Spectrum of Blumenol B **71**

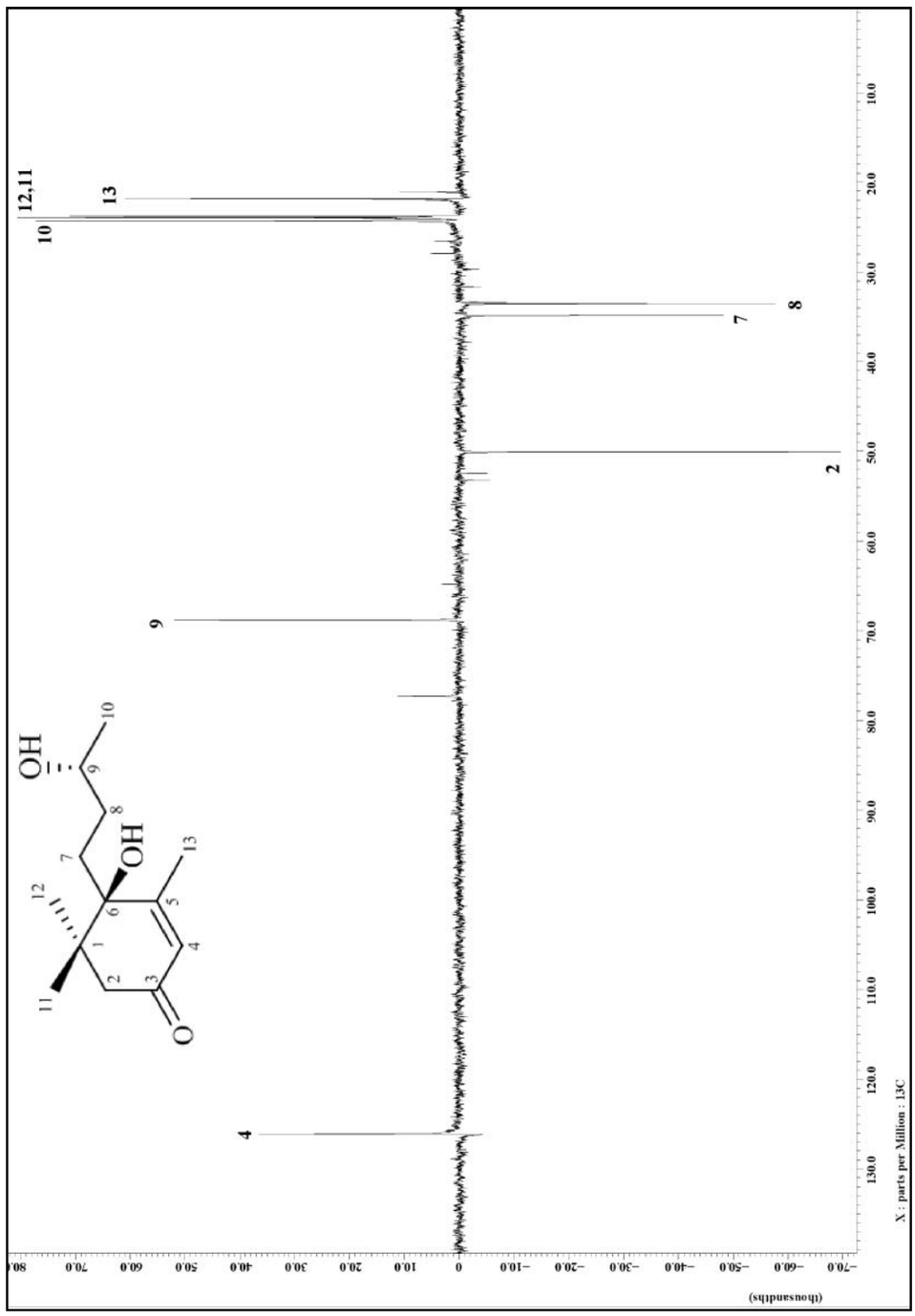

Figure 3.127: DEPT 135 NMR Spectrum of Blumenol B **71**

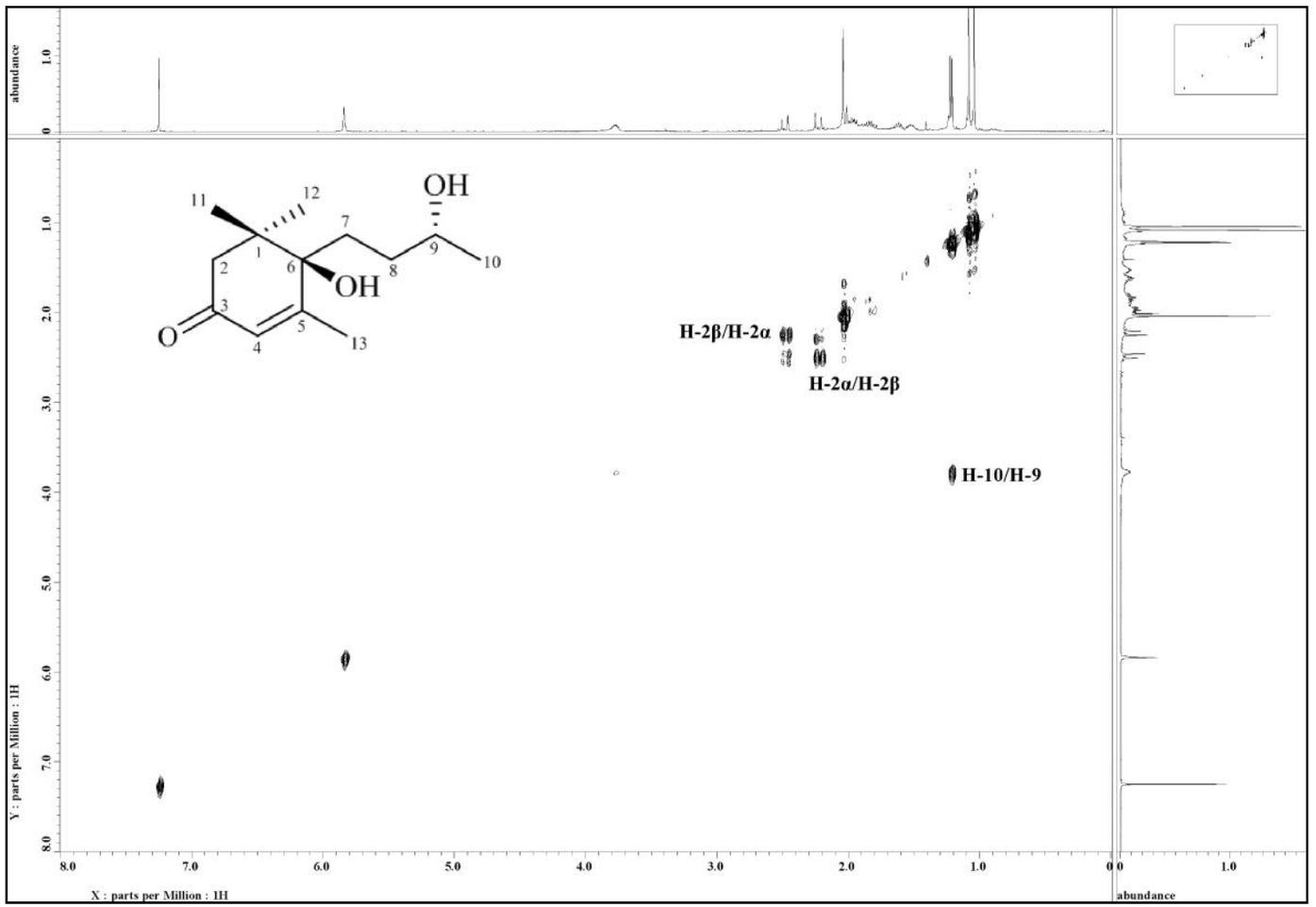

Figure 3.128: COSY Spectrum of Blumenol B **71**

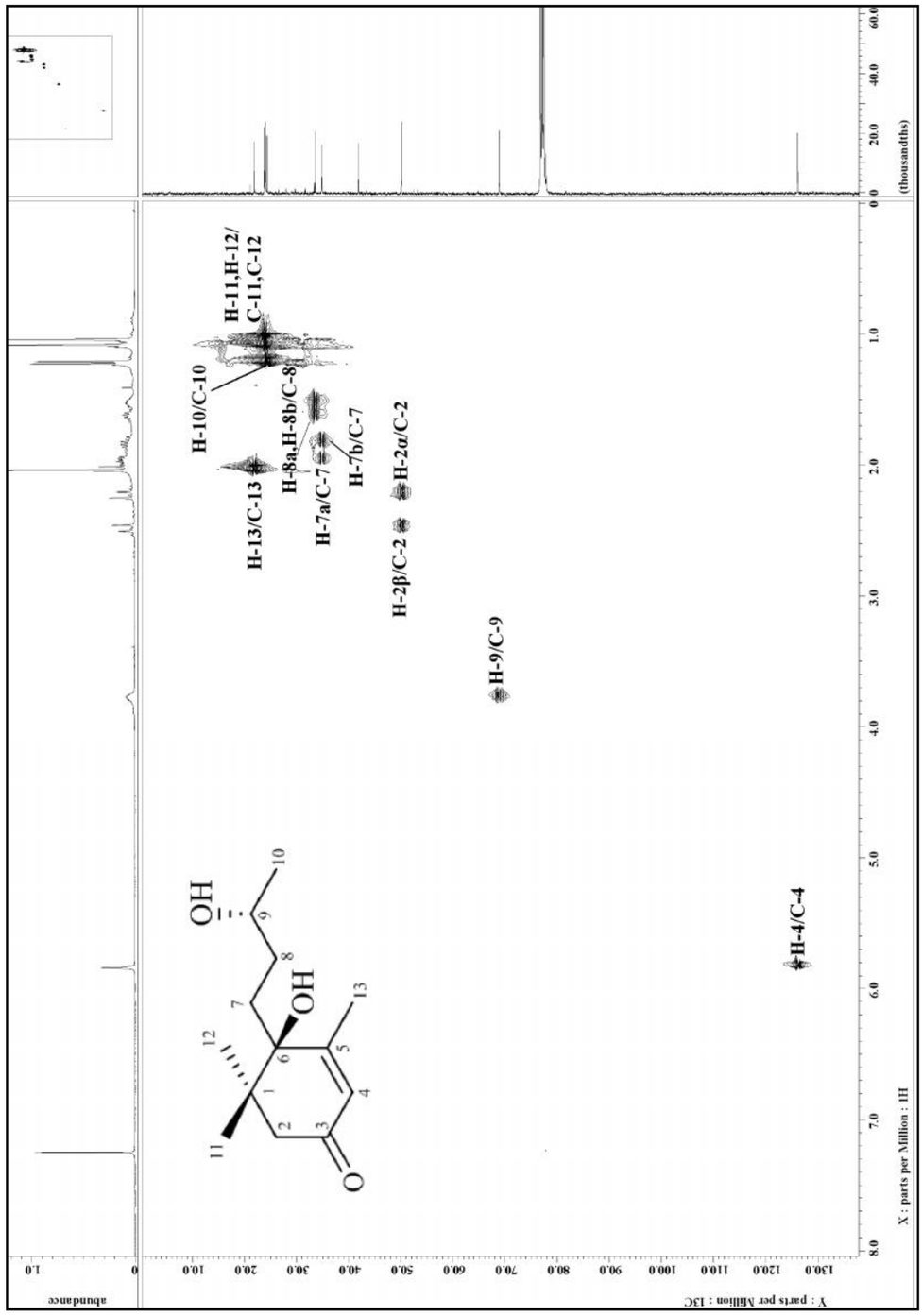

Figure 3.129: HSQC Spectrum of Blumenol B **71**

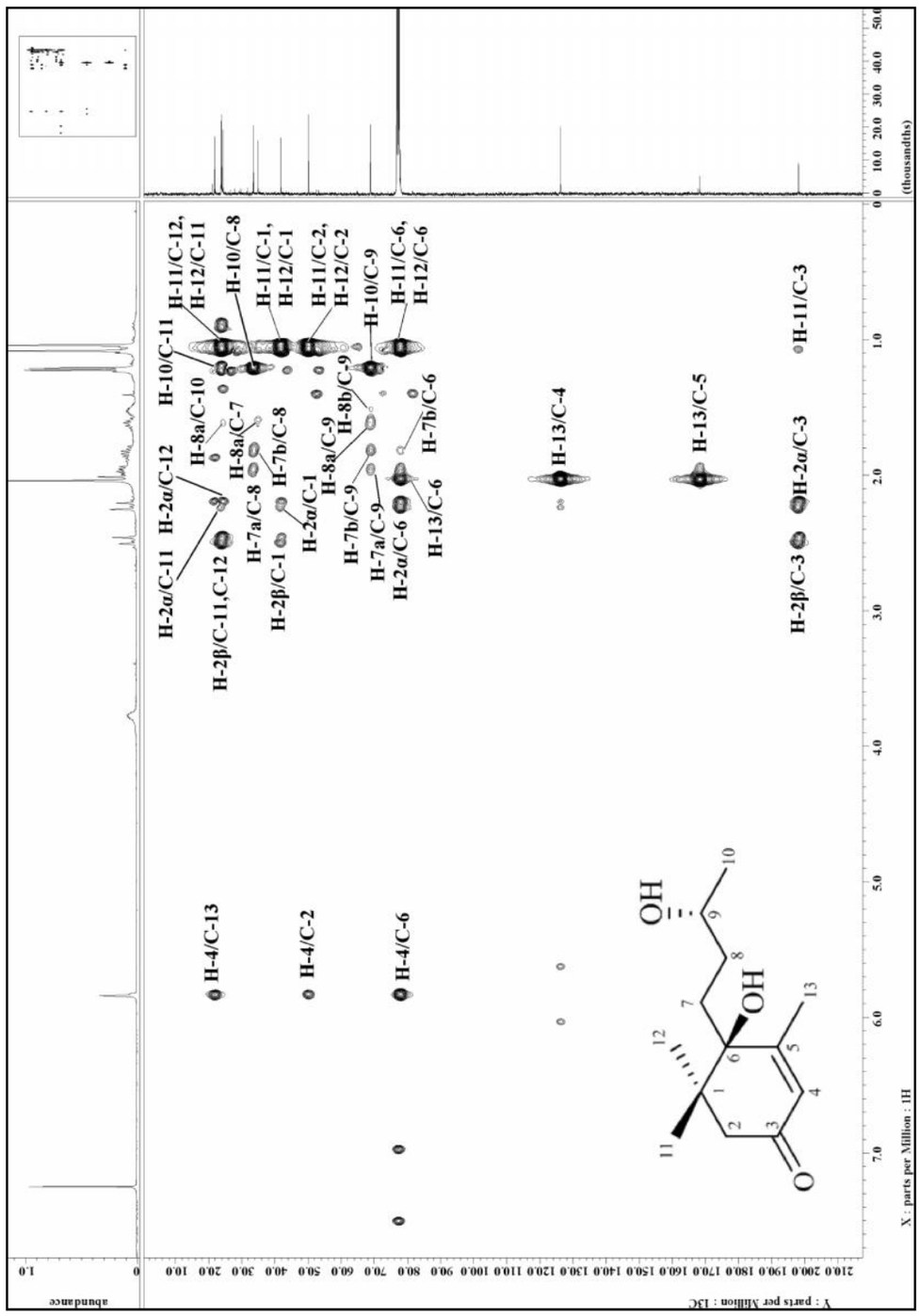

Figure 3.130: HMBC Spectrum of Blumenol B **71**

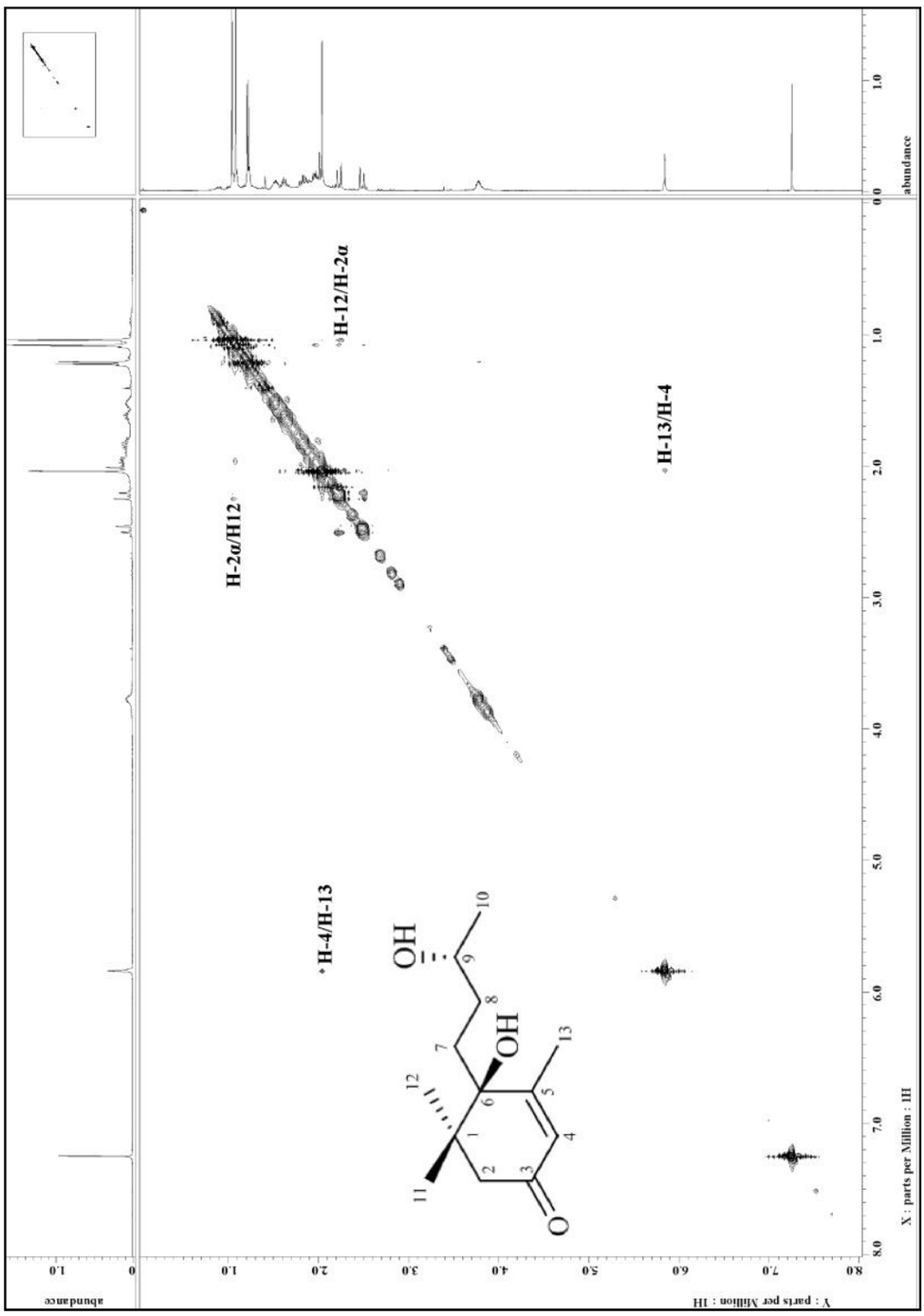

Figure 3.131: NOESY Spectrum of Blumenol B **71**

3.2.18 Blumenol A 66

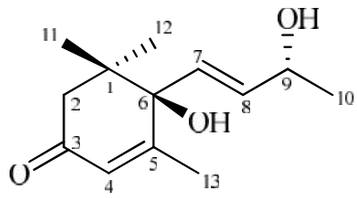

66

Blumenol A **66** $[\alpha]_D^{23}$ +146.6º (*c* 0.58, $CHCl_3$) was afforded as a white amorphous solid. The ESIMS (Figure 3.133) revealed a pseudomolecular ion peak $[M+H]^+$ at *m/z* 225.1665, corresponding to the molecular formula of $C_{13}H_{20}O_3$ (calc. 225.1485). In UV spectrum, absorption maxima were observed at 237 nm.[102] The IR spectrum of showed an absorption peak at 3402, 1655 and 1124 cm^{-1}which were due to OH, C=O and C-O stretching vibrations respectively.[102]

This compound had similar structural skeleton with blumenol B **71**. The only difference was at C-7 and C-8. In ^{1}H-NMR spectrum (Figure 3.134), a doublet and a multiplet peaks were observed at δ_H 5.75 and δ_H 5.84 with coupling constant, *J* = 16.0 Hz which was attributed to H-7 and H-8, respectively indicating the presence of *trans* double bond instead of two methylene protons in blumenol B **71**. Two singlets were observed at δ_H 1.05 and δ_H 0.98 which attributed to two methyl protons of H_3-11 and H_3-12 respectively. The other two methyl protons resonated at δ_H 1.27 as doublet (3H, *d*, *J* = 6.4 Hz, H_3-10) and δ_H 1.87 (3H, *d*, *J* = 1.4 Hz, H_3-13)

The ^{13}C-NMR spectrum (Figure 3.135) of blumenol A **66** indicated a total of thirteen carbon signals like blumenol B **71**; four methyl, one methylenes, four methines, three quaternary carbons and one carbonyl carbon which represented a C13 nor-isoprenoid skeleton.[103] The stereochemistry of this compound was assumed to be the same as blumenol B **71** since both compounds were obtained from the same plant,

therefore they are most probably biogenetically related. This hypothesis is supported by the NMR data from the synthesized blumenol B by Yamano and Ito (2005).[102]

From the analysis of the spectroscopic data obtained (Table 3.19) and comparison with the literature values,[101,102,103,104,105,106,107] the structure of blumenol A **66** was confirmed.

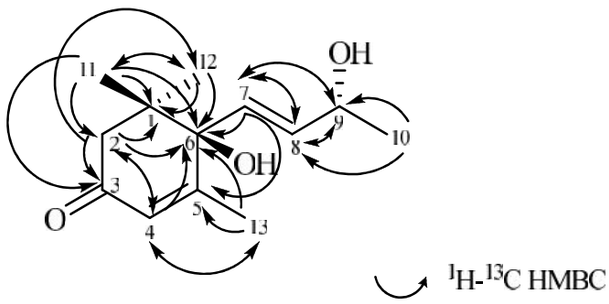

Figure 3.132: HMBC Correlations of Blumenol A **66**

Table 3.19: ^{1}H-NMR (400 MHz) and ^{13}C-NMR (100 MHz) Spectral Data of Blumenol A **66** in $CDCl_3$.

Position	**^{1}H**		**^{13}C**	
	δ_H (multiplicity, *J* in Hz)		**δ_C**	
	Experimental ($CDCl_3$)	**Reference* ($CDCl_3$)**	**Experimental ($CDCl_3$)**	**Reference* ($CDCl_3$)**
1	-	-	41.3	41.1
2β	2.42 (*d*, 17.2)	2.44 (*d*, 17.5)	49.8	49.7
2α	2.21 (*d*, 17.2)	2.23 (*d*, 17.5)		
3	-	-	198.3	197.9
4	5.88 (*br s*)	5.90 (*br s*)	126.1	126.9
5	-	-	163.2	162.7
6	-	-	79.1	79.0
7	5.75 (*d*, 16.0)	5.78 (*d*, 16.0)	129.1	129.0
8	5.84 (*m*)	5.85 (*dd*, 16.0, 5.0)	135.8	135.7
9	4.38 (*quintet*, 6.4, 5.9)	4.40 (*qd*, 6.5, 5.0)	68.1	68.0
10	1.27 (*d*, 6.4)	1.29 (*d*, 6.5)	23.8	23.7
11	1.05 (*s*)	1.08 (*s*)	22.9	22.9
12	0.98 (*s*)	1.02 (*s*)	24.1	24.0
13	1.87 (*d*, 1.4)	1.90 (*s*)	19.1	18.9

*Literature value from Yamano and Ito (2005), Feng et al. (2010).

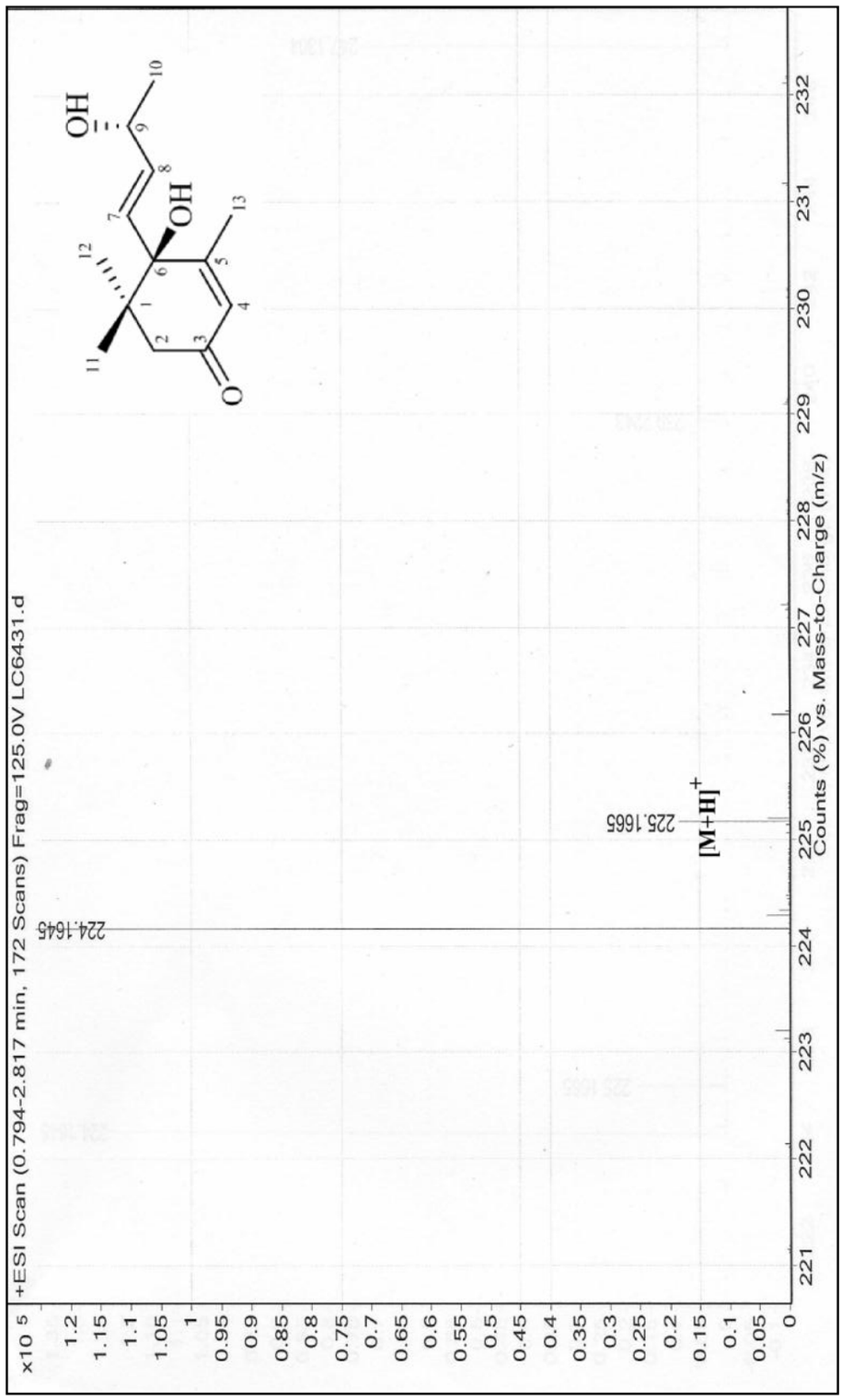

Figure 3.133: LCMS Spectrum of Blumenol A **66**

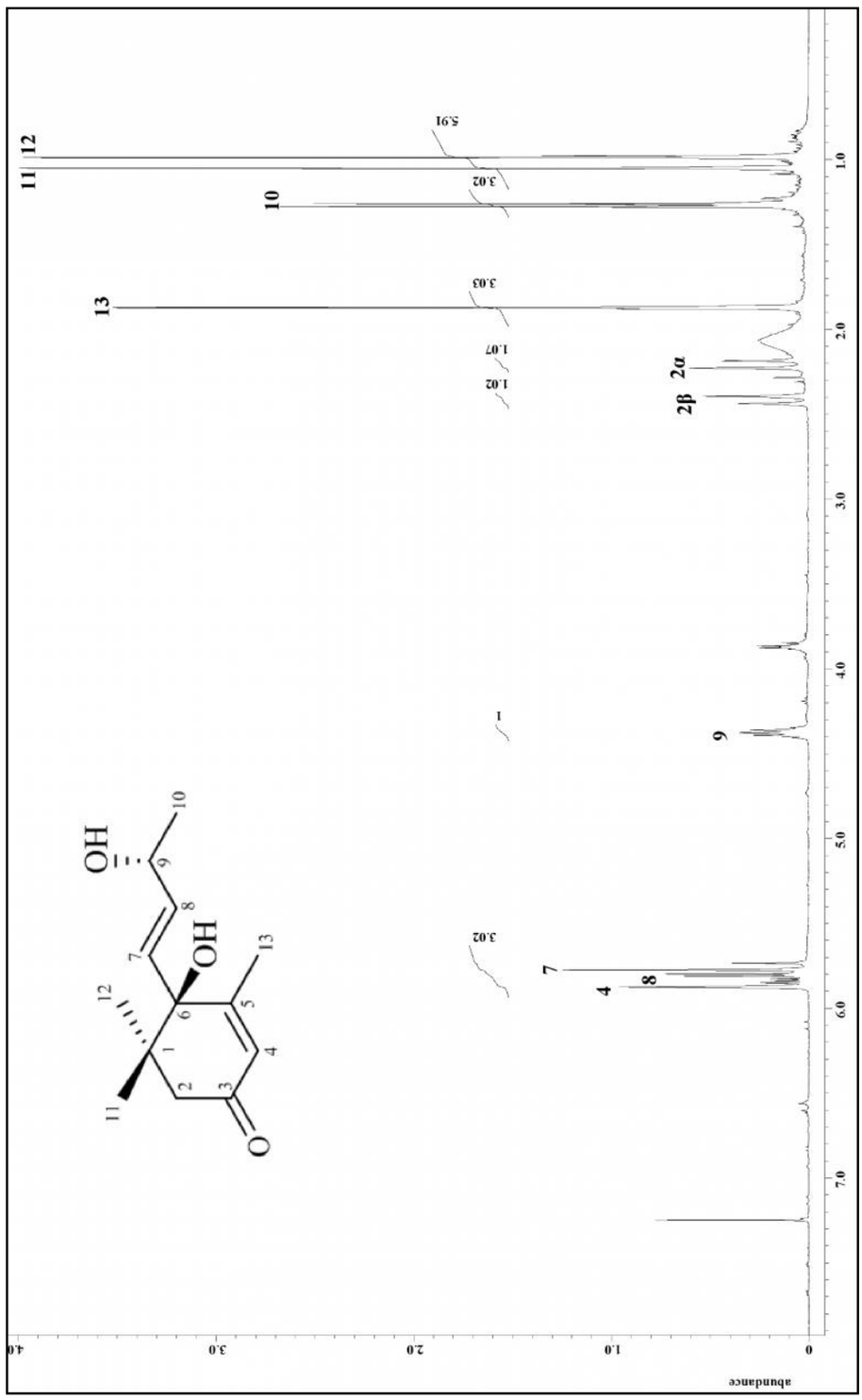

Figure 3.134: ^{1}H NMR Spectrum of Blumenol A **66**

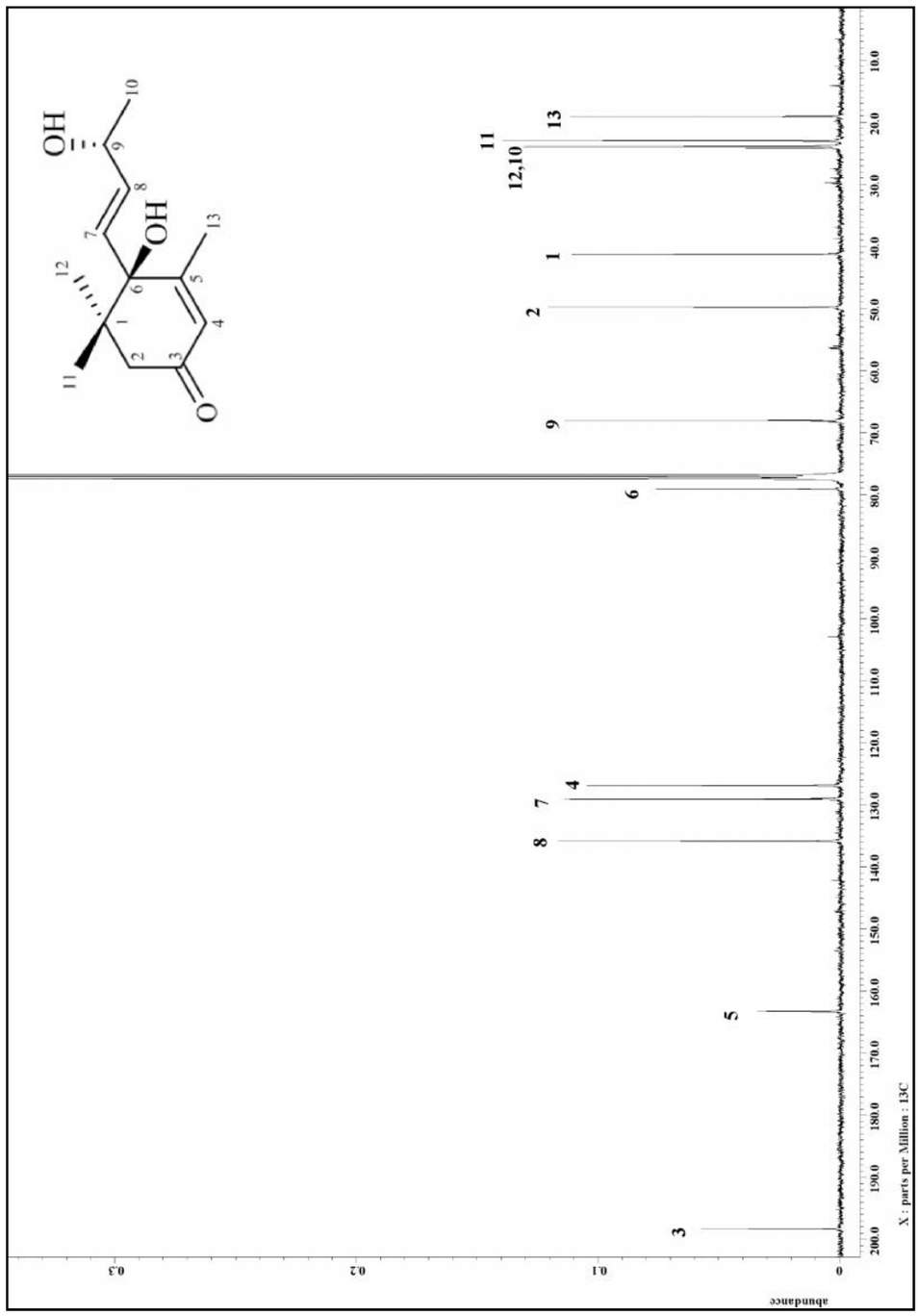

Figure 3.135: ^{13}C NMR Spectrum of Blumenol *A* **66**

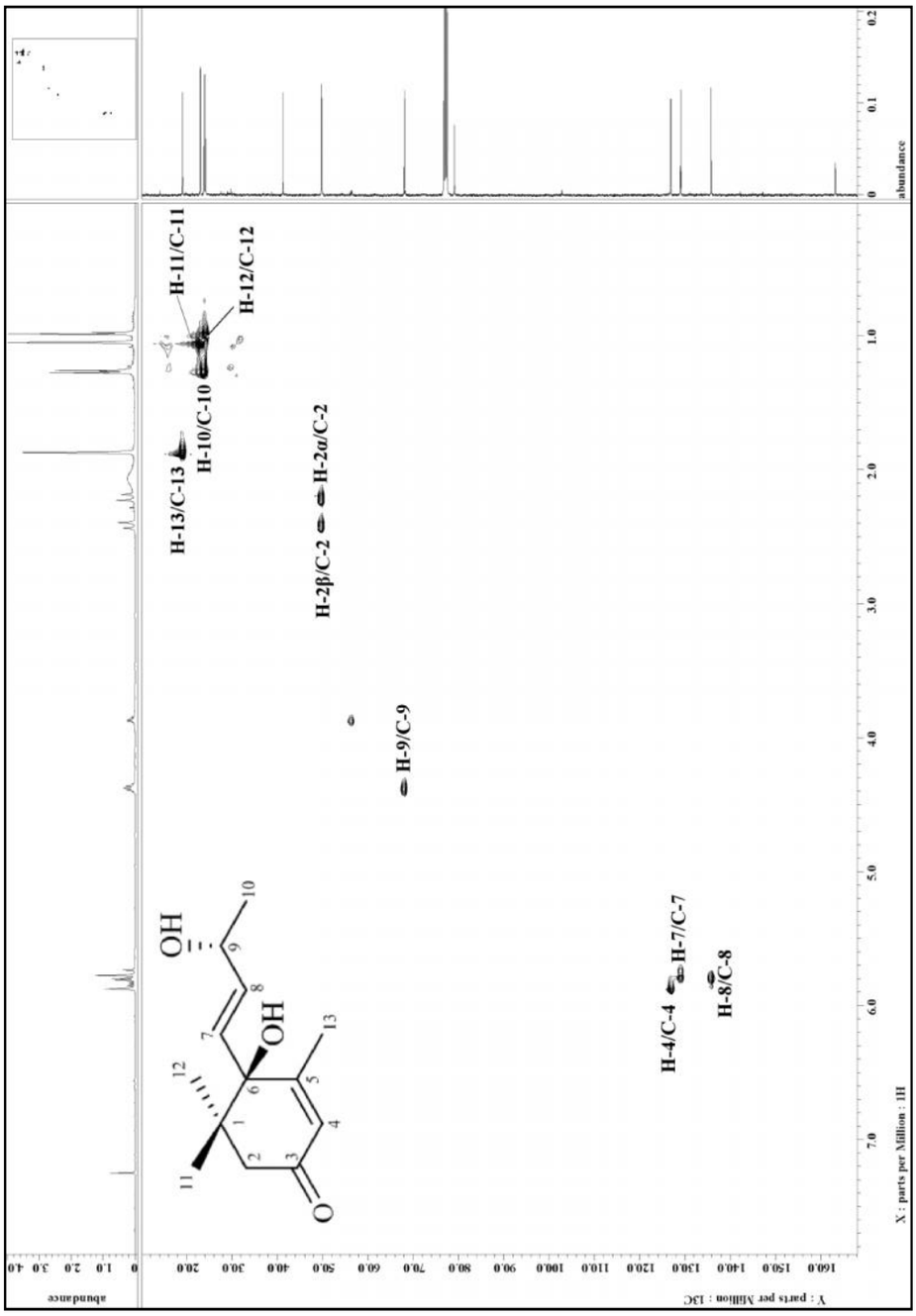

Figure 3.136: HSQC Spectrum of Blumenol A **66**

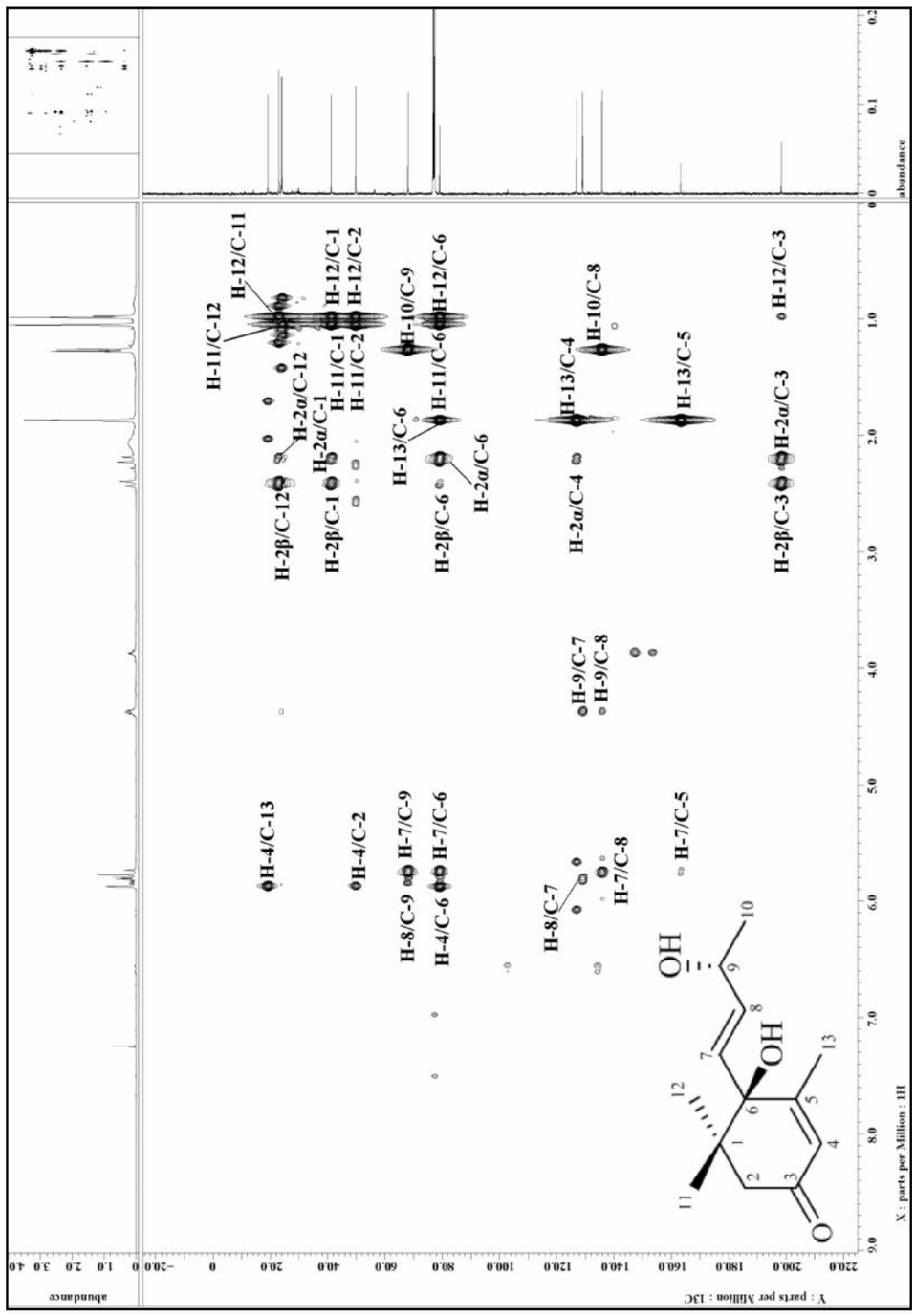

Figure 3.137: HMBC Spectrum of Blumenol A **66**

3.2.19 β-sitosterol 73

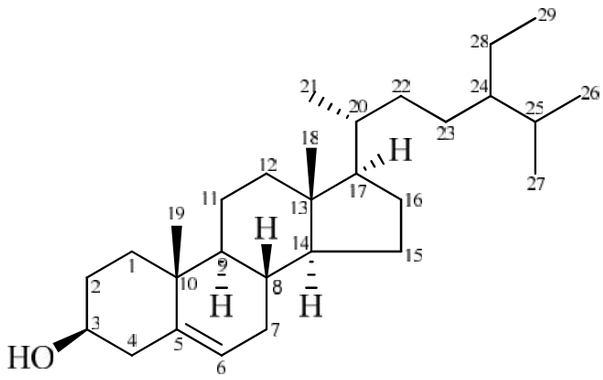

73

β-sitosterol **73** $[\alpha]_D^{23}$ -55.6º (*c* 0.09, $CHCl_3$) was obtained as a white amorphous solid . The ESIMS (Figure 3.138) showed a pseudomolecular ion peak $[M+H]^+$ at *m/z* 415.3561, corresponding to the molecular formula of $C_{29}H_{50}O$ (calc. 415.3934). UV spectrum showed absorption maxima at 203 nm.[108] In IR spectrum, absorption peaks at 3425 and 2925 cm^{-1} were observed, indicating OH and sp^3 C-H stretching vibration respectively.[108] The other peaks at 1465 and 1375 cm^{-1} were due to CH_2 and CH_3 bending.

In the ^{1}H-NMR spectrum (Figure 3.139), a broad singlet at downfield region of δ_H 5.34 which attributed to H-6 indicative of the presence of double bond functionality between C-5 and C-6. Two singlet of methyl groups were observed at δ_H 0.67 and δ_H 0.99 which attributed to H_3-18 and H_3-19 respectively. Two methyl protons of H_3-21 and H_3-29 were observed as multiplets at δ_H 0.89-0.91 and δ_H 0.84-0.86 respectively while the another two methyl protons; H_3-26 and H_3-27 were overlapped at δ_H 0.78-0.83.

The ^{13}C-NMR and DEPT spectra (Figure 3.140 and Figure 3.141) of β-sitosterol **73** indicated a total of twenty nine carbon signals; six methyl, eleven methylenes, nine methines and three quaternary carbons which was in agreement with the molecular

formula of β-sitosterol **73**. The carbon signal at δ_C 71.9 indicated the presence of oxymethine proton at C-3.

Complete ^{1}H and ^{13}C-NMR assignments (Table 3.20) were established by thorough analysis of 2D-NMR data as well as reported data,[37,108,109,110] thus the compound was identified as β-sitosterol **73**.

Table 3.20: ^{1}H-NMR (400 MHz) and ^{13}C-NMR (100 MHz) Spectral Data of β-sitosterol **73** in $CDCl_3$.

Position	^{1}H		^{13}C	
	δ_H (multiplicity, *J* in Hz)		δ_C	
	Experimental ($CDCl_3$)	Reference* ($CDCl_3$)	Experimental ($CDCl_3$)	Reference* ($CDCl_3$)
1a	1.81-1.85 (*m*)		37.3	37.3
1b	1.03-1.08 (*m*)			
2a	1.94-2.02 (*m*)		32.0	31.6
2b	1.42-1.63 (*m*)			
3	3.48-3.55 (*m*)	3.52 (*m*)	71.9	71.8
4	2.18-2.27 (*m*)		42.3	42.2
5	-	-	140.8	140.8
6	5.34 (*br s*)	5.36 (*br* s)	121.8	121.7
7a	1.94-2.02 (*m*)		32.0	31.9
7b	1.42-1.63 (*m*)			
8	1.81-1.85 (*m*)		31.7	31.9
9	0.89-0.91 (*m*)		50.2	51.2
10	-	-	36.6	36.5
11	1.42-1.63 (*m*)		21.2	21.1
12a	1.94-2.02 (*m*)		39.8	39.8
12b	1.03-1.18 (*m*)			
13	-	-	42.4	42.3
14	0.99 (*s*)		56.8	56.8
15	1.03-1.18 (*m*)		24.8	24.3
16	1.81-1.85 (*m*)		28.3	28.3
17	1.03-1.18 (*m*)		56.1	56.0
18	0.67 (*s*)	0.68 (*s*)	11.9	11.9
19	0.98 (*s*)	1.01 (*s*)	19.5	19.4
20	1.24-1.38 (*m*)		36.2	36.2
21	0.89-0.91 (*m*)	0.92 (*d*, 6.4)	18.9	18.8
22a	2.30-2.35 (*m*)		33.8	33.9
22b	0.94-0.98 (*m*)			
23	1.03-1.18 (*m*)		26.1	26.1
24	0.89-0.91 (*m*)		45.9	45.9
25	1.59-1.63 (*m*)		29.2	29.2
26	0.78-0.83 (*m*)	0.81 (*d*, 6.5)	19.9	19.8
27	0.78-0.83 (*m*)	0.83 (*d*, 6.5)	19.1	19.3
28	1.24-1.38 (*m*)		23.1	23.1
29	0.84-0.86 (*m*)	0.85 (*t*, 7.5)	12.1	12.2

*Literature values from Pateh et al. (2008).

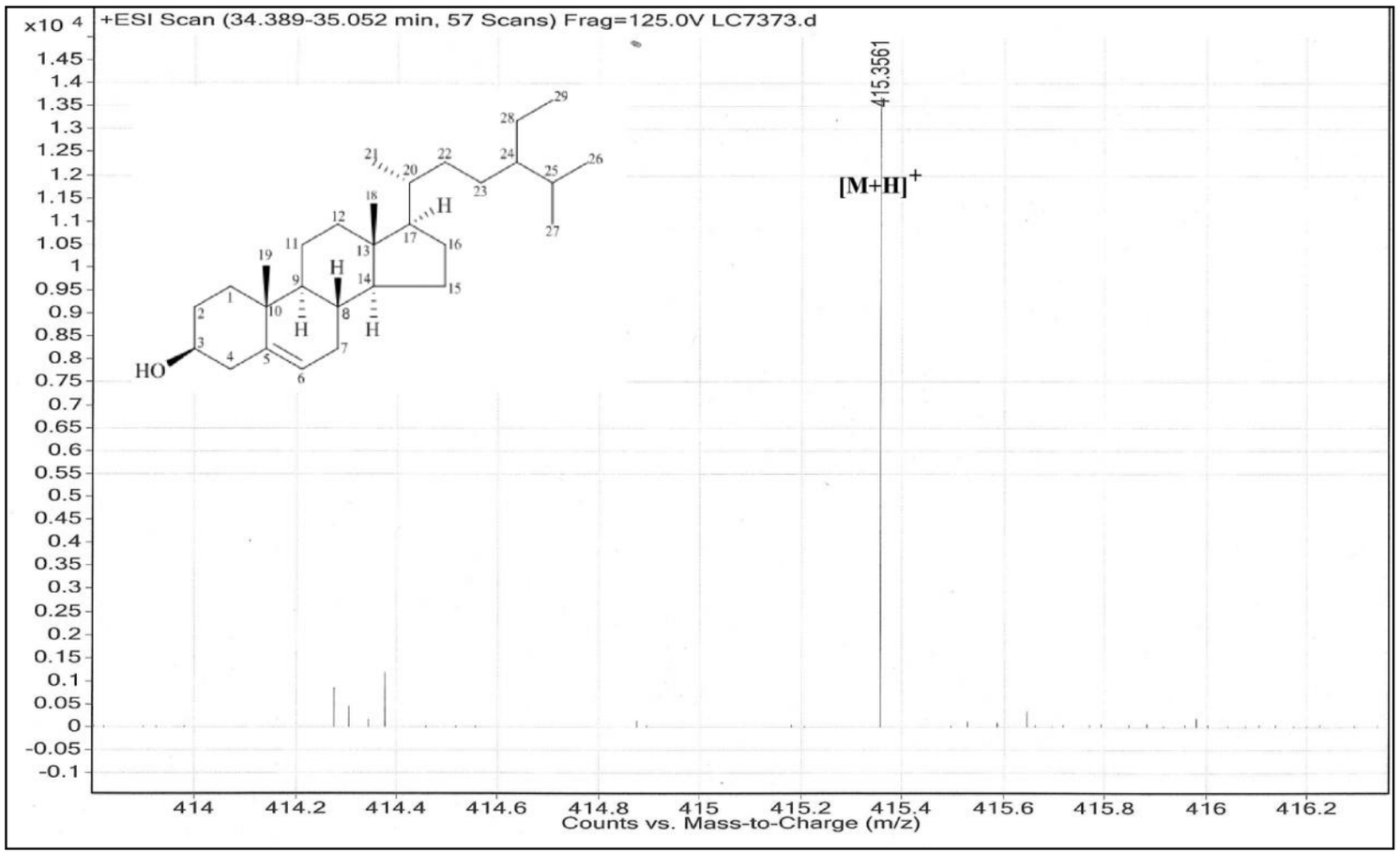

Figure 3.138: LCMS Spectrum of β-sitosterol **73**

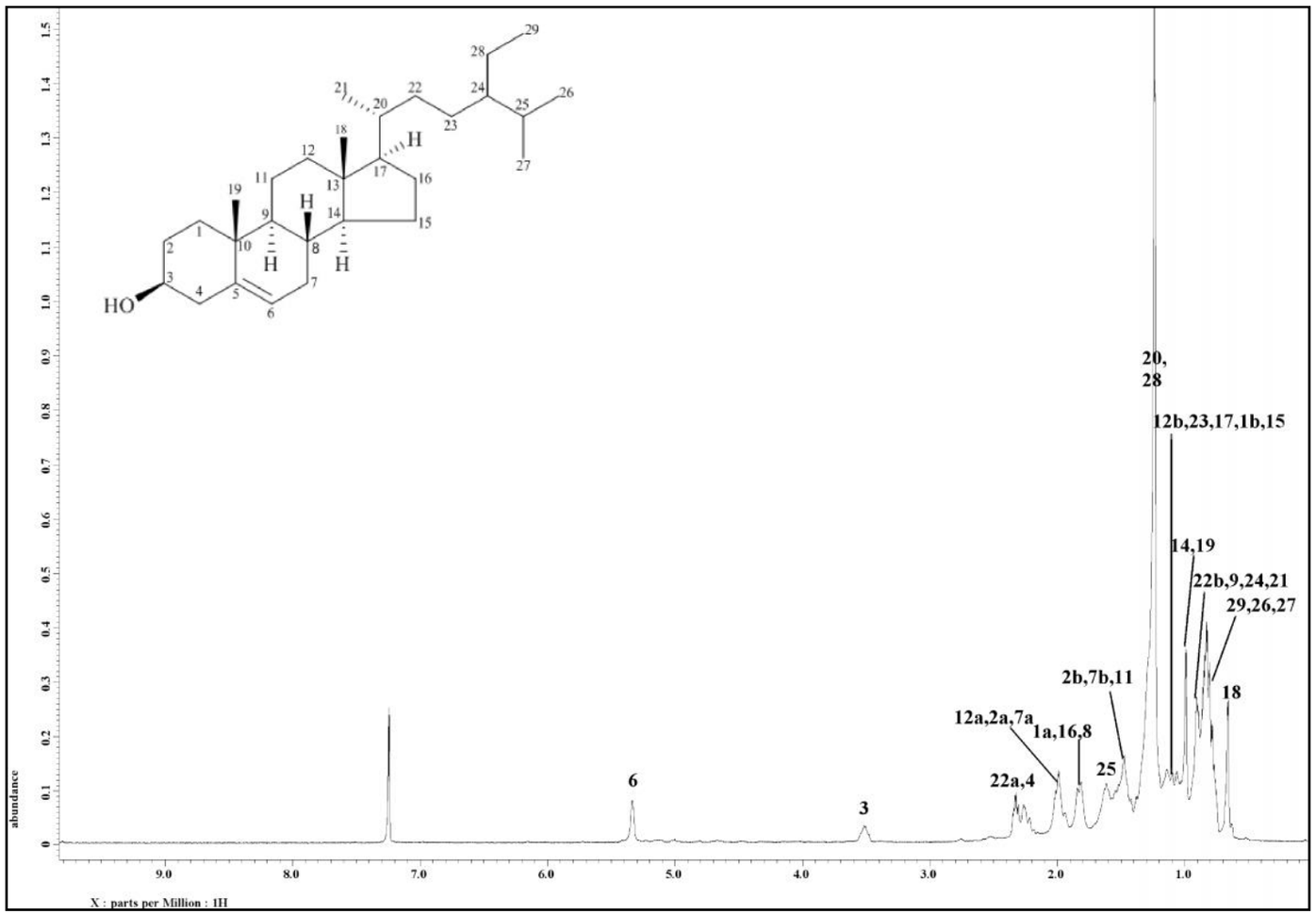

Figure 3.139: ^{1}H NMR Spectrum of β-sitosterol **73**

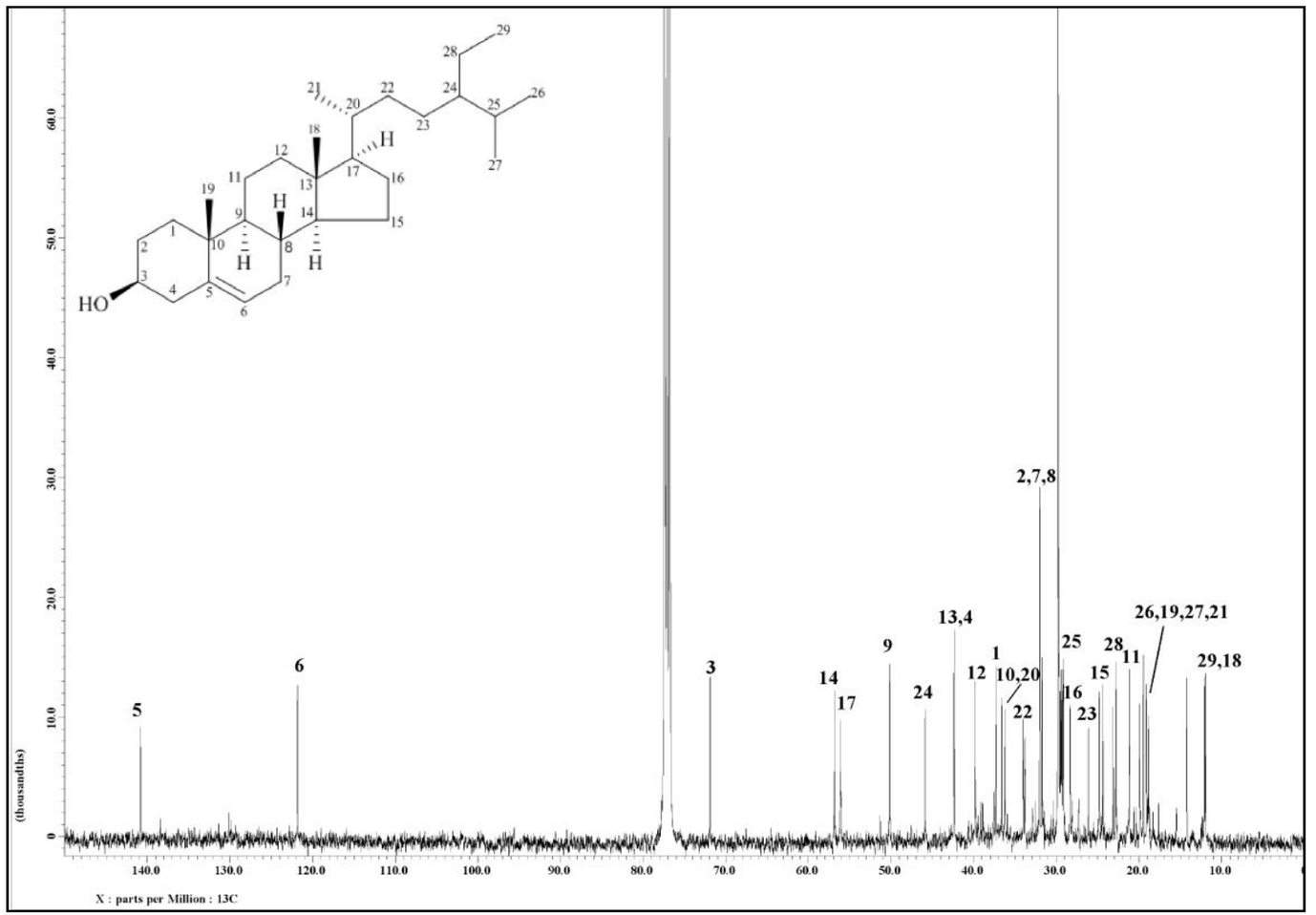

Figure 3.140: ^{13}C NMR Spectrum of β-sitosterol **73**

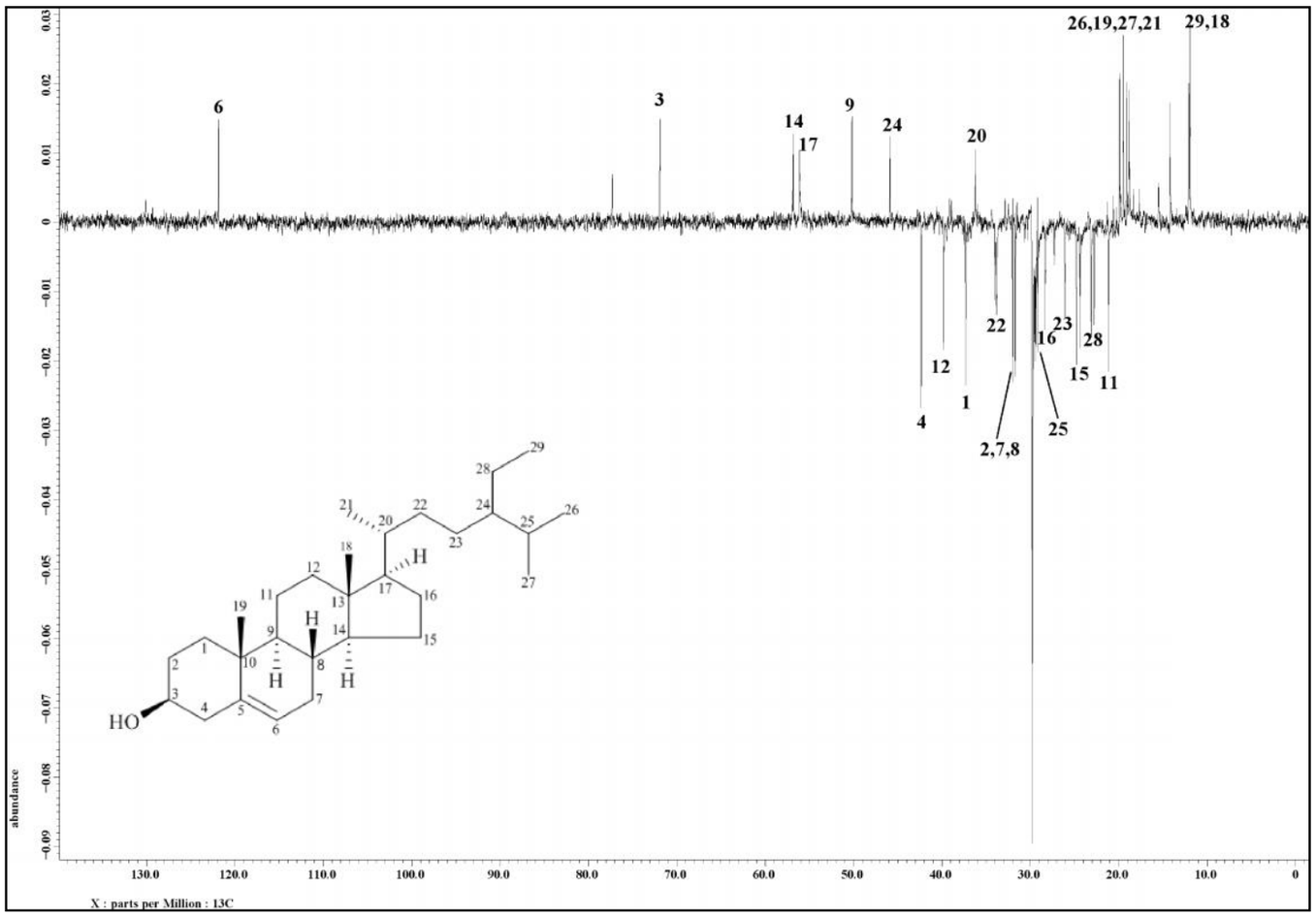

Figure 3.141: DEPT 135 Spectrum of β-sitosterol **73**

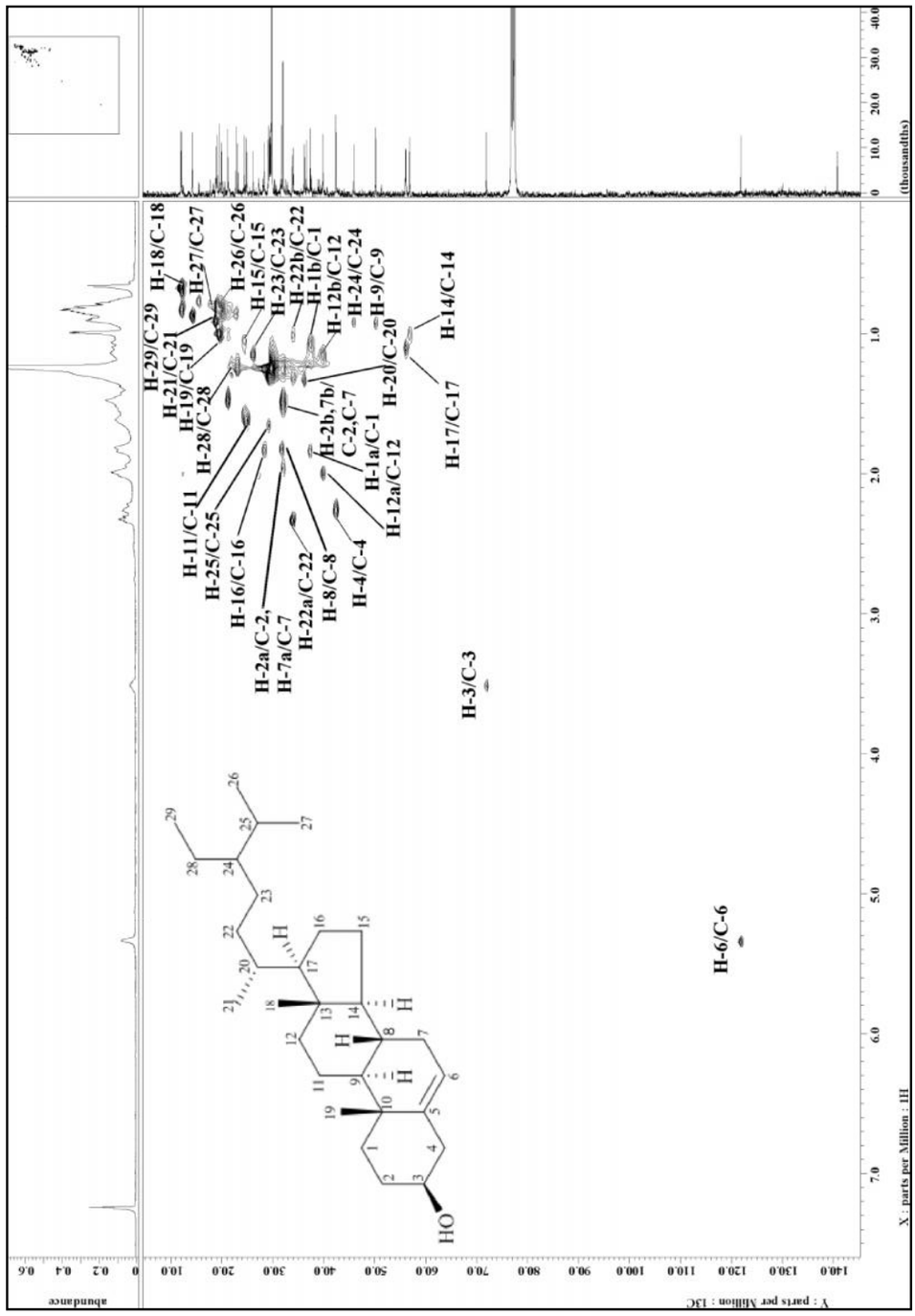

Figure 3.142: HSQC Spectrum of β-sitosterol **73**

3.2.20 Stigmast-4-en-3-one 57

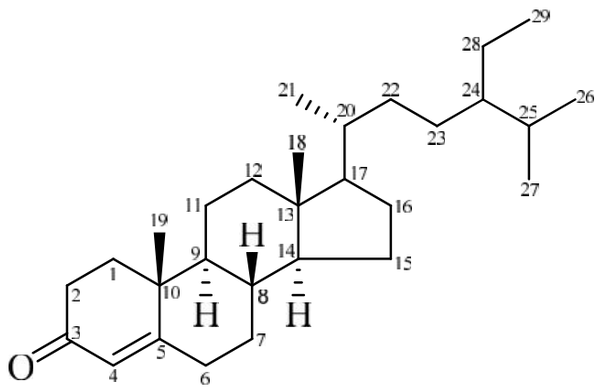

57

Stigmast-4-en-3-one **57** $[\alpha]_D^{23}$ +75.0º (*c* 0.12, $CHCl_3$) was yielded as a white amorphous solid. The ESIMS (Figure 3.143) showed a pseudomolecular ion peak $[M+H]^+$ at *m/z* 413.2660, corresponding to the molecular formula of $C_{29}H_{48}O$ (calc. 413.3778). UV spectrum showed absorption maxima at 241 nm.[108] The IR spectrum of showed absorption peak at 1675cm^{-1} indicated the presence of C=O group while absorption peaks at 1468 and 1375 cm^{-1} were due to CH_3 and CH_2 bending respectively.[108]

The ^{1}H-NMR spectrum (Figure 3.144) of stigmast-4-en-3-one **57** closely resemble that of β-sitosterol **73**. The presence of a broad singlet at downfield region of δ_H 5.73 were attributed to olefinic proton H-4. Two singlets of methyl groups were observed at δ_H 0.71 and δ_H 1.18 which could be assigned to H_3-18 and H_3-19 respectively. Three methyl protons; H_3-21, H_3-26 and H_3-27 were observed as doublet at δ_H 0.92, δ_H 0.82 and δ_H 0.82 and δ_H 0.86 respectively while remaining methyl protons (H_3-29) resonated at δ_H 0.85-0.86 as multiplet.

The ^{13}C-NMR spectrum (Figure 3.145) of stigmast-4-en-3-one **57** indicated a total of twenty nine carbon signals; six methyl, eleven methylenes, nine methines and three quaternary carbons. A downfield carbon signal was observed at δ_C 199.8 indicated

the presence of carbonyl group at C-3. The other two downfield carbon signals of δ_C 123.7 and δ_C 171.8 were attributed to the olefinic carbons C-4 and C-5.

Based on the spectral data obtained (Table 3.21) and comparison with literature data,[37,108,110] the structure stigmast-4-en-3-one **57** was confirmed without doubt.

Table 3.21: ^{1}H-NMR (400 MHz) and ^{13}C-NMR (100 MHz) Spectral Data of stigmast-4-en-3-one **57** in $CDCl_3$.

Position	**^{1}H**		**^{13}C**	
	δ_H (multiplicity, *J* in Hz)		**δ_C**	
	Experimental ($CDCl_3$)	**Reference* ($CDCl_3$)**	**Experimental ($CDCl_3$)**	**Reference* ($CDCl_3$)**
1a	2.00-2.05 (*m*)		35.6	35.7
1b	1.65-1.72 (*m*)			
2a	2.32-2.37 (*m*)		34.0	33.9
2b	1.30-1.33 (*m*)			
3	-	-	199.8	198.9
4	5.73 (*br s*)	5.74 (*d*, 2.2)	123.7	123.6
5	-	-	171.8	171.0
6	2.25-2.28 (*m*)		33.0	32.9
7a	1.82-1.89 (*m*)		32.1	32.1
7b	1.04-0.98 (*m*)			
8	1.49-1.53 (*m*)		35.7	35.7
9	0.92-0.94 (*m*)		53.8	53.8
10	-	-	38.6	38.6
11	1.42-1.44 (*m*)		21.0	21.0
12a	2.00-2.05 (*m*)		39.6	39.5
12b	1.15-1.10 (*m*)			
13	-	-	42.4	42.4
14	1.07-1.12 (*m*)		55.9	55.9
15a	1.62-1.63 (*m*)		24.2	24.1
15b	1.07-1.12 (*m*)			
16a	1.82-1.88 (*m*)		28.2	28.1
16b	1.25-1.27 (*m*)			
17	0.98-1.04 (*m*)		55.9	56.1
18	0.71 (*s*)	0.72 (*s*)	11.9	12.0
19	1.18 (*s*)	1.19 (*s*)	17.4	17.4
20	1.34-1.38 (*m*)		36.1	36.1
21	0.92 (*d*, 6.5)	0.93 (*d*, 6.6)	18.6	18.7
22	2.38-2.43 (*m*)		33.9	34.0
23	1.13-1.15 (*m*)		26.0	26.0
24	0.92-0.94 (*m*)		45.8	45.8
25	1.65-1.72 (*m*)		29.1	29.1
26	0.82 (*d*, 6.8)	0.84 (*d*, 6.8)	19.8	19.8
27	0.81 (*d*, 6.8)	0.82 (*d*, 6.8)	19.0	19.2
28	1.21-1.24 (*m*)		23.1	23.1
29	0.85-0.86 (*m*)	0.85 (*d*, 7.2)	12.0	11.1

*Literature values from Kolak et al. (2005).

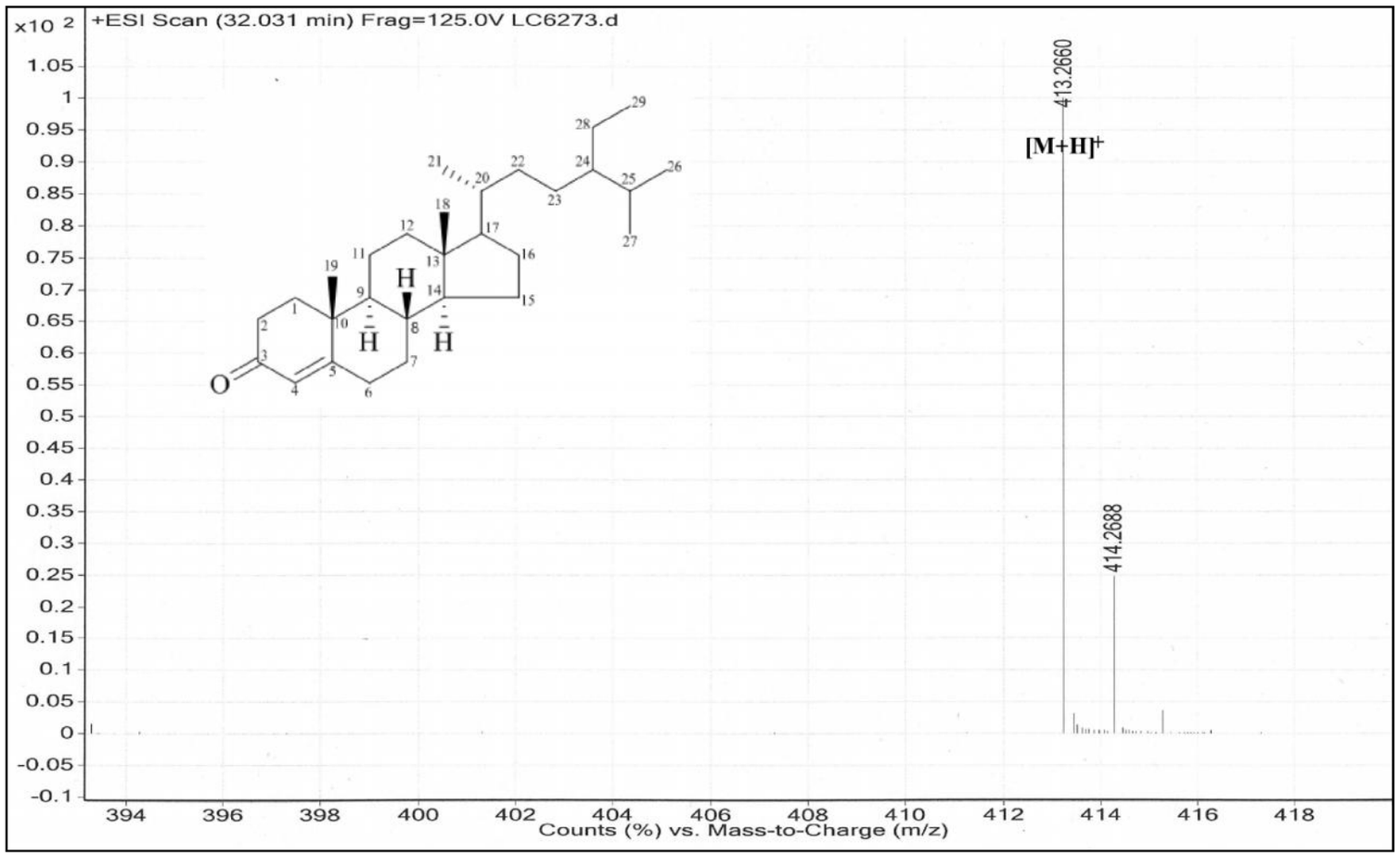

Figure 3.143: LCMS Spectrum of Stigmast-4-en-3-one **57**

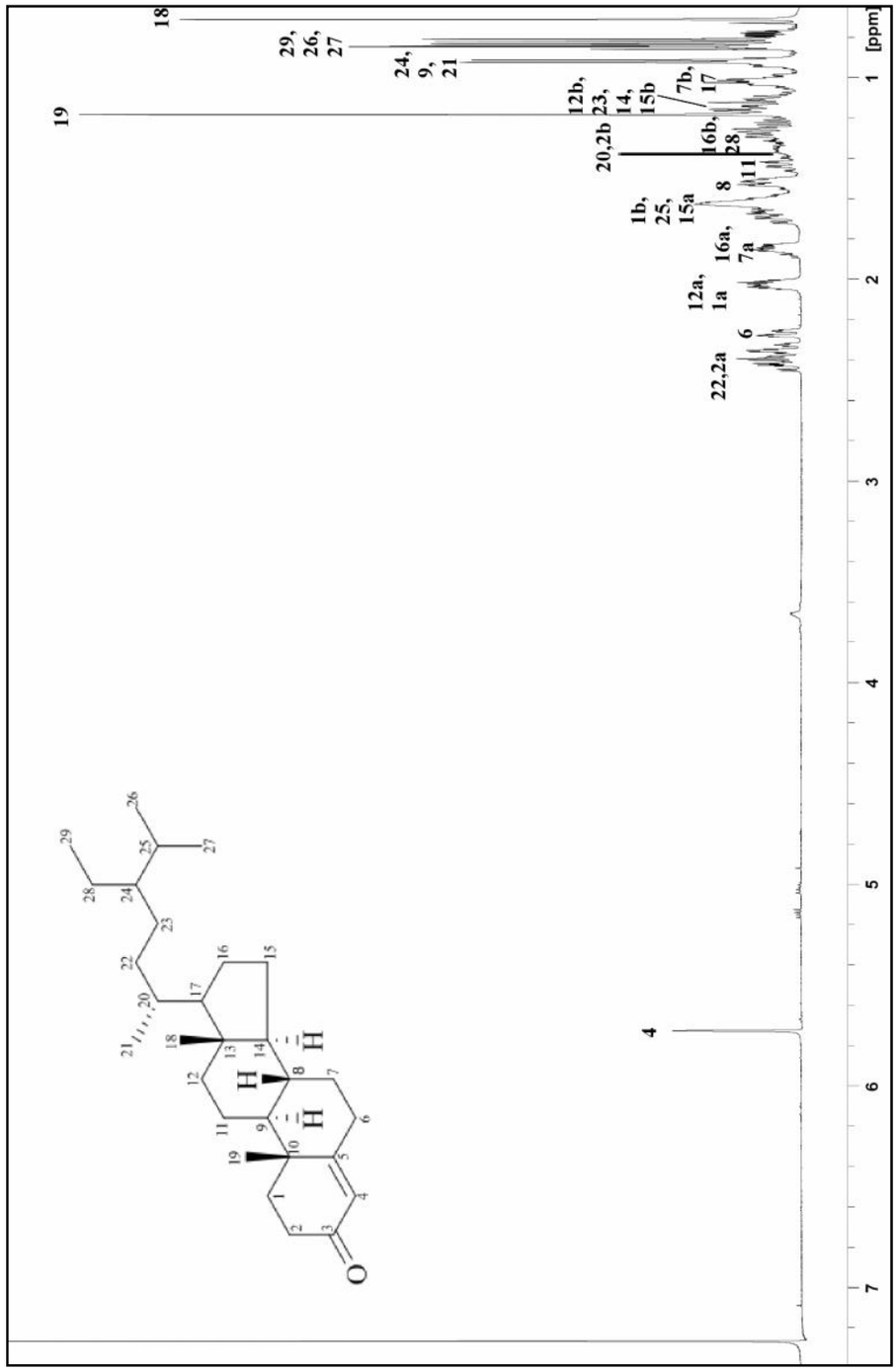

Figure 3.144: ^{1}H NMR Spectrum of stigmast-4-en-3-one **57**

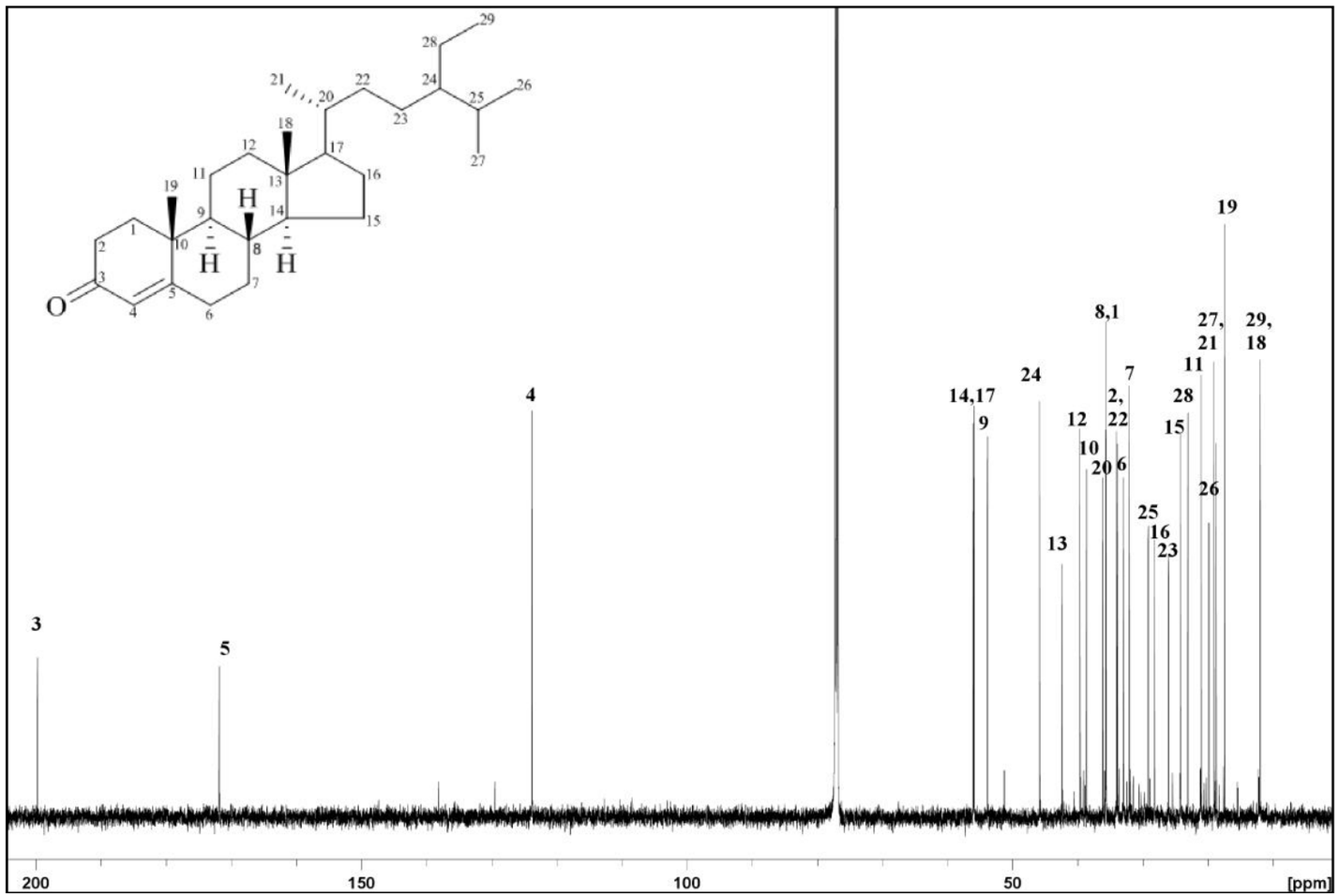

Figure 3.145: ^{13}C NMR Spectrum of stigmast-4-en-3-one **57**

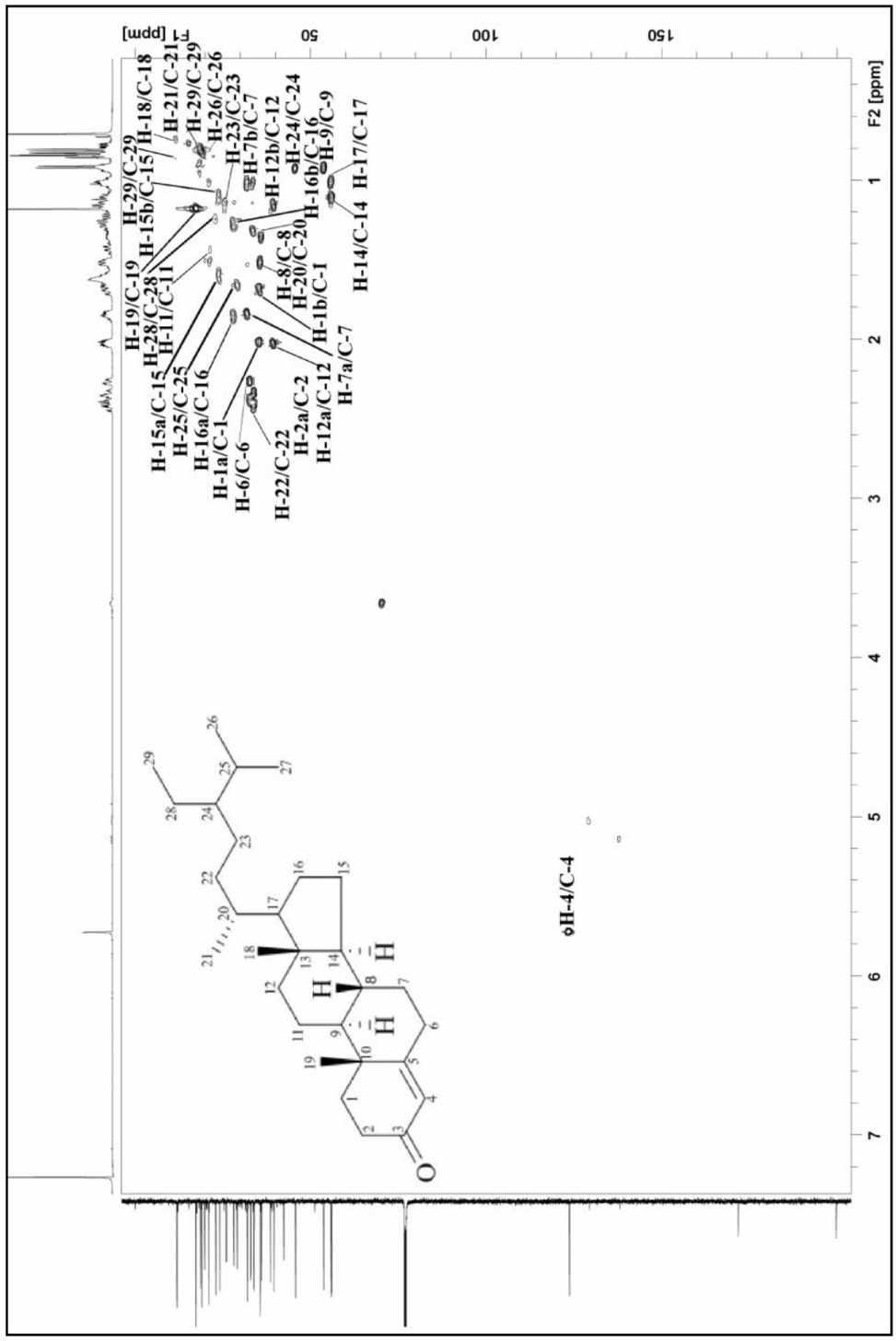

Figure 3.146: HSQC Spectrum of stigmast-4-en-3-one **57**

3.2.21 Vanillin 58

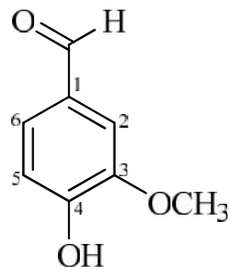

58

Vanillin **58** was isolated as a light brownish amorphous solid. The ESIMS (Figure 3.148) displayed a pseudomolecular ion peak $[M+H]^+$ at *m/z* 153.0555, corresponding to the molecular formula of $C_8H_8O_3$ (calc. 153.0546). In UV spectrum, absorption bands at 308 and 277 nm were observed.[111] The IR spectrum of showed absorption peaks at 3365, 1661 and 1155 cm^{-1} which indicated OH, C=O and C-O stretching vibrations respectively.[112,113]

In ^{1}H-NMR spectrum (Figure 3.149), H-5 resonated as a doublet at δ_H 7.03 (1H, *d*, *J* = 8.7 Hz, H-5) while signals of H-2 and H-6 were seen to be overlapped between δ_H 7.40-7.42 (2H, *m*, overlapped, H-2, H-6). The presence of two singlets at δ_H 9.81 and δ_H 3.95 were attributed to the aldehyde and methoxyl groups respectively. A broad singlet at δ_H 6.28 indicated the presence of a hydroxyl group. In addition, this signal did not correlate to any carbon signal in the HSQC spectrum.

The ^{13}C-NMR and DEPT spectra (Figure 3.150 and Figure 3.151) of vanillin **58** indicated a total of eight carbon signals; one methoxyl, three methines, three quaternary carbons and one carbonyl carbon. Three quaternary carbons at δ_C 129.9, δ_C 147.2 and δ_C 151.8 was attributed to C-1, C-3 and C-4 respectively due to the connectivity of aldehyde, methoxyl and hydroxyl group.

Complete ^{1}H and ^{13}C-NMR assignments (Table 3.22) were established by thorough analysis of COSY, HMBC (Figure 3.148) and HSQC data. From the analysis

of the spectroscopic data obtained and comparison with the literature,[114,115] thus the compound was identified as vanillin **58**.

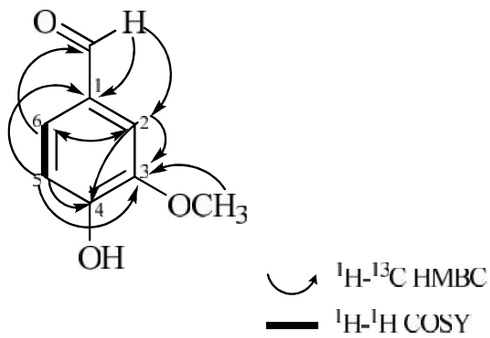

Figure 3.147: COSY and HMBC Correlations of Vanillin **58**

Table 3.22: ^{1}H-NMR (400 MHz) and ^{13}C-NMR (100 MHz) Spectral Data of Vanillin **58** in $CDCl_3$.

Position	**^{1}H**		**^{13}C**	
	δ_H (multiplicity, *J* in Hz)		**δ_C**	
	Experimental ($CDCl_3$)	**Reference* ($CDCl_3$)**	**Experimental ($CDCl_3$)**	**Reference* ($CDCl_3$)**
1	-	-	129.9	129.5
2	7.40-7.42 (*m*, overlapped)	7.42 (*d*, 2.0)	108.8	109.4
3	-	-	147.2	147.5
4	-	-	151.8	152.3
5	7.03 (*d*, 8.7)	7.04 (*d*, 8.0)	114.5	114.8
6	7.40-7.42 (*m*, overlapped)	7.43 (*dd*, 8.0, 2.0)	127.7	127.4
CHO	9.81 (*s*)	9.83 (*s*)	191.0	191.3
OMe	3.95 (*s*)	3.96 (*s*)	56.2	56.0
OH	6.28 (*br s*)	6.38 (*s*)	-	-

*Literature value from Xuan et al. (2005) and Pelter et al. (1976).

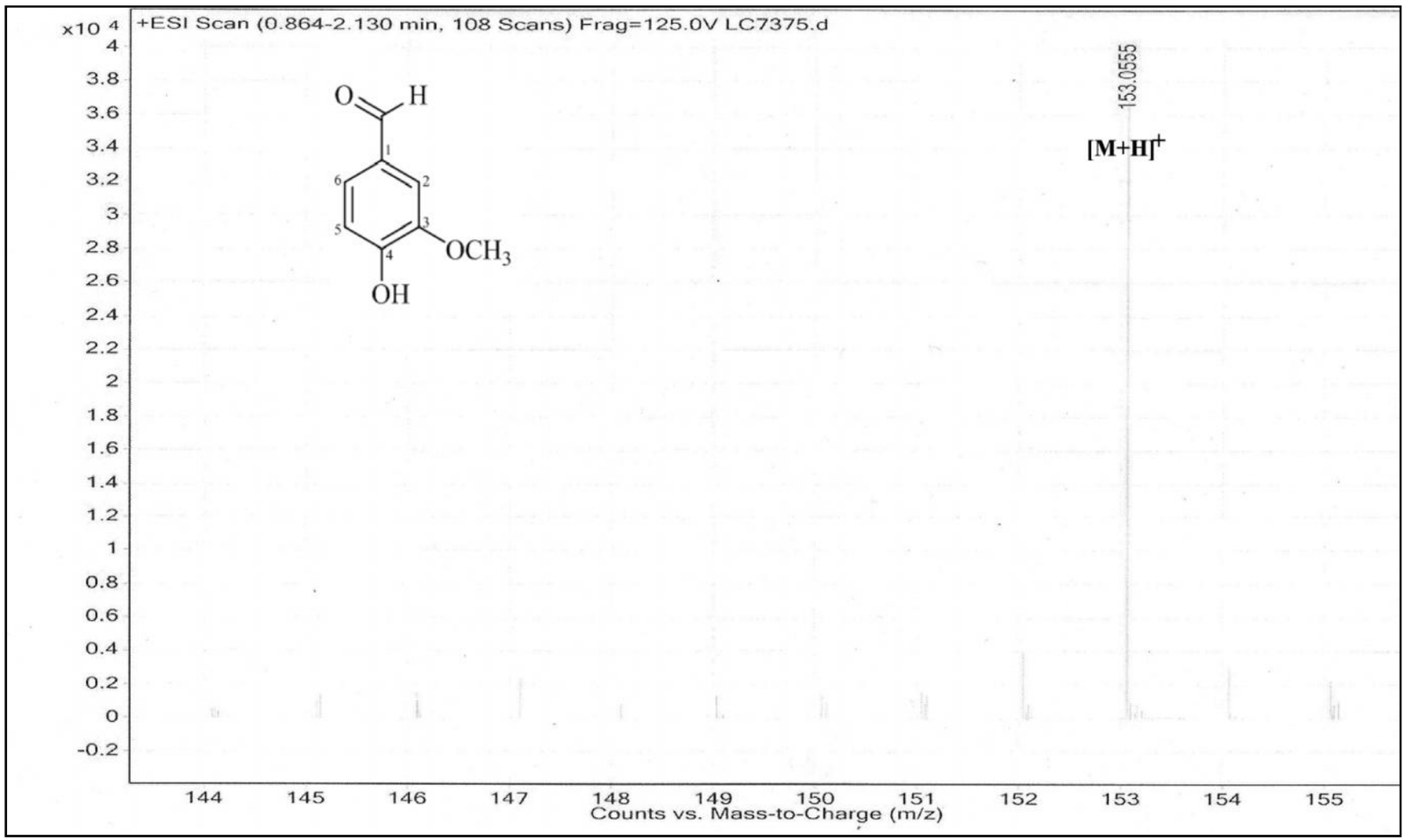

Figure 3.148: LCMS Spectrum of Vanillin **58**

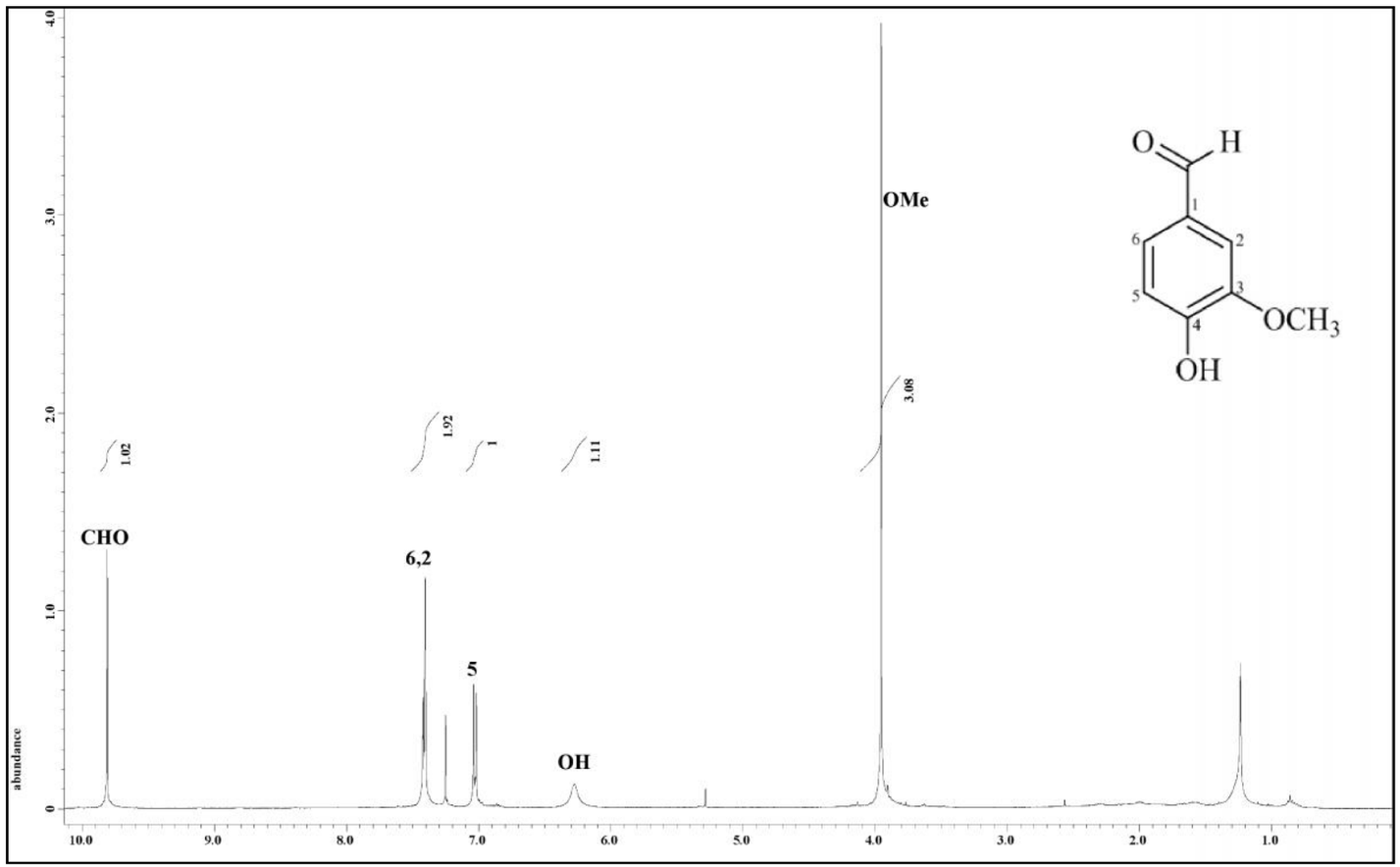

Figure 3.149: ^{1}H NMR Spectrum of Vanillin **58**

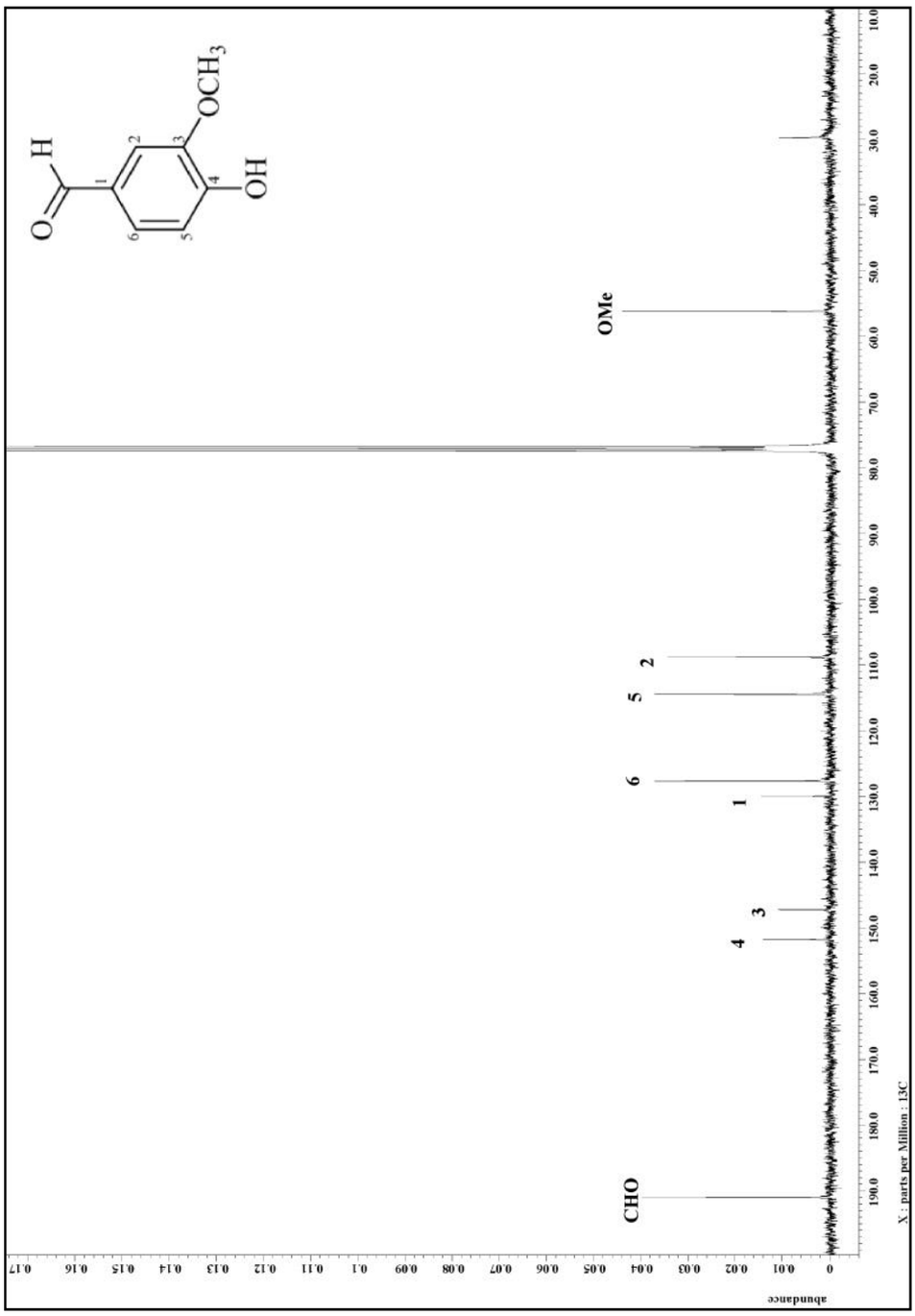

Figure 3.150: ^{13}C NMR Spectrum of Vanillin **58**

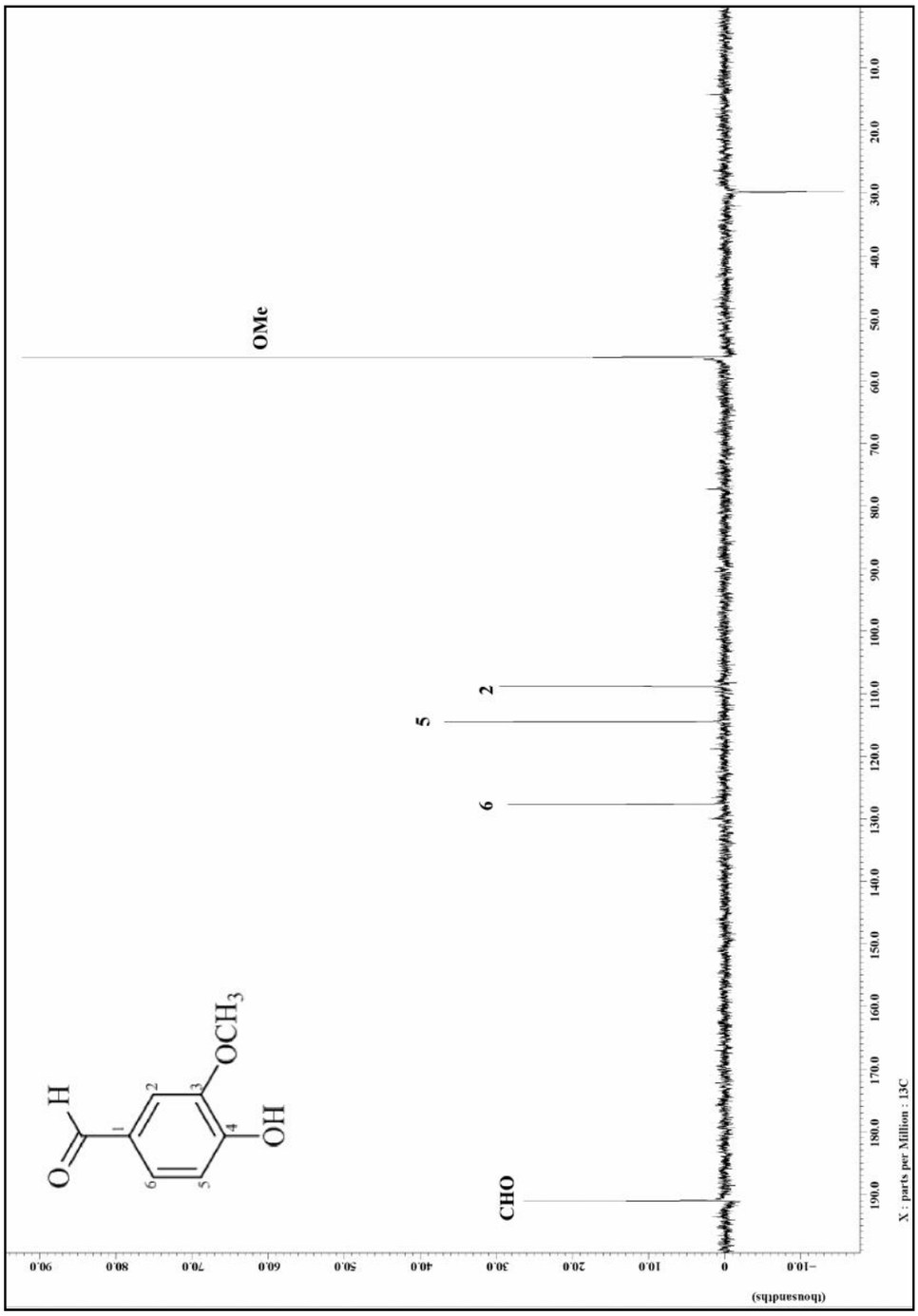

Figure 3.151: DEPT 135 Spectrum of Vanillin **58**

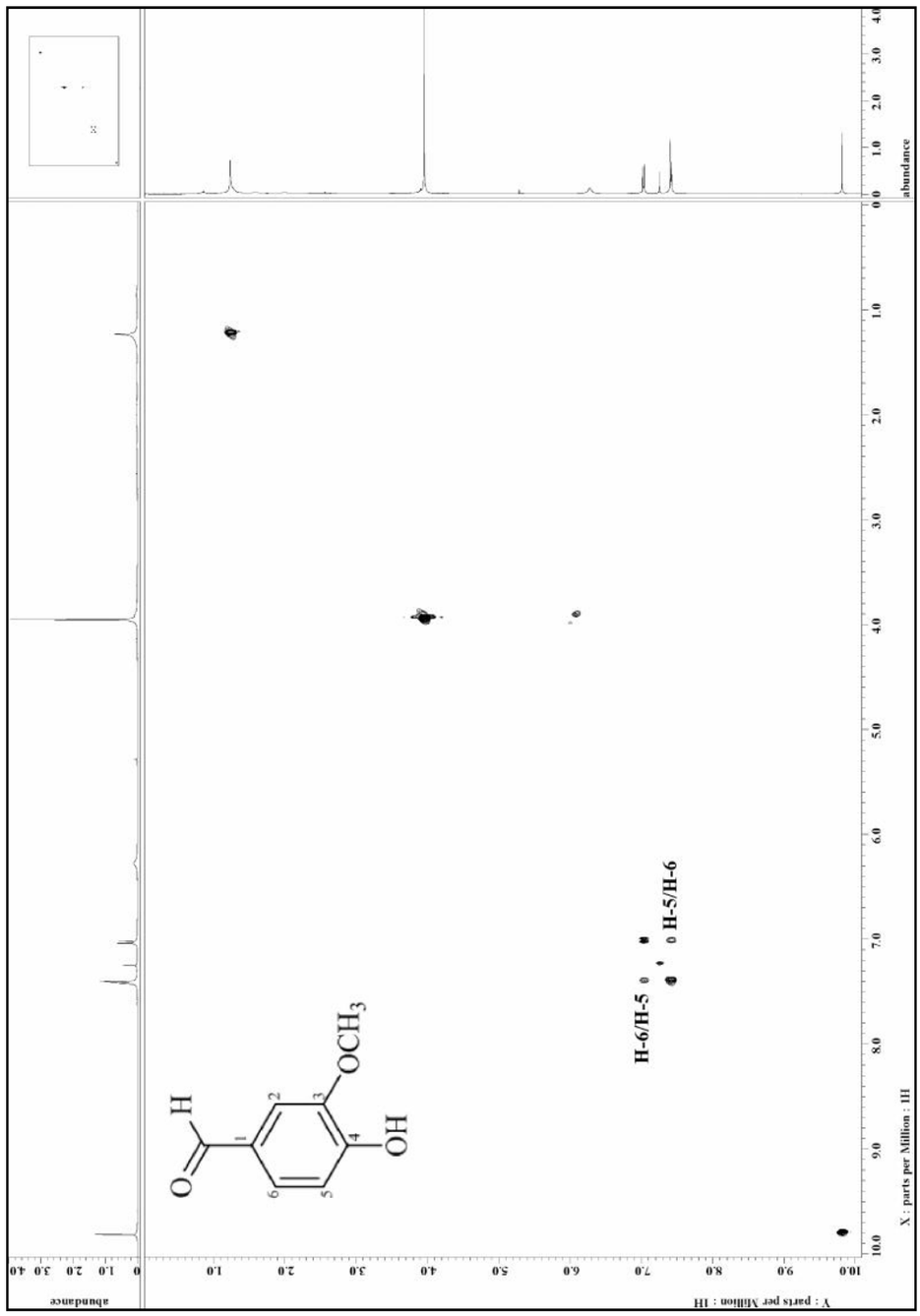

Figure 3.152: COSY Spectrum of Vanillin **58**

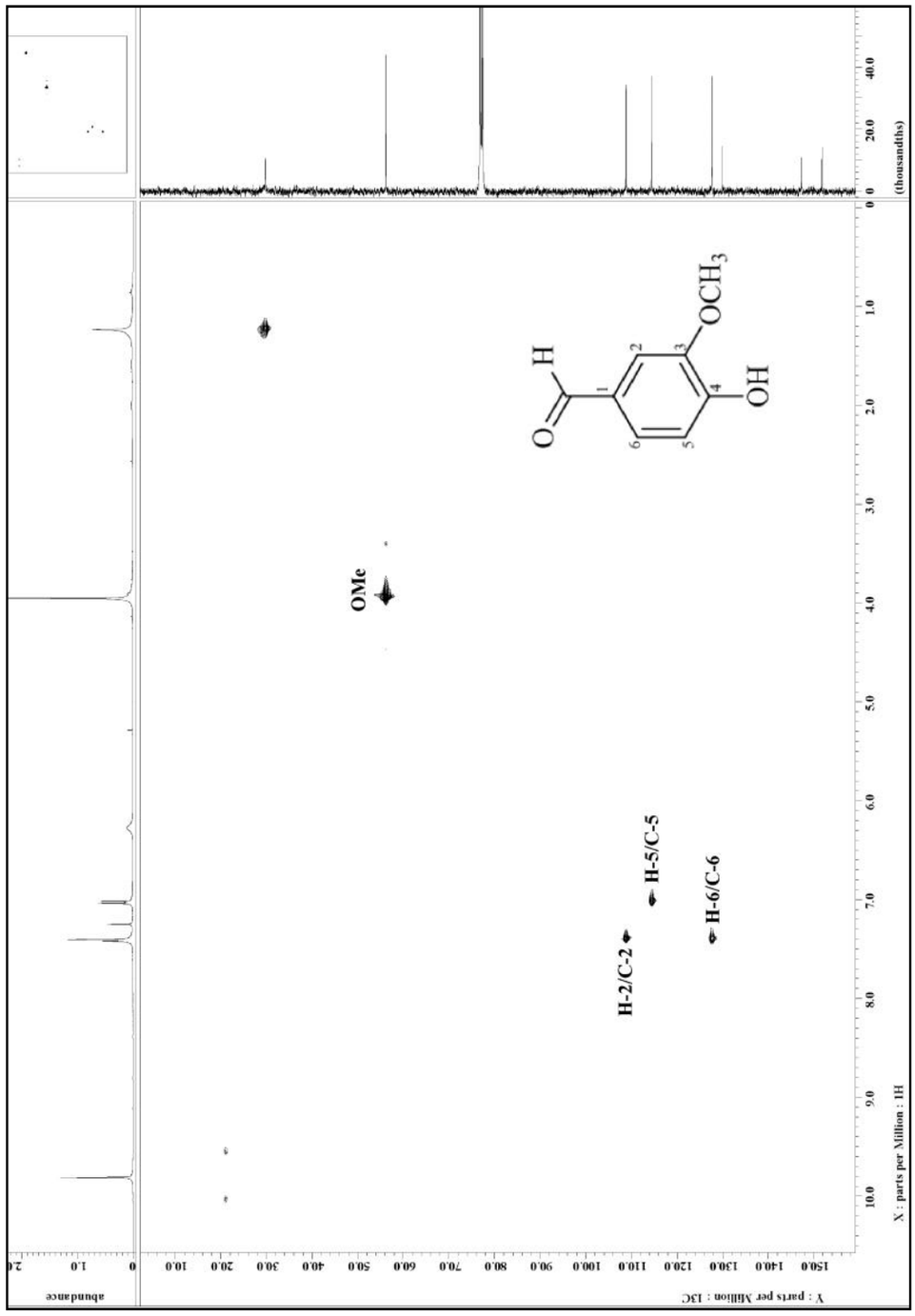

Figure 3.153: HSQC Spectrum of Vanillin **58**

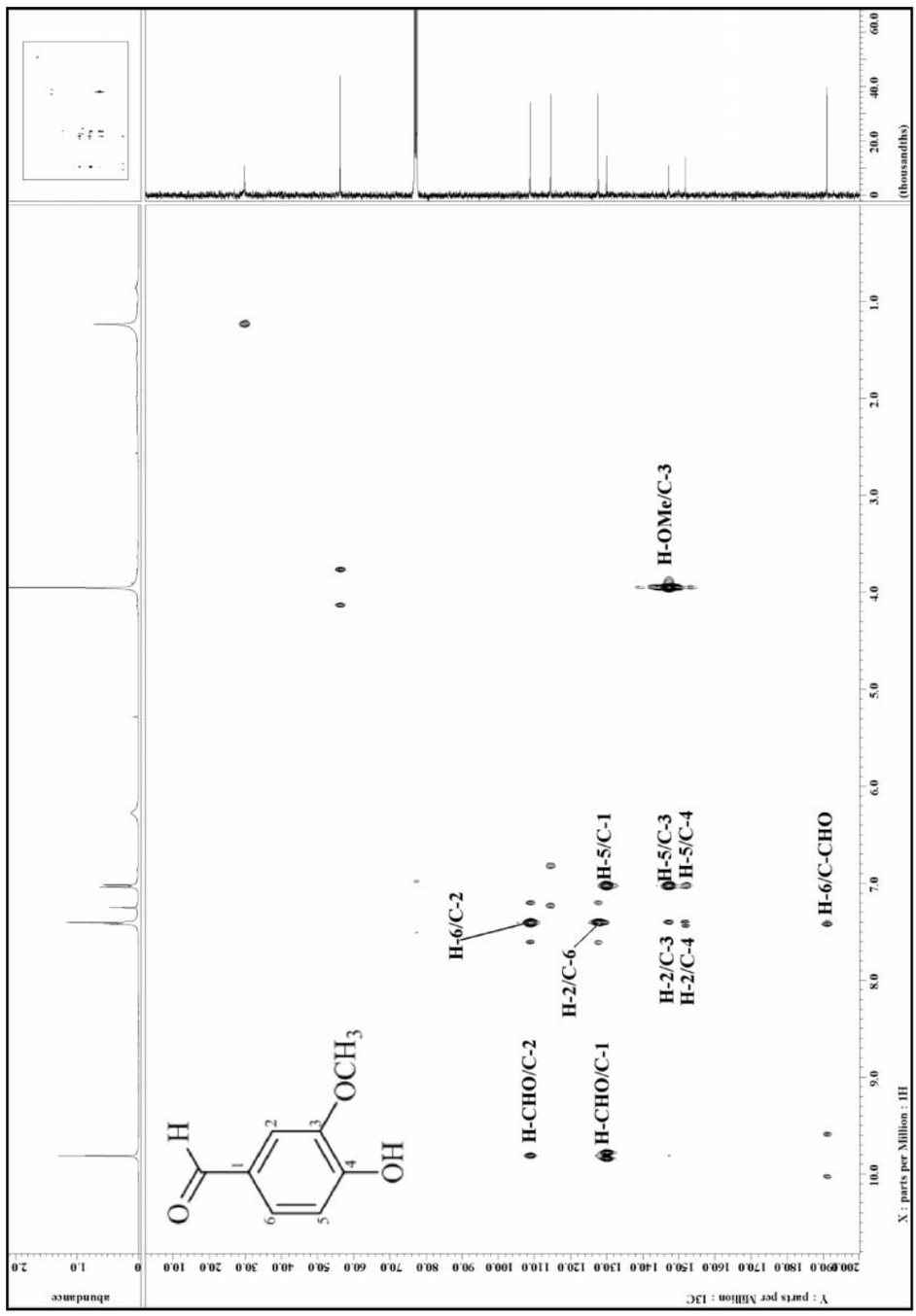

Figure 3.154: HMBC Spectrum of Vanillin **58**

4.1 General

Corynanthe type of indole alkaloids are known to possess anti-proliferative, cytotoxic and anti-cholinesterase activities. Angustine **42** and 10-hydroxyangustine **6** which isolated from *Nauclea orientalis* exhibited good anti-proliferative activity against both T-24 and EGF dependent MK cells.[15] Besides, Sichaem et al. (2012) reported that naucleficine **64** and naucleidinal showed significant cytotoxic activity against both HeLa and KB cell lines.[116] In addition, angustine **42** also exhibited good anti-cholinesterase activity where it has been shown to be potent inhibitor toward BChE.[117]

4.2 Cytotoxic activity

Prostate cancer is the most frequently diagnosed cancer among men in the developed world. An estimated 238,590 new cases will be diagnosed and 29,720 deaths will result from prostate cancer in the United States in 2013 (Cancer Facts and Figures 2013, American Cancer Society, 2013). Although the mechanisms that drive prostate cancer have not been completely understood, age, race, and family history of the prostate cancer patients have been shown to be potential factors closely associated with this terminal disease.[118]

4.2.1 Cell culture

Human prostate normal cell line (RWPE-1) and human prostate cancer cell lines; LNCaP and PC-3, were purchased from the American Type Culture Collection (ATCC, Manassas, Virginia, USA). LNCaP and PC-3 cells were grown in *Roswell Park Memorial Institute medium (RPMI)* supplemented with 10% heat-inactivated fetal bovine serum (FBS, Sigma-Aldrich, St. Louis, MO), 1% penicillin and streptomycin. RWPE-1 cells were maintained in Keratinocyte Serum Free Medium (K-SFM, ATCC) supplemented with bovine pituitary extract (BPE) and human recombinant epidermal

growth factor (EGF). Mediums were supplemented with 10% heat-inactivated fetal calf serum (Sigma.), 100 U/mL penicillin and 100 mg/ml streptomycin (Flowlab, Sydney, Australia). All cells were maintained in a humidified atmosphere of 5% CO_2 in air at 37°C incubator.

4.2.2 Cell proliferation assay

The anti-proliferative activity of the compounds was evaluated by performing MTT assays as previously described with minor modifications.[119] Briefly, cells were seeded 24 hours prior to treatment in a 96-well plate at 5×10^4 cells/well in order to obtain 70% to 80% confluent cultures. The compounds were dissolved in DMSO (Sigma Chemical Co., St. Louis, Missouri, USA) followed by a 2× serial dilution for 10 points ranged from 0.825 µM to 100 µM. The 96-well plate was incubated for 24 hours at 37°C in a humidified atmosphere with 5% CO_2. At the end of incubation, 50 µl of MTT solution (2 mg/mL; Sigma) was added to each well. The plate was then incubated for 4 hours. All medium was removed and the purple formazan crystal formed at the bottom of the wells was dissolved with 200 µl DMSO for 20 minutes. The absorbance at 570 nm was read on a spectrophotometric plate reader (Hidex). The proportion of surviving cells was calculated as:

(OD of drug-treated sample – OD of blank)/(OD of control – OD of blank) × 100%.

Dose-response curves were constructed to obtain the IC_{50} values. Experimental data were derived from 3 independent experiments. The selectivity index was obtained by mean IC_{50} RWPE-1 / mean IC_{50} of LNCaP or PC-3.

4.2.3 Results and discussion

The cytotoxic effect of dichloromethane crude, subditine **72**, angustoline **43**, angustidine **44**, angustine **42** and nauclefine **63** were evaluated on human prostate

cancer cells LNCaP and PC-3 by MTT assays. IC_{50} values (dose required to inhibit the proliferative response by 50%) for each compound was shown in Table 4.1. Subditine **72** showed great inhibitory effect towards LNCaP cells at IC_{50} 12.24 ± 0.19 μM while IC_{50} for angustoline **43**, angustidine **44**, angustine **42** and nauclefine **63** were 58.09 ± 0.05 μM, 140.27 ± 0.10 μM, 149.16 ± 0.09 μM and 86.35 ± 0.09 μM respectively. Similar findings were obtained on PC-3 cells, where subditine **72** exhibited the highest activity (IC_{50} = 13.97 ± 0.32 μM) compared to the other compounds. These findings indicate that subditine **72** is the most potent cytotoxic compound among the five tested.

Subsequently, the cytotoxicity effect of subditine **72** was tested on on RWPE-1 (human normal prostate epithelial cells). MTT assay showed a higher IC_{50} value at 30.48 ± 0.08 μM, indicating that subditine **72** is 2.5 and 2.2 folds more potent against LNCaP and PC-3 (selectivity index (SI): [LNCaP/PC-3] = 2.49/2.18) prostate cancer cells than the normal prostate cells; RWPE-1. In contrast, standard anti-cancer drug paclitaxel showed less selectivity (SI: [LNCaP/PC-3] = 1.24/1.19) by exhibiting IC_{50} values of 1.27 ± 0.04 μM, 1.33 ± 0.02 μM and 1.58 ± 0.06 μM against LNCaP, PC-3 and RWPE-1 respectively.

Table 4.1: Subditine **72**, angustoline **43**, angustidine **44**, angustine **42** and nauclefine **63** and standard drug paclitaxel screening on LNCaP and PC-3 human prostate cancer and RWPE human normal prostate epithelial cell-lines using MTT assays. 24 hours post treatment, MTT salt was dissolved with DMSO and the absorbance was measured with Hidex microplate reader at 570 nm.

Compounds	IC_{50} values at 24 hours (μM)		
	LNCaP	PC-3	RWPE-1
Subditine **72**	12.24 ± 0.19	13.97 ± 0.32	30.48 ± 0.08
Angustoline **43**	58.09 ± 0.05	67.31 ± 0.87	65.94 ± 0.04
Angustidine **44**	140.27 ± 0.10	84.91 ± 1.48	36.07 ± 0.05
Angustine **42**	149.16 ± 0.09	121.59 ± 3.73	98.39 ± 0.10
Nauclefine **63**	86.35 ± 0.09	92.07 ± 1.28	72.85 ± 0.06
Paclitaxel (Reference drug)	1.27 ± 0.04	1.33 ± 0.02	1.58 ± 0.06

4.3 Cholinesterase inhibition assay

Alzheimer's disease (AD) is a neurodegenerative disease characterized by neuronal loss in the brain region involved in cognitive functions.[120] Based on the cholinergic hypothesis, the neuronal loss eventually results in low levels of acetylcholine (ACh) neurotransmitter in the affected region of the brain leading to impaired cholinergic neurotransmission and clinical symptoms of AD. Cholinesterases, namely the acetylcholinesterase (AChE) and butyrylcholinesterase (BChE) are the enzymes that catalyze the hydrolysis of acetylcholine, an essential process in cholinergic neurotransmission.[121] Therefore the enhancement of ACh level using cholinesterase inhibitors (ChEIs) is one of the approaches to treat AD. AChE inhibitors such as donepezil, rivastigmine and galanthamine are currently still the best available pharmacotherapy for AD patients, producing symptomatic improvements in mild to

moderate AD patients.[122] The recent development of inhibitors includes drugs with high selectivity for BChE, which also showed enhancement of ACh levels in rats brain, without triggering severe peripheral or central cholinergic adverse effects.[123,124]

Despite the long history of AD, there are very few ChEIs available for the treatment of AD. Natural products especially the plant-based alkaloids, have been viewed as promising drug candidates and had contributed significantly in drug discovery and development of ChEIs for AD. For example, ChEIs inhibitors, including those used clinically such as galanthamine, huperzine A and physostigmine are alkaloids isolated from plants; *Galanthus* spp., *Huperzia serrata* and *Physostigma venenosum*, respectively.[125]

4.3.1 Chemicals and enzymes

Acetylcholinesterase from electric eel, 5,5′-dithiobis(2-nitrobenzoic acid), acetylthiocholine iodide (ATCI), butyrylcholine esterase from equine serum, S-butyrylthiocholine chloride and galanthamine hydrobromide were purchased from Sigma (St Louis, MO). Sodium dihydrogen phosphate anhydrous was purchased from R&M Chemicals (Essex, UK) while disodium hydrogen phosphate anhydrous was purchased from Merck (Darmstadt, Germany). All the other solvents and reagents used were of analytical grade.

4.3.2 In vitro cholinesterase inhibitory assay

Cholinesterase inhibitory activity of the extracts and isolated compounds was evaluated following Ellman's microplate assay as described by Ahmed and Gilani (2009).[126] Briefly, for AChE inhibitory assay, 140 µL of 0.1 M sodium phosphate buffer (pH 8) was first added to each well of a 96-well microplate followed by 20 µL of the

test sample; naucletine **61**, angustidine **44**, nauclefine **63**, angustine **42**, naucline **56**, angustoline **43**, harmane **67**, 3,14-dihydroangustoline **68**, strictosamide **70** and pumiloside **69** (in 10 % methanol) and 20 µL of 0.09 unit/ml AChE. After 15 minutes of pre-incubation at 25 °C, 10 µL of 10 mM 5,5′-dithiobis(2-nitrobenzoic acid) was added into each well followed by 10 µL of 14 mM acetylthiocholine iodide (ATCI). The absorbance of the colored end-product was measured at 412 nm at designated intervals for 30 minutes after the initiation of enzymatic reaction by Tecan Infinite 200 ProMicroplate Spectrometer (Switzerland). For BChE inhibitory assay, the same procedure was followed except that the enzyme and substrate used were BChE from the equine serum and S-butyrylthiocholine chloride respectively. Galanthamine was used as the reference standard. Each sample test was conducted in triplicate. Absorbance of the test sample was corrected by subtracting the absorbance of its respective blank. A set of five concentrations was used to estimate the 50 % inhibitory concentration (IC_{50}) for the active compounds.

4.3.3 Molecular docking

Molecular docking of angustidine **44** and nauclefine **63** were performed using Autodock 3.0.5 along with AutoDockTools (ADT).[127] The compounds were built by sing Hyperchem 8 and energy minimization was performed with a convergence criterion of 0.05 kcal/(molA). Crystal structures of AChE from *Torpedo californica* in complex with galanthamine and BChE from *Homo sapiens* were obtained from Protein Data Bank with PDB ID: 1W6R[128] and PDB ID: 2WIJ[129], respectively. Both proteins were edited using ADT to remove all water molecules and hydrogen atoms were added. Non-polar hydrogens and lone pairs were then merged and each atom was assigned with Gasteiger partial charges. A grid box of 60 × 60 × 60 points, with a spacing of 0.375 Å was positioned at the center of active site gorge. One hundred independent dockings

were carried out for each docking experiment. The lowest docked energy of each conformation in the most populated cluster was selected. Analysis and visualization of the docking results were done using VMD[130] and Acceryls Discovery Studio 2.5 (Accelrys Inc., San Diego, CA, USA).

4.3.4 BChE kinetic study

Kinetic studies of BChE inhibition was determined by constructing Lineweaver-Burk (LB) plots; reciprocal plots of 1/V versus 1/[S] at different concentrations of substrate S-butyrylthiocholine chloride (1.75 mM to 14.0 mM) in the absence and presence of two different concentrations of inhibitors (33.2 and 66.4 µM). The *Ki* value was estimated from the replots of the slope of the individual LB plots versus the inhibitor concentrations.

4.3.5 Results and Discussion

Results and discussion for anti-cholinesterase activity were divided into three parts; cholinesterase inhibition studies, molecular docking of angustidine **44** and nauclefine **63** and BChE kinetic study of angustidine **44**.

4.3.5.1 Cholinesterase inhibition studies

The CH_2Cl_2 (bark) and MeOH (leaves) extract from *Nauclea officinalis* showed moderate BChE inhibition; IC_{50} values of 97.33 ± 5.07 µg/mL and 132 ± 12.7 µg/mL respectively. Therefore, the phytochemicals from both extracts were isolated and then tested for both BChE and AChE. The determination of cholinesterase inhibitory activity on AChE and BChE were evaluated according to colorimetric Ellman's method[131]. Table 4.2 summarizes the cholinesterase inhibitory activity of the extracts, while Table 4.3 summarizes the IC_{50} and selectivity indices of the isolated alkaloids and the standard,

galanthamine. Naucletine **61**, angustidine **44**, nauclefine **63**, angustine **42**, naucline **56** and angustoline **43** were obtained from bark of CH_2Cl_2 extract while harmane **67** and 3,14-dihydroangustoline **68** were isolated from leaves of CH_2Cl_2 extract. Strictosamide **70** and pumiloside **69** were obtained from the leaves of MeOH extract. All the indole alkaloids except pumiloside **69** displayed strong to weak BChE inhibitory effect with the IC_{50} values in the range of 1.02-168.55 µM while three compounds (angustidine **44**, angustoline **43** and pumiloside **69**) showed moderate to weak AChE inhibition with IC_{50} values in the range of 21.71-261.89 µM. It is interesting to note that five compounds; harmane **67**, angustidine **44**, angustine **42**, nauclefine **63** and angustoline **43** were more potent BChE inhibitors than galanthamine. Angustidine **44** was found to be the most potent inhibitor of both AChE and BChE among the isolated alkaloids with higher selectivity toward BChE (selectivity index = 21.09).

Table 4.2: Cholinesterase inhibitory activities of *N. officinalis* extracts

Extracts	AChE		BChE	
	% inhibition at 200 µg/mL	IC_{50} (µg/mL)	% inhibition at 200 µg/mL	IC_{50} (µg/mL)
CH_2Cl_2 (Bark)	0.55	ND	82.51	97.33 ± 5.07
MeOH (Bark)	28.55	ND	NA	ND
CH_2Cl_2 (Leaves)	NA	ND	5.44	ND
MeOH (Leaves)	11.67	ND	54.13	132 ± 12.7

ND = not determined

NA= no activity

Table 4.3: Cholinesterase inhibitory activities of alkaloids from *N. officinalis*

Compounds	% inhibition at 100 µg/ml		IC_{50}				Selectivity	
	AChE	BChE	AChE		BChE		AChE[a]	BChE[b]
			µg/mL	µM	µg/mL	µM		
Naucletine **61**	34.19 ± 7.06	62.02 ± 1.37	ND	ND	20.78 ± 3.06	63.14	-	-
Angustidine **44**	82.62 ± 2.35	95.88 ± 0.50	6.54 ± 0.37	21.72	0.31 ± 0.07	1.03	0.05	21.09
Nauclefine **63**	34.61 ± 4.84	75.31 ± 16.61	ND	ND	2.21 ± 0.03	7.70	-	-
Angustine **42**	40.19 ± 0.65	83.97 ± 1.35	ND	ND	1.56 ± 0.05	4.98	-	-
Naucline **56**	35.27 ± 4.74	82.47 ± 1.10	ND	ND	12.17 ± 2.23	38.25	-	-
Angustoline **43**	77.53 ± 4.40	82.5 ± 0.67	86.72 ± 5.41	261.89	8.31 ± 1.25	25.10	0.10	10.43
Harmane **67**	58.42 ± 4.98	96.72 ± 1.53	54.75 ± 0.88	300.68	2.4 ± 0.13	13.18	0.04	22.81
3,14-dihydroangustoline **68**	38.55 ± 5.94	72.82 ± 1.60	ND	ND	16.58 ± 1.35	49.77	-	-
Strictosamide **70**	34.76 ± 3.27	56.01 ± 0.93	ND	ND	83.97 ± 0.61	168.54	-	-
Pumiloside **69**	54.96 ± 12.15	17.38 ± 5.47	60.62 ± 4.98	118.36	ND	ND	-	-
Galanthamine (standard)	-	-	0.27 ± 0.07	0.94	8.12 ± 0.61	28.29	30.10	0.03

Data presented as Mean ± SD (n=3)
ND = not determined

[a] Selectivity for AChE is defined as IC_{50}(BChE)/IC_{50}(AChE)
[b] Selectivity for BChE is defined as IC_{50}(AChE)/IC_{50}(BChE)

There are few studies reporting on the cholinesterase inhibitory activity of alkaloids, for instance Torres et al. (2012) reported similar results for harmane **67** with IC_{50} values of 330 and 90 μM against AChE and BChE respectively.[132] In contrast, Zhao et al. (2013) reported that harmane **67** had better AChE inhibitory activity than on BChE, with IC_{50} values of 7.11 and 76.91 μM respectively.[133] The difference may be due to the fact that Torres et al. (2012) used the same concentration of both AChE and BChE while Zhao et al. (2013) used a higher concentration for AChE than BChE (0.087 unit/mL for AChE and 0.035 unit/mL for BChE). In the present study, the author has used the same concentration for both enzymes (0.09 unit/mL) and the results obtained agreed with the finding of Torres et al. (2012).

Passos et al. (2013) reported the inhibitory activity of angustine **42** and strictosamide **70**.[117] The former showed good inhibitory activity against BChE with IC_{50} of 3.47 μM, while the latter showed a weak activity with IC_{50} of more than 100 μM. Both compounds showed poor AChE inhibitory activity with IC_{50} of more than 100 μM.

On the selectivity, it is interesting to note that all the alkaloids except pumiloside **69** were selective inhibitor of BChE, unlike galanthamine that was an AChE selective inhibiting alkaloid. Despite being 23 times less potent than galanthamine against AChE, on a molar basis comparison, angustidine **44** was 28 times more potent inhibitor of BChE than galanthamine. AChE is of prime importance as compared to BChE, but both enzymes complements one another for their role in cholinergic neurotransmission. From some recent studies, it was postulated that progressive decline in activity of AChE in certain brain regions during the progression of AD, is replaced by progressive increase in BChE activity, which may act as a compensatory mechanism for ACh hydrolysis[134]. Owing to the growing importance of BChE, an agent that inhibits BChE would be beneficial especially during the later stages of AD. In addition, a BChE selective inhibitor would be expected to cause less peripheral cholinergic adverse effects.

In a review on cholinesterase from medicinal plants, alkaloids in general were reported to have IC_{50} values in the range of $6x10^{-4}$ μM up to more than 2000 μM. A closer look reveals that indole and lycopodane-type alkaloids are weak inhibitor of AChE, while isoquinoline, quinazoline, quinolizidine, triterpenoidal and steroidal alkaloids are good to moderate AChE inhibitors. On the other hand, some triterpenoidal alkaloid, in particular buxakashmiramine (IC_{50} 0.74 μM) showed good to potent BChE inhibitory activity. Likewise, isoquinoline and steroidal alkaloids are good to moderate BChE inhibitors, but lycopodane-type alkaloids lack BChE inhibitory activity[135]. The indole alkaloids isolated in the present study showed comparable inhibitory activity with previously reported alkaloids, however these alkaloids were more BChE selective. This is the first report on the BChE inhibition potential of of naucletine **61**, nauclefine **63**, naucline **56**, angustoline **43**, 3,14-dihydroangustoline **68** and angustidine **44**, which exhibited the most potent activity.

*4.3.5.2 Molecular docking of angustidine **44** and nauclefine **63***

The BChE inhibition studies have shown that angustidine **44** revealed the most potent activity followed by angustine **42** and nauclefine **63**. In order to understand the binding mechanisms of these compounds with cholinesterase enzyme, molecular docking study was performed on both angustidine **44** and nauclefine **63**. The molecular docking of angustine **42** was not performed as it has been reported before[117]. Passos et al. (2013) reported that the binding of angustine **42** with *h*BChE involved hydrophobic interaction of Trp 82, Trp 231, Leu 286 and Phe 329 with its aromatic moieties.[117] The interaction sites, residue involved and bonding types as well as the ligand interacting moiety are summarized in Table 4.4. The findings indicate that angustidine **44** docked deep into the bottom gorge of *h*BChE, forming hydrogen bonds with Ser 198 and His 438 (Figure 4.1). The hydrogen bonds formed with the amino acid residues at the

catalytic site could be responsible for the potency of angustidine **44** as BChE inhibitor. On the other hand, angustidine **37** was well accommodated, forming π-π stacking interaction with Trp84 at choline binding site, which anchored this compound to the *Tc*AChE active site gorge (Figure 4.2). Meanwhile, nauclefine **63** formed hydrogen bond with Gly 116 at the oxyanionic hole and π-π interactions were observed between His 438 of *h*BChE and aromatic ring of nauclefine **63** (Figure 4.3). Since the active site of BChE has many of the channel-lining aromatic residues replaced by residues with aliphatic side chains, it is able to accomodate bulkier compounds compared to AChE. Due to space availability, both angustidine **44** and nauclefine **63** were able to accomodate and docked completely into the base of the active site and held in place by the hydrogen bond. In contrast, Passos et al. (2013) reported that angustine **42** was mainly stabilized by hydrophobic interactions involving its aromatic moieties with Trp 82, Trp 231, Leu 286 and Phe 329 residues of BChE.[117]

Table 4.4: Binding interaction data for bioactive alkaloids from *N. officinalis* docked into active site gorge of AChE and BChE

Compound	Enzyme	Binding Energy (kcal)	Interacting site	Residue	Type of Interaction	Distance (Å)	Ligand Interacting
Angustidine **44**	*Tc*AChE	-11.53	CBS*	Trp 84	Hydrophobic	3.47	Aromatic ring
	*h*BChE	-10.14	CS**	Ser 198	Hydrogen	1.83	C-19
				His 438		2.76	C-19
Nauclefine **63**	*h*BChE	-10.15	CS**	His 438	Hydrophobic	3.44	Aromatic ring
						4.09	Aromatic ring
						5.21	Aromatic ring
			OH***	Gly 116	Hydrogen	2.25	C-18

*Choline binding site
**Catalytic site
*** Oxyanion hole

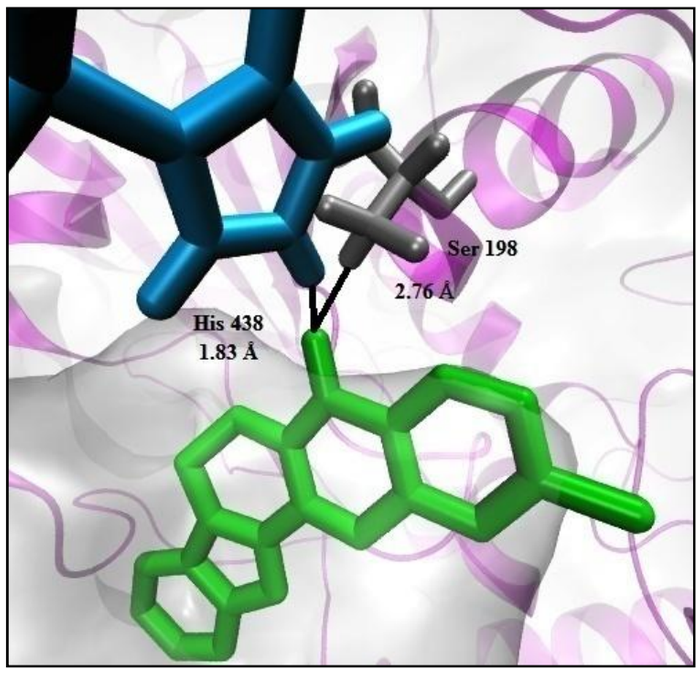

Figure 4.1: Binding interaction of angustidine **44** with active site residue *h*BChE

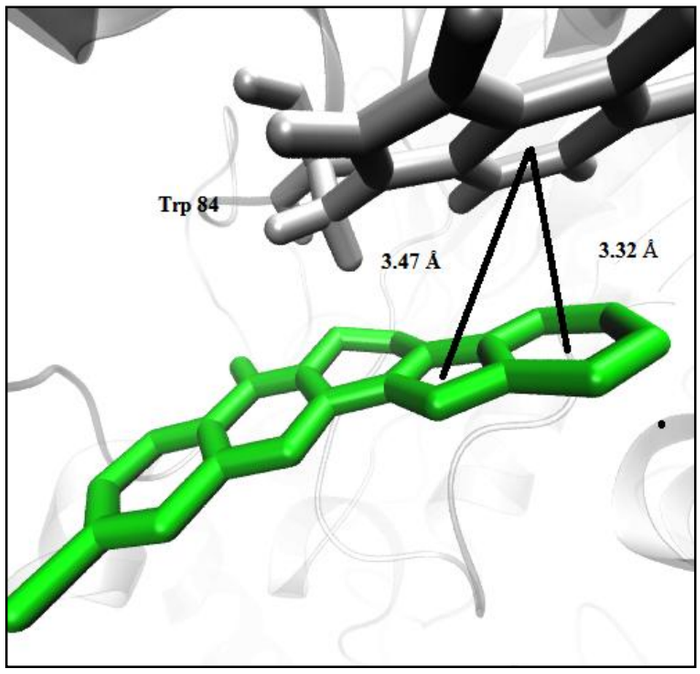

Figure 4.2: Binding interaction of angustidine **44** with active site residues of *Tc*AChE

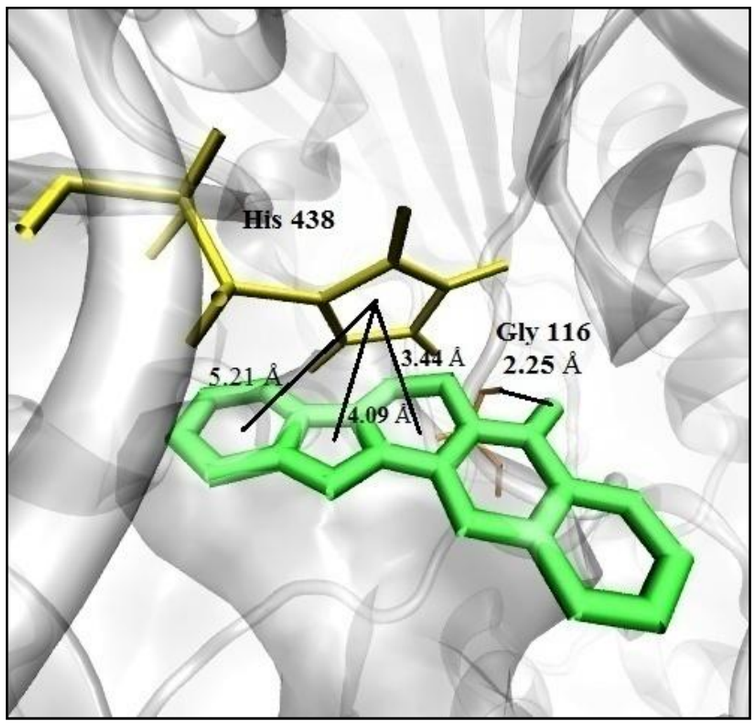

Figure 4.3: Binding interaction of nauclefine **63** with active site residue *h*BChE

*4.3.5.3 BChE kinetic study of angustidine **44***

The mode of inhibition for angustidine **44** on BChE was further investigated to determine their inhibition constant, *Ki* values. The catalytic rates of BChE were measured in the absence of inhibitor and presence of two concentrations of inhibitor; angustidine **44** (33.2 and 66.4 µM) by constructing Lineweaver-Burk (LB) plot over a range of substrate concentrations (1.75 to 14.0 mM) (Figure 4.4). Graphical analysis of LB plot constructed for BChE suggested mixed type inhibition. In addition, *Ki* value of 6.12 µM was obtained by plotting the slope of the individual LB plots versus the inhibitor concentrations (Figure 4.5).

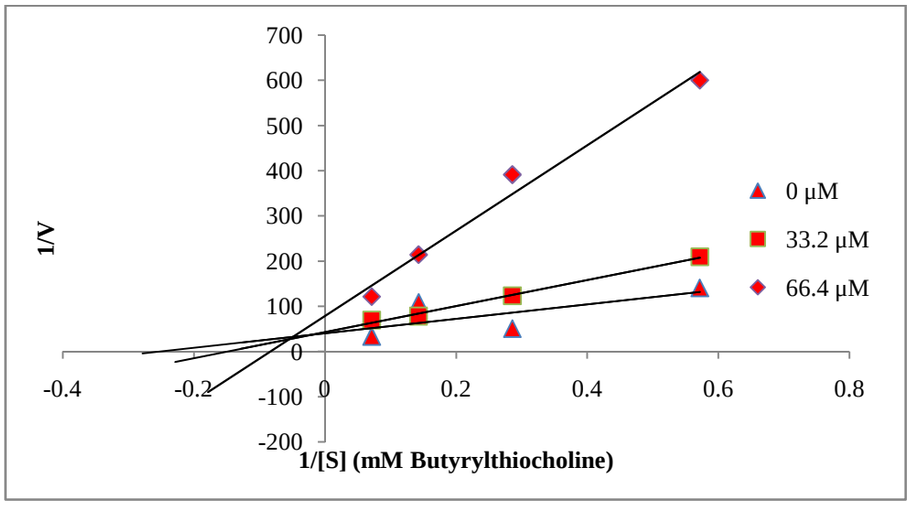

Figure 4.4: Lineweaver-Bulk (LB) plot of BChE activity over a range of substrate concentration (1.75 to 14.0 µM) for angustidine **44**.

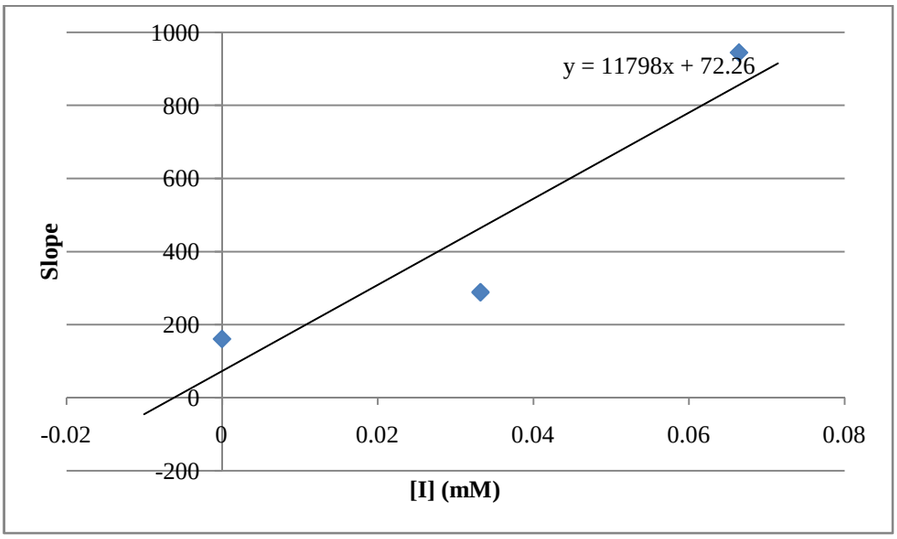

Figure 4.5: The *Ki* value (6.12 µM) for BChE inhibition by angustidine **44** was obtained by plotting the slopes of LB plots versus inhibitor concentrations.

CONCLUSION

Phytochemical study on bark and leaves of two species of Rubiaceae; *Nauclea officinalis* (KL 5655 and KL 4745) and *Nauclea subdita* (KL 5254) were carried out. *Nauclea officinalis* were collected from Hutan Simpan Madek, Keluang, Johor and Hutan Simpan Mersing Johor while *Nauclea subdita* were collected from Hutan Simpan Bukit Kinta, Chemor, Perak.

The chemical investigation of this three plants afforded twenty one compounds including two new indole alkaloids; naucline **56** and subditine **72** along with eleven known indole alkaloids; nauclefine **63**, naucletine **61**, angustine **42**, angustoline **43**, 3,14-dihydroangustoline **68**, angustidine **42**, strictosamide **70**, naucleficine **64**, naucleactonin C **65**, harmane **67** and 1,2,3,4-tetrahydro-1-oxo-β-carboline **60**, one quinoline alkaloid glycoside; pumiloside **69**, two triterpenes; stigmast-4-en-3-one **57** and β-sitosterol **73**, two amides; benzamide **62** and cinnamide **59**, two C13 nor-isoprenoids; blumenol A **66** and blumenol B **71** as well as one benzaldehyde; vanillin **58**. The structure of all these compounds were elucidated with extensive spectroscopic methods namely 1D-NMR (^{1}H, ^{13}C, DEPT), 2D-NMR (COSY, HSQC, HMBC, NOESY) and comparison with reported data.

Subditine **72** showed potent inhibitory effect towards LNCaP cells at IC_{50} 12.24 ± 0.19 μM and PC-3 cells at IC_{50} = 13.97 ± 0.32 μM comparable to standard drug; palitaxel (1.27 ± 0.04 and 1.33 ± 0.22 for LNCaP and PC-3 respectively). Angustoline **43**, angustidine **44**, angustine **42** and nauclefine **63** exhibited moderate to weak inhibitory effect toward both prostate cancer cell lines. Besides, MTT assay showed that subditine **72** exhibited a higher IC_{50} value at 30.48 ± 0.08 μM on RWPE-1 (human normal prostate epithelial cells), indicating that subditine **72** is 2.5 and 2.2 folds more potent against LNCaP and PC-3 (selectivity index (SI): [LNCaP/PC-3] = 2.49/2.18)

prostate cancer cells than the normal prostate cells; RWPE-1. On the other hand, standard drug paclitaxel had less selectivity (SI: [LNCaP/PC-3] = 1.24/1.19) with IC_{50} values of 1.27 ± 0.04 µM, 1.33 ± 0.02 µM and 1.58 ± 0.06 µM against LNCaP, PC-3 and RWPE-1 respectively.

For cholinesterase inhibitory studies, all the indole alkaloids except pumiloside **69** displayed strong to weak BChE inhibitory effect with the IC_{50} values in the range of 1.02 -168.55 µM while angustidine **44**, angustoline **43** and pumiloside **69** showed moderate to weak AChE inhibition with the IC_{50} values in the range of 21.71-261.89 µM. Angustidine **44** was the most active inhibitor of both AChE and BChE with IC_{50} values of 21.72 µM and 1.03 µM, respectively. All the alkaloids except pumiloside **69** were BChE selective inhibitors. Interestingly, five compounds; angustidine **44**, nauclefine **63**, angustine **42**, angustoline **43** and harmane **67** exhibited more potent inhibitory toward BChE than galanthamine. Angustidine **44**, nauclefine **63**, angustine **42**, angustoline **43** and harmane **67** acts at different sites of the cholinesterases, interacting with the choline binding site of AChE and catalytic site of BChE. Angustidine **44** docked deep into the bottom gorge of *h*BChE, forming hydrogen bonding with Ser 198 and His 438. The nature of protein-ligand interactions is mainly hydrophobic with AChE and via hydrogen bonding with BChE. Kinetic study shown that angustidine **44** exhibited mixed type inhibition with estimated *Ki* value of 6.12 µM. Overall, the nine indole alkaloids; naucletine **61**, angustidine **44**, nauclefine **63**, angustine **42**, naucline **56**, angustoline **43**, harmane **67**, 3,14-dihydroangustoline **68**, strictosamide **70** had potent to moderate BChE inhibitory activity and could serve as potential lead compounds for further drug research study of AD agents.

In conclusion, it may be deduced that both plants; *Nauclea officinalis* and *Nauclea subdita* are rich source of indole alkaloids with interesting activity and skeletal features. These compounds could be investigated further for various type of maladies

such as diabetes and inflammation. More extensive studies may also be performed on the active compounds such as subditine **72** and angustidine **44** in moves to develop therapeutic agents for cancer and Alzheimer's disease, respectively.

6.1 Plant Material

The plant materials were collected and identified by the phytochemical group of the Department of Chemistry, Faculty of Science, University of Malaya. They were deposited at the Herbarium of the Department of Chemistry, University of Malaya, Kuala Lumpur, Malaysia. The plant species and their respective localities are shown in Table 6.1 below.

Table 6.1: Plant species and locality

Voucher specimen	Species	Part of plant	Locality and date of collection
KL 5655	*N. officinalis*	Bark and leaves	Hutan Simpan Madek, Keluang, Johor, Malaysia. 22nd April 2009
KL 4745	*N. officinalis*	Bark and leaves	Hutan Simpan Mersing, Johor, Malaysia. 22nd October 1997
KL 5254	*N. subdita*	Bark and leaves	Hutan Simpan Bukit Kinta, Chemor, Perak, Malaysia. 20nd June 2006

6.2 Solvent

All solvents were of AR grade. Those used for bulk extraction were distilled prior to use. The solvents used were hexane, dichloromethane, methanol, ammonia solution, hydrochloric acid.

6.3 Instrumentation

The 1D- and 2D-NMR spectra were recorded either in deuterated chloroform ($CDCl_3$), deuterated methanol (CD_3OD), deuterated pyridine (C_5D_5N) and deuterated *N*,*N*-Dimethyl formamide (DMF-d_7) using the JEOL LA 400 FT NMR, JEOL ECA 400 FT NMR, BRUKER Advance III 400 NMR and BRUKER Advance III 600 NMR spectrometers.

The ESIMS and LCMS-IT-TOF spectra were obtained from Agilent Technologies 6530 Accurate-Mass Q-TOF LC/MS and UPLC Shimadzu liquid chromatography with an SPD-M20A diod array detector coupled to an IT-TOF mass spectrometer respectively.

The ultraviolet absorption spectra were recorded using a Shimadzu UV-250 Ultraviolet-Visible Spectrophotometer. Solvent used was spectroscopic grade methanol (CH_3OH).

IR spectra were recorded on a Perkin Elmer Spectrum FTIR Spectrometer RX1 with spectroscopic grade chloroform as the solvent.

A Jasco P-1020 polarimeter was used to record the optical rotation.

6.4 Chromatography

Purification processes were performed using various chromatography techniques such as column chromatoghraphy and preparative thin layer chromatography.

6.4.1 Thin Layer Chromatography (TLC)

Aluminum supported silica gel 60 F_{254} (Merck) were used for Thin Layer Chromatography (TLC). The crude extract, fractions from column chromatography and isolated compounds were examined using TLC. By using a piece of fine glass capillary tube, the TLC plates were spotted and placed in chromatographic tanks saturated with

the developing solvent system. The spots developed on the TLC plates were visualized under a UV Lamp Model UVGL-58 (254 and 365 nm), followed by spraying with Dragendorff"s reagent.

6.4.2 Column Chromatography (CC)

Silica gel 60, 70 - 230 mesh ASTM (0.063 - 0.200 mm) and 230 - 400 mesh ASTM (0.040 - 0.063 mm) (Merck) were used for column chromatography. A slurry of silica gel 60 was prepared and poured into a glass column with a particular dimension. The crude extract was dissolved in minimum amount of solvent and applied on to the top of the column. The extract was loaded to column and eluted from the column with gradient solvent system.

6.4.3 Preparative Thin Layer Chromatography (PTLC)

PTLC silica gel 60 F254 glass plate (20 x 20 cm) were used for isolation of compounds that cannot be achieved by conventional column chromatography. Bands on the PTLC were visualized using a UV Lamp Model UVGL-58.

6.5 Reagents

Reagents used for detection of alkaloid contents were Mayer's reagent and Dragendorff's reagent.

6.5.1 Mayer's Reagent (potassium mercuric iodide)

For Mayer's reagent, 1.4g of mercuric iodide in 60 mL of distilled water was mixed with 5.0 g of potassium iodide in 10 mL of distilled water. The mixture was then made up to a 100 mL solution. A positive test result was indicated by the formation of

white precipitate when the aqueous layer (acidified) is treated with 2 to 3 drops of Mayer's reagent.

6.5.2 Dragendorff's Reagent (potassium bismuth iodide)

Bismuth (III) nitrate (0.85 g) in a mixture of glacial acetic acid (10 mL) and distilled water (40 mL) as solution A. Potassium iodide (8.0 g) in distilled water (200 mL) as solution B. Stock solution was prepared by mixing solution A and solution B in equal volumes. The stock solution (20 mL) was then diluted in a mixture of acetic acid (20 mL) and distilled water (60 mL) to prepare the spray reagent. A positive test result was indicated by the formation of on orange spot.

6.6 Extraction of the bark

First, the respective dried, grounded samples (*N. officinalis* from Madek, *N. officinalis* from Mersing and *N. subdita*) were defatted with hexane (17 L) for three days at room temperature (Scheme 6.1). Then, the hexane extract was filtered and dried on the rotary evaporator. The residues were dried and then later moistened with 28% of ammonia solution (NH_3) and left for 2 hours. They were then re-extracted with dichloromethane (CH_2Cl_2) (17 L) for three days at room temperature and the CH_2Cl_2 extract was dried using a rotarary evaporator to obtain the CH_2Cl_2 crude. Finally, the residues were soaked with methanol (MeOH) (17 L) at room temperature for three day period and the MeOH crude was dried using a rotarary evaporator. The hexane crude was obtained as a yellowish residue while the CH_2Cl_2 and MeOH crudes were each obtained in the form of a dark brown residue.

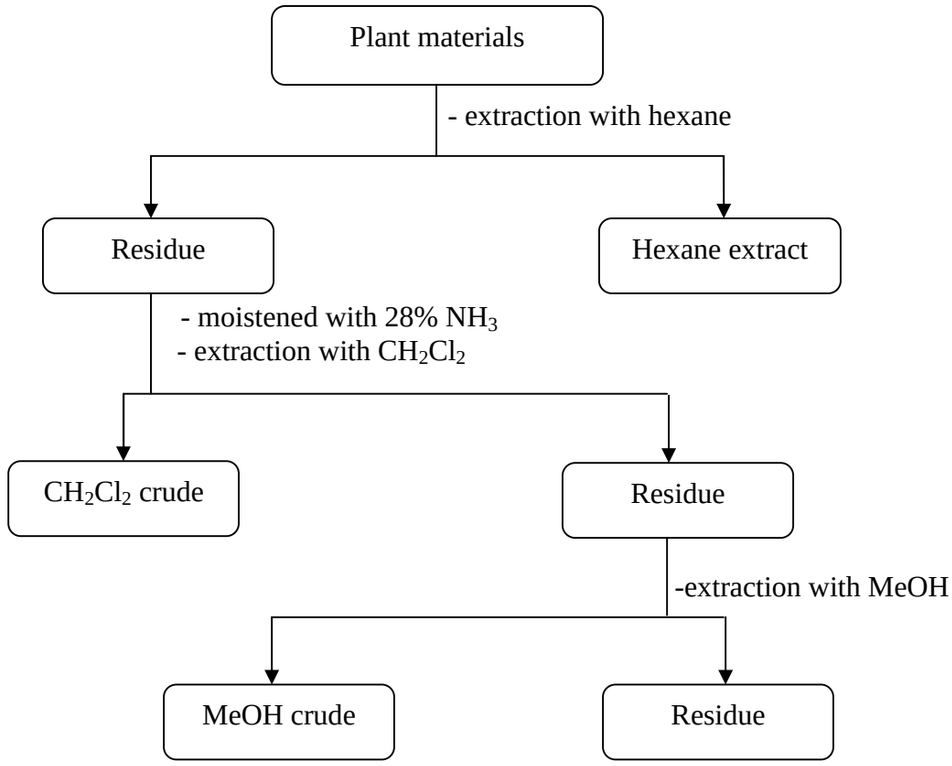

Scheme 6.1: Extraction of bark.

6.7 Extraction of leaves

Extraction procedures for leaves were almost the same as bark but with additional acid-base extraction for CH_2Cl_2 extract (Scheme 6.2). First, the dried plant materials were soaked with hexane (17 L) for three days at room temperature. Then, the hexane crude was obtained by filtration followed by the drying using rotarary evaporator. The residues were dried at room temperature and then moistened with 28% of NH_3 and left for 2 hours. They were then re-extracted with CH_2Cl_2 (17 L) for three days at room temperature to obtained CH_2Cl_2 extract.

Next, the CH_2Cl_2 extract was concentrated under reduced pressure to a volume of approximately 500 mL. The alkaloid content in the extract was tested using TLC and spraying the developed TLC plate with Dragendroff's reagent. The dichloromethane extract was then extracted with 5% of hydrochloric acid and monitered with the

Mayer's reagent test. The hydrochloric acid solution obtained was basified with NH_3 solution to a pH of 11 followed by extraction with CH_2Cl_2 again. The CH_2Cl_2 extract then was washed with distilled water and dried with sodium sulphate anhydrous and finally concentrated under reduced pressure to give the CH_2Cl_2 crude.

The residues were soaked again with MeOH (17 L) for three day period at room temperature to obtain MeOH crude. The hexane crude, CH_2Cl_2 crude and MeOH crude were each obtained in the form of a dark green residue.

The same procedures were applied on all the leaves for the three plants. The amount of the plant materials used for extraction and the yield for all the crudes are listed in Table 6.2.

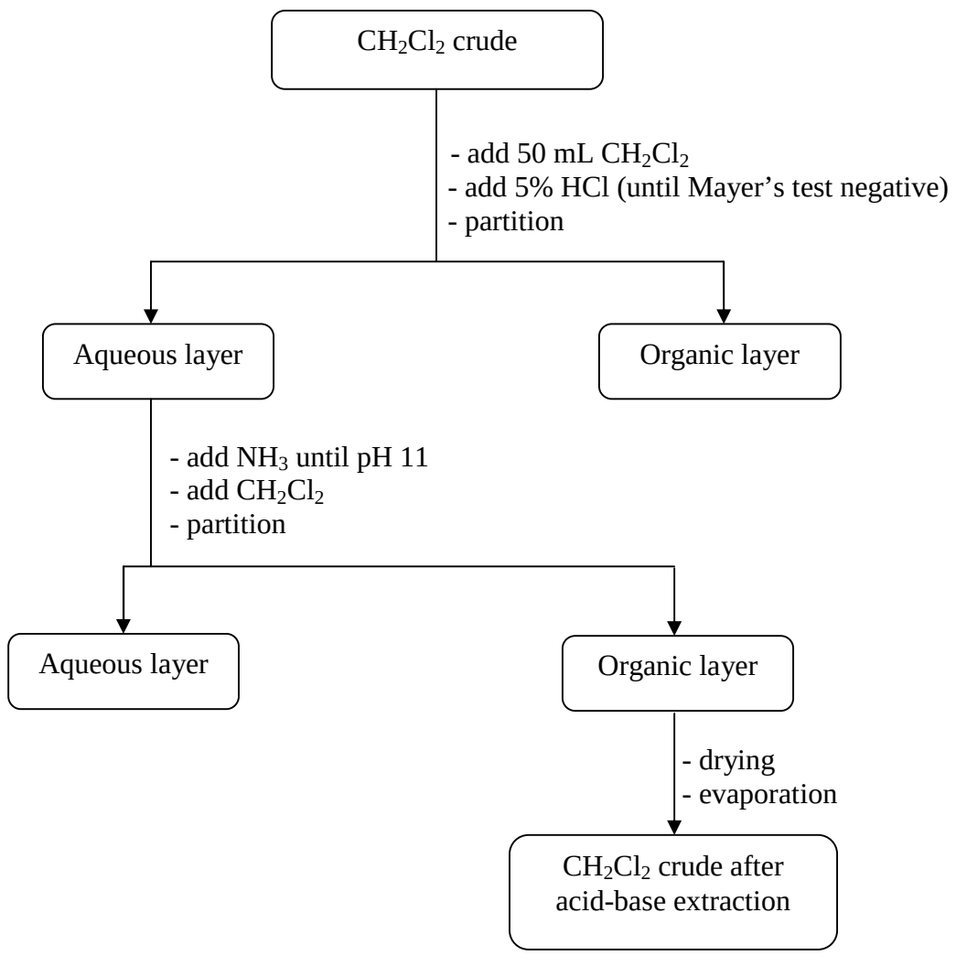

Scheme 6.2: Extraction of leaves.

Table 6.2: Amount of each plant material used for extraction and percentage yield of the crudes.

Plant material	Part of plant	Amount	Yield of crude (g)	Percentage yield (%)
N. officinalis - Madek	Bark	2.0 kg	Hexane- 3.83 CH_2Cl_2- 11.00 MeOH- 23.62	Hexane- 0.19 CH_2Cl_2- 0.55 MeOH- 1.18
	Leaves	1.9 kg	Hexane- 21.80 *CH_2Cl_2- 1.54 MeOH- 57.39	Hexane- 1.15 CH_2Cl_2- 0.08 MeOH- 3.02
N. officinalis - Mersing	Bark	1.5 kg	Hexane- 2.17 CH_2Cl_2-6.24 MeOH- 18.02	Hexane- 0.14 CH_2Cl_2- 0.42 MeOH- 1.20
	Leaves	1.3 kg	Hexane- 19.16 *CH_2Cl_2- 3.54 MeOH- 37.05	Hexane- 1.47 CH_2Cl_2- 0.27 MeOH- 2.85
N. subdita	Bark	1.7 kg	Hexane- 1.66 CH_2Cl_2- 5.81 MeOH- 26.45	Hexane- 0.10 CH_2Cl_2- 0.34 MeOH- 1.56
	Leaves	2.0 kg	Hexane- 16.82 *CH_2Cl_2- 1.13 MeOH- 34.72	Hexane- 0.84 CH_2Cl_2- 0.06 MeOH- 1.74

*Weight of crude after acid-base extraction

6.8 Isolation and Purification

The CH_2Cl_2 crude was subjected to column chromatography using silica gel 60 as the stationary phase. The solvent used was CH_2Cl_2 with increasing portion of MeOH (gradient elution system). Solvent systems used for for column chromatography separation of CH_2Cl_2 crude of *N. officinalis* (Madek and Mersing) and *N. subdita* were shown in Table 6.3.

Table 6.3: Solvent system for the isolation and purification of the CH_2Cl_2 crude of bark and leaves of *N. officinalis* (Madek and Mersing) and *N. subdita*.

Dichloromethane (CH_2Cl_2)	**Methanol (MeOH)**
100	0
99	1
98	2
97	3
96	4
95	5
94	6
90	10
83	17
75	25
0	100

The fractions which were collected were monitored using TLC and those with the same TLC profile were combined which were later subjected to column chromatography or preparative TLC in order to isolate and purify compounds. For the

MeOH crude of leaves of *N. officinalis* (Madek), HPLC was used for the isolation and purification of compounds. The solvent system applied is shown in Table 6.4.

Table 6.4: Solvent system for the purification of the MeOH crude of the leaves of *N. officinalis* (Madek)

Time (min)	Flow rate (mL/min)	%A2 (H_2O + FA)	%B2 (MeOH + FA)
0	3	70	30
2	3	70	30
32	3	0	100
35	3	0	100
37	3	70	30
40	3	70	30

The structures of the isolated compounds were elucidated with the aid of spectroscopic methods such as 1D NMR (^{1}H, ^{13}C, DEPT), 2D NMR (COSY, HMBC, HMQC/HSQC, NOESY), UV, IR and ESIMS/LCMS-IT-TOF. The optical rotations for the optically active compounds were also determined.

The isolated compounds from the bark and leaves of *N. officinalis* (Madek), *N. officinalis* (Mersing) and *N. subdita* are listed in Table 6.5 - Table 6.10. The isolation and purification of the compounds from these species are shown in Scheme 6.3- Scheme 6.11.

Table 6.5: Compounds isolated from the bark of *N. officinalis* (Madek) and their chromatography solvent systems.

Compounds	Type of crude	Solvent system	Weight (mg)
Stigmast-4-en-3-one **57**	Hexane	80:20 (Hexane:CH_2Cl_2)	2.2
Vanillin **58**	CH_2Cl_2	100:0 (CH_2Cl_2:MeOH)	3.0
Cinnamide **59**	CH_2Cl_2	99:1 (CH_2Cl_2:MeOH)	2.4
1,2,3,4-tetrahydro-1-oxo-β-carboline **60**	CH_2Cl_2	99.1 (CH_2Cl_2:MeOH)	4.1
Naucletine **61**	CH_2Cl_2	99:1 (CH_2Cl_2:MeOH)	11.8
Angustine **42**	CH_2Cl_2	98:2 (CH_2Cl_2 :MeOH)	15.2
Benzamide **62**	CH_2Cl_2	98:2 (CH_2Cl_2 :MeOH)	2.3
Angustidine **44**	CH_2Cl_2	98:2 (CH_2Cl_2 :MeOH)	5.5
Nauclefine **63**	CH_2Cl_2	98:2 (CH_2Cl_2 :MeOH)	8.5
Naucline **56**	CH_2Cl_2	97:3 (CH_2Cl_2 :MeOH)	12.8
Angustoline **43**	CH_2Cl_2	97:3 (CH_2Cl_2 :MeOH)	4.6

Table 6.6: Compounds isolated from the leaves of *N. officinalis* (Madek) and their chromatography solvent systems.

Compounds	Type of crude	Solvent system	Weight (mg)
Angustine **42**	CH_2Cl_2	97:3 (CH_2Cl_2 :MeOH)	4.1
Blumenol A **66**	CH_2Cl_2	97:3 (CH_2Cl_2 :MeOH)	3.5
Harmane **67**	CH_2Cl_2	96:4 (CH_2Cl_2 :MeOH)	3.2
3,14-dihydroangustoline **68**	CH_2Cl_2	95:5 (CH_2Cl_2 :MeOH)	2.3

Pumiloside **69**	MeOH	(MeOH:H_2O - HPLC)	5.7
Strictosamide **70**	MeOH	(MeOH:H_2O - HPLC)	6.4

Table 6.7: Compounds isolated from the bark of *N. officinalis* (Mersing) and their chromatography solvent systems.

Compounds	Type of crude	Solvent system	Weight (mg)
Naucleficine **64**	CH_2Cl_2	100:0 (CH_2Cl_2:MeOH)	5.2
Naucleactonin C **65**	CH_2Cl_2	100:0 (CH_2Cl_2:MeOH)	2.4
Angustine **42**	CH_2Cl_2	98:2 (CH_2Cl_2:MeOH)	7.2
Angustidine **44**	CH_2Cl_2	97:3 (CH_2Cl_2:MeOH)	4.3
Nauclefine **63**	CH_2Cl_2	97:3 (CH_2Cl_2:MeOH)	6.1

Table 6.8: Compounds isolated from the leaves of *N. officinalis* (Mersing) and their chromatography solvent systems.

Compounds	Type of crude	Solvent system	Weight (mg)
Benzamide **62**	CH_2Cl_2	99:1 (CH_2Cl_2:MeOH)	2.5
Angustine **42**	CH_2Cl_2	98:2 (CH_2Cl_2:MeOH)	4.2
Nauclefine **63**	CH_2Cl_2	97:3 (CH_2Cl_2:MeOH)	2.9
Blumenol B **71**	CH_2Cl_2	97:3 (CH_2Cl_2:MeOH)	2.7
Blumenol A **66**	CH_2Cl_2	97:3 (CH_2Cl_2:MeOH)	3.3
Angustoline **43**	CH_2Cl_2	96:4 (CH_2Cl_2:MeOH)	3.1

Table 6.9: Compounds isolated from the bark of *N. subdita* and their chromatography solvent systems.

Compounds	Type of crude	Solvent system	Weight (mg)
Stigmast-4-en-3-one **57**	Hexane	80:20 (Hexane:CH_2Cl_2)	3.7
β-sitosterol **73**	Hexane	80:20 (Hexane:CH_2Cl_2)	2.5
Naucleactonin C **65**	CH_2Cl_2	100:0 (CH_2Cl_2:MeOH)	2.3
Subditine **72**	CH_2Cl_2	98:2 (CH_2Cl_2:MeOH)	18.1
Benzamide **62**	CH_2Cl_2	98:2 (CH_2Cl_2:MeOH)	4.6
Cinnamide **59**	CH_2Cl_2	98:2 (CH_2Cl_2:MeOH)	2.2
1,2,3,4-tetrahydro-1-oxo-β-carboline **60**	CH_2Cl_2	98:2 (CH_2Cl_2:MeOH)	3.4
Angustine **42**	CH_2Cl_2	98:2 (CH_2Cl_2:MeOH)	20.7
Angustidine **44**	CH_2Cl_2	97:3 (CH_2Cl_2:MeOH)	8.1
Nauclefine **63**	CH_2Cl_2	97:3 (CH_2Cl_2:MeOH)	10.5
Harmane **67**	CH_2Cl_2	96:4 (CH_2Cl_2:MeOH)	2.7
Angustoline **43**	CH_2Cl_2	96:4 (CH_2Cl_2:MeOH)	8.2

Table 6.10: Compounds isolated from the leaves of *N. subdita* and their chromatography solvent systems.

Compounds	Type of crude	Solvent system	Weight (mg)
Angustine **42**	CH_2Cl_2	98:2 (CH_2Cl_2:MeOH)	3.1
Harmane **67**	CH_2Cl_2	96:4 (CH_2Cl_2:MeOH)	2.5

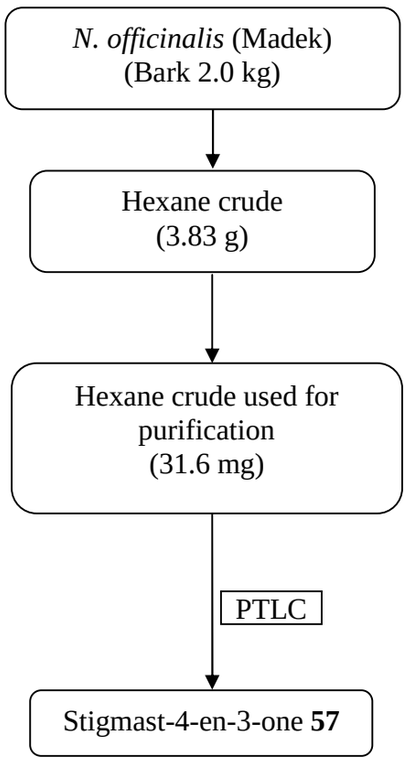

Scheme 6.3: Isolation and purification of compounds from the hexane crude of the bark of *N. officinalis* from Madek.

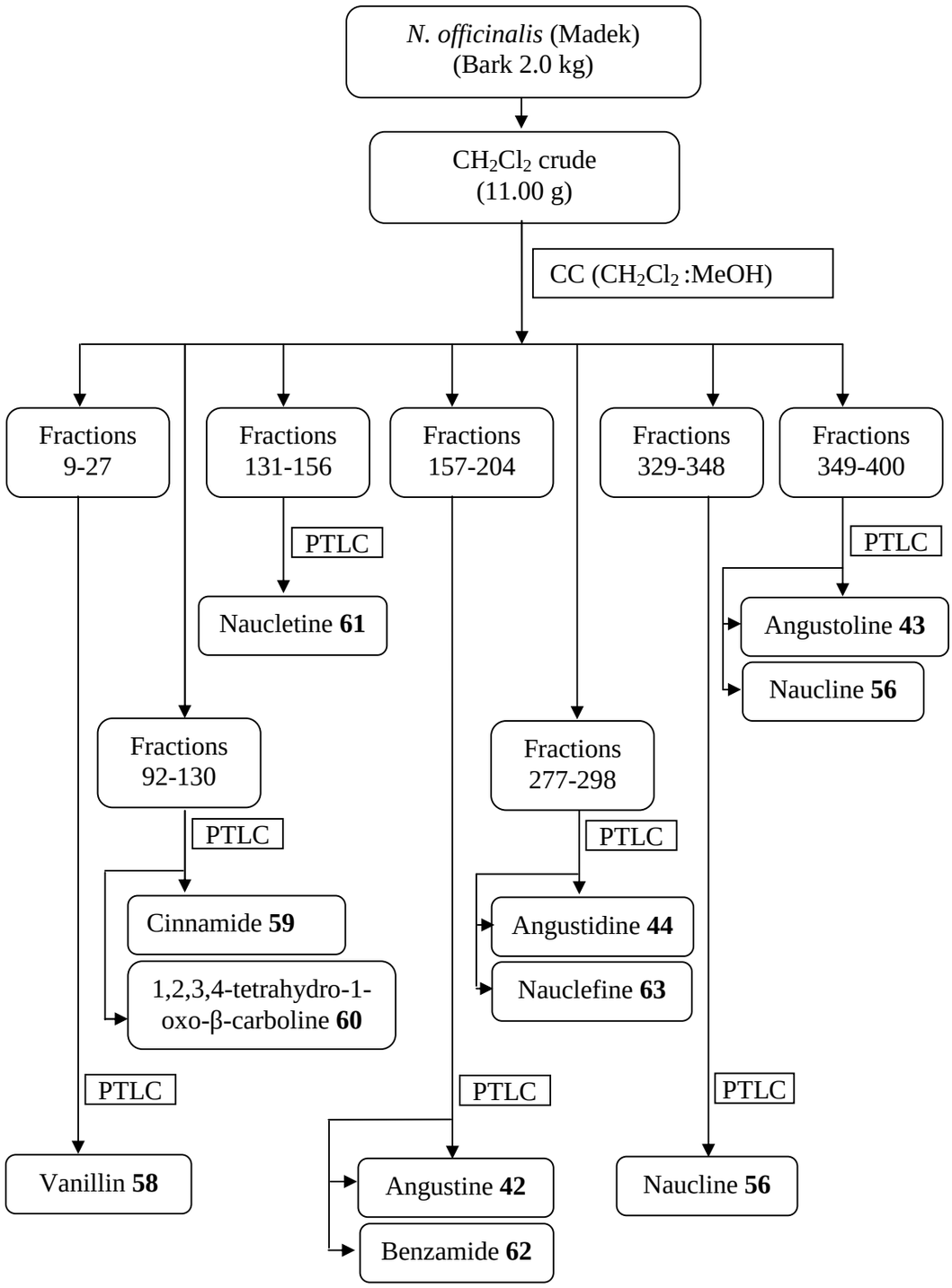

Scheme 6.4: Isolation and purification of the compounds from the CH_2Cl_2 crude of the bark of *N. officinalis* from Madek.

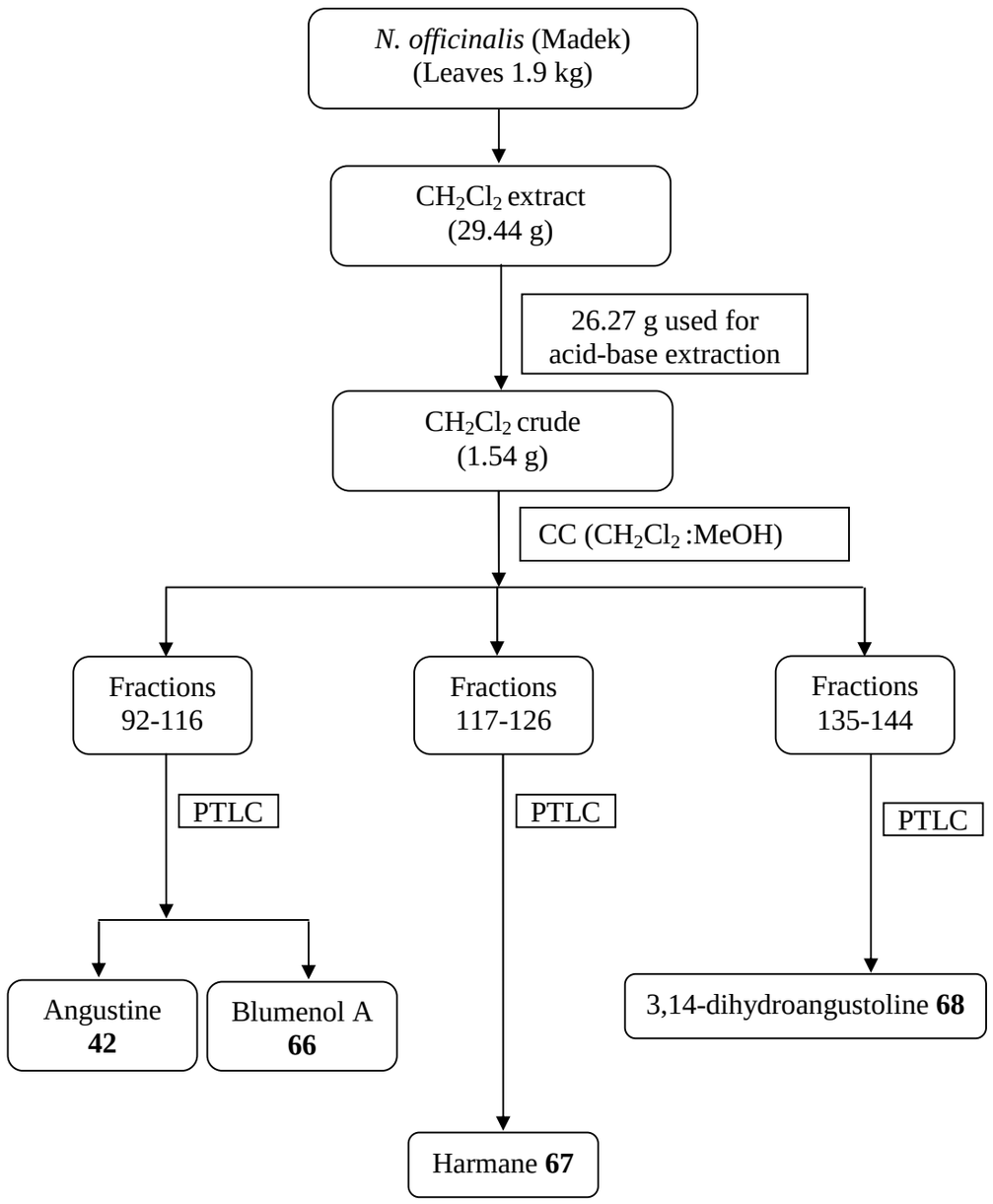

Scheme 6.5: Isolation and purification of the compounds from the CH_2Cl_2 crude of the leaves of *N. officinalis* from Madek.

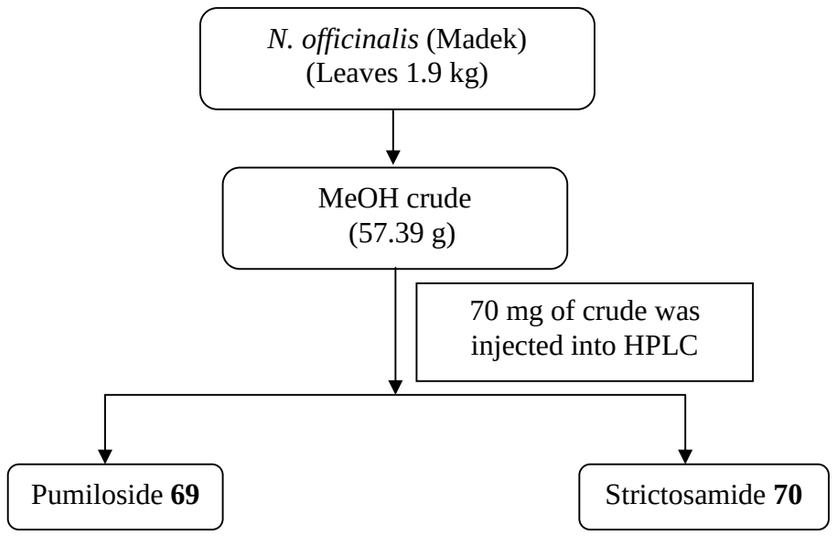

Scheme 6.6: Isolation and purification of the compounds from the MeOH crude of the leaves of *N. officinalis* from Madek

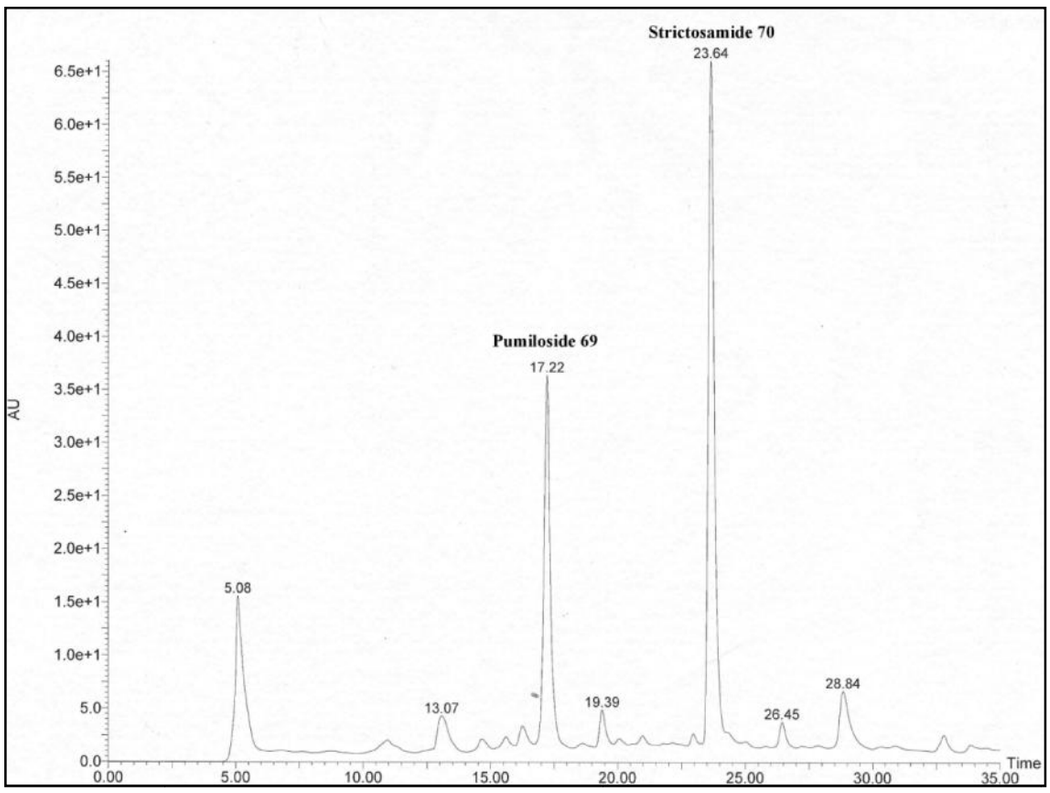

HPLC :Prep (Waters)

Column : C18 reversed phase (5 µM)

Column brand : X-bridge

Column size : 10 X 150 mm

Injection volume : 200 µL per injection

Retention time : 17.22 min - Pumiloside **69**

23.64 min – Strictosamide **70**

Figure 6.1: Chromatogram of isolated compounds; pumiloside **69** and strictosamide **70** at retention time of 17.22 min and 23.64 min respectively.

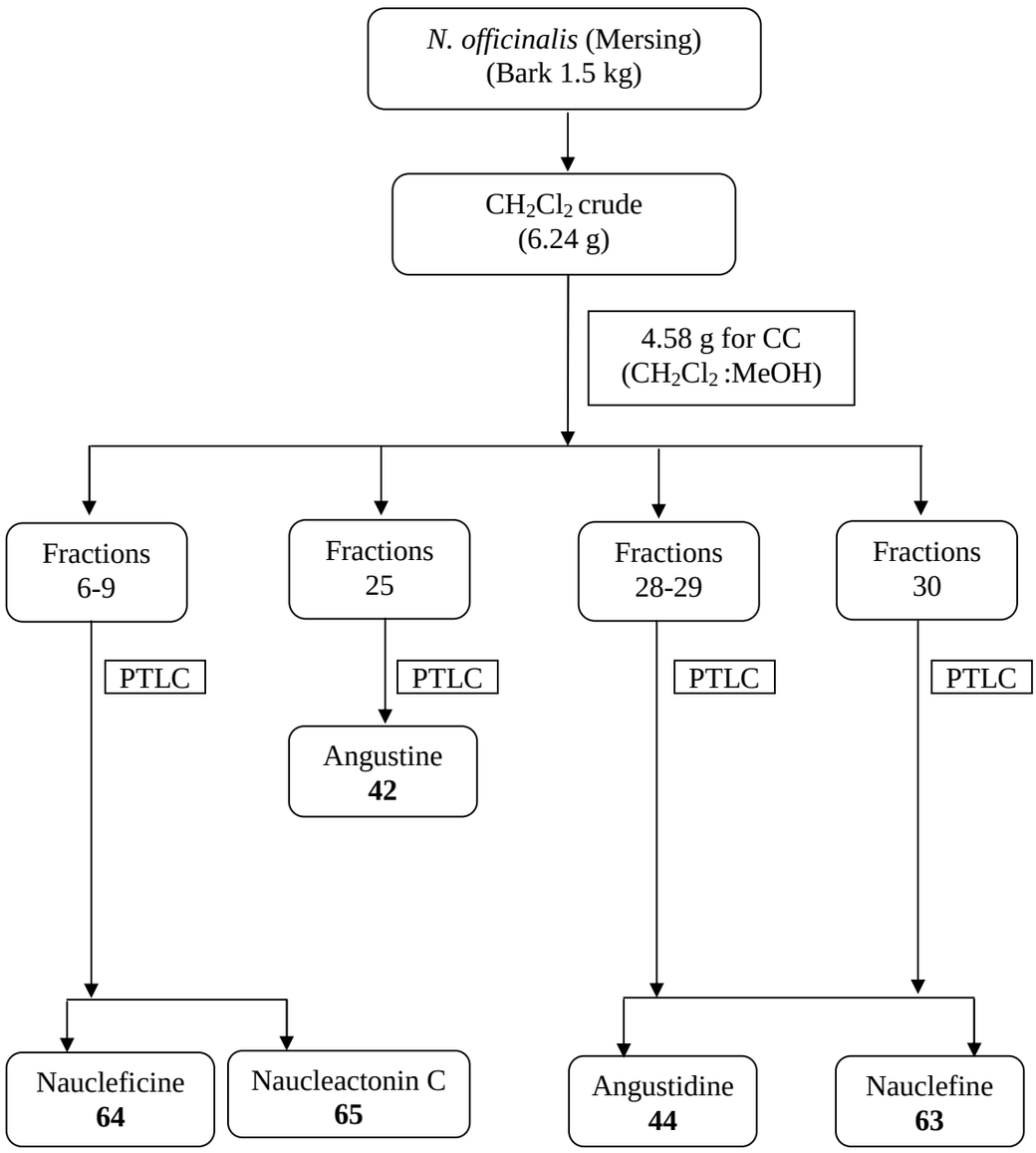

Scheme 6.7: Isolation and purification of the compounds from the CH_2Cl_2 crude of the bark of *N. officinalis* from Mersing.

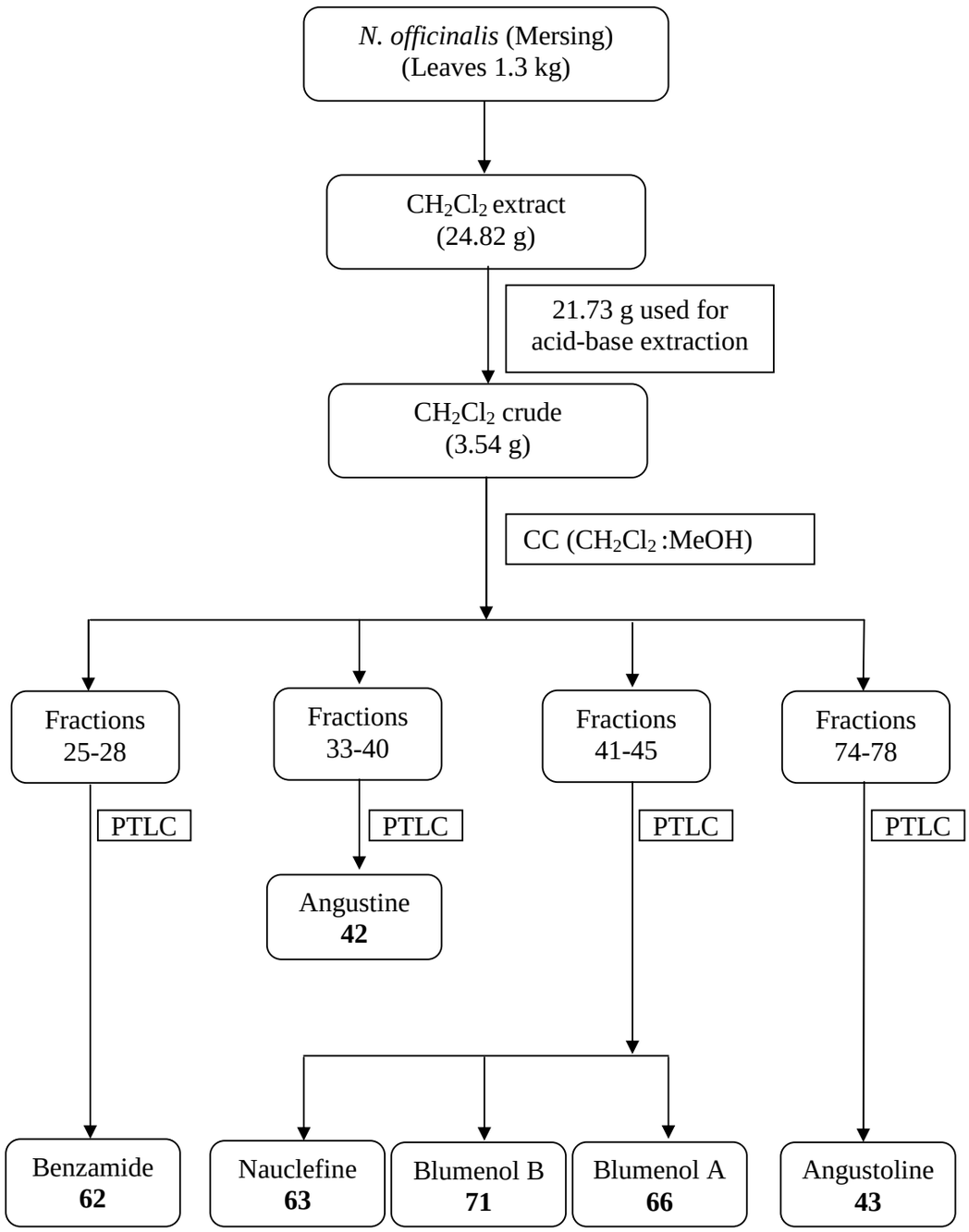

Scheme 6.8: Isolation and purification of the compounds from the CH_2Cl_2 crude of the leaves of *N. officinalis* from Mersing.

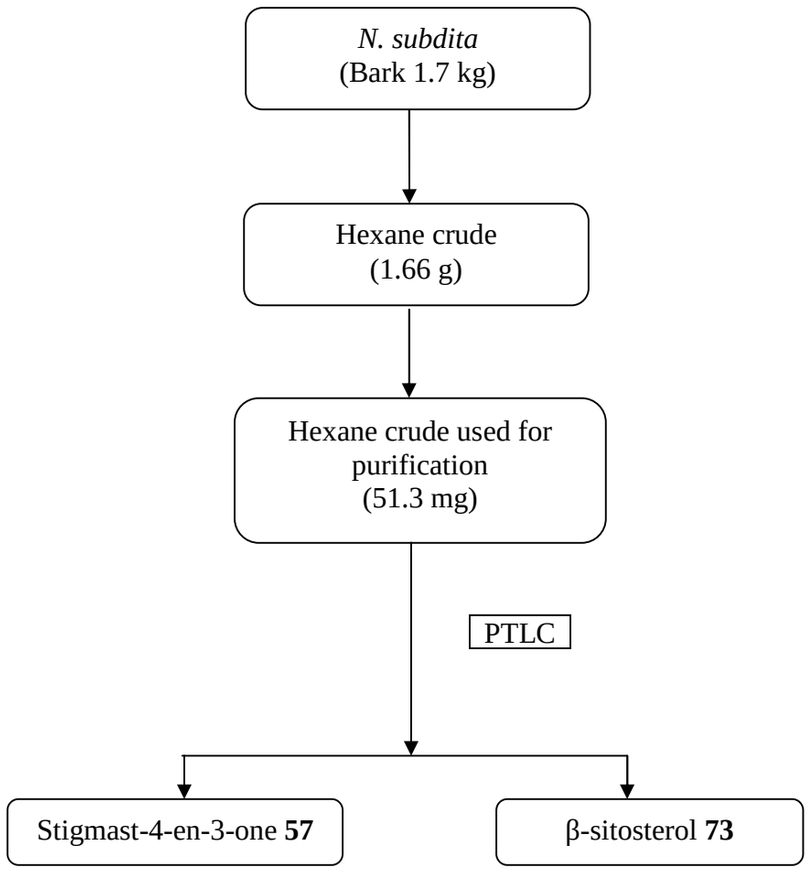

Scheme 6.9: Isolation and purification of the compounds from the heaxane crude of the bark of *N. subdita*.

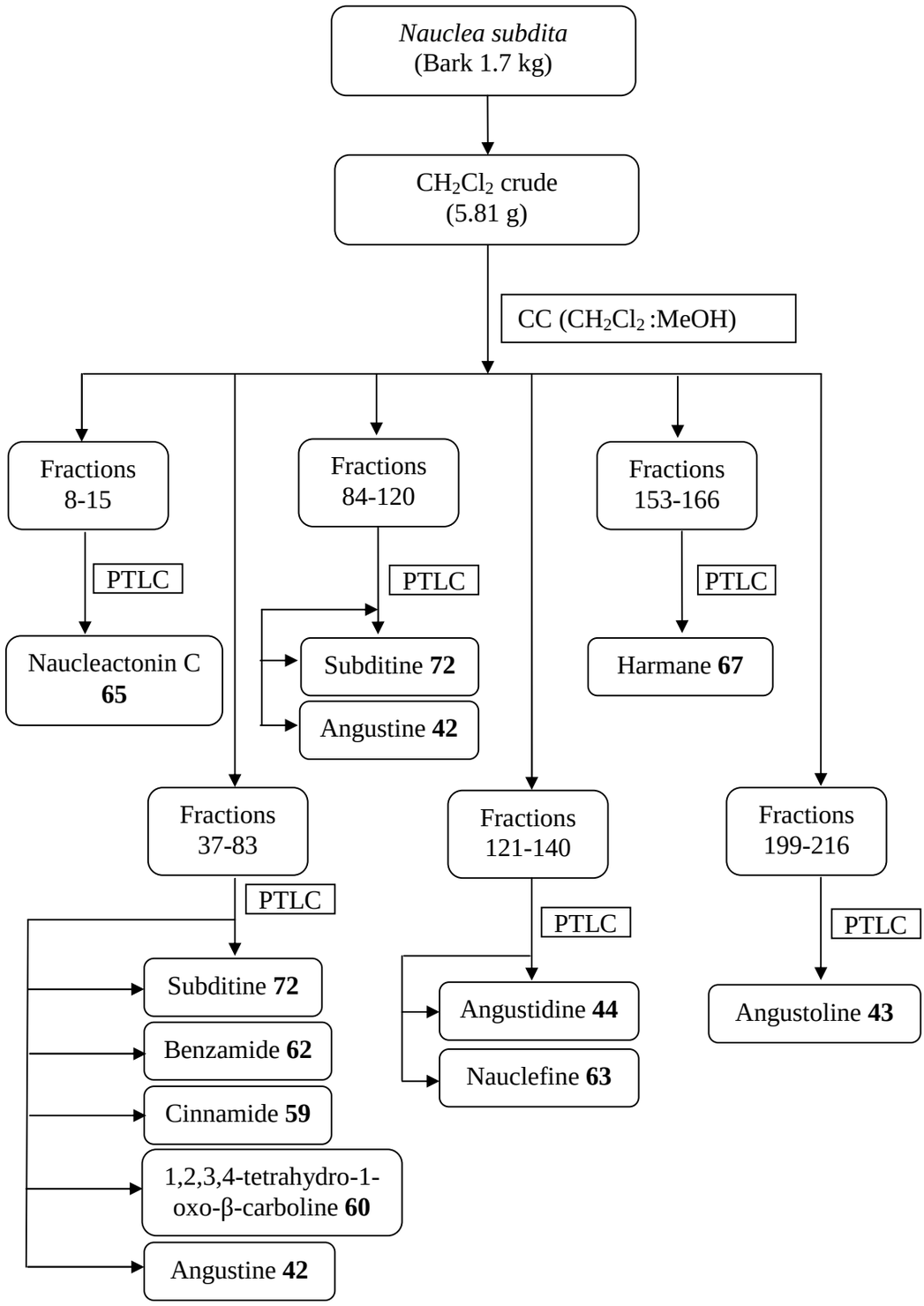

Scheme 6.10: Isolation and purification of the compounds from the CH_2Cl_2 crude of the bark of *N. subdita*.

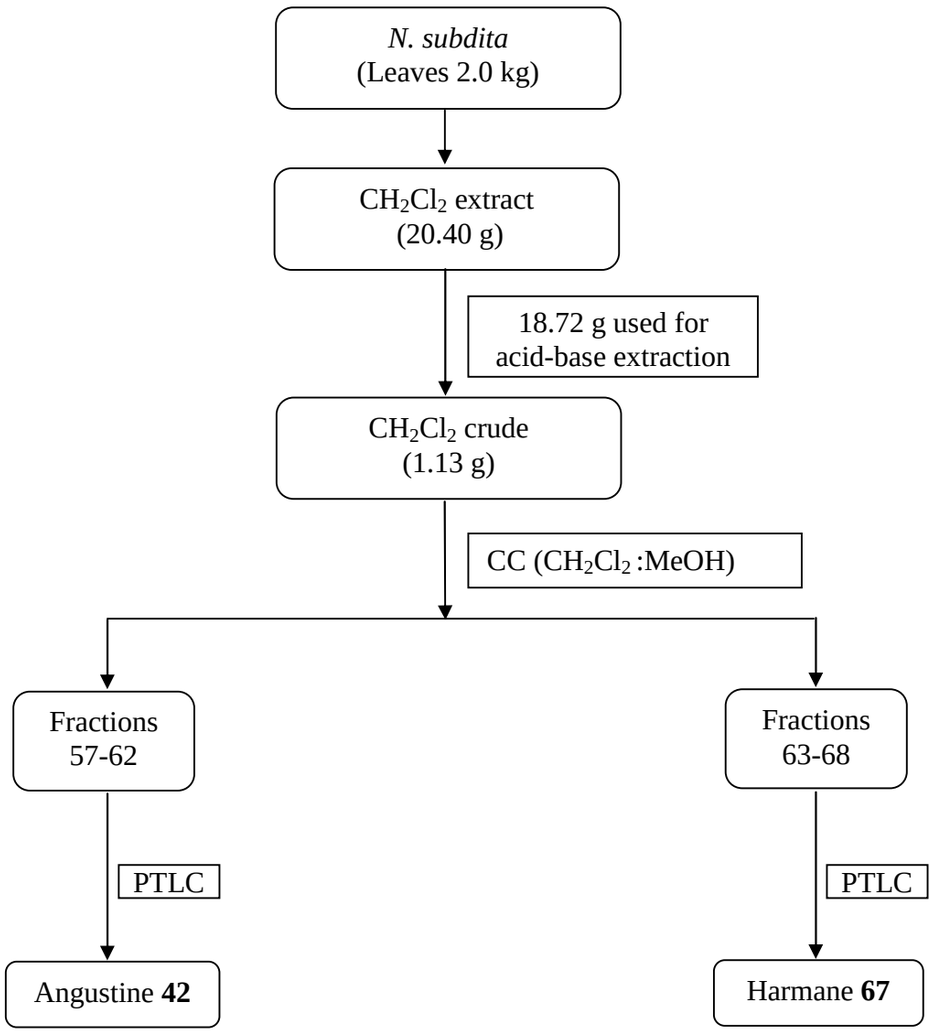

Scheme 6.11: Isolation and purification of the compounds from the CH_2Cl_2 crude of the leaves of *N. subdita*.

6.9 Physical and Spectral Data of Isolated Compounds

Naucline 56 : Brownish amorphous solid

Molecular formula : $C_{20}H_{18}N_2O_2$

UV λ_{max}, nm : 391, 374, 214

IR v_{max} (NaCl), cm^{-1} : 1638

Mass spectrum *m/z* : 319.1450 ($[M+H]^+$)

^1H NMR ($CDCl_3$) δ ppm : See Table 3.2

^{13}C NMR ($CDCl_3$) δ ppm : See Table 3.2

Nauclefine 63 : Yellowish amorphous solid

Molecular formula : $C_{18}H_{13}N_3O$

UV λ_{max}, nm : 391, 372, 220, 204

IR v_{max} (NaCl), cm^{-1} : 3415, 1650

Mass spectrum *m/z* : 288.1155 ($[M+H]^+$)

^1H NMR ($CDCl_3$) δ ppm : See Table 3.3

^{13}C NMR ($CDCl_3$) δ ppm : See Table 3.3

Naucletine 61 : Yellowish amorphous solid

Molecular formula : $C_{20}H_{15}N_3O_2$

UV λ_{max}, nm : 402, 312, 260, 210

IR v_{max} (NaCl), cm^{-1} : 1675, 1653

Mass spectrum *m/z* : 330.1266 ($[M+H]^+$)

^1H NMR ($CDCl_3$) δ ppm : See Table 3.4

^{13}C NMR ($CDCl_3$) δ ppm : See Table 3.4

Angustine 42 : Orange amorphous solid

Molecular formula : $C_{20}H_{15}N_3O$

UV λ_{max}, nm : 399, 381, 305, 293, 210

IR v_{max} (NaCl), cm^{-1} : 3425, 1645

Mass spectrum *m/z* : 314.1361 ($[M+H]^+$)

^1H NMR ($CDCl_3$) δ ppm : See Table 3.5

^{13}C NMR ($CDCl_3$) δ ppm : See Table 3.5

Angustoline 43 : Orange amorphous solid

Molecular formula : $C_{20}H_{17}N_3O_2$

$[\alpha]_D^{24}$: -72.7º (*c* 0.1, $CHCl_3$)

UV λ_{max}, nm : 394, 375, 210

IR v_{max} (NaCl), cm^{-1} : 1653, 1103

Mass spectrum *m/z* : 332.1096 ($[M+H]^+$

^1H NMR (C_5D_5N) δ ppm : See Table 3.6

^{13}C NMR (C_5D_5N) δ ppm : See Table 3.6

3,14-dihydroangustoline 68 : Yellowish amorphous solid

Molecular formula : $C_{20}H_{19}N_3O_2$

$[\alpha]_D^{24}$: -88.9º (*c* 0.09, $CHCl_3$)

UV λ_{max}, nm : 393, 375, 219

IR v_{max} (NaCl), cm^{-1} : 1640, 1101

Mass spectrum *m/z* : 334.1267 ($[M+H]^+$)

^1H NMR ($CDCl_3$) δ ppm : See Table 3.7

^{13}C NMR ($CDCl_3$) δ ppm : See Table 3.7

Angustidine 44 : Orange amorphous solid

Molecular formula : $C_{19}H_{15}N_3O$

UV λ_{max}, nm : 391, 288, 229

IR v_{max} (NaCl), cm^{-1} : 3401, 1644

Mass spectrum *m/z* : 302.1317 ($[M+H]^+$)

^1H NMR (C_5D_5N) δ ppm : See Table 3.8

^{13}C NMR (C_5D_5N) δ ppm : See Table 3.8

Subditine 72 : Yellowish amorphous solid

Molecular formula : $C_{20}H_{15}N_3O_2$

UV λ_{max}, nm : 393, 377, 210

IR v_{max} (NaCl), cm^{-1} : 3305, 1645

Mass spectrum *m/z* : 330.1018 ($[M+H]^+$)

^1H NMR ($CDCl_3$) δ ppm : See Table 3.9

^{13}C NMR ($CDCl_3$) δ ppm : See Table 3.9

Strictosamide 70 : Light yellowish amorphous solid

Molecular formula : $C_{26}H_{30}N_2O_8$

$[\alpha]_D^{23}$: -40.0º (*c* 0.1, MeOH)

UV λ_{max}, nm : 387, 328, 225, 203

IR v_{max} (NaCl), cm^{-1} : 1653, 1050

Mass spectrum *m/z* : 512.1875 ($[M+Na]^+$)

^1H NMR (CD_3OD) δ ppm : See Table 3.10

^{13}C NMR (CD_3OD) δ ppm : See Table 3.10

Pumiloside 69 : Light yellowish amorphous solid

Molecular formula : $C_{26}H_{28}N_2O_9$

$[\alpha]_D^{24}$: -93.5º (*c* 0.31, MeOH)

UV λ_{max}, nm : 328, 314, 244, 210

IR v_{max} (NaCl), cm^{-1} : 3415, 1653

Mass spectrum *m/z* : 535.1649 ($[M+Na]^+$)

^1H NMR (DMF-d_7) δ ppm : See Table 3.11

^{13}C NMR (DMF-d_7) δ ppm : See Table 3.11

Naucleficine 64 : Orange amorphous solid

Molecular formula : $C_{20}H_{14}N_2O_2$

UV λ_{max}, nm : 379, 364, 298, 263, 229

IR v_{max} (NaCl), cm^{-1} : 3271, 1676, 1642

Mass spectrum *m/z* : 315.1126 ($[M+H]^+$)

^1H NMR ($CDCl_3$) δ ppm : See Table 3.12

^{13}C NMR ($CDCl_3$) δ ppm : See Table 3.12

Naucleactonin C 65 : Yellowish amorphous solid

Molecular formula : $C_{19}H_{14}N_2O_2$

UV λ_{max}, nm : 368, 353, 211

IR v_{max} (NaCl), cm^{-1} : 3281, 1653

Mass spectrum *m/z* : 303.1127 ($[M+H]^+$)

^1H NMR ($CDCl_3$) δ ppm : See Table 3.13

^{13}C NMR ($CDCl_3$) δ ppm : See Table 3.13

Harmane 67 : Brownish amorphous solid

Molecular formula : $C_{12}H_{10}N_2$

UV λ_{max}, nm : 348, 288, 233

IR v_{max} (NaCl), cm^{-1} : 3145

Mass spectrum *m/z* : 183.0942 ($[M+H]^+$)

^1H NMR ($CDCl_3$) δ ppm : See Table 3.14

^{13}C NMR ($CDCl_3$) δ ppm : See Table 3.14

1,2,3,4-tetrahydro-1-oxo-β-carboline 60 : Brownish amorphous solid

Molecular formula : $C_{11}H_{10}N_2O$

UV λ_{max}, nm : 298, 240

IR v_{max} (NaCl), cm^{-1} : 3415, 1734

Mass spectrum *m/z* : 187.9447 ($[M+H]^+$)

^1H NMR ($CDCl_3$) δ ppm : See Table 3.15

^{13}C NMR ($CDCl_3$) δ ppm : See Table 3.15

Benzamide 62 : Light yellowish armorphous solid

Molecular formula : C_7H_7NO

UV λ_{max}, nm : 222

IR v_{max} (NaCl), cm^{-1} : 3390, 3187

Mass spectrum *m/z* : 122.0601 ($[M+H]^+$)

^1H NMR ($CDCl_3$) δ ppm : See Table 3.16

^{13}C NMR ($CDCl_3$) δ ppm : See Table 3.16

Cinnamide 59 : Light yellowish amorphous solid

Molecular formula : C_9H_9NO

UV λ_{max}, nm : 272, 217

IR v_{max} (NaCl), cm^{-1} : 3369, 3172

Mass spectrum *m/z* : 148.0750 ($[M+H]^+$)

^1H NMR ($CDCl_3$) δ ppm : See Table 3.17

^{13}C NMR ($CDCl_3$) δ ppm : See Table 3.17

Blumenol B 71 : White amorphous solid

Molecular formula : $C_{13}H_{22}O_3$

$[\alpha]_D^{23}$: +36.4º (*c* 0.11, $CHCl_3$)

UV λ_{max}, nm : 242

IR v_{max} (NaCl), cm^{-1} : 3401, 1651, 1126

Mass spectrum *m/z* : 227.1733 ($[M+H]^+$)

^1H NMR ($CDCl_3$) δ ppm : See Table 3.18

^{13}C NMR ($CDCl_3$) δ ppm : See Table 3.18

Blumenol A 66 : White amorphous solid

Molecular formula : $C_{13}H_{20}O_3$

$[\alpha]_D^{23}$: +146.6º (*c* 0.58, $CHCl_3$)

UV λ_{max}, nm : 237

IR v_{max} (NaCl), cm^{-1} : 3402, 1655, 1124

Mass spectrum *m/z* : 225.1665 ($[M+H]^+$)

^1H NMR ($CDCl_3$) δ ppm : See Table 3.19

^{13}C NMR ($CDCl_3$) δ ppm : See Table 3.19

β-sitosterol 73 : White amorphous solid

Molecular formula : $C_{29}H_{50}O$

$[\alpha]_D^{24}$: -55.6º (*c* 0.09, $CHCl_3$)

UV λ_{max}, nm : 203

IR v_{max} (NaCl), cm^{-1} : 3425, 2925, 1465, 1375

Mass spectrum *m/z* : 415.3561 ($[M+H]^+$)

^1H NMR ($CDCl_3$) δ ppm : See Table 3.20

^{13}C NMR ($CDCl_3$) δ ppm : See Table 3.20

Stigmast-4-en-3-one 57 : White amorphous solid

Molecular formula : $C_{29}H_{48}O$

$[\alpha]_D^{24}$: +75.0º (*c* 0.12, $CHCl_3$)

UV λ_{max}, nm : 241

IR v_{max} (NaCl), cm^{-1} : 1675, 1468, 1375

Mass spectrum *m/z* : 413.2660 ($[M+H]^+$)

^1H NMR ($CDCl_3$) δ ppm : See Table 3.21

^{13}C NMR ($CDCl_3$) δ ppm : See Table 3.21

Vanillin 58 : Light brownish amorphous solid

Molecular formula : $C_8H_8O_3$

UV λ_{max}, nm : 308, 277

IR v_{max} (NaCl), cm^{-1} : 3365, 1661, 1155

Mass spectrum *m/z* : 153.0555 ($[M+H]^+$)

^1H NMR ($CDCl_3$) δ ppm : See Table 3.22

^{13}C NMR ($CDCl_3$) δ ppm : See Table 3.22

Reference

1. Kumar, S., Kumar, R. & Khan, A. (2011). Medicinal Plant Resources: Manifestation and Prospects of Life-Sustaining Healthcare System. *Continental J. Biological Sciences* Q(1), 19-29.

2. Tzanavaras, P. D. & Zacharis, C. K. (2010). *Reviews in Pharmaceutical and Biomedical Analysis*. Bentham e Books.

3. Fathalla, M. A.-E.-K., Abd-El Kawy, A. M. & Taha, H. S. (2011). Effect of Heavy Metal ($HgCl_2$) on Accumulation and Production of Total Indole Alkaloids, Vinblastine And/or Vincristine from Egyptian *Catharanthus Roseus* (L.) G. Don. Calli Cultures. *Journal of Applied Sciences Research*, *7*(4), 542-549.

4. Okoro, I. O., Osagie, A. & Asibor, E. O. (2010). Antioxidant and Antimicrobial activities of polyphenols from ethnomedicinal plants of Nigeria. *African Journal of Biotechnology*, *9*(20), 2989-2993.

5. Newman, D. J. & Cragg, G. M. (2012). Natural products as sources of new drugs over the 30 years from 1981 to 2010. *Journal of Natural Products*, *75*(3), 311-315.

6. Okwu, D. E. & Uchenna, N. F. (2009). Exotic multifacceted medicinal plants of drugs and pharmaceutical industries. *African Journal of Biotechnology*, *8*(25), 7271-7282.

7. Okwu, D. E. & Ezenagu, V. (2008). International Journal of Chemical Sciences. *6*, *2*(705-716).

8. Dongmo, G. I. F., Enyong, J. O., Noumessing, C. E. M. & Enyegue, D. M. (2007). Phytochemical Constituents and Antioxidant Potential of Some Cameroonian Medicinal Plant. *Pharmacologyonline*, *2* 436-452.

9. Eswani, N., Kudus, K. A., Nazre, M. & Noor, A. G. A. (2010). Medicinal Plant Diversity and Vegetation Analysis of Logged over Hill Forest of Tekai Tembeling Forest Reserve, Jerantut, Pahang. *Journal of Agricultural Science*, *2*(3), 189-210.

10. Hanum, I. F., Ibrahim, A. Z., Khamis, S., Nazre, M., Lepun, P., Rusea, G., et al. (2001). An annotated checklist of higher plants in Ayer Hitam Forest Reserve, Puchong, Selangor. *Pertanika Journal Tropical Agricultural Science*, *24*(1), 62-75.

11. Hanum, I. F., Rahim, A., Lepun, P., Edham, I. & Nazre, M. (2001). Tree taxa inventory at Ayer Hitam Forest Base-Camp. *Pertanika Journal Tropical Agricultural Science*, *24*(1), 29-34.

12. Abdelwahab, S. I., Mohan, S., Mohamed Elhassan, M., Al-Mekhlafi, N., Mariod, A. A., Abdul, A. B., et al. (2011). Antiapoptotic and Antioxidant Properties of *Orthosiphon stamineus* Benth (Cats Whiskers): Intervention in the Bcl-2-Mediated Apoptotic Pathway. *Evidence-Based Complementary and Alternative Medicine, 2011*.

13. Ng, F. S. P. & Whitmore, T. C. (1989). *Tree flora of Malaya: a manual for foresters*. Longman Malaysia.

14. Takayama, H., Tsutsumi, S.-i., Kitajima, M., Santiarworn, D., Liawruangrath, B. & Aimi, N. (2003). Gluco-indole Alkaloids from *Nauclea cadamba* in Thailand and Transformation of 3α-Dihydrocadambine into the Indolopyridine Alkaloid, 16-Carbomethoxynaufoline. *Chemical & Pharmaceutical Bulletin, 51*(2), 232-233.

15. Erdelmeier, C. A. J., Regenass, U., Rali, T. & Sticher, O. (1992). Indole Alkaloids with in vitro Antiproliferative Activity from the Ammoniacal Extract of *Nauclea orientalis*. *Planta Med, 58*(01), 43-48.

16. Agomuoh, A. A., Ata, A., Udenigwe, C. C., Aluko, R. E. & Irenus, I. (2013). Novel indole alkaloids from *Nauclea latifolia* and their renin-inhibitory activities. *Chemistry & Biodiversity*, NM(3), 401-410.

17. Ahmad, R., Mahbob, E. N. M., Noor, Z. M., Ismail, N. H., Lajis, N. H. & Shaari, K. (2010). Evaluation of antioxidant potential of medicinal plants from Malaysian Rubiaceae (subfamily Rubioideae). *Afr. J. Biotechnol., 9*(46), 7948-7954.

18. Mongrand, S., Badoc, A., Patouille, B., Lacomblez, C., Chavent, M. & Bessoule, J.-J. (2005). Chemotaxonomy of the Rubiaceae family based on leaf fatty acid composition. *Phytochemistry, 66*(5), 549-559.

19. Manns, U. & Bremer, B. (2010). Towards a better understanding of intertribal relationships and stable tribal delimitations within Cinchonoideae s.s. (Rubiaceae). *Molecular Phylogenetics and Evolution, 56*(1), 21-39.

20. Karou, S. D., Tchacondo, T., Ilboudo, D. P. & Simpore, J. (2011). Sub-Saharan Rubiaceae: a review of their traditional uses, phytochemistry and biological activities. *Pakistan Journal of Biological Sciences, 14*(3), 149-169.

21. Pedersen, O., Gurib-Fakim, A., Subratty, H. & Adsersen, A. (1999). Pharmacological Properties of Seven Medicinal Plants of the Rubiaceae from Mauritius. *Pharmaceutical Biology, 37*(3), 202-207.

22. Ismail, N. H. Chemistry and Biological Activity of Anthraquinones from Morinda Elliptica (Rubiaceae). University of Putra Malaysia, 1999.

23. Duke, J. A. (2000). *The Green Pharmacy Herbal Handbook: Your Comprehensive Reference to the Best Herbs for Healing*. (1 ed.). Rodale Books.

24. Duke, J. A. (2000). *The Green Pharmacy Herbal Handbook: Your Comprehensive Reference to the Best Herbs for Healing*. Rodale Books.

25. Singh, P. & Ali, S. J. (2012). Ethnomedicinal Plants of Family Rubiaceae of Eastern U.P. *Indian Journal of Life Sciences, 1*(2), 83-86.

26. Sichaem, J., Surapinit, S., Siripong, P., Khumkratok, S., Jong-aramruang, J. & Tip-pyang, S. (2010). Two new cytotoxic isomeric indole alkaloids from the roots of *Nauclea orientalis*. *Fitoterapia, 81*(7), 830-833.

27. Chen, T. & Taylor, C. M. (2011). *Nauclea Linnaeus, Sp.* P1. *Flora of China*, *19* 249.

28. *The Plant List*. http://www.theplantlist.org/browse/A/Rubiaceae/Nauclea/.

29. Ridsdale, C. E. (1978). A Revision of the Tribe Naucleeae s.s. (Rubiaceae). *Blumea*, *24* 307-366.

30. Maitera, O. N., Khann, M. E. & James, T. F. (2011). Phytochemical analysis and the chemotherapeutics of leaves and stem-bark of Nauclea latifolia grown in Hong, Adamawa State Nigeria. *Asian Journal of Plant Science and Research*, *1*(3), 16-22.

31. Deeni, Y. Y. & Hussain, H. S. N. (1991). Screening for antimicrobial activity and for alkaloids of *Nauclea latifolia*. *Journal of Ethnopharmacology*, *35*(1), 91-96.

32. Benoit-Vical, F., Valentin, A., Cournac, V., Pélissier, Y., Mallié, M. & Bastide, J.-M. (1998). In vitro antiplasmodial activity of stem and root extracts of *Nauclea latifolia S.M.* (Rubiaceae). *Journal of Ethnopharmacology*, *61*(3), 173-178.

33. Orwa, C., Mutua, A., Kindt, R., Jamnadass, R. & Anthony, S., Agroforestree Database: a tree reference and selection guide version 4.0. World Agroforestry Centre, Kenya: 2009.

34. Ruzaik, F. In *Plants used in the Indigenous System of Medicine in Sri Lanka-(Dawatagolla Forest Plantation)*, 2013; pp 44-53.

35. Sun, J. Y., Lou, H. X., Dai, S. J., Xu, H., Zhao, F. & Liu, K. (2008). Indole alkoloids from *Nauclea officinalis* with weak antimalarial activity. *Phytochemistry*, *69*(6), 1405-1410.

36. Sun, J. Y., Lou, H. X., Xu, H., Dai, S. J. & Liu, K. (2007). Two new indole alkaloids from *Nauclea officinalis*. *Chinese Chemical Letters*, *18* 1084-1086.

37. Su, K., Gong, M., Zhou, J. & Deng, S. (2009). Study of Chemical Composition of *Nauclea Officinalis* Leaves. *International Journal of Chemistry*, *1*(2), 77-81.

38. Fatin, R. J., Wahab, R., Daud, J. M., Sudin, M., Rasat, M. S. & Sulaiman, O. (2012). Study on Methanolic Extracts of *Nauclea subdita* (Korth) Steud. Heartwood Parts for the Total Phenolic Contents and Free Radical Scavenging Activities. *Current Research Journal of Biological Sciences*, *4*(5), 600-607.

39. Pelletier, S. W. (1983). *The nature and definition of an alkaloid*. New York: Wiley.

40. Hesse, M. (1981). *Alkaloid Chemistry*. John Wiley & Sons, Inc.

41. IUPAC. (1997). *Compendium of Chemical Terminology-the Gold Book*. (2nd ed.). Blackwell Scientific Publications, Oxford.

42. Snieckus, V. (1968). *The Alkaloids :Chemistry and Physiology*. New York: Academic Press Inc.

43. Cordell, G. A. (1981). *Introduction to Alkaloids: A Biogenetic Approach*. John Wiley & Sons.

44. Cai, S.-X., Li, D.-H., Zhu, T.-J., Wang, F.-P., Xiao, X. & Gu, Q.-Q. (2010). Two New Indole Alkaloids from the Marine-Derived Bacterium *Aeromonas sp.* CB101. *Helvetica Chimica Acta*, *93*(4), 791-795.

45. Martínez-Luis, S., Gómez, J. F., Spadafora, C., Guzmán, H. M. & Gutiérrez, M. (2012). Antitrypanosomal Alkaloids from the Marine Bacterium *Bacillus pumilus*. *Molecules*, *17*(9), 11146-11155.

46. Kar, A., Pharmacognosy and Pharmacobiotechnology. 2 ed.; New Age International (P) Limited Publishers: 2007.

47. Wink, M. & Waterman, P. G. (1999). *Chemotaxonomy in relation to molecular phylogeny of plants*. Sheffeld Academic Press and CRC Press.

48. Hesse, M., Chapter 2 Classification of Alkaloids. In *Alkaloids: Nature's Curse Or Blessing?*, Verlag Helvetica Chimica Acta: 2002; p 400.

49. Aniszewski, T., Chapter 1 - Definition, Typology and Occurrence of Alkaloids. In *Alkaloids - Secrets of Life*, Elsevier: Amsterdam, 2007; pp 1-59.

50. (1998). *Alkaloids: Biochemistry, Ecology, and Medicinal Applications*. (1 ed.). Springer.

51. Watt, G. (1972). *Dictionary of Economic Products of India*.

52. Nadkarni, A. K. (1976). *Nadkarni's Indian Materia Medica Popular Prakashan*. Pvt. Ltd. Bombay.

53. Chopra, R. N., Nayar, S. L. & Chopra, I. C. (1996). *Glossary of Indian medicinal plants*. Council of Scientific and Industrial Research.

54. Singh, A., Duggal, S., Kaur, N. & Singh, J. (2010). Berberine: Alkaloid with wide spectrum of pharmacological activities *Journal of Natural Products, 3* 64-75.

55. Atta-Ur-Rahman & Basha, A. (1982). *Biosynthesis of Indole Alkaloids*.

56. Qureshi, A. A. & Scott, A. I. (1968). Interconversion of Corynanthe, aspidosperma, and Iboga alkaloids. A model for indole alkaloid biosynthesis. *Chemical Communications (London)*, (16), 945-946.

57. Nakanishi, K. (1983). *Natural Products Chemistry*. Kodansha.

58. Thomas, R. (1961). A possible biosynthetic relationship between the cyclopentanoid monoterpenes and the indole alkaloids. *Tetrahedron Letters*, *2*(16), 544-553.

59. Perkin, W. H. & Robinson, R. (1919). LXXIX.-Harmine and harmaline. Part III. *Journal of the Chemical Society, Transactions*, *115* 933-967.

60. Battersby, A. R., Burnett, A. R. & Parsons, P. G. (1969). Alkaloid biosynthesis. Part XV. Partial synthesis and isolation of vincoside and isovincoside: biosynthesis of the three major classes of indole alkaloids from vincoside. *Journal of the Chemical Society C: Organic*, (8), 1193-1200.

61. Dewick, P. M., Alkaloids. In *Medicinal Natural Products*, John Wiley & Sons, Ltd: 2001; pp 291-403.

62. Jackson, A. H. & Smith, P. (1967). A new theory of electrophilic substitution in 3-substituted indoles. *Chemical Communications (London)*, (6), 264-266.

63. Stöckigt, J. & Zenk, M. H. (1977). Isovincoside (strictosidine), the key intermediate in the enzymatic formation of indole alkaloids. *FEBS Letters*, *79*(2), 233-237.

64. Stockigt, J. & Zenk, M. H. (1977). Strictosidine (isovincoside): the key intermediate in the biosynthesis of monoterpenoid indole alkaloids. *Journal of the Chemical Society, Chemical Communications*, (18), 646-648.

65. Scott, A. I., Lee, S.-L., De Capite, P., Culver, M. G. & Hutchinson, C. R. (1977). The Role of Isovincoside (Strictosidine) in the Biosynthesis of the Indole Alkaloids. *Heterocycles*, *7*(2), 979-984.

66. Stöckigt, J. (1979). Enzymatic formation of intermediates in the biosynthests of ajmalicine: Strictosidine and cathenamine. m¦·²-¡¦£«§±²°·, *18*(6), 965-971.

67. Treimer, J. F. & Zenk, M. H. (1979). Purification and properties of strictosidine synthase, the key enzyme in indole alkaloid formation. *Eur J Biochem*, *101*(1), 225-233.

68. Smith, G. N. (1968). Strictosidine: a key intermediate in the biogenesis of indole alkaloids. *Chemical Communications (London)*, (15), 912-914.

69. Battersby, A. R. (1967). Biosynthesis of the indole and Colchicum alkaloids. *Pure Appl Chem*, *14*(1), 117-36.

70. Phillipson, J. D., Zenk, H. & Europe, P. S. o. (1980). *Indole and biogenetically related alkaloids*. Academic Press.

71. O'Connor, S. E. & Maresh, J. J. (2006). Chemistry and biology of monoterpene indole alkaloid biosynthesis. *Natural Product Reports*, *23*(4), 532-547.

72. Au, T. Y., Cheung, H. T. & Sternhell, S. (1973). New corynanthe alkaloids from *Strychnos angustiflora*. *J Chem Soc Perkin 1*, (1), 13-16.

73. Phillipson, J. D., Hemingway, S. R., Bisset, N. G., Houghton, P. J. & Shellard, E. J. (1974). Angustine and related alkaloids from species of *Mitragyna*, *nauclea*, *uncaria*, and *Strychnos*. *Phytochemistry*, *13*(6), 973-978.

74. Mao, L., Xin, L. & Dequan, Y. (1984). Alkaloids of *Nauclea officinalis*. *Planta Medica*, *50*(06), 459-461.

75. Shigemori, H., Kagata, T., Ishiyama, H., Morah, F., Ohsaki, A. & Kobayashi, J. (2003). Naucleamides A-E, New Monoterpene Indole Alkaloid from *Nauclea latifolia*. *Chemical & Pharmaceutical Bulletin*, *51*(1), 58-61.

76. Sainsbury, M. & Uttley, N. L. (1976). Synthesis of the indolo[2',2':3,4]pyrido[1,2-b][2,7]naphthyridinone alkaloid nauclefine and its ring-E isomers. *J Chem Soc Perkin 1*, (22), 2416-2418.

77. Sainsbury, M. & Webb, B. (1975). Parvine, a new angustine-type alkaloid from *Nauclea parva*. *Phytochemistry*, *14*(12), 2691-2693.

78. Abreu, P. & Pereira, A. (1998). A New Indole Alkaloid from *Sarcocephalus latifolius*. *Heterocycles*, *48*(5), 885-891.

79. Hotellier, F., Delaveau, P. & Pousset, J.-L. (1975). Nauclefine et naucletine deux nouveaux alcaloides de type indoloquinolizidine isoles du *Nauclea latifolia*. *Phytochemistry*, *14*(5–6), 1407-1409.

80. Ninomiya, I., Naito, T. & Takasugi, H. (1976). Photocyclisation of enamides. Part X. Total syntheses of the yohimbine skeleton: demethoxycarbonyldihydrogambirtannine, angustidine, naucletine, (+/-)-angustoline, and related compounds. *Journal of the Chemical Society, Perkin Transactions 1*, (17), 1865-1868.

81. Lavilla, R., Gallon, F. & Bosch, J. (1995). Regioselective syntheses of the indolopyridine alkaloids nauclefine, angustine, dihydroangustine and naucletine from a common intermediate. *Journal of the Chemical Society, Chemical Communications*, (16), 1675-1676.

82. Liew, S. Y., Mukhtar, M. R., Hadi, A. H. A., Awang, K., Mustafa, M. R., Zaima, K., et al. (2012). Naucline, a New Indole Alkaloid from the Bark of *Nauclea officinalis*. *Molecules*, *17*(4), 4028-4036.

83. Fan, L., Fan, C., Wang, Y., Zhang, X., Zhang, Q., Zhang, J., et al. (2010). Alkaloids from the leaves of *Nauclea officinalis*. *Yao Xue Xue Bao*, *45*(6), 747-751.

84. Zhang, Z., ElSohly, H. N., Jacob, M. R., Pasco, D. S., Walker, L. A. & Clark, A. M. (2001). New Indole Alkaloids from the Bark of *Nauclea orientalis*. *Journal of Natural Products*, *64*(8), 1001-1005.

85. Erdelmeier, C. A. J., Wright, A. D., Orjala, J., Baumgartner, B., Rali, T. & Sticher, O. (1991). New Indole Alkaloid Glycosides from *Nauclea orientalis*. *Planta Med*, *57*(02), 149-152.

86. Sun, J., Lou, H., Dai, S., Xu, H., Zhao, F. & Liu, K. (2008). Indole alkoloids from *Nauclea officinalis* with weak antimalarial activity. *Phytochemistry*, *69*(6), 1405-1410.

87. Sivasothy, Y., Hadi, A. H. A., Mohamad, K., Leong, K. H., Ibrahim, H., Sulaiman, S. F., et al. (2012). Spectaflavoside A, a new potent iron chelating dimeric flavonol glycoside from the rhizomes of *Zingiber spectabile* Griff. *Bioorganic & Medicinal Chemistry Letters*, *22*(11), 3831-3836.

88. Donfack, E. V., Lenta, B. N., Kongue, M. D. T., Fongang, Y. F., Ngouela, S., Tsamo, E., et al. (2012). Naucleactonin D, an Indole Alkaloid and other Chemical Constituents from Roots and Fruits of *Mitragyna inermis*. *Zeitschrift für Naturforschung B*, *11*(67b), 1159-1165.

89. Naito, T., Kuroda, E., Miyata, O. & Ninomiya, I. (1991). Photocyclization of Enamides. XXXIV. A Practical Total Synthesis of Aromatic Yohimboid Alkaloids, Oxogambirtannine and Naucleficine. *Chemical & Pharmaceutical Bulletin*, *39*(9), 2216-2218.

90. Nagoor, N. H., Shah Jehan Muttiah, N., Soon Lim, C., In, L. L. A., Mohammad, K. & Awang, K. (2011). Regulation of Apoptotic Effects by Erythrocarpine E, a Cytotoxic Limonoid from *Chisocheton erythrocarpus* in HSC-4 Human Oral Cancer Cells. *PLoS ONE*, *6*(8), e23661.

91. Aassila, H., Bourguet-Kondracki, M. L., Rifai, S., Fassouane, A. & Guyot, M. (2003). Identification of Harman as the Antibiotic Compound Produced by a Tunicate-Associated Bacterium. *Mar. Biotechnol.*, *5*(2), 163-166.

92. Seki, H., Hashimoto, A. & Hino, T. (1993). The ^{1}H- and ^{13}C-Nuclear Magnetic Resonance Spectra of Harman. Reinvestigation of the Assignments by One- and Two-Dimensional Methods. *Chemical & Pharmaceutical Bulletin*, *41*(6), 1169-1172.

93. Seki, H., Tokunaga, T., Utsumi, H. & Yamaguchi, K. (2000). Determination of Heteronuclear Long-Range 1H–13C and 1H–15N Coupling Constants of Harman by Modified J-HMBC 2D NMR Techniques. *Tetrahedron*, *56*(19), 2935-2939.

94. Fadaeinasab, M., Hadi, A., Kia, Y., Basiri, A. & Murugaiyah, V. (2013). Cholinesterase Enzymes Inhibitors from the Leaves of *Rauvolfia Reflexa* and Their Molecular Docking Study. *Molecules*, *18*(4), 3779-3788.

95. Lide, D. R. & Milne, G. W. A. (1995). *Handbook of Data on Common Organic Compounds*. Taylor & Francis.

96. Saidi, N. (2010). Cinnamide and benzamide from species of Cryptocarya crassinervia *Jurnal Natural*, *10*(2), 7-11.

97. Matsunami, K., Otsuka, H., Takeda, Y. & Miyase, T. (2010). Reinvestigation of the Absolute Stereochemistry of Megastigmane Glucoside, Icariside B_5. *Chemical and Pharmaceutical Bulletin*, *58*(10), 1399-1402.

98. Almeida, M. d. F. O., Melo, A. C. R. d., Pinheiro, M. L. B., Silva, J. R. d. A., Souza, A. D. L. d., Barison, A., et al. (2011). Constituintes químicos e atividade Leishmanicida de *Gustavia elliptica* (Lecythidaceae). *Química Nova*, *34* 1182-1187.

99. Weiss, G., Koreeda, M. & Nakanishi, K. (1973). Stereochemistry of theaspirone and the blumenols. *Journal of the Chemical Society, Chemical Communications*, (16), 565-566.

100. Miyase, T., Ueno, A., Takizawa, N., Kobayashi, H. & Oguchi, H. (1987). Studies on the Glycosides of *Epimedium grandiflorum* MORR. var. thunbergianum (MIQ.) NAKAI. II(Pharmacognosy,Chemical). *Chemical & Pharmaceutical Bulletin*, *35*(9), 3713-3719.

101. Galbraith, M. N. & Horn, D. H. S. (1972). Structures of the natural products blumenols A, B, and C. *Journal of the Chemical Society, Chemical Communications*, (3), 113-114.

102. Yamano, Y. & Ito, M. (2005). Synthesis of Optically Active Vomifoliol and Roseoside Stereoisomers. *Chemical and Pharmaceutical Bulletin*, *53*(5), 541-546.

103. González, A. G., Guillermo, J. A., Ravelo, A. G., Jimenez, I. A. & Gupta, M. P. (1994). 4,5-Dihydroblumenol A, a New Nor-isoprenoid from *Perrottetia multiflora*. *Journal of Natural Products*, *57*(3), 400-402.

104. Ren, J., Qin, J., Cheng, X., Yan, S., Jin, H. & Zhang, W. (2013). Five new sesquiterpene lactones from *Inula hupehensis*. *Arch. Pharm. Res.*, *36*(11), 1319-1325.

105. Andersson, R. & Lundgren, L. N. (1988). Monoaryl and cyclohexenone glycosides from needles of *Pinus sylvestris*. *Phytochemistry*, *27*(2), 559-562.

106. Çalış, İ., Kuruüzüm-Uz, A., Lorenzetto, P. A. & Rüedi, P. (2002). (6S)-Hydroxy-3-oxo-α-ionol glucosides from *Capparis spinosa* fruits. *Phytochemistry*, *59*(4), 451-457.

107. Feng, Z., Yang, Y., Jiang, J. & Zhang, P. (2010). Chemical constituents from flowers of *Chrysanthemum indicum*. *Zhongguo Zhong Yao Za Zhi*, *35*(24), 3302-3305.

108. Kolak, U., Topçu, G., Seher Birteksöz, Ötük, G. & Ulubelen, A. (2005). Terpenoids and Steroids from the Roots of *Salvia blepharochlaena*. *Turkish Journal of Chemistry*, *29*(177-186).

109. Pateh, U. U., Haruna, A. K., Garba, M., Iliya, I., Sule, I. M., Abubakar, M. S., et al. (2008). Isolation of stigmasterol, β-sitosterol and 2-hydroxyhexadecanoic acid methyl ester from the rhizomes of *Stylochiton lancifolius* pyer and Kotchy (Araceae). *Nigerian Journal of Pharmaceutical Sciences 7*(1), 19-25.

110. Su, K., Gong, M., Zhou, J. & Deng, S. (2010). Chemical Constituents from *Nauclea Officinalis* Leaves. *Journal of Shihezi University (Natural Science)*, *28*(6), 757-760.

111. Azarpira, A., Lu, F. & Ralph, J. (2011). Reactions of dehydrodiferulates with ammonia. *Organic & Biomolecular Chemistry*, *9*(19), 6779-6787.

112. Zheng, D., Hu, C., Peng, Y. & Hu, S. (2009). A carbon nanotube/polyvanillin composite film as an electrocatalyst for the electrochemical oxidation of nitrite and its application as a nitrite sensor. *Electrochimica Acta*, *54*(21), 4910-4915.

113. Pouységu, L., Sylla, T., Garnier, T., Rojas, L. B., Charris, J., Deffieux, D., et al. (2010). Hypervalent iodine-mediated oxygenative phenol dearomatization reactions. *Tetrahedron*, *66*(31), 5908-5917.

114. Xuan, W.-D., Chen, H. S., Yuan, Z.-X. & Zhu, P. (2005). Chemical Constituents of *Nauclea officinalis*. *Chinese Journal of Natural Medicines*, *3*(3), 181-183.

115. Pelter, A., Ward, R. S. & Gray, T. I. (1976). The carbon-13 nuclear magnetic resonance spectra of flavonoids and related compounds. *Journal of the Chemical Society, Perkin Transactions 1*, (23), 2475-2483.

116. Sichaem, J., Worawalai, W. & Tip-pyang, S. (2012). Chemical constituents from the roots of *Nauclea orientalis*. *Chem Nat Compd*, *48*(5), 827-830.

117. Passos, C. S., Simões-Pires, C. A., Nurisso, A., Soldi, T. C., Kato, L., de Oliveira, C. M. A., et al. (2013). Indole alkaloids of Psychotria as multifunctional cholinesterases and monoamine oxidases inhibitors. *Phytochemistry*, *86* 8-20.

118. Costello, L. C. & Franklin, R. B. (2000). The intermediary metabolism of the prostate: a key to understanding the pathogenesis and progression of prostate malignancy. *Oncology*, *59*(4), 269-282.

119. Gummadi VR, Rajagopalan S, Looi CY, Paydar M, Renukappa GA, Ainan BR, et al. (2013). Discovery of 7- azaindole based anaplastic lymphoma kinase (ALK) inhibitors: Wild type and mutant (L1196M) active compounds with unique binding mode. *Bioorg Med Chem Lett*, *23*(17), 4911-4918.

120. Eckert, A., Marques, C. A., Keil, U., Schussel, K. & Muller, W. E. (2003). Increased apoptotic cell death in sporadic and genetic Alzheimer's disease. *Annals of the New York Academy of Sciences* 604-609.

121. Giacobini, E. (2004). Cholinesterase inhibitors: new roles and therapeutic alternatives. *Pharmacological Research*, *50*(4), 433-440.

122. Martinez, A. & Castro, A. (2006). Novel cholinesterase inhibitors as future effective drugs for the treatment of Alzheimer's disease. *Expert Opinion on Investigational Drugs 15*(1), 1-12.

123. Giacobini, E. (2001). Selective inhibitors of butyrylcholinesterase: a valid alternative for therapy of Alzheimer's disease? *Drugs Aging*, *18*(12), 891-898.

124. Greig, N. H., Utsuki, T., Ingram, D. K., Wang, Y., Pepeu, G., Scali, C., et al. (2005). Selective butyrylcholinesterase inhibition elevates brain acetylcholine, augments learning and lowers Alzheimer beta-amyloid peptide in rodent. *Proceedings of the National Academy of Sciences of the United States of America*, *102*(47), 17213-17218.

125. Dall'Acqua, S. (2013). Plant-derived acetylcholinesterase inhibitory alkaloids for the treatment of Alzheimer's disease. *Botanics: Targets & Therapy*, *3* 19-28.

126. Ahmed, T. & Gilani, A.-H. (2009). Inhibitory effect of curcuminoids on acetylcholinesterase activity and attenuation of scopolamine-induced amnesia may explain medicinal use of turmeric in Alzheimer's disease. *Pharmacology Biochemistry and Behavior*, *91*(4), 554-559.

127. Morris, G. M., Goodsell, D. S., Halliday, R. S., Huey, R., Hart, W. E., Belew, R. K., et al. (1998). Automated docking using a Lamarckian genetic algorithm and an empirical binding free energy function. *Journal of Computational Chemistry*, *19*(14), 1639-1662.

128. Greenblatt, H. M., Guillou, C., Guénard, D., Argaman, A., Botti, S., Badet, B., et al. (2004). The Complex of a Bivalent Derivative of Galanthamine with Torpedo Acetylcholinesterase Displays Drastic Deformation of the Active-Site Gorge: Implications for Structure-Based Drug Design. *Journal of the American Chemical Society*, *126*(47), 15405-15411.

129. Carletti, E., Aurbek, N., Gillon, E., Loiodice, M., Nicolet, Y., Fontecilla Camps, J. C., et al. (2009). Structure–activity analysis of aging and reactivation of human butyrylcholinesterase inhibited by analogues of tabun. *Biochemical Journal*, *421*(1), 97-106.

130. Humphrey, W., Dalke, A. & Schulten, K. (1996). VMD: Visual molecular dynamics. *Journal of Molecular Graphics*, *14*(1), 33-38.

131. Ellman, G. L., Courtney, K. D., Andres jr, V. & Featherstone, R. M. (1961). A new and rapid colorimetric determination of acetylcholinesterase activity. *Biochemical Pharmacology*, *7*(2), 88-95.

132. Torres, J. M., Lira, A. F., Silva, D. R., Guzzo, L. M., Sant'Anna, C. M. R., Kümmerle, A. E., et al. (2012). Structural insights into cholinesterases inhibition by harmane β-carbolinium derivatives: A kinetics – molecular modeling approach. *Phytochemistry*, *81* 24-30.

133. Zhao, T., Ding, K.-m., Zhang, L., Cheng, X.-m., Wang, C.-h. & Wang, Z.-t. (2013). Acetylcholinesterase and Butyrylcholinesterase Inhibitory Activities of β-Carboline and Quinoline Alkaloids Derivatives from the Plants of Genus *Peganum*. *Journal of Chemistry*, *2013* 6.

134. Çokuğraş, A. N. (2003). Butyrylcholinesterase: structure and physiological importance. *Turk J Biochem*, *28*(2), 54-61.

135. Ahmed, F., Mueen Ahmed, K., Sasikala, P. & Ghalib, R. (2013). Cholinesterase inhibitors from botanicals. *7*(14), 121-130.

APPENDIX

Publications and Journals

1. Sook Yee Liew, Chung Yeng Looi, Mohammadjavad Paydar, Foo Kit Cheah, Kok Hoong Leong, Won Fen Wong, Mohd Rais Mustafa, Marc Litaudon, Khalijah Awang. Subditine, a New Monoterpenoid Indole Alkaloid from Bark of *Nauclea subdita* (Korth.) Steud. Induces Apoptosis in Human Prostate Cancer Cells. PLoS ONE 2014, 9 (2), e87286.

2. Sook Yee Liew, Mat Ropi Mukhtar, A. Hamid A. Hadi, Khalijah Awang, Mohd Rais Mustafa, Kazumasa Zaima, Hiroshi Morita, Marc Litaudon. Naucline, a New Indole Alkaloid from the Bark of *Nauclea officinalis*. *Molecules* 2012, *17* (4), 4028-4036.

3. Sook Yee Liew, Mat Ropi Mukhtar, Khalijah Awang, Mohd Rais Mustafa, Seik Weng Ng. 1-(1-Hydroxyethyl)-7,8-dihydroindolo[2,3-a]pyridine[3,4-g]quinolizin-5(13H)-one (angustoline) monohydrate from *Nauclea subdita* (Rubiaceae). *Acta Crystallographica Section E* 2011, 67 (7), o1727-o1728.

4. Sook Yee Liew, Kooi Yeong Khaw, Vikneswaran Murugaiyah, Chung Yeng Looi, Yi Li Wong, Mohd Rais Mustafa, Marc Litaudon, Khalijah Awang. Natural Indole BChE Inhibitors from *Nauclea officinalis*. *Phytomedicine* 2014, Submitted.

5. Sook Yee Liew, Marc Litaudon, Hazrina Hazni, Khalijah Awang. Chemical constituents from *Nauclea officinalis* and its chemotaxonomic study. *Biochemical Systematics and Ecology* 2014, *S*ubmitted.

Articles/Presentations in Conference/Congress/Meeting.

1. Sook Yee Liew, Khalijah Awang , Mohd Rais Mustafa. Cytotoxic Indole Alkaloids from *Nauclea subdita* (Rubiaceae). 9th Mathematics and Physical Sciences Graduate Congress (MPSGC). (8th - 10th January 2014). Universiti Malaya (UM), Kuala Lumpur, Malaysia.

2. Liew Sook Yee, Mat Ropi Mukhtar, A.Hamid A.Hadi, Khalijah Awang, Mohd Rais Bin Mustafa, Kazumasa Zaima, Hiroshi Morita, and Marc Litaudon. Alkaloids from The Bark and Leaves of *Nauclea officinalis* (Rubiaceae). 8th Mathematics and Physical Sciences Graduate Congress (MPSGC). (8th - 10th December 2012). Chulalongkorn University (CU), Thailand.

3. Sook Yee Liew. Alkaloids from The Bark and Leaves of *Nauclea Officinalis* (Rubiaceae). 4th Hope Meetings. (7th-11th March 2012). “Chemistry for Creating the Future”. Tsukuba International Congress Center, Tsukuba, Japan.

4. Sook Yee Liew, Mat Ropi Mukhtar, A. Hamid A. Hadi, Khalijah Awang, Mohd Rais Mustafa, Kazumasa Zaima, Hiroshi Morita, Marc Litaudon. Chemical Constituents from *Nauclea officinalis* (Rubiaceae). 7th Mathematics and Physical Sciences Graduate Congress (MPSGC). (12th - 14th December 2011). National University of Singapore (NUS), Singapore.

OPEN ACCESS Freely available online

PLOS | ONE

Subditine, a New Monoterpenoid Indole Alkaloid from Bark of *Nauclea subdita* (Korth.) Steud. Induces Apoptosis in Human Prostate Cancer Cells

Sook Yee Liew[1], Chung Yeng Looi[2], Mohammadjavad Paydar[2], Foo Kit Cheah[3], Kok Hoong Leong[3], Won Fen Wong[4], Mohd Rais Mustafa[2], Marc Litaudon[5], Khalijah Awang[1]*

1 Department of Chemistry, Faculty of Science, University of Malaya, Kuala Lumpur, Malaysia, **2** Department of Pharmacology, Faculty of Medicine, University of Malaya, Kuala Lumpur, Malaysia, **3** Department of Pharmacy, Faculty of Medicine, University of Malaya, Kuala Lumpur, Malaysia, **4** Department of Medical Microbiology, Faculty of Medicine, University of Malaya, Kuala Lumpur, Malaysia, **5** Institut de Chimie des Substances Naturelles, Centre National de la Recherche Scientifique, Gif-sur-Yvette, Cedex, France

Abstract

In this study, a new apoptotic monoterpenoid indole alkaloid, subditine (**1**), and four known compounds were isolated from the bark of *Nauclea subdita*. Complete ^{1}H- and ^{13}C- NMR data of the new compound were reported. The structures of isolated compounds were elucidated with various spectroscopic methods such as 1D- and 2D- NMR, IR, UV and LCMS. All five compounds were screened for cytotoxic activities on LNCaP and PC-3 human prostate cancer cell-lines. Among the five compounds, the new alkaloid, subditine (**1**), demonstrated the most potent cell growth inhibition activity and selective against LNCaP with an IC_{50} of 12.24±0.19 μM and PC-3 with an IC_{50} of 13.97±0.32 μM, compared to RWPE human normal epithelial cell line (IC_{50} = 30.48±0.08 μM). Subditine (**1**) treatment induced apoptosis in LNCaP and PC-3 as evidenced by increased cell permeability, disruption of cytoskeletal structures and increased nuclear fragmentation. In addition, subditine (**1**) enhanced intracellular reactive oxygen species (ROS) production, as reflected by increased expression of glutathione reductase (GR) to scavenge damaging free radicals in both prostate cancer cell-lines. Excessive ROS could lead to disruption of mitochondrial membrane potential (MMP), release of cytochrome c and subsequent caspase 9, 3/7 activation. Further Western blot analyses showed subditine (**1**) induced down-regulation of Bcl-2 and Bcl-xl expression, whereas p53 was up-regulated in LNCaP (p53-wild-type), but not in PC-3 (p53-null). Overall, our data demonstrated that the new compound subditine (**1**) exerts anti-proliferative effect on LNCaP and PC-3 human prostate cancer cells through induction of apoptosis.

Citation: Liew SY, Looi CY, Paydar M, Cheah FK, Leong KH, et al. (2014) Subditine, a New Monoterpenoid Indole Alkaloid from Bark of *Nauclea subdita* (Korth.) Steud. Induces Apoptosis in Human Prostate Cancer Cells. PLoS ONE 9(2): e87286. doi:10.1371/journal.pone.0087286

Editor: Chih-Pin Chuu, National Health Research Institutes, Taiwan

Received August 16, 2013; **Accepted** December 20, 2013; **Published** February 14, 2014

Funding: The work was funded by University of Malaya Research Grant RP001/2012; University of Malaya High Impact Research Grant UM.C/625/1/HIR/MOHE/SC/37 and HIR: E00002-20001; French National Center for Scientific Research CNRS grant 57-02-03-1007; and Postgraduate Research Funds of University of Malaya (PV050/2012A). This work was carried out within the framework of an official agreement between the CNRS and the University of Malaya (Malaysia). The funders had no role in study design, data collection and analysis, decision to publish, or preparation of the manuscript.

Competing Interests: The authors have declared that no competing interests exist.

* E-mail: khalijah@um.edu.my

Introduction

The Rubiaceae family (Madder family) is one of the largest of the angiosperms with more than 637 genera and almost 10,700 species [1]. The genus *Nauclea* which belongs to this family, consists of about 35 species worldwide [2] and in Malaysia, there are two *Nauclea* species; *N. officinalis* and *N. subdita* [3]. *Nauclea subdita* (Korth.) Steud. is a tropical plant that grows in lowland to hill forests, in swampy places and frequently along streams and rivers [4]. It is a small or medium tree to 25 m tall and 60 cm girth [3]. The plants from this genus are known to produce interesting monoterpenoid indole alkaloids with high structural diversity such as naucline [5], nauclealines B [6] and naufoline [7]. Many of them exhibited significant biological activities; anti-convulsant [8], anti-proliferative [9] and vasorelaxant activities [5].

Prostate cancer is the most frequently diagnosed cancer among men in the developed world. An estimated 238,590 new cases will be diagnosed and 29,720 deaths will result from prostate cancer in the United States in 2013 (Cancer Facts and Figures 2013, American Cancer Society, 2013). Although the mechanisms that drive prostate cancer have not been completely understood, age, race, and family history of the prostate cancer patients have been shown to be the potential factors closely associated with this fatal disease [10].

In our continuous effort to search for new and bioactive chemical constituents from the Malaysia flora [11–15], a new cytotoxic and apoptotic monoterpenoid indole alkaloid, subditine (**1**), has been isolated from the bark of *Nauclea subdita* together with the four known alkaloids; angustoline (**2**) [11,16,17], angustidine (**3**) [18,19], angustine (**4**) [20,21], nauclefine (**5**) [22,23] (Figure 1). In the present paper, we report the isolation and characterization of subditine (**1**), the cytotoxic activities of alkaloids **1**–**5** as well as the apoptotic mechanism of **1** against human prostate cancer cells LNCaP and PC-3.

Molecules **2012**, *17*, 4028-4036; doi:10.3390/molecules17044028

OPEN ACCESS

molecules

ISSN 1420-3049

www.mdpi.com/journal/molecules

Article

Naucline, a New Indole Alkaloid from the Bark of *Nauclea officinalis* †

Sook Yee Liew [1], Mat Ropi Mukhtar [1], A. Hamid A. Hadi [1], Khalijah Awang [1,*], Mohd Rais Mustafa [2], Kazumasa Zaima [3], Hiroshi Morita [3] and Marc Litaudon [4]

[1] Department of Chemistry, Faculty of Science, University of Malaya, 50603 Kuala Lumpur, Malaysia; E-Mails: joeyliew5382@um.edu.my (S.Y.L.); ahamid@um.edu.my (A.H.A.H.)

[2] Department of Pharmacology, Faculty of Medicine, University of Malaya, 50603 Kuala Lumpur, Malaysia; E-Mail: rais@um.edu.my

[3] Faculty of Pharmaceutical Sciences, Hoshi University, Shinagawa-ku, Tokyo 142-8501, Japan; E-Mail: moritah@hoshi.ac.jp

[4] Institut de Chimie de la Substances Naturelles, Centre Nationale de la Recherches Scientifique, 91198, Gif-sur Yvette, Cedex, France; E-Mail: marc.litaudon@icsn.cnrs-gif.fr

† We wish to dedicate this article to our dearest colleague, Dr. Mat Ropi bin Mukhtar who has been a great inspiration to natural product research in Malaysia and globally.

* Author to whom correspondence should be addressed; E-Mail: khalijah@um.edu.my; Tel.: +603-7967-4064; Fax: +603-7967-4193.

Received: 9 February 2012; in revised form: 27 March 2012 / Accepted: 28 March 2012 / Published: 2 April 2012

Abstract: A new indole alkaloid, naucline (**1**) together with four known alkaloids, angustine (**2**), angustidine (**3**), nauclefine (**4**) and naucletine (**5**), were isolated from the bark of *Nauclea officinalis*. The structures of all isolated compounds were elucidated with various spectroscopic methods such as 1D- and 2D- NMR, IR, UV and LCMS-IT-TOF. In addition to that of alkaloid **1**, the complete ^{13}C-NMR data of naucletine (**5**) were also reported. Naucline (**1**) showed a moderate vasorelaxant activity (90% relaxation at 1×10^{-5} M) whereas, angustine (**2**), nauclefine (**4**), and naucletine (**5**) showed potent vasorelaxant activity (more than 90% relaxation at 1×10^{-5} M) on an isolated rat aorta.

Keywords: naucline; angustine; angustidine; nauclefine; naucletine; Rubiaceae; vasorelaxant activity

Acta Crystallographica Section E
Structure Reports Online
ISSN 1600-5368

1-(1-Hydroxyethyl)-7,8-dihydroindolo-[2,3-*a*]pyridine[3,4-*g*]quinolizin-5(13*H*)-one (angustoline) monohydrate from *Nauclea subdita* (Rubiaceae)

Sook Yee Liew,[a] Mat Ropi Mukhtar,[a] Khalijah Awang,[a] Mohd Rais Mustafa[b] and Seik Weng Ng[a]*

[a]Department of Chemistry, University of Malaya, 50603 Kuala Lumpur, Malaysia, and [b]Department of Pharmacology, Faculty of Medicine, University of Malaya, 50603 Kuala Lumpur, Malaysia
Correspondence e-mail: seikweng@um.edu.my

Received 12 June 2011; accepted 13 June 2011

Key indicators: single-crystal X-ray study; T = 100 K; mean σ(C–C) = 0.003 Å; R factor = 0.036; wR factor = 0.098; data-to-parameter ratio = 13.0.

The title compound (trivial name: angustoline monohydrate), $C_{20}H_{17}N_3O_2\cdot H_2O$, features a fused-ring system formed by one five- and four six-membered rings. The nearly planar benzimidazole portion (r.m.s. deviation = 0.008 Å) and the nearly planar 2,7-naphthyridin-1-one portion (r.m.s. deviation = 0.022 Å) of the fused-ring system are slightly twisted, with a dihedral angle of 9.47 (8)°, owing to the tetrahedral nature of the two methylene linkages in the central six-membered ring. The secondary N atom acts as a hydrogen-bond donor to the water molecule of crystallization. In the crystal, the amino and hydroxy groups, and the water molecule are engaged in hydrogen bonding, generating a three-dimensional network.

Related literature

For the isolation of the title compound from other plants, see: Abreu & Pereira (1998, 2001); Au *et al.* (1973); Carte *et al.* (1990); Erdelmeier *et al.* (1992); Fan *et al.* (2010); Hotellier *et al.* (1975); Kakuguchi *et al.* (2009); Lin *et al.* (1988); Sun *et al.* (2008); Xuan *et al.* (2007); Zeches *et al.* (1985).

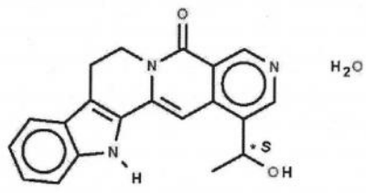

Experimental

Crystal data

$C_{20}H_{17}N_3O_2\cdot H_2O$
M_r = 349.38
Monoclinic, $P2_1$
a = 8.8350 (3) Å
b = 6.7002 (2) Å
c = 14.7347 (4) Å
β = 103.117 (3)°
V = 849.48 (4) Å^3
Z = 2
Cu $K\alpha$ radiation
μ = 0.76 mm^{-1}
T = 100 K
0.30 × 0.03 × 0.03 mm

Data collection

Agilent SuperNova Dual with an Atlas detector diffractometer
Absorption correction: multi-scan (*CrysAlis PRO*; Agilent, 2010)
T_{min} = 0.803, T_{max} = 0.978
6453 measured reflections
3252 independent reflections
3015 reflections with $I > 2\sigma(I)$
R_{int} = 0.027

Refinement

$R[F^2 > 2\sigma(F^2)]$ = 0.036
$wR(F^2)$ = 0.098
S = 1.02
3252 reflections
251 parameters
1 restraint
H atoms treated by a mixture of independent and constrained refinement
$\Delta\rho_{max}$ = 0.29 e Å^{-3}
$\Delta\rho_{min}$ = −0.23 e Å^{-3}
Absolute structure: Flack (1983), 1395 Friedel pairs
Flack parameter: 0.1 (2)

Table 1
Hydrogen-bond geometry (Å, °).

D—H···A	D—H	H···A	D···A	D—H···A
O2—H2···N3^{i}	0.97 (4)	1.77 (4)	2.732 (2)	171 (3)
O1w—H11···O1^{ii}	0.85 (4)	2.08 (4)	2.928 (2)	169 (3)
O1w—H12···O2^{iii}	0.83 (4)	1.95 (4)	2.762 (2)	167 (3)
N1—H1···O1w	0.85 (3)	2.02 (3)	2.861 (2)	177 (2)

Symmetry codes: (i) $-x+1, y-\frac{1}{2}, -z+1$; (ii) $x+1, y, z$; (iii) $-x+2, y-\frac{1}{2}, -z+1$.

Data collection: *CrysAlis PRO* (Agilent, 2010); cell refinement: *CrysAlis PRO*; data reduction: *CrysAlis PRO*; program(s) used to solve structure: *SHELXS97* (Sheldrick, 2008); program(s) used to refine structure: *SHELXL97* (Sheldrick, 2008); molecular graphics: *X-SEED* (Barbour, 2001); software used to prepare material for publication: *publCIF* (Westrip, 2010).

This work was carried under the aegis of a University of Malaya–CNRS (France) collaborative framework. We thank the Ministry of Higher Education (grant No. FRGS-FP016/2010 A) for financial support.

Supplementary data and figures for this paper are available from the IUCr electronic archives (Reference: XU5242).

References

Abreu, P. & Pereira, A. (1998). *Heterocycles*, **48**, 885–891.
Abreu, P. & Pereira, A. (2001). *Nat. Prod. Lett.* **15**, 43–48.
Agilent (2010). *CrysAlis PRO*. Agilent Technologies, Yarnton, Oxfordshire, England.
Au, T. Y., Cheung, H. T. & Sternhell, S. (1973). *J. Chem. Soc. Perkin Trans. 1*, pp. 13–16.
Barbour, L. J. (2001). *J. Supramol. Chem.* **1**, 189–191.
Carte, B. K., Debrosse, C., Eggleston, D., Hemling, M., Mentzer, M., Poehland, B., Troupe, N. & Westley, J. W. (1990). *Tetrahedron*, **46**, 2747–2760.
Erdelmeier, C. A. J., Regenass, U., Rali, T. & Sticher, O. (1992). *Planta Med.* **58**, 43–48.


9th Mathematics and Physical Sciences Graduate Congress
Faculty of Science
University of Malaya
8-10 Jan 2014
KUALA LUMPUR 2014
MPSGC
CU UM NUS
9th
Hosted By
Participating Universities:
UNIVERSITY OF MALAYA
The Leader in Research & Innovation
NUS
National University of Singapore
Chulalongkorn University

Cytotoxic Indole Alkaloids from *Nauclea subdita* (Rubiaceae)

*Sook Yee Liew[a] , Khalijah Awang[a] , Mohd Rais Mustafa[b].

[a]*Department of Chemistry, Faculty of Science, University of Malaya, 50603, Kuala Lumpur, Malaysia.*
[b] *Department of Pharmacology, Faculty of Medicine, University of Malaya, Kuala Lumpur, 50603 Kuala Lumpur, Malaysia.*

Abstract. In this study, a new monoterpenoid indole alkaloid, subditine (**1**), and seven known compounds; angustine (**2**), angustidine (**3**), angustoline (**4**), nauclefine (**5**), 1,2,3,4-tetrahydro-1-oxo-beta-carboline (**6**), harmane (**7**) and benzamide (**8**) were isolated from the bark of *Nauclea subdita*. Complete ^{1}H- and ^{13}C- NMR data of the new compound were reported. The structures of isolated compounds were elucidated with various spectroscopic methods such as 1D- and 2D- NMR, IR, UV and LCMS. Subditine (**1**), angustine (**2**), angustidine (**3**), angustoline (**4**) and nauclefine (**5**) were screened for cytotoxic activities on LNCaP human prostate cancer cell-line. Among the five compounds, the new alkaloid, subditine (**1**), demonstrated the most potent cell growth inhibition activity and selective against LNCaP with an IC_{50} of 12.24 ± 0.19μM, compare to RWPE human normal epithelial cell line (IC_{50} = 30.48 ± 0.08μM).

Keywords: Rubiaceae, *Nauclea subdita*, subditine, cytotoxic


Chulalongkorn University
จุฬาลงกรณ์มหาวิทยาลัย
Pillar of the Kingdom
Abstract Book
The 8th Mathematics and Physical Science
Graduate Congress
2012
Connect Science
Connect ASEAN
8 - 10 December 2012
Faculty of Science
Chulalongkorn University, Thailand
Participating Universities :
UNIVERSITY OF MALAYA
The Leader in Research & Innovation
NUS
National University of Singapore

The 8th Mathematics and Physical Sciences Graduate Congress MPSGC 2012
Connect Science Connect ASEAN 8-10 December 2012

Alkaloids from The Bark and Leaves of *Nauclea officinalis* (Rubiaceae)

Liew Sook Yee[1*], Mat Ropi Mukhtar[1], A.Hamid A.Hadi[1], Khalijah Awang[1], Mohd Rais Bin Mustafa[2], Kazumasa Zaima[3], Hiroshi Morita[3], and Marc Litaudon[4]

[1]Department of Chemistry, Faculty of Science, University of Malaya, 50603 Kuala Lumpur, Malaysia
[2]Department of Pharmacology, Faculty of Medicine, University of Malaya, 50603 Kuala Lumpur, Malaysia
[3]Faculty of Pharmaceutical Sciences, Hoshi University, Shinagawa-ku, Tokyo 142-8501, Japan
[4]*Institut de Chimie de la Substances Naturelles, Centre Nationale de la Recherches Scientifique, 91198, Gif-sur Yvette, Cedex, France.*
**Corresponding author. E-mail: joeyliew5382@gmail.com*

Abstract

Plant material of *Nauclea officinalis* was collected at Hutan Simpan Madek, Keluang, Johor. A phytochemical study on the bark and leaves of *Nauclea officinalis* was conducted using solvents such as dichloromethane, hexane and methane to extract crude compounds from the bark. The crude of dichloromethane extract of the bark and leaves produced a new compound named as naucline (1) and 7 known compounds which are angustine (2), nauclefine (3), naucletine (4), angustidine (5) angustoline (6), dihydroangsutoline (7) and harmane (8). The compounds were isolated and purified using column chromatography and preparative TLC. The structures of isolated compounds were elucidated with spectroscopy methods such as NMR and LCMS. Naucline (1), angustine (2), nauclefine (3) and naucletine (4) have been tested for vasorelaxant activity. Four of them showed potent vasorelaxant activity on an isolated rat aorta.

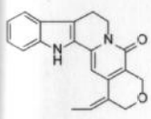
(1)

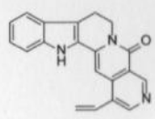
(2)

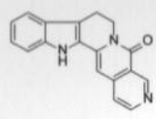
(3)

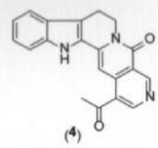
(4)

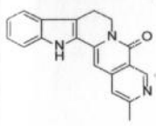
(5)

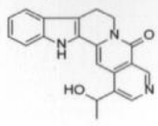
(6)

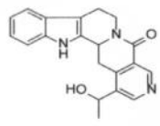
(7)

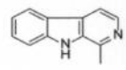
(8)

Keywords: Naucline, *nauclea officinalis*, vasorelaxant activity

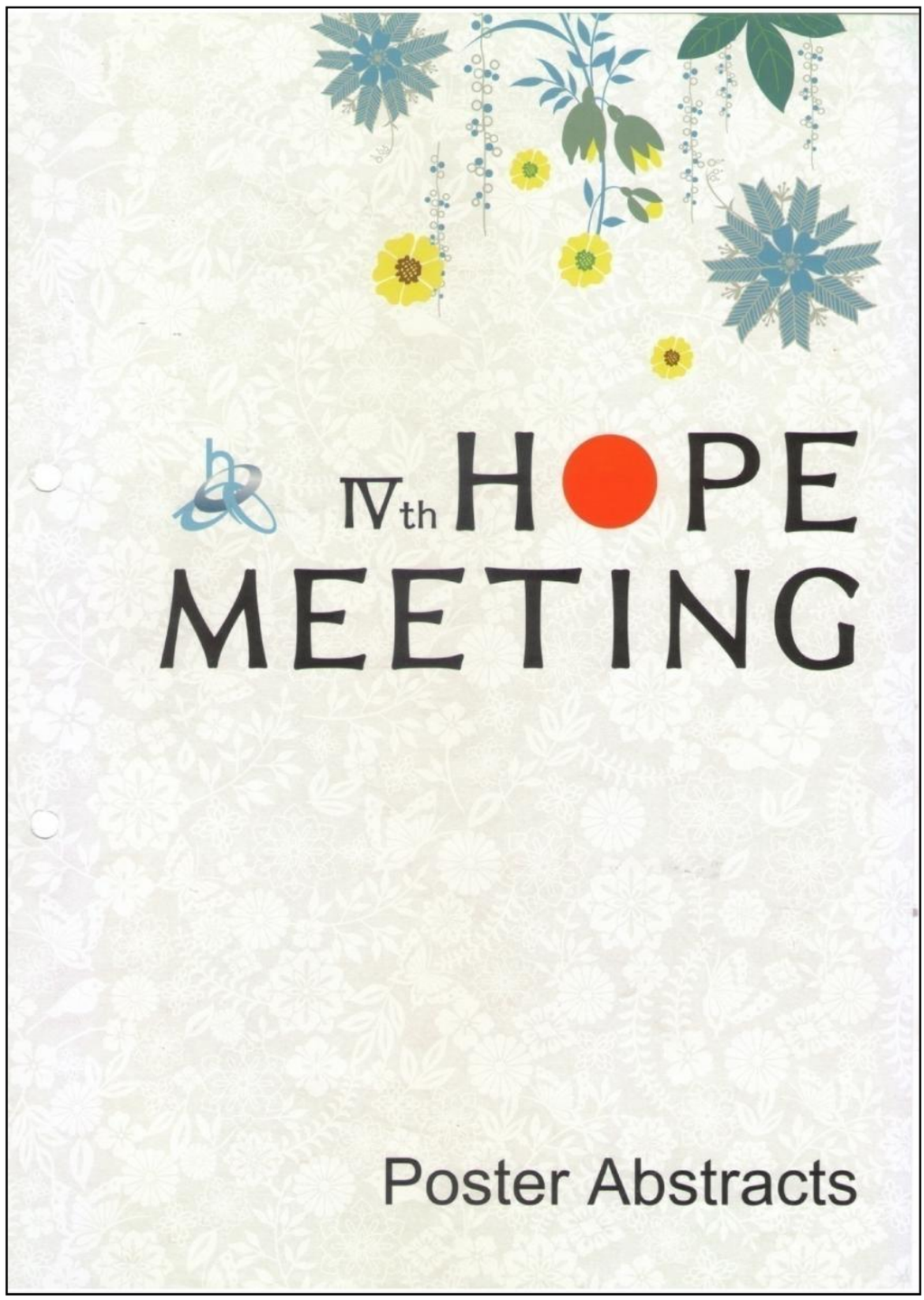
IVth HOPE
MEETING
Poster Abstracts

Title	Alkaloids from The Bark and Leaves of Nauclea Officinalis (Rubiaceae)	
Name	Liew Sook Yee	MY1102
Institution	University of Malaya	

Introduction: Rubiaceae which is also known as Madder or Bedstraw, comprising of 650 genres and 10,500 species worldwide. Majority of them distributed primarily in the tropical regions and are mainly woody trees and shrubs. The genus *Nauclea* (Rubiaceae) is known to have many types of indole alkaloid. A number of monoterpenoid indole alkaloids have been isolated from this genus. *Nauclea officinalis* (Rubiaceae) is a traditional Chinese medicine and major components in this plant are alkaloids and triterpenes.

Objectives: The study was conducted to extract and isolate the chemical constituents from the bark and leaves of *Nauclea officinalis* as well as to study biological activities of the compounds.

Material and Methods: Plant material of *Nauclea officinalis* was collected at Hutan Simpan Madek, Keluang, Johor. A phytochemical study on the bark and leaves of *Nauclea officinalis* was conducted using solvents such as dichloromethane, hexane and methane to extract crude compounds from the bark.

Results: The crude of dichloromethane extract of the bark and leaves produced a new compound named as naucline (**1**) and 7 known compounds which are angustine (**2**), nauclefine (**3**), naucletine (**4**), angustidine (**5**) angustoline (**6**), dihydroangsutoline (**7**) and harmane (**8**). The compounds were isolated and purified using column chromatography and preparative TLC. The structures of isolated compounds were elucidated with spectroscopy methods such as NMR and LCMS. Naucline (**1**), angustine (**2**), nauclefine (**3**) and naucletine (**4**) have been tested for vasorelaxant activity. Four of them showed potent vasorelaxant activity on an isolated rat aorta.

Conclusion: Extraction from bark and leaves of *Nauclea officinalis* followed by isolation, purification and structural elucidation of the compounds produced naucline, angustine, nauclefine, naucletine, angustidine angustoline, dihydroangsutoline and harmane. Further investigation will be done to obtain more compounds in bark as well as leaves of this species and bioactivity study of all the compounds.

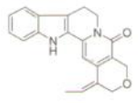

(1)

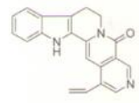

(2)

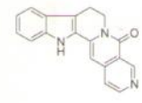

(3)

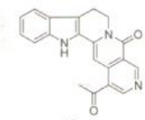

(4)

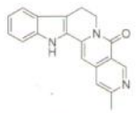

(5)

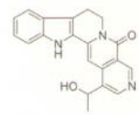

(6)

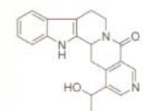

(7)

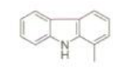

(8)

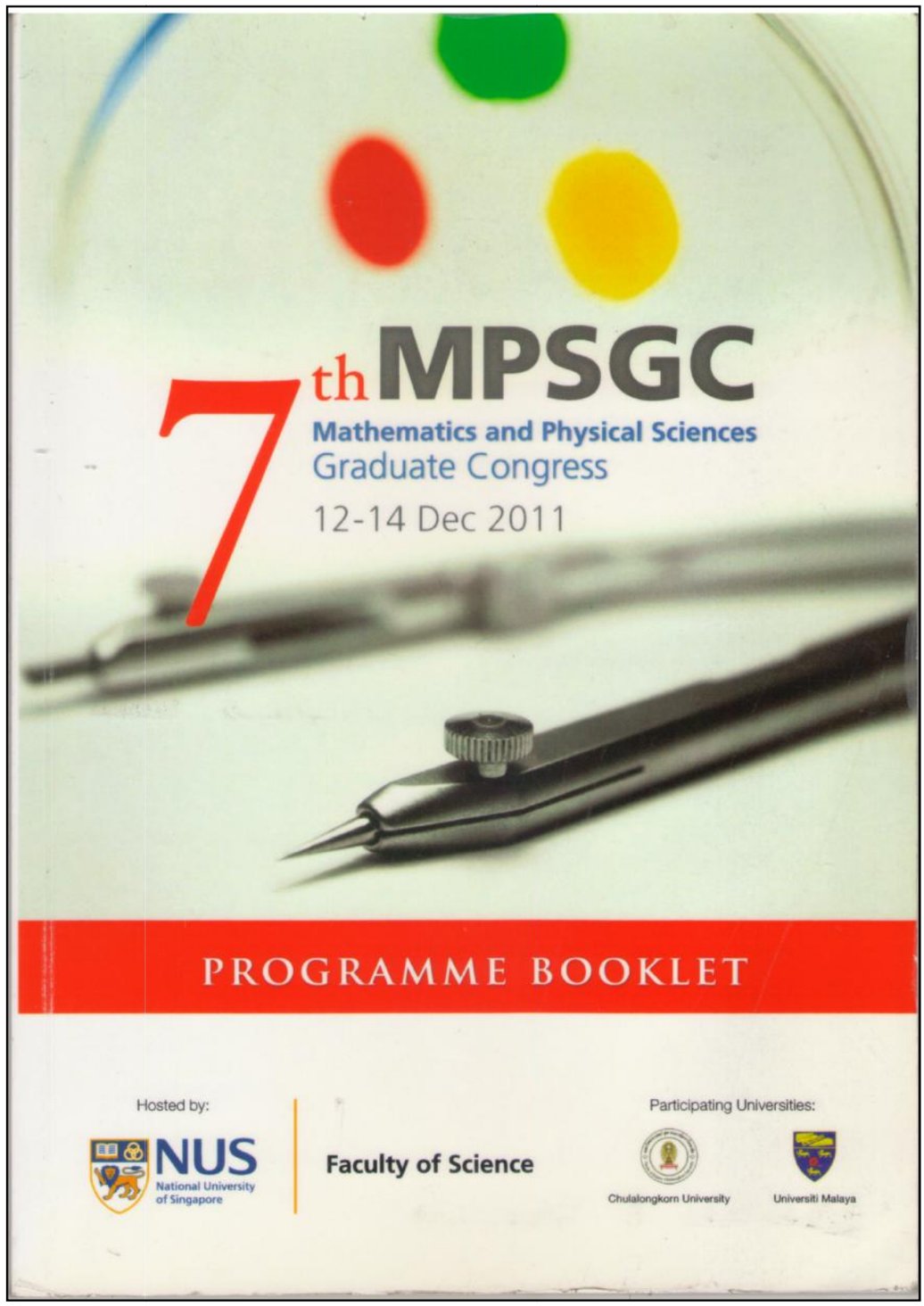
7th MPSGC
Mathematics and Physical Sciences
Graduate Congress
12-14 Dec 2011
PROGRAMME BOOKLET
Hosted by:
NUS
National University of Singapore
Faculty of Science
Participating Universities:
Chulalongkorn University
Universiti Malaya

Detailed Schedule of Oral Presentations

12th December 2011, Monday, PM session

Chemistry Session 1,
Chairpersons: Mr. CHEN Baisheng and Mr. Ramakrishna MALLAMPATI

TIME	TITLE
1300	Plenary speech: Metal Speciation Contributing to Everyday Life *(by Dr. Nor Kartini Abu Bakar)*
1315	Preparation of Industrial-Waste Based Gypsum Binder
1335	Fabrication Of A Nitrocellulose Based Automated Multi-Step Lab-On-Paper For Elisa By Inkjet Printing
1355	Study of Cytotoxic Effects of Green Synthesized Silver Nanoparticles with Mint Ginger and Coffee Extracts on Tumor Cells
1415	Chemical Constituents from Nauclea officinalis (Rubiaceae)
1435	Break (15 mins)
1450	Biological Applications And Electrochemistry Of The Newly Synthesized N,N',N" Donor Schiff Base Transition Metal Complexes
1510	Cycloartane Triterpones From Gardenia spp. And Their Cytotxic Effect
1530	Evaluation of Physicochemical Properties of Ethanol Using RF-GC Methodologies
1550	Synthesis Of Conduritol-F And Inositols From Natural Chiral Building Block (+)-proto-Quercitol And Their Alpha-Glucosidase Inhibition
1610	Synthesis, Characterization and Potential Application of Copper Sulfide for Mercury Trapping in Aqueous System
1630	Synthesis Of Bioconjugated Quercityl-Cinnamate Derivatives From Naturally Available (+)-proto-Quercitol And Their Alpha-Glucosidase Inhibition
1650	Break (15 mins)
1705	Modeling of Heat Transfer During Steaming of Steamed Bread Fortified with Green Tea Extract
1725	Studies on the Water Absorption Behavior of Treated and Untreated Red Balau Saw Dust (Shorea dipterocarpaceae) Filled LDPE Composites
1745	Practical Colorimetric Evaluation for Polydiacetylene Paper-Based Thermal Indicators
1805	Assessment of Poly(3-hydroxyalkanoates) and its Oligoesters as Natural based Plasticizers for Poly(vinyl chloride)

Chemical constituents from *Nauclea officinalis* (Rubiaceae)

Liew Sook Yeea, Mat Ropi Mukhtara, A.Hamid A.Hadia, Khalijah Awanga, Mohd Rais Bin Mustafab, Kazumasa Zaimac, Hiroshi Moritac, and Marc Litaudond

a.Department of Chemistry, Faculty of Science, University of Malaya
b. Department of Pharmacology, Faculty of Medicine, University of Malaya
c. Faculty of Pharmaceutical Sciences, Hoshi University
d. Institut de Chimie de la Substances Naturelles, Centre Nationale de la Recherches Scientifique,

Email: joeyliew5382@hotmail.com

Four known alkaloids, angustine (**1**), angustidine (**2**), nauclefine (**3**) and naucletine (**4**) were isolated from the bark of *Nauclea officinalis* The compounds were isolated and purified using column chromatography and preparative TLC. The structures of isolated compounds were elucidated with spectroscopy methods such as NMR and LCMS. Angustine (**1**), nauclefine (**3**), and naucletine (**4**) showed potent vasorelaxant activity (more than 90% relaxation at 1×10^{-5}M) on an isolated rat aorta.

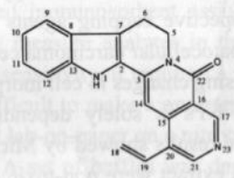

(1)

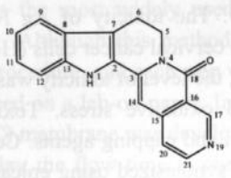

(2)

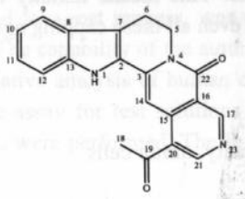

(3)

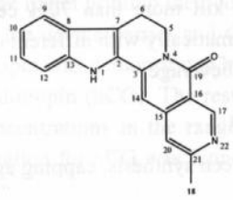

(4)

Figure 1. Structures of angustine **(1)**, angustidine **(2)**, nauclefine **(3)**, and naucletine **(4)**.